

Transfer, Development, and Splice Length for Strand/Reinforcement in High-Strength Concrete

DETAILS

122 pages | | PAPERBACK

ISBN 978-0-309-11747-0 | DOI 10.17226/13916

AUTHORS

Bruce W Russell; Julio A Ramirez; Transportation Research Board

BUY THIS BOOK

FIND RELATED TITLES

Visit the National Academies Press at NAP.edu and login or register to get:

- Access to free PDF downloads of thousands of scientific reports
- 10% off the price of print titles
- Email or social media notifications of new titles related to your interests
- Special offers and discounts



Distribution, posting, or copying of this PDF is strictly prohibited without written permission of the National Academies Press. (Request Permission) Unless otherwise indicated, all materials in this PDF are copyrighted by the National Academy of Sciences.

NCHRP REPORT 603

**Transfer, Development, and
Splice Length for
Strand/Reinforcement in
High-Strength Concrete**

Julio A. Ramirez

PURDUE UNIVERSITY
West Lafayette, IN

Bruce W. Russell

OKLAHOMA STATE UNIVERSITY
Stillwater, OK

Subject Areas

Bridges, Other Structures, Hydraulics and Hydrology

Research sponsored by the American Association of State Highway and Transportation Officials
in cooperation with the Federal Highway Administration

TRANSPORTATION RESEARCH BOARD

WASHINGTON, D.C.

2008

www.TRB.org

NATIONAL COOPERATIVE HIGHWAY RESEARCH PROGRAM

Systematic, well-designed research provides the most effective approach to the solution of many problems facing highway administrators and engineers. Often, highway problems are of local interest and can best be studied by highway departments individually or in cooperation with their state universities and others. However, the accelerating growth of highway transportation develops increasingly complex problems of wide interest to highway authorities. These problems are best studied through a coordinated program of cooperative research.

In recognition of these needs, the highway administrators of the American Association of State Highway and Transportation Officials initiated in 1962 an objective national highway research program employing modern scientific techniques. This program is supported on a continuing basis by funds from participating member states of the Association and it receives the full cooperation and support of the Federal Highway Administration, United States Department of Transportation.

The Transportation Research Board of the National Academies was requested by the Association to administer the research program because of the Board's recognized objectivity and understanding of modern research practices. The Board is uniquely suited for this purpose as it maintains an extensive committee structure from which authorities on any highway transportation subject may be drawn; it possesses avenues of communications and cooperation with federal, state and local governmental agencies, universities, and industry; its relationship to the National Research Council is an insurance of objectivity; it maintains a full-time research correlation staff of specialists in highway transportation matters to bring the findings of research directly to those who are in a position to use them.

The program is developed on the basis of research needs identified by chief administrators of the highway and transportation departments and by committees of AASHTO. Each year, specific areas of research needs to be included in the program are proposed to the National Research Council and the Board by the American Association of State Highway and Transportation Officials. Research projects to fulfill these needs are defined by the Board, and qualified research agencies are selected from those that have submitted proposals. Administration and surveillance of research contracts are the responsibilities of the National Research Council and the Transportation Research Board.

The needs for highway research are many, and the National Cooperative Highway Research Program can make significant contributions to the solution of highway transportation problems of mutual concern to many responsible groups. The program, however, is intended to complement rather than to substitute for or duplicate other highway research programs.

NCHRP REPORT 603

Project 12-60
ISSN 0077-5614
ISBN: 978-0-309-11747-0
Library of Congress Control Number 2008907268

© 2008 Transportation Research Board

COPYRIGHT PERMISSION

Authors herein are responsible for the authenticity of their materials and for obtaining written permissions from publishers or persons who own the copyright to any previously published or copyrighted material used herein.

Cooperative Research Programs (CRP) grants permission to reproduce material in this publication for classroom and not-for-profit purposes. Permission is given with the understanding that none of the material will be used to imply TRB, AASHTO, FAA, FHWA, FMCSA, FTA, or Transit Development Corporation endorsement of a particular product, method, or practice. It is expected that those reproducing the material in this document for educational and not-for-profit uses will give appropriate acknowledgment of the source of any reprinted or reproduced material. For other uses of the material, request permission from CRP.

NOTICE

The project that is the subject of this report was a part of the National Cooperative Highway Research Program conducted by the Transportation Research Board with the approval of the Governing Board of the National Research Council. Such approval reflects the Governing Board's judgment that the program concerned is of national importance and appropriate with respect to both the purposes and resources of the National Research Council.

The members of the technical committee selected to monitor this project and to review this report were chosen for recognized scholarly competence and with due consideration for the balance of disciplines appropriate to the project. The opinions and conclusions expressed or implied are those of the research agency that performed the research, and, while they have been accepted as appropriate by the technical committee, they are not necessarily those of the Transportation Research Board, the National Research Council, the American Association of State Highway and Transportation Officials, or the Federal Highway Administration, U.S. Department of Transportation.

Each report is reviewed and accepted for publication by the technical committee according to procedures established and monitored by the Transportation Research Board Executive Committee and the Governing Board of the National Research Council.

The Transportation Research Board of the National Academies, the National Research Council, the Federal Highway Administration, the American Association of State Highway and Transportation Officials, and the individual states participating in the National Cooperative Highway Research Program do not endorse products or manufacturers. Trade or manufacturers' names appear herein solely because they are considered essential to the object of this report.

Published reports of the

NATIONAL COOPERATIVE HIGHWAY RESEARCH PROGRAM

are available from:

Transportation Research Board
Business Office
500 Fifth Street, NW
Washington, DC 20001

and can be ordered through the Internet at:

<http://www.national-academies.org/trb/bookstore>

Printed in the United States of America

THE NATIONAL ACADEMIES

Advisers to the Nation on Science, Engineering, and Medicine

The **National Academy of Sciences** is a private, nonprofit, self-perpetuating society of distinguished scholars engaged in scientific and engineering research, dedicated to the furtherance of science and technology and to their use for the general welfare. On the authority of the charter granted to it by the Congress in 1863, the Academy has a mandate that requires it to advise the federal government on scientific and technical matters. Dr. Ralph J. Cicerone is president of the National Academy of Sciences.

The **National Academy of Engineering** was established in 1964, under the charter of the National Academy of Sciences, as a parallel organization of outstanding engineers. It is autonomous in its administration and in the selection of its members, sharing with the National Academy of Sciences the responsibility for advising the federal government. The National Academy of Engineering also sponsors engineering programs aimed at meeting national needs, encourages education and research, and recognizes the superior achievements of engineers. Dr. Charles M. Vest is president of the National Academy of Engineering.

The **Institute of Medicine** was established in 1970 by the National Academy of Sciences to secure the services of eminent members of appropriate professions in the examination of policy matters pertaining to the health of the public. The Institute acts under the responsibility given to the National Academy of Sciences by its congressional charter to be an adviser to the federal government and, on its own initiative, to identify issues of medical care, research, and education. Dr. Harvey V. Fineberg is president of the Institute of Medicine.

The **National Research Council** was organized by the National Academy of Sciences in 1916 to associate the broad community of science and technology with the Academy's purposes of furthering knowledge and advising the federal government. Functioning in accordance with general policies determined by the Academy, the Council has become the principal operating agency of both the National Academy of Sciences and the National Academy of Engineering in providing services to the government, the public, and the scientific and engineering communities. The Council is administered jointly by both the Academies and the Institute of Medicine. Dr. Ralph J. Cicerone and Dr. Charles M. Vest are chair and vice chair, respectively, of the National Research Council.

The **Transportation Research Board** is one of six major divisions of the National Research Council. The mission of the Transportation Research Board is to provide leadership in transportation innovation and progress through research and information exchange, conducted within a setting that is objective, interdisciplinary, and multimodal. The Board's varied activities annually engage about 7,000 engineers, scientists, and other transportation researchers and practitioners from the public and private sectors and academia, all of whom contribute their expertise in the public interest. The program is supported by state transportation departments, federal agencies including the component administrations of the U.S. Department of Transportation, and other organizations and individuals interested in the development of transportation. www.TRB.org

www.national-academies.org

COOPERATIVE RESEARCH PROGRAMS

CRP STAFF FOR NCHRP REPORT 603

Christopher W. Jenks, *Director, Cooperative Research Programs*
Crawford F. Jencks, *Deputy Director, Cooperative Research Programs*
David B. Beal, *Senior Program Officer*
Eileen P. Delaney, *Director of Publications*
Ellen M. Chafee, *Assistant Editor*

NCHRP PROJECT 12-60 PANEL **Field of Design—Area of Bridges**

R. Scott Christie, *Pennsylvania DOT (Chair)*
Theresa Ahlborn, *Michigan Technological University*
Thomas Beitelman, *Sound Structures Engineering, Inc., Tallahassee, FL*
Vijay Chandra, *PB Americas, Inc., Herndon, VA*
Allan W. Frank, *Kentucky Transportation Cabinet*
Gregg A. Freeby, *Texas DOT*
Bijan Khaleghi, *Washington State DOT*
David H. Sanders, *University of Nevada—Reno*
Joey Hartmann, *FHWA Liaison*
Eric P. Munley, *FHWA Liaison*
Stephen F. Maher, *TRB Liaison*

AUTHOR ACKNOWLEDGMENTS

The research reported herein was performed under NCHRP Project 12-60 by Purdue Research Foundation through the School of Civil Engineering at Purdue University with subcontracting services being provided by the School of Civil and Environmental Engineering of Oklahoma State University (OSU).

The Principal Investigator on this project was Julio A. Ramirez of Purdue University. The other author of this report was Bruce W. Russell of Oklahoma State University. The work was done under the general supervision of Julio A. Ramirez. The work at OSU was under the supervision of Bruce W. Russell.

FOREWORD

By David B. Beal

Staff Officer

Transportation Research Board

This report documents research performed to develop recommended revisions to the *AASHTO LRFD Bridge Design Specifications* to extend the applicability of the transfer, development, and splice length provisions for prestressed and non-prestressed concrete members to concrete strengths greater than 10 ksi. The report details the research performed and includes recommended revisions to the *AASHTO LRFD Bridge Design Specifications*. The material in this report will be of immediate interest to bridge designers.

The *AASHTO LRFD Bridge Design Specifications* contain barriers to the use of high-strength concrete. These barriers restrict the application of existing and new technology to bridges. The *AASHTO LRFD Bridge Design Specifications* state that design concrete compressive strengths above 10 ksi shall be used only when allowed by specific articles or when physical tests are made to establish the relationships between the concrete strength and other properties. When the *AASHTO LRFD Bridge Design Specifications* were written, there was a lack of data to demonstrate that the provisions were applicable to concrete compressive strengths above 10 ksi. Recent research has started to address design issues with higher strength concretes. FHWA Showcase Projects encourage the use of high-performance concretes—including high-strength concrete—in bridge structures. As the industry moves toward the use of high-strength concrete, the need to revise the *AASHTO LRFD Bridge Design Specifications* is more urgent. There is, therefore, a need to expand the *AASHTO LRFD Bridge Design Specifications* to allow greater use of high-strength concrete.

Two recent NCHRP reports complement the work accomplished in NCHRP Project 12-60 in removing barriers to the use of high-strength concrete. *NCHRP Report 579: Application of LRFD Bridge Design Specifications to High-Strength Structural Concrete: Shear Provisions* identifies all barriers in the *AASHTO LRFD Bridge Design Specifications* to the use of high-strength concrete and provides research findings to remove the barriers related to shear. *NCHRP Report 595: Application of the LRFD Bridge Design Specifications to High-Strength Structural Concrete: Flexure and Compression Provisions* addresses flexural and compression issues. Recommendations from these reports have already been adopted into the *AASHTO LRFD Bridge Design Specifications*.

The objective of NCHRP Project 12-60 was to develop recommended revisions to the *AASHTO LRFD Bridge Design Specifications* for normal-weight concrete having compressive strengths up to 15 ksi, relating to transfer and development length of prestressing strand with diameters up to 0.62 in. and development and splice length in tension and compression of individual bars, bundled bars, and welded wire reinforcement and development length of standard hooks. This research was performed by Purdue University and Oklahoma State University. The report fully documents the research leading to the recommended revisions to Section 5 of the *AASHTO LRFD Bridge Design Specifications*. AASHTO is expected to consider these recommendations for adoption in 2008.

CONTENTS

1	Summary
4	Chapter 1 Introduction and Research Approach
4	1.1 Problem Statement and Research Objective
4	1.2 Research Approach
6	Chapter 2 Literature Review
6	2.1 Introduction
7	2.2 Literature Review
18	2.3 Identification of Issues and Needs
21	2.4 Issues Related to Testing Protocols
25	2.5 Summary
26	Chapter 3 Experimental Program and Results
26	3.1 Introduction to the Experimental Program
26	3.2 The Standard Test Method for the Bond of Prestressing Strands
31	3.3 The NASP Bond Test in Concrete
38	3.4 Measured Transfer Lengths versus Varying Concrete Strengths and Varying NASP Bond Test Values
54	3.5 Development Length Tests
72	3.6 Discussion of Design Recommendations
77	3.7 The Effect of Concrete Strength on Bond Performance— Summary, Conclusions, and Recommendations
78	3.8 Experimental Program—Mild Steel Anchorage of Uncoated Bars in Tension
89	3.9 Anchorage of Epoxy-Coated Bars in Tension
99	3.10 Anchorage of Bars Terminated with Standard Hooks in Tension
110	Chapter 4 Design Recommendations
110	4.1 Introduction
110	4.2 Design Recommendations
111	4.3 Details of the Design Recommendations
119	References
122	Appendices

S U M M A R Y

Transfer, Development, and Splice Length for Strand/Reinforcement in High-Strength Concrete

Article 5.4.2.1 of the 3rd edition of the *AASHTO LRFD Bridge Design Specifications* limits the applicability of the specifications for concrete compressive strengths of 10,000 psi or less unless physical tests are made to establish the relationships between concrete strength and other properties (AASHTO 2004). A comprehensive, article-by-article review of Section 5 of the *AASHTO LRFD Bridge Design Specifications* pertaining to transfer, development, and splice length for strand/reinforcement was performed under NCHRP Project 12-60 to identify all the provisions that have to be revised to extend their use to high-strength, normal-weight concrete up to 15 ksi. Upon completion of the experimental work under NCHRP Project 12-60, draft specifications and accompanying commentary for provisions to extend the application of the LRFD bridge design specifications to high-strength concrete were developed. The provisions cover the transfer and development length of prestressing strand and the development and splice length of reinforcement in normal-weight concrete with compressive strengths up to 15 ksi. Researchers from Purdue University and Oklahoma State University have jointly prepared this report.

Transfer Length and Development Length for Strand

Recommendations include new transfer length and development length equations for incorporation into Articles 5.11.4.1 and 5.11.4.2 of the *AASHTO LRFD Bridge Design Specifications*. Also, a new requirement is introduced for addition to Article 5.4.4.1 for the purpose of qualifying the basic bonding properties of prestressing strand.

Article 5.4.4.1 addresses the material properties of prestressing strand. Heretofore, Article 5.4.4.1 addressed the mechanical properties of strand only, i.e., breaking strength, yield strength, and strand size. Based on research described in this report, a “Standard Test Method for the Bond of Prestressing Strands” (also called the “Standard Test for Strand Bond”) is recommended for inclusion by reference in Article 5.4.4.1. Details for testing procedures and material acceptance are included in Appendix H. The Standard Test Method for the Bond of Prestressing Strand requires that prestressing strands obtain an average minimum pull-out value of 10,500 lb for 0.5-in. strands and 12,600 lb for 0.6-in. strands.

Further, the research supports, and this report recommends, that transfer length and development length equations include a parameter for concrete strength. The research shows a clear correlation between shortening of transfer and development lengths and increasing concrete strength. Therefore, a new transfer length expression is recommended for inclusion into Article 5.11.4.2 of the *AASHTO LRFD Bridge Design Specifications*:

$$l_t = \left[\frac{120d_b}{\sqrt{f'_c}} \right] \leq 40d_b$$

where

d_b = strand diameter,
 f'_{ci} = concrete strength at release, and
 l_t = transfer length.

At a concrete release strength of 4 ksi, the recommended expression provides for a transfer length of 60 strand diameters, which matches historic design procedures. The recommended expression also provides for a transfer length of at least 40 strand diameters, effectively limiting the benefits from release strength to about 9 ksi.

Increases in concrete strength also result in shorter development lengths. Therefore a new development length expression is recommended for inclusion in Article 5.11.4.3 of the *AASHTO LRFD Bridge Design Specifications*:

$$l_d = \left[\frac{120}{\sqrt{f'_{ci}}} + \frac{225}{\sqrt{f'_c}} \right] d_b \geq 100d_b$$

This expression provides a development length of about 150 strand diameters for concrete with release strength of 4 ksi and design strength of 6 ksi. The expression is different in form than the current expression, but more “user friendly” to the designer. In the development length equation, l_d is the development length (in.), d_b is the strand diameter (in.), f'_{ci} is the concrete strength at release (ksi), and f'_c is the concrete design strength (ksi). The expression provides for a development length of at least 100 strand diameters.

Recommendations are also made to revise the part of Article 5.11.4.3 of the *AASHTO LRFD Bridge Design Specifications* dealing with debonded, or shielded, strands. In brief, recommendations contained in this report would remove the 2.0 multiplier applied to debonded strands, but add some restrictions to the use of debonded strands.

Development Length and Splice Length for Reinforcement

The proposed recommendations stemming from the work conducted under NCHRP Project 12-60 cover two aspects for mild steel:

1. Development length of black and epoxy-coated reinforcing bars anchored by means of straight embedment length and splices and
2. Development length of black and epoxy-coated bars terminated with a standard hook.

Based on observations from tests conducted during NCHRP Project 12-60 on 18 top cast beam-splice specimens and the examination of an extensive database of previous tests compiled by ACI Committee 408, it is proposed that extension of the *AASHTO LRFD Bridge Design Specifications* to concrete strengths up to 15 ksi follow a format similar to the one used in *ACI: 318-05: Building Code Requirements for Structural Concrete and Commentary* (ACI 2005), with the following exceptions:

- Removal of the bar size factor for #6 bars and smaller bars (thus $\gamma = 1.0$ in all cases).
- Use of a single factor for epoxy-coated bars of 1.5 regardless of the ratio of cover to bar diameter.
- Exclusion of evaluations of beam splice specimens with bottom cast bars in this study. ACI Committee 408 has indicated that the current approach in the 318 Code (ACI 2005) overestimates the bar force at failure in many specimens with bottom bars available in the ACI Committee 408 database, especially for specimens with concrete compressive strengths greater than 10 ksi (ACI Committee 408 2003). ACI Committee 408 proposed a modified expression

for development and splice length in addition to removal of the bar size factor to address this issue. In the evaluation of test data conducted under NCHRP Project 12-60, the researchers found that the use of a bottom cast modification factor of 1.2 for uncoated bars anchored in concrete with compressive strengths greater than 10 ksi appeared to address the safety concerns raised by ACI Committee 408. This factor would not be needed for bottom cast epoxy-coated bars (because of the single modification factor of 1.5) or for uncoated top bars. This approach could be used as an alternative to the approach suggested by ACI Committee 408. The researchers note that additional testing of bottom cast uncoated splices is justified with higher strength concretes.

Article 5.11.2.4 of the *AASHTO LRFD Bridge Design Specifications* (AASHTO 2004) was verified for high-strength concrete in the experimental work plan for NCHRP Project 12-60 with the exception of the lightweight aggregate factor. Based on the analysis of tests conducted during NCHRP Project 12-60 (21 full-scale tests of hooked bar anchorages) and the analysis of tests of additional specimens in the literature, it is possible to support the extension of the approach in the 318 Code (ACI 2005) provision for anchorage of bars terminated with standard hooks, black and epoxy-coated, to normal-weight concrete with concrete compressive strength of up to 15 ksi, with these two modifications:

1. A minimum amount of transverse reinforcement (at least #3 U bars at $3d_b$ spacing) needs to be provided to improve the bond strength of both epoxy-coated and black #11 bars and larger bars in tension anchored by means of standard hooks.
2. A modification factor of 0.8 instead of the current factor of 0.7 for #11 and smaller hooks with side cover (normal to plane of hook) not less than 2.5 in. and for 90-deg hooks with cover on bar extension beyond hook not less than 2 in.

Tension lap splices were also evaluated under NCHRP Project 12-60. Splices of bars in compression were not part of the experimental program. Class C splices were eliminated based on the modifications to development length provisions. The proposed modifications to Article 5.11.2.1 of the *AASHTO LRFD Bridge Design Specifications* contain several changes that eliminated many of the concerns regarding tension splices due to closely spaced bars with minimal cover; however, development lengths, on which splice lengths are based, have in some cases increased. A two-level splice length was retained primarily to encourage designers to splice bars at points of minimum stress and to stagger splices to improve behavior of critical details; however, such provisions are not intended to reflect the strength of the splice.

CHAPTER 1

Introduction and Research Approach

1.1 Problem Statement and Research Objective

This final report documents research findings regarding the transfer length and development length of prestressing strand and the development length and splice length of reinforcement in normal-weight concrete with compressive strengths up to 15 ksi. Recommended revisions to the 4th edition of the *AASHTO LRFD Bridge Design Specifications* were also developed in the research (AASHTO 2007).

Structural engineers have continually tried to optimize building materials by improving their durability and effectiveness. An example of such efforts is the use of high-strength concrete in bridge members. High-strength concrete, defined for this report as concrete having a compressive strength in excess of 10 ksi, is more brittle than normal-strength concrete; consequently, the designer has to be cautious in extending empirically based rules to this new material. The 2004 *AASHTO LRFD Bridge Design Specifications* (with 2005 and 2006 interim revisions) states that concrete with compressive strengths above 10 ksi should be used only when physical tests are made to establish the relationships between concrete strength and other properties (AASHTO 2004). This requirement reflects the lack of data to demonstrate that the provisions were applicable to concrete strengths above 10 ksi at the time the specification was written.

The objective of this study was to develop recommended revisions as appropriate to the 4th edition of the *AASHTO LRFD Bridge Design Specifications* for normal-weight concrete having compressive strengths up to 15 ksi, relating to the following (AASHTO 2007):

- Transfer and development length of prestressing strand with diameters up to 0.62 inches; and
- Development and splice length in tension and compression of individual bars, bundled bars, and welded wire reinforcement and development length of standard hooks.

The knowledge gained and the resulting improvements to the 4th edition of the *AASHTO LRFD Bridge Design Specifications* will assist engineers in the safe design of high-strength concrete bridge members (AASHTO 2007).

The 4th edition of the *AASHTO LRFD Bridge Design Specifications* provides a good starting point for higher strength concrete bridge members (AASHTO 2007). However, the existing provisions were optimized for concrete strengths between 5 and 10 ksi and require modifications if they are to be extended to higher strength concretes. Because of its brittle nature, high-strength concrete must be properly utilized in both design and construction. The more brittle nature of high-strength concrete means that if cracks form, they may propagate more extensively than they would in lower strength concretes. This may result in the loss of effectiveness of the concrete cover and raise safety concerns regarding the bond strength of strand and deformed bars embedded in high-strength concrete.

1.2 Research Approach

Chapter 2 of this report provides a review of relevant practice, performance data, research findings, and other relevant information related to the transfer and development length of prestressing strand and the development and splice length of mild reinforcement. This chapter presents an information summary on the factors that affect the behavior of transfer and development length of prestressing strand and the development and splice length of mild reinforcement. Chapter 2 includes a critical review of existing testing protocols for determining bond characteristics and presents the testing protocols used in NCHRP Project 12-60.

Article 5.4.2.1 of the 3rd edition of the *AASHTO LRFD Bridge Design Specifications* limits the applicability of the specifications to concrete compressive strengths of 10,000 psi or less unless physical tests are made to establish the relationships between concrete strength and other properties (AASHTO

2004). A comprehensive, article-by-article review of Section 5 of the 2nd edition of the *AASHTO LRFD Bridge Design Specifications* (with Update 2000) was performed under NCHRP Project 12-56 to identify all the provisions that directly or indirectly have the potential to prevent the extension of the specifications in their current form to high-strength concrete (AASHTO 1998; Hawkins and Kuchma 2002). In addition, a comprehensive, article-by-article review of Section 5 of the 2nd edition of the *AASHTO LRFD Bridge Design Specifications* with the 1999, 2000, and 2001 interim revisions (AASHTO 1998) was performed as part of the FHWA study, *Compilation and Evaluation of Results from High Performance Concrete Bridge Projects* (Russell et al. 2006). The provisions identified

by both of these reports as having the potential for preventing the extension of development and splice length specifications to high-strength concrete were reviewed and considered during the work conducted under NCHRP Project 12-60.

The results of the expanded plan of research are included in Chapter 3. The findings of the extensive literature review and the experimental program conducted under NCHRP Project 12-60 were used to recommend revisions as appropriate to the *AASHTO LRFD Bridge Design Specifications* for transfer, development, and splice lengths for strand/reinforcement in normal-weight concrete having compressive strengths up to 15 ksi. Chapter 4 contains design recommendations supported by the research conducted under NCHRP Project 12-60.

CHAPTER 2

Literature Review

2.1 Introduction

The comprehensive and critical literature review undertaken during NCHRP Project 12-60 is described in this chapter. In this report, important findings from prior research are reviewed, with particular attention to the impact of these findings on the work plan for NCHRP Project 12-60.

The objective of the work related to prestressing strand was to gather and synthesize existing data and information on the transfer length and development length of strand with diameters up to 0.6 in. In the area of mild reinforcement, the effort concentrated on development and splice length in tension of individual bars and development length of bars in tension anchored with standard hooks. The database constructed from this effort includes 71 tension development and splice tests of specimens with top cast uncoated reinforcing bars, 493 specimens with bottom cast uncoated reinforcing bars, 27 specimens with top cast epoxy-coated bars, and 48 with bottom cast epoxy-coated bars. In addition, 33 specimens with uncoated bars terminated with standard hooks and 13 specimens reinforced with epoxy-coated bars have been reviewed.

A comprehensive analysis of the data collected was conducted to identify issues and needs related to bond of strand and mild steel in high-strength concrete. This analysis assisted in the identification of several key variables that are likely to affect the transfer and development of prestressing strands, development/splice length of bars in tension, and development length of bars in tension terminated with standard hooks. Some of these variables are currently included in the *AASHTO LRFD Bridge Design Specifications* while some are not. In the area of transfer length and development length of prestressing strand, specifications do not account for variables such as concrete strength, strand size, “top bar” effects, epoxy coating, bond quality of individual strand samples, and structural behavior issues (e.g., the interaction of shear and bond). The work plan for NCHRP Project 12-60 included procedures and testing to evaluate some, but not all, of these effects. Other

issues that may influence the transfer and development of prestressing strands include confining reinforcement and strand spacing. The research reported in the literature indicates that 0.6-in. strand can be spaced at 2.0 in. center to center (c/c) or that 0.5-in. strands may be spaced at 1.75 in. without penalty to the transfer and development of strands. The reported research also indicates that confining reinforcement has little or no effect on transfer length of strands, but it can be quite beneficial to strand development. Standardized confinement details were employed in beam testing where warranted.

In the area of bond of mild reinforcement, the single most important issue not currently accounted for in the *AASHTO LRFD Bridge Design Specifications* is the effect of confining reinforcement on the bond strength of tension reinforcement in the case of splitting type failures. This parameter is especially important as bars are being developed in higher strength concretes. The review also revealed that for epoxy-coated bar development/splice length and development length of bars terminated with standard hooks there is a paucity of data on concretes with cylinder strengths above 10 ksi.

A significant effort during the initial 6 months of the NCHRP Project 12-60 study was focused on identifying and evaluating testing protocols related to the experimental work to be conducted. In the area of bond in concrete of prestressing strand, particular attention was given to the surface characterization tests to evaluate strand “bond-ability.” There are three tests that have been offered in recent years as possible tests to standardize acceptance of strand based on its “bond-ability”: (1) the Moustafa Test, where untensioned strands are pulled from large concrete blocks; (2) the PTI Bond Test, where untensioned strands are pulled from a neat cement mortar; and (3) the NASP Bond Test, where untensioned strands are pulled from a sand cement mortar. In testing performed by the North American Strand Producers (NASP), the NASP Bond Test has proven to be the most reliable test of the three. It has produced test results from “blind trials” with the best repeatability and reproducibility.

In three separate rounds of testing, the Moustafa Test (now called the Large Block Pull-Out Test) was performed at different sites to determine its reproducibility across sites. In NASP Round I testing, the Moustafa Test was performed at Coreslab Structures in Colorado and at Florida Wire and Cable Co. (FWC). For the purpose of carrying out Moustafa Tests, FWC built a completely automated testing machine so that the Moustafa procedures could be precisely followed. Round I testing showed widely dissimilar results from the two testing sites. In NASP Round II, the Moustafa Test and the PTI Bond Tests were performed at three testing sites: Coreslab Structures, FWC, and the University of Oklahoma. Additionally, the NASP Bond Test was introduced in an early form as a test very similar to the PTI Bond Test except that a sand-cement mortar was used. Seven different strand samples were shipped to the different testing sites. The trials were blind. Again, the Moustafa Test failed to produce reproducible results across testing sites. Of the three tests, the NASP Bond Test showed the highest statistical correlation across testing sites. In the NASP Round III testing, a more refined version of the NASP Bond Test again outperformed the Moustafa Test in blind trials at the three testing sites. In all three rounds of testing, when the Moustafa Test was used, it failed to produce results that were consistent across sites. The NASP Bond Test proved more reliable at providing the same or similar results across testing sites in Rounds II, III, and IV. Because of the NASP Bond Test's more consistent results, the NCHRP Project 12-60 testing program was built upon the NASP Bond Test.

The review conducted on testing for development/splice length of deformed bars in tension showed that the generally recommended testing protocol for full-scale specimens because of both the relative ease of fabrication and the realistic state of stress achieved during testing is the beam-splice specimen. Thus, beam splice specimens were used in the development of experimental data related to development/splice length of mild reinforcement during the course of the NCHRP Project 12-60 study. It is well established that testing protocols to evaluate development and splice length requirements for deformed bars and wire in tension must be of an appropriate scale, containing more than one bar or wire, with due regard for a realistic transfer of force between concrete and steel reinforcement and cover/bar spacing effects. Splice tests have in the past been accurate simulations of real conditions in structures; however, development length tests have been largely conducted using pull-out tests, in which splitting failures are purposely avoided. As a result, the bond stresses developed along splices are low compared with the bond stresses along a bar in a pull-out test. This difference in test methods is responsible for large differences in code-required anchorage lengths for splices and development of single bars. Pull-out failures occur in cases of high confinement and short bonded lengths. In most structural applications, however, splitting failures tend to control. Beam-splice specimens are deemed to represent larger-scale specimens designed

to directly measure development and splice strength in full-scale members.

The experimental work supporting the current requirements in the *AASHTO LRFD Bridge Design Specifications* and *ACI 318-05: Building Code Requirements for Structural Concrete and Commentary* (2005) for development of standard hooks in tension was conducted using a test setup representing an exterior beam column joint. Because of the paucity of data on concrete strengths above 10 ksi, the evaluation of uncoated and epoxy-coated bars terminated with standard hooks in tension to normal-weight concrete with compressive strength up to 15 ksi was performed using a similar exterior beam column joint test setup.

The results of the initial work of NCHRP Project 12-60 confirmed the basic premises stated in the original project proposal. Thus, the efforts of the experimental program and the order of priority of these efforts remained as originally stated. The experimental program focused on the following major efforts listed in priority order:

1. **Determining design equations for transfer and development length of strand in prestressed concrete bridge members.** Variables included concrete strength at release, concrete strength at time of development length testing, use of air-entraining admixtures, "top bar effects," and strand size.
2. **Development and splice length in tension of reinforcing bars.** Variables included concrete strength, bar size, concrete cover/bar spacing, amount of transverse reinforcement, epoxy coating, and casting position.
3. **Development length in tension of bars terminated with standard hooks.** Variables included concrete strength, bar size, concrete cover/bar spacing, amount of transverse reinforcement, and epoxy coating.

A comprehensive article-by-article review of Section 5 of the 2nd edition of the *AASHTO LRFD Bridge Design Specifications* with the 1999, 2000, and 2001 interim revisions (AASHTO 1998) was conducted during the initial 6 months of the NCHRP Project 12-60 study. In this review, the provisions of Section 5 that directly or indirectly affect transfer and development length of prestressing strand and development/splice length of mild reinforcement by the use of high-strength concrete were extracted and critically reviewed.

2.2 Literature Review

2.2.1 Strand Transfer and Development Length

A number of experimental investigations related to high-strength concrete have been conducted in North America and overseas. Hence, a significant body of knowledge currently exists with respect to the performance of high-strength concrete

members. Amongst the experimental data are various studies dealing with transfer length and development length of prestressing strand and splice length and development length of black and epoxy-coated reinforcement. In this study, a comprehensive and critical literature review was undertaken to gather and synthesize existing data and information related to the transfer length and development length of prestressing strand with diameters up to 0.6 in., and development and splice length in tension and compression of individual bars, bundled bars, and welded wire reinforcement and development length of standard.

The literature review centered on collecting information on testing protocols for determining surface bond characteristics of strand, performance of members containing transverse reinforcement, bond and transfer length, and tests addressing deformation capacity. Information available from the field—including FHWA showcase projects and the unpublished experiences of engineers, bridge owners, and producers—was reviewed and used to supplement other work conducted in this study.

The development of reliable code expressions for transfer and development of prestressing strand is made more difficult by the large experimental scatter reported by researchers over the past 40 years. The original code expressions for transfer and development length of pretensioned strands were developed from testing performed in the late 1950s and early 1960s on Grade 250, stress-relieved strand (Hanson and Kaar 1959; Kaar, LaFraugh, and Mass 1963; Tabatabai and Dickson 1993). Based on these early tests, the ACI Building Code (ACI 2005) and the *AASHTO LRFD Bridge Design Specifications* adopted provisions governing the design for strand transfer and development. Manufacturing innovation has brought about Grade 270 low-relaxation strand as the industry standard, while the code expressions for transfer and development length have changed very little.

Furthermore, contemporary strand production employs induction heating to stress relieve strand, whereas convection heating was used in the late 1950s and early 1960s. Convection heating created hotter surface temperatures on strand that may have burned off much of the surface residues remaining from the wire drawing process. Today's processes, using induction heating, may have created surface temperatures lower than those created by convection heating and thereby may have effectively changed the bonding characteristics of the surface of prestressing strands (Rose and Russell 1997).

In the mid-1980s, Cousins, Johnston, and Zia (1990) measured transfer lengths that exceeded the standard design predictions by a wide margin. Their findings led FHWA to adopt a moratorium on the use of 0.6 in. diameter strands and to increase the development length for other sizes of prestressing strands. The FHWA action led to the creation of a

large number of research programs intent on measuring the transfer and development of prestressing strands. Research was performed at the University of Texas (Russell and Burns 1996, 1997), Florida DOT (Shahawy, Issa, and Batchelor 1992), McGill University (Mitchell et al. 1993), and Auburn University (Cousins et al. 1993). The arbitrary 1.6 multiplier from the original FHWA moratorium is now incorporated into the *AASHTO LRFD Bridge Design Specifications*.

By the mid-1990s, it became apparent that the studies examining the transfer and development of prestressing strands had not resulted in a consensus on design standards. As a whole, the research displayed a large scatter of the test results, with measured transfer lengths for 0.5-in. strand ranging from a low of less than 20 in. to a high of more than 60 in. Thus, it became apparent that other variables were in play and that such variables were not properly accounted for in either design equations or specifications.

Since the mid-1990s, research work has concentrated on developing a standardized test to assess the bond characteristics of individual prestressing strands. It was suspected that different strand manufacturers produced strand with quite dissimilar bonding characteristics. Hence, it was important to quantify the bonding characteristics of an individual strand before the transfer length and development length data would be meaningful. To that end, three or four different testing programs were undertaken to assess the viability of various "standardized tests" and the suitability of such tests for predicting the "bond-ability" of prestressing strand.

The first such testing program was developed by Rose and Russell (1997). The various testing programs found little correlation between a "simple pull-out" test and measured transfer lengths. From these research programs, the precast concrete industry adopted a set of standard test procedures that were to be employed in performing "pull-out" tests. The set adopted is known as the "Moustafa Test." Early results using the Moustafa Test indicated that the test could be used to compare the bonding characteristics of strand on a relative basis. Logan (1997) demonstrated that the Moustafa Test, at the recommended threshold value, would provide strand with bonding capability more than adequate to meet current design assumptions.

In the meantime, the Post-Tensioning Institute commissioned a study at Queen's University in Ontario (Hyett, Dube, and Bawden 1994). The study produced yet another bond test, the "PTI Bond Test." The PTI Bond Test's primary purpose was to assess the bond characteristics of 0.6 in. diameter strand and show the strand's suitability for use as a rock anchor. In an appendix to ASTM A 416, the ASTM has adopted the PTI Bond Test on a provisional basis for 0.6 in. diameter strand that is to be used as rock anchors.

Subsequent testing sponsored by the North American Strand Producers Association (NASP) led to the development

of a third bond test, now called the “NASP Bond Test” (Russell and Paulsgrove 1999b). In “blind trial” testing, the Moustafa Test, the PTI Bond Test, and the NASP Bond Test were performed at multiple sites. The results of the blind trial testing indicated that the NASP Bond Test provided the best repeatability. Based on these results and on as yet unpublished results from NASP Round III testing, the NASP recommended the use of the NASP Bond Test as the standardized test to assess the bond characteristics of prestressing strands. Overall, experimental results clearly show that inherent quality differences exist in the bond of prestressing strands from various manufacturers. Accordingly, it is imperative in a testing program to evaluate the bonding characteristics of the prestressing strands used. The standardization process will make possible nationwide adoption by trans-

portation agencies of the experimental results on transfer length and development length of strand in concrete.

Round II of the NASP tests examined the proposed standardized tests for repeatability and reproducibility. The results clearly indicated that the NASP Bond Test was the most reliable test of the three tests examined. Results from the Moustafa Test are shown in Figures 2.1 and 2.2. Note that in the Moustafa Test, results from a majority of strands tended to cluster near the threshold level, and a more poorly performing strand was inconsistently rated. In a similar plot, Figure 2.3 compares results from two different test series performed at the University of Oklahoma (OU) featuring the NASP Bond Test. Finally, Figure 2.4 compares the NASP Bond Test results at two different test sites. The reproducibility of test results proved to be quite remarkable and

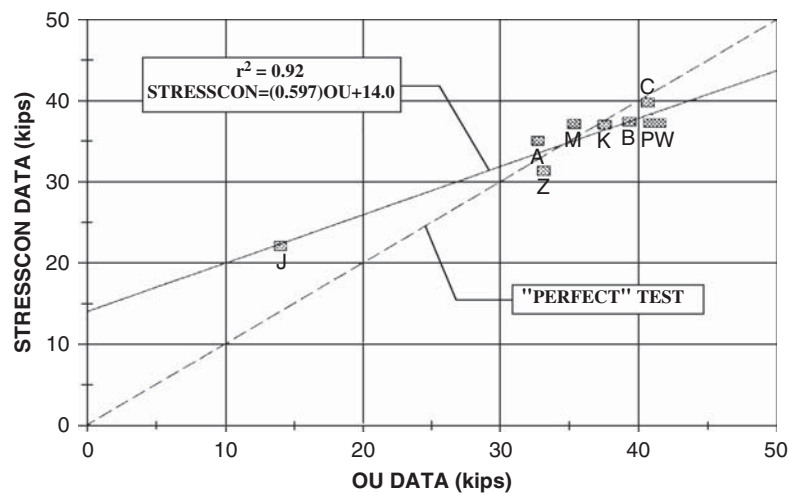


Figure 2.1. Comparison of Moustafa pull-out values from Stresscon and OU.

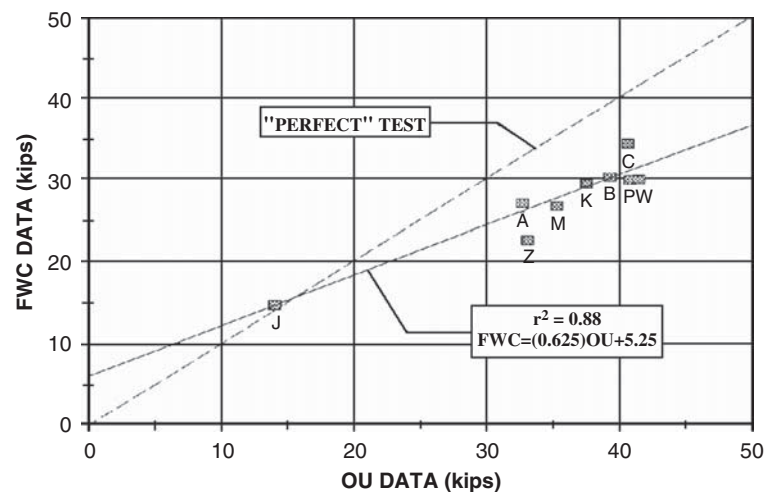


Figure 2.2. Comparison of Moustafa pull-out values from FWC and OU.

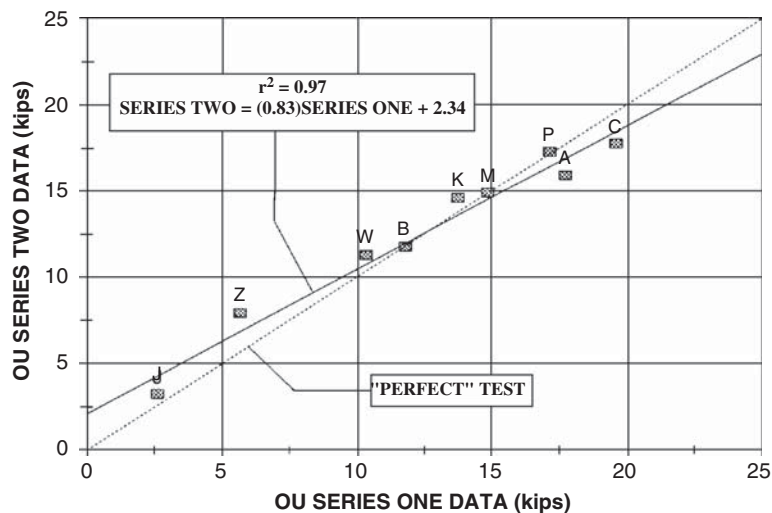


Figure 2.3. Comparison of NASP Bond Test results at OU in separate test series.

can be seen in the figures. The test has received unanimous endorsement by the NASP as its testing standard.

2.2.1.1 Effects of Strand Spacing

Historically, AASHTO limited the strand clear spacing to a minimum of three times the strand diameter ($3d_b$). In bridge codes prior to the *AASHTO LRFD Bridge Design Specifications*, this provision was made an explicit part of the design code. It is likely that this code provision mirrored the standard of placing 0.5-in. strands at 2.0 in. c/c . If this provision were extended to the larger diameter 0.6-in. strands, then the 0.6-in. strands would have to be placed at 2.4 in. c/c . Nevertheless, using this strand spacing would cancel out the economic value inherent in the use of 0.6-in. strand and would

also cancel out the most compelling reasons to use high-strength concrete in pretensioned girder applications. Russell (1994) showed that 0.6-in. strands must be placed at a spacing of about 2.0 in. c/c to enable designs to take advantage of high-strength concrete.

The Auburn report (Cousins et al. 1993) was one of the more recent works dedicated to investigating the effects of strand spacing on transfer and development lengths of pretensioned strands. In the Auburn study, 0.5-in. pretensioned strands were fully stressed and placed at 1.75 in. c/c in some beams and 2.0 in. c/c in others. The research demonstrated that there was no substantive difference in transfer lengths measured on beams. For beams with strands spaced at 2.0 in. c/c , the measured transfer lengths averaged 44 in. For beams with strands spaced at 1.75 in. c/c , the measured transfer

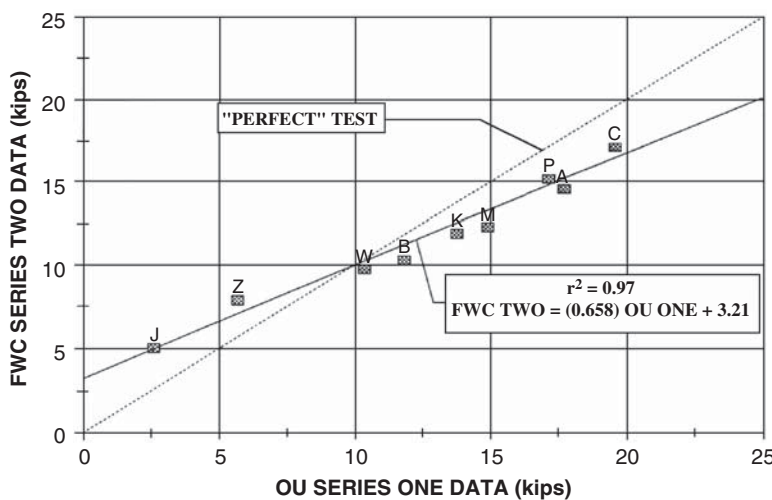


Figure 2.4. Comparison of NASP Bond Test results at two different test sites.

lengths averaged 47 in. The researchers concluded that the strand spacing had no effect on the measured transfer lengths.

In the same study, beams were also tested for strand development. As with the transfer length measurements, the data demonstrated that beams performed similarly regardless of whether strands were spaced at 1.75 in. or 2.0 in. *c/c*. The researchers concluded that spacing 0.5-in. strand at 1.75 in. *c/c* did not adversely affect transfer or development length of the strands. The researchers also concluded that the research results could be extended to the use of 0.6-in. strands at 2.0 in. *c/c*.

From their research, Cousins et al. (1993) drew two conclusions. First, “decreasing the strand spacing in pretensioned, prestressed members from 2.0 inches to 1.75 inches has no significant effect on transfer length and does not result in splitting of members at transfer of prestressing force.” Second, “decreasing the strand spacing in pretensioned, prestressed members from 2.0 inches to 1.75 inches has no significant effect on development length or nominal moment capacity.” With regard to 0.6-in. strand, Cousins et al. (1993) make the following statement, “. . . for the results reported herein for specimens prestressed with 0.5 inch diameter strand, the use of 0.6 inch diameter strand at a spacing of 2.0 inches does appear reasonable.”

Deatherage, Burdette, and Chew (1994) also reported on research performed to determine the effect that strand spacing had on transfer and development lengths. In their study, 0.5 in. diameter strand was placed in pretensioned beams with 1.75-in. and 2.0-in. spacing. Also, strands of three different diameters (0.5 in., 0.525 in., and 9/16 in.) were placed in beams with 2.0-in. spacing. In their studies, Deatherage, Burdette, and Chew (1994) concluded that a *c/c* spacing of 1.75 in. should be permitted for 0.5 in. diameter strands. Also, the researchers stated that their data indicated that the bond strength of pretensioned strand was roughly proportional to its strand diameter, indicating that strand spacing did not influence the bond characteristics of strand appreciably. Accordingly, the authors recommended that the spacing requirements for 0.5-in. strand be reduced from 4.0 strand diameters to 3.5 diameters. If this principle is applied to 0.6-in. strands, the authors would effectively recommend a 2.1-in. spacing for 0.6 in. diameter strands.

2.2.1.2 Strand from Different Manufacturers

Deatherage, Burdette, and Chew (1994) included 0.5 in. diameter strands from various manufacturers. The researchers provide strand transfer and development length test data, but provide little comment on differences between manufacturers. The data indicate that differences in measured transfer lengths exist among strands made by different manufacturers. In the Deatherage, Burdette, and Chew study (1994), the 0.5-in. strand provided by FWC (as designated in their arti-

cle) had transfer lengths that varied between 18 and 36 in. Other strand manufacturers provided strand that varied between 18 in. and 21 in. In NASP Round II testing, nine different strand samples were tested. The NASP Bond Test demonstrated significant and measurable differences between strands. In the NASP Round III testing, 10 different strand samples were tested. In these tests, the differences in pull-out test results were demonstrated to correlate directly with strand transfer and development lengths.

2.2.1.3 Influence of Concrete Strength

Cousins et al. (1993) also tested for transfer and development lengths in two different strength classes of concrete. The normal-strength concrete mixture resulted in concrete strengths between 6,000 and 8,000 psi. The high-strength concrete mixture resulted in concrete strengths between 10,000 and 12,000 psi. Transfer lengths measured in the high-strength concrete were, on average, 37 in.; the transfer lengths measured in the normal-strength concrete were, on average, 51 in. The higher concrete strength resulted in transfer lengths that were about 25 percent shorter. The researchers concluded that “increasing the concrete strength . . . reduces the transfer length and development length.”

Two other significant research programs examined the effects of concrete strength on transfer and development length. The first, undertaken by Zia and Moustafa (1977), recommended code expressions for transfer and development length that included the concrete strength parameter. Nearly 20 years later, Abrishami and Mitchell (1993) also performed transfer and development length tests. They also recommended that concrete strength be incorporated into the code provisions. However, as noted above, the lack of data that are consistent from one research program to another has prevented the development of a consensus for code expressions related to transfer and development length of pretensioned strands.

2.2.1.4 Tests of Strands Pretensioned in High-Performance Concrete

In the 1990s, several research programs were undertaken by various states to design and build bridges using high-performance concrete (HPC). Most, if not all, of these projects incorporated high-strength concrete as part of the HPC. In several of the projects, strand transfer length was measured, and development length tests were conducted to ensure adequate bonding properties from the pretensioned strands and to add to the body of knowledge regarding the transfer and development of pretensioned strands in high-strength concrete.

Perhaps the first of these tests was performed in Texas by Gross and Burns (1995). In this research, two rectangular

beams, 42 in. deep, were fabricated. Each beam employed pretensioned 0.6 in. diameter strands with 2.0 in. spacing. Transfer lengths were measured and development length tested at each of the four ends. Concrete strengths were 7,040 psi at release and 13,160 psi at the time of development length testing.

From the four beam ends, an average transfer length of 14.3 in. was measured. This value is significantly less than the current transfer length provision of $60 d_b$ found in the *AASHTO LRFD Bridge Design Specifications*. Similarly, the development length for these 0.6-in. strands was found to be less than 78 in., which roughly corresponds to the development length given by current AASHTO provisions. The history of these beams is also interesting. They were dubbed the “Hoblitzell-Buckner” beams. Hoblitzell was employed by FHWA and was instrumental in developing the federal programs encouraging the use of HPC. Buckner authored a report for FHWA titled, *An Analysis of Transfer and Development Lengths for Pretensioned Concrete Structures* (Buckner 1994). Buckner reviewed transfer length and development length data prior to 1992/1993 and developed some design recommendations based on that earlier data. In his report, Buckner recommended that the design provision for transfer lengths be changed to reflect the stress in the pretensioned strand prior to release (f_{pi}) as opposed to using the “effective prestress” after all losses, which is still found in the 318-02 Code (ACI 2002). Effectively, Buckner’s recommendation would have increased the requirement for transfer length by about 25 percent.

More interesting was Buckner’s design equation for development length. In reviewing the data, Buckner concluded that the strain experienced by the prestressing steel at flexural strength level was an important component in the development of strand. His design equation required the design engineer to increase development length requirements as the steel strain at flexural strength level increased. The Hoblitzell-Buckner beams were designed, therefore, to develop extremely large strains in the prestressing steel at flexural strength and test Buckner’s proposal. In the subsequent development length tests reported by Gross and Burns (1995), the strands were able to achieve their ultimate tensile capacity, undergo very large elongation strains, and adequately develop their tension capacities within the current AASHTO design provision. The results of these tests suggested that strand strain did not play an important role in strand development, and therefore it would not be necessary to recommend that the *AASHTO LRFD Bridge Design Specifications* should contain a development length provision based on predicted strand strain at flexural strength levels.

The state of Colorado sponsored a research program specifically designed to assess the transfer length and development length of 0.6-in. strands pretensioned in HPC box beams (Cooke, Shing, and Frangopol 1998). In these beams, 0.6-in. strands were spaced at 2 in. *c/c*. The average measured

transfer length was 23.4 in. The concrete strength at release was 7,800 psi.

The box beams were also tested for development length. Concrete strength at the time of development length testing was 11,000 psi. For embedment lengths in excess of 60 in., the strands demonstrated the ability to develop adequate tension force to support the flexural capacity of the beams. Subsequent failures were labeled as flexural failures. However, when the strand embedment length was set at 60 in. and 59 in., web shear cracking formed in the webs of the box beams, and strand anchorage failures ensued. The researchers reported that the development length for the strand was 60 in.

Additionally, several research projects were undertaken in the 1990s in part to investigate the transfer and development length of 0.6-in. strands. Uniformly, these projects featured pretensioned 0.6 in. diameter strands and spaced at 2 in. *c/c*. The projects were sponsored by Texas (Barnes and Burns 2000), Virginia (Roberts-Wollmann et al. 2000; Ozyildirim and Gomez 1999), and Georgia (Khan, Dill, and Reutlinger 2002). Uniformly, these researchers concluded that 0.6 in. diameter strands could be deployed safely using 2-in. spacing.

The state of Virginia has also supported transfer length testing of 0.6 in. diameter strands in HPC. Results reported by Ozyildirim and Gomez (1999) and Roberts-Wollmann et al. (2000) indicate that transfer lengths measured in HPC were substantially less than the transfer length predicted by the current code expressions.

Barnes and Burns (2000) reported on transfer lengths that were measured on 36 AASHTO Type I beams pretensioned with 0.6-in. strands. Strand spacing was 2 in. *c/c*. Concrete compressive strengths at release ranged from 3,950 to 11,000 psi. Altogether, transfer lengths from 192 independent measurements are discussed, and the report includes data on strands that are fully bonded to the ends of the member and strands that are shielded, or debonded, at the ends of the member. The results of the Barnes and Burns study (2000) indicate a definite trend in which transfer lengths tend to decrease in inverse proportion to the square root of the concrete strength at release. A “best fit” line reported by the authors includes the square root of the concrete strength at release in the denominator. This relationship is shown in Figure 2.5. However, the data demonstrate wide variation, and the statistical correlation is relatively weak. Nonetheless, it appears that concrete strength is an important factor that may affect the bond of pretensioned strand.

Barnes and Burns (2000) also reported results on transfer lengths of strand from various strand manufacturers. Their results are illustrated in Figure 2.6. The data illustrated in Figure 2.6 demonstrate that wide variations in measured transfer length may be the result of differences among strand manufacturers. This finding highlights the need to establish an industry standard for the “bond-ability” of prestressing strand.

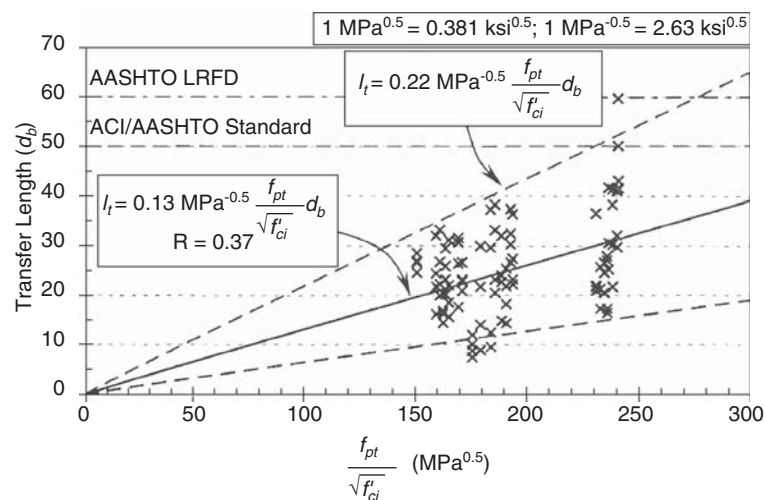


Figure 2.5. Data comparing transfer lengths to concrete strength at release (Barnes and Burns 2000).

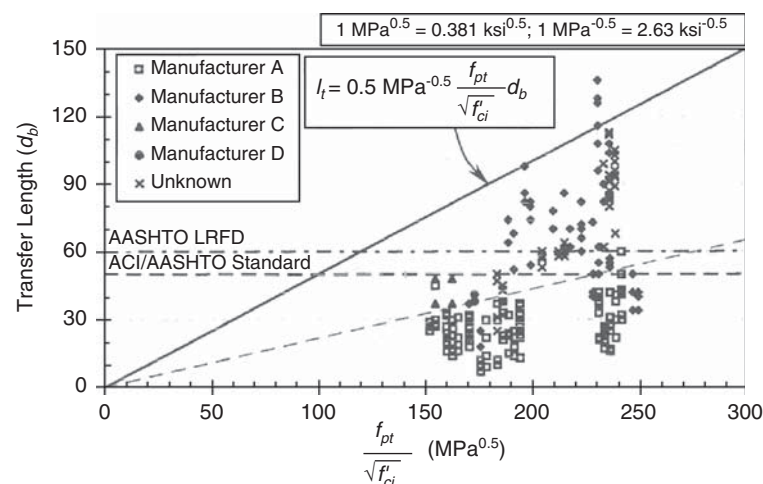


Figure 2.6. Data highlighting differences among strand manufacturers (Barnes and Burns 2000).

In addition to the research projects explicitly discussed herein, there have been other projects across the United States that have incorporated the use of 0.6 in. diameter strands and spaced at 2.0 in. *c/c*. Many of those projects have measured transfer lengths. One of the projects was performed by Kahn, Dill, and Reutlinger (2002). In some cases, the research reports are still in a preliminary format and use of the data is being reserved by the authors and the research sponsors. However, it is safe to say that, uniformly, these projects are employing 0.6 in. diameter strands at 2.0-in. spacing without adverse effects.

2.2.1.5 Effects of Air Entrainment

There is no evidence that a systematic testing program examining the effects of air entrainment on the transfer and development of prestressing strands exists. There is a need to

examine the effects of air entrainment on pretensioned bond. The research reported herein incorporates the use of air entrainment; however, it should be noted that air entrainment is not usually specified in combination with high-strength concrete/HPC because air entrainment directly causes a decline in concrete strengths.

2.2.1.6 Water Reducers and High Range Water Reducers

There is no evidence of a systematic testing program examining the effects of water reducers (WRs) or high range water reducers (HRWRs) on the transfer and development of prestressing strands. Since WRs and HRWRs are used in more than 95 percent of the pretensioned prestressing plants throughout North America, this is an important variable that warrants investigation.

2.2.2 Development and Splice Length for Mild Reinforcement

To identify needed experimental research, the literature review focused on the analysis of test results from bond tests on development and splice length in tension of coated and uncoated bars and development length of coated and uncoated bars terminated with standard hooks in tension. Based on the reported bond performance of individual and bundled bars in compression, it was determined that no additional experimental work was required in this area. Compression development lengths are considerably shorter than tension development lengths because there are no transverse cracks in compression zones; the harmful effect of such cracks in initiating splitting is absent. However, the major difference between tension and compression development and splice lengths is the ability of the bars in compression to transfer load to the concrete directly by bearing. In tests conducted by Pfister and Mattock (1963), bearing stresses equal to five times the cylinder strength of the concrete were attained at the square-cut ends of bars in compression splices. Additional experimental work conducted at the Otto-Graf-Institute of the University of Stuttgart by Leonhardt and Teichen (1972) conclusively showed the following:

- End bearing is responsible for the majority of splice failures in compression irrespective of the splice length tested. The splice lengths varied between 9 and 38 bar diameters.
- The bearing capacity of the concrete at the bearing ends of the bars was increased by the presence of confining reinforcement. Under such conditions, concrete bearing stresses of 17 ksi were measured (for concrete with a uniaxial compressive strength around 4 ksi).
- An increase in the thickness of the concrete cover over the compression splice resulted only in very minor improvements in bond performance.
- Under long-term loading, the bearing pressure under the ends of the compression bars diminishes because of creep; hence, the splice performance improves.

The available information on the anchorage in tension of welded wire reinforcement indicated that a significant experimental effort was not required as part of NCHRP Project 12-60 (Furlong, Fenves, and Kasl 1991; Griezic, Cook, and Mitchell 1994; and Guimaraes, Kreger, and Jirsa 1992). In the case of plain wire fabric, the development in tension depends on the mechanical anchorage from at least two cross wires. Deformed welded wire reinforcement derives anchorage from bond stresses along the deformed wires and from mechanical anchorage from the cross wires. Current code expressions for development length in tension of deformed welded wire reinforcement assume that at least one cross wire

is present in the development length. Tests have also shown that the development length of deformed welded wire reinforcement is not affected by epoxy coating, and thus the epoxy coating factor in the current ACI Code is 1.0 for epoxy-coated deformed wire fabric. In recent years, welded wire fabric (WWF) has been used widely as shear reinforcement in thin-webbed girders because of the ease of construction over the use of conventional stirrups. Research conducted to date, with concrete compressive strengths up to 12 ksi, indicates that this reinforcement can be used effectively to resist shear (Mansur, Lee, and Lee 1987; Xuan, Rizkalla, and Maruyama 1988; Pincheira, Rizkalla, and Attiogbe 1989; and Zhongguo, Tadros, and Baishya 2000). It was shown that two cross wires welded at a spacing of 2 in. at the open ends (top and bottom) of WWF cages provide satisfactory anchorage. Such anchorage was found to be more effective for deformed WWF than smooth WWF. The increase in concrete compressive strength has been shown to further improve the anchorage of this reinforcement.

2.2.2.1 Databases

There are two databases. One consists of 71 tension development and splice tests of specimens with top cast uncoated reinforcing bars, 493 specimens with bottom cast uncoated reinforcing bars, 27 specimens with top cast epoxy-coated bars, and 48 specimens with bottom cast epoxy-coated bars, for a total of 639 specimens. The other database consists of 33 specimens with uncoated bars terminated with standard hooks and 13 specimens with epoxy-coated bars, for a total of 46 specimens.

The provisions for development length of reinforcement in Section 5 of the *AASHTO LRFD Bridge Design Specifications* are based on the provisions of ACI 318-89 (ACI 1989). The 1989 provisions in the ACI Code were extensively modified in the 1995 version of the ACI Code (ACI 1995) with a view to formulating a more “user-friendly” format while maintaining the same general agreement with professional judgment and research results. Tests conducted by Azizinamini et al. (1993, 1999a) have indicated that in the case of high-strength concrete, some minimum amount of transverse reinforcement is needed to ensure adequate ductility from the splice at failure. A proposed modification to ACI 318-99 (ACI 1999), based on these tests, called for the determination of a basic straight development length for bars in tension without including the presence of transverse reinforcement, together with a minimum area of transverse steel in the form of stirrups, A_{sp} , crossing potential splitting planes. In these studies, over 70 specimens with concrete compressive strengths ranging between 5 ksi and 16 ksi were tested (Azizinamini et al. 1993, 1999a).

Although the modification proposed in another paper by Azizinamini and colleagues (1999b) was not adopted in the 2002 version of the 318 Code (ACI 2002), it was deemed an improvement over the current AASHTO LRFD provisions. Therefore, the 2005 318 Code (ACI 2005) provisions were used in NCHRP Project 12-60 as the basis for further extension of the AASHTO provisions to higher strength concrete. The experimental work conducted in the mild steel phase of NCHRP Project 12-60 was focused on filling the gaps identified in order to extend the applicability of the present AASHTO LRFD *Bridge Design Specifications* to normal-weight concrete with compressive strengths up to 15 ksi.

The 639-specimen database is shown in Figures 2.7 through 2.10 by plotting the bond strength, u_{test} , versus the concrete compressive strength, f'_c . The bond strength is defined as

$$u_{\text{test}} = \frac{A_b f_{su}}{\pi d_b l_s} \quad (2.1)$$

In Equation 2.1, A_b is the area of bar being developed or spliced, f_{su} is the stress in the bar estimated at failure using moment-curvature type analysis and compatibility of deformations, d_b is the diameter of the bar, and l_s is anchorage/splice length. As can be seen from Figures 2.7 and 2.8, there is a lack of data for development and splice lengths of uncoated bars in tension above 16 ksi. Figures 2.9 and 2.10 show that there are limited data for epoxy-coated bars in tension

above 8 ksi. In order to assess whether the limit on f'_c can be removed by examining the existing data for development and splice length of uncoated and epoxy-coated bars in tension, the ratio of test to calculated bond strength is plotted versus the concrete compressive strength (f'_c) evaluated throughout the range of concrete cylinder strengths. The bond strength ratio is determined in terms of bar stresses at failure versus calculated bar stress, using Equations 2.2 through 2.5:

$$\frac{l_s}{d_b} = \frac{3}{40} \frac{f_s}{\sqrt{f'_c} \left(\frac{c + K_{tr}}{d_b} \right)} \quad (2.2)$$

$$c = (c_{\min} + 0.5 * d_b) \quad (2.3)$$

$$K_{tr} = \frac{A_{tr} * f_{yt}}{1500 * s * n} \quad (2.4)$$

To limit the probability of a pull-out failure, 318 Code (ACI 2005) requires that

$$\frac{c + K_{tr}}{d_b} \leq 2.5 \quad (2.5)$$

The additional parameters in the equations are the following: f_s is the stress in the reinforcing bar; c_{\min} is the smaller of minimum cover or one-half of the clear spacing between bars; A_{tr} represents the area of each stirrup or tie crossing the potential plane of splitting adjacent to the reinforcement

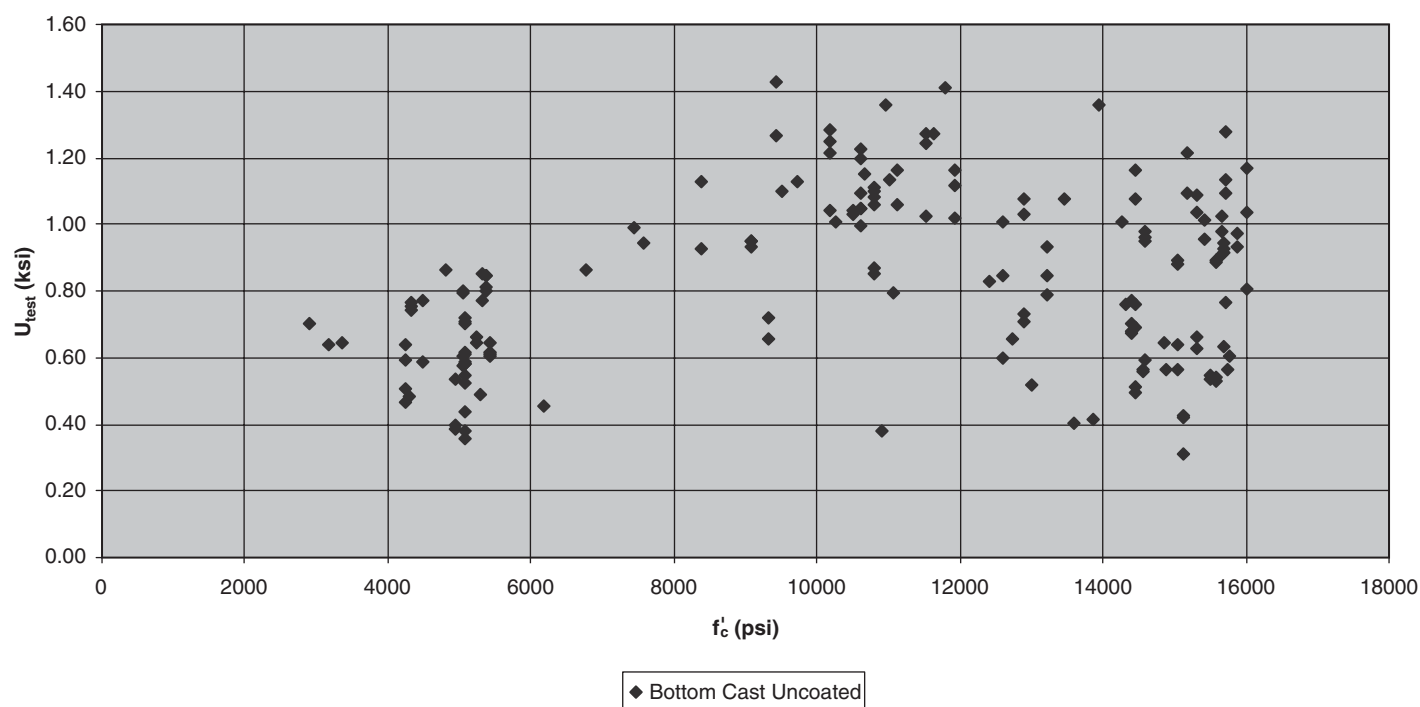


Figure 2.7. Bond stress at failure (u_{test}) versus the concrete compressive strength ($\sqrt{f'_c}$) of bottom cast uncoated specimens.

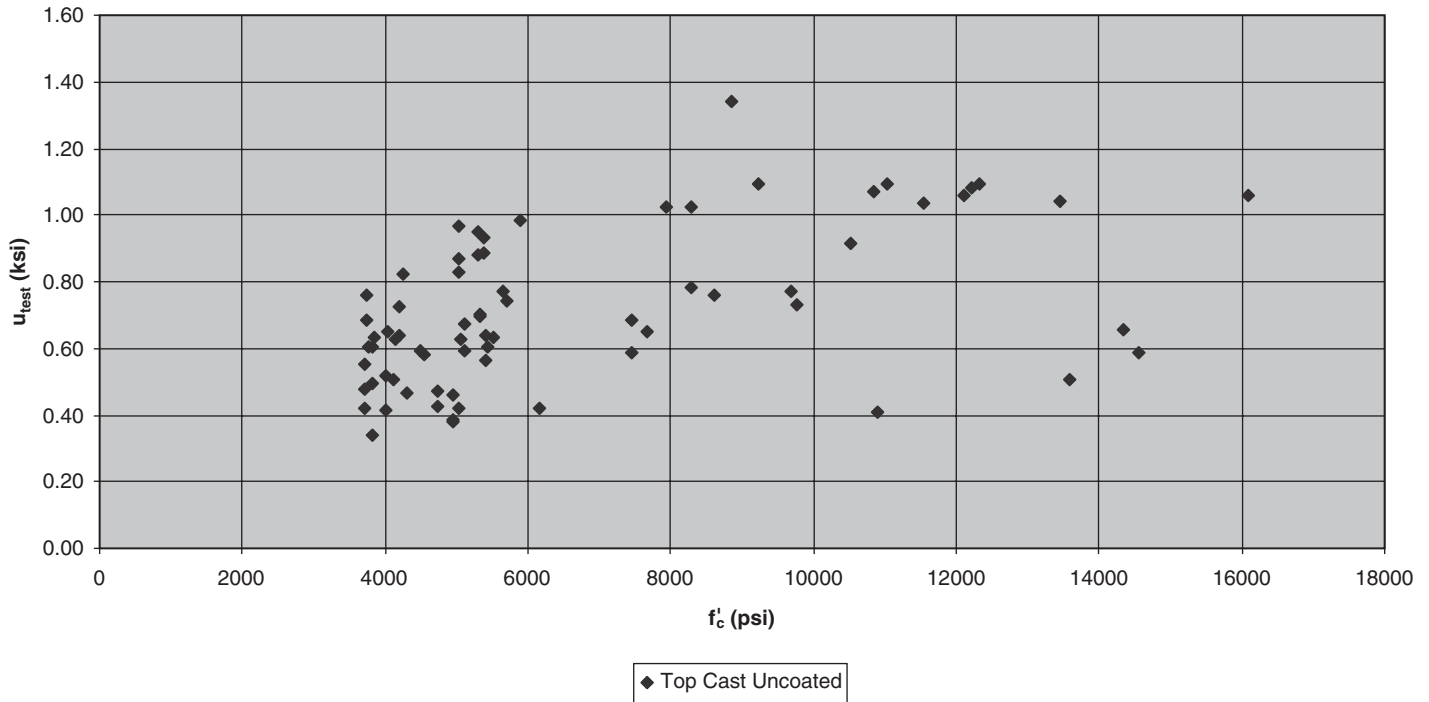


Figure 2.8. Bond stress at failure (u_{test}) versus the concrete compressive strength ($\sqrt{f'_c}$) of top cast uncoated specimens.

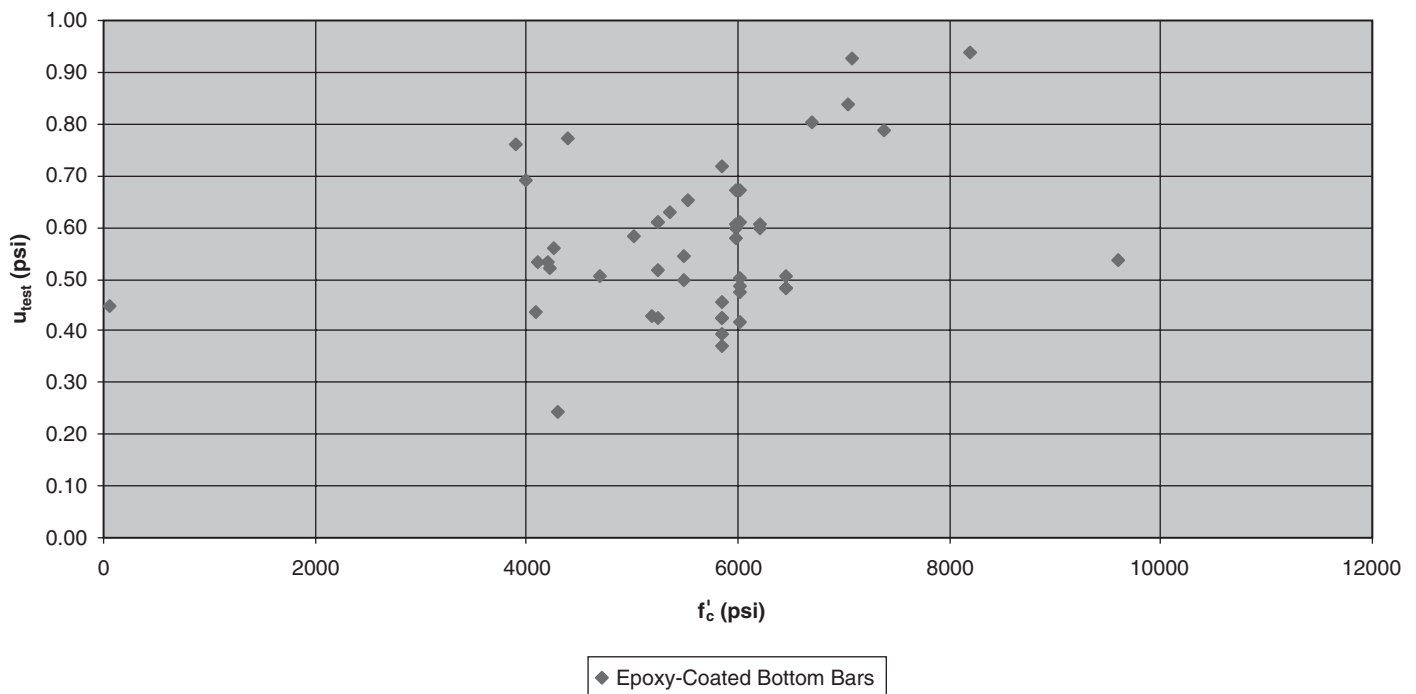


Figure 2.9. Bond stress at failure (u_{test}) versus the concrete compressive strength ($\sqrt{f'_c}$) of bottom cast epoxy-coated specimens.

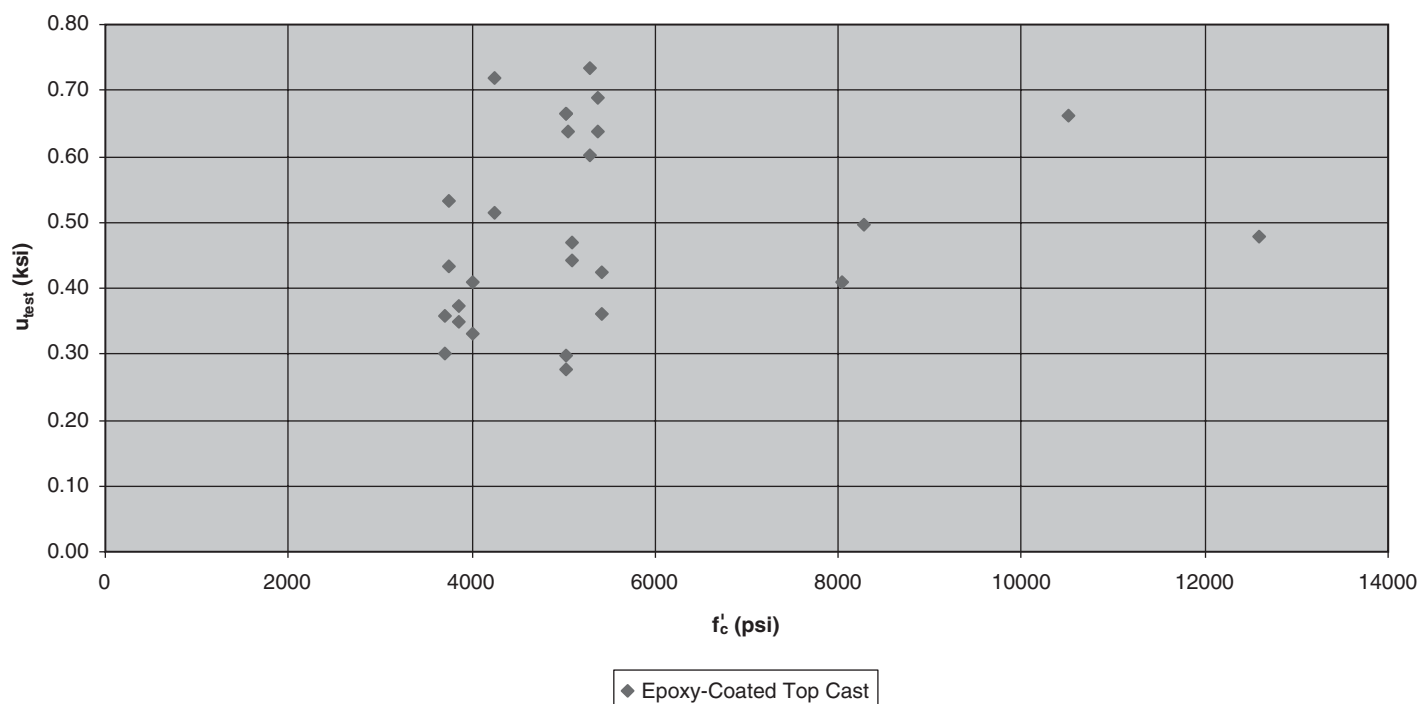


Figure 2.10. Bond stress at failure (u_{test}) versus the concrete compressive strength ($\sqrt{f'_c}$) of top cast epoxy-coated specimens.

being developed, spliced, or anchored; f_{yt} is the yield strength of the stirrup reinforcement; s is the spacing of stirrups; and n is the number of bars being developed or spliced. The results of the evaluation indicated that the average of the ratio for bars not confined by stirrups is 1.23 with a standard deviation of 0.28 for all f'_c values, and 1.23 with a standard deviation of 0.23 for concrete compressive strengths below 10 ksi. In the case of bars confined by stirrups, the average is 1.23, and the standard deviation is 0.3 for all f'_c values. For f'_c values below 10 ksi, the average is 1.24 and the standard deviation is 0.30. In members with confined bars, the stirrups are assumed to be uniformly spaced throughout the splice/development length. The value for the members in the database, calculated by the ACI provisions, gives approximately the same scatter throughout the range of concrete compressive strengths up to a maximum of 16 ksi for members with and without stirrups. This conclusion supports the extension of these provisions to higher concrete compressive strengths with a few verification tests of uncoated bars at the upper limit, mainly to establish the role of the minimum amount of transverse reinforcement on the mode of failure of splices in tension recommended in the Azizinamini et al. studies (1993, 1999a). On the other hand, it is recognized that there is a paucity of data on the performance of epoxy-coated bars in concretes with compressive strengths above 10 ksi. Therefore, a more intense verification testing effort was carried out in this study to close this gap.

Tests have shown that the bar force is transferred rapidly into the concrete, and the portion following a hook is generally ineffective and can potentially be limited by the tensile strength of the concrete. Marques and Jirsa (1975) reported on the results of 22 tests conducted using two #7 or two #11 uncoated bars. Standard 90- or 180-deg hooks conforming to the 318 Code were used (ACI 2005). The concrete compressive strength was around 5 ksi. The specimens simulated exterior beam column joints. Hamad, Jirsa, and D'Abreu de Paulo (1993) reported on the results of 24 tests to evaluate the anchorage performance of epoxy-coated hooked bars. Based on these results, a 20-percent increase on the basic development length was recommended for epoxy-coated hooked bars. It was shown that the relative anchorage strength of uncoated and epoxy-coated hooked bars was independent of bar size, concrete strength, side concrete cover, or hook geometry. The maximum concrete strength of the specimens was 7 ksi. These tests serve as the basis of the 318 Code anchorage provisions for bars anchored by means of standard hooks (ACI 2005). The specimen and the test setup used in NCHRP Project 12-60 was similar to the one used in the Marques and Jirsa (1975) and Hamad, Jirsa, and D'Abreu de Paulo (1993) studies. However, only 90-deg hooks were evaluated, since Hamad, Jirsa, and D'Abreu de Paulo found little difference in the performance of 90- and 180-deg hooks. It should be noted that sections of the *AASHTO LRFD Bridge Design Specifications* dealing with the anchorage of bars in tension

terminated with a standard hook are similar to those in the 2005 version of the ACI Code.

2.3 Identification of Issues and Needs

The work described in the previous section was used to assemble a comprehensive list of issues pertaining to transfer length, development length, and splice length of strand/reinforcement to normal-weight concrete with compressive strengths in excess of 10 ksi and up to 15 ksi. In this section, a discussion of the main issues related to bond performance of reinforcement is presented, and gaps found in the existing database are addressed. The experimental program described in Chapter 3 of this report was directed at addressing the identified needs in order to extend the *AASHTO LFRD Bridge Design Specifications* to allow greater use of high-strength concrete.

In reinforced and prestressed concrete structures, sufficient transfer of forces between concrete and reinforcement is required for a satisfactory design. The transfer of forces occurs through a combination of chemical surface adhesion, friction, and bearing of bar deformations against the surrounding concrete. Initially, the transfer of forces occurs mainly by chemical adhesion; after initial slip, most of the force is transferred by bearing and friction. In the case of plain bars or wires, slip-induced friction—resulting from shape and surface roughness—plays an important role in the force transfer. In the case of deformed reinforcement, as slip increases, bearing of the ribs against the surrounding concrete becomes the principal mechanism of force transfer between concrete and steel. The forces on the bar surface are balanced by compressive and shearing stresses in the concrete (see Figure 2.11). The concrete stresses result in tensile stresses that, if high enough, can lead to cracking in planes both parallel and perpendicular to the reinforcement, as shown in Figure 2.12. These transverse cracks can lead to splitting failure.

If the concrete cover, bar spacing, or amount of transverse reinforcement is sufficient to prevent or delay the splitting failure, then failure can occur along a surface surrounding the

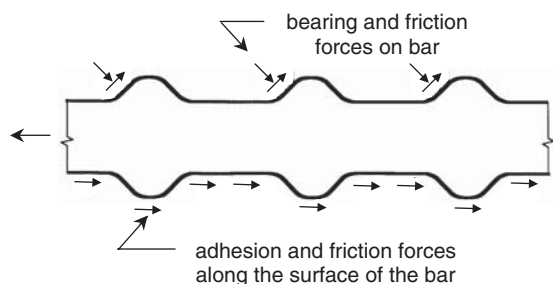


Figure 2.11. Mechanisms of force transfer between concrete and reinforcement-deformed bars.

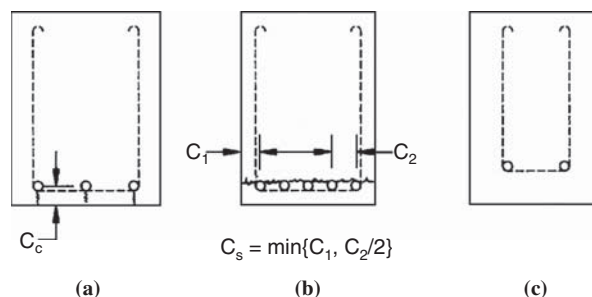


Figure 2.12. Anchorage failure modes: (a) vertical splitting, (b) splitting in the horizontal plane of the bars, and (c) pull-out without splitting (ACI 408 2003).

perimeter of the bar, resulting in a pull-out type failure. Tests have shown that these two types of failures can take place at stresses close to the tensile strength of the reinforcement. Pull-out failures occur in cases of high confinement and low bonded lengths. However, splitting failures are more common in structural applications. For this reason, it is recommended that experimental data considered for development of design equations should have a minimum embedment length. Another important observation is that transverse reinforcement has been observed to rarely yield during splitting failures (Maeda, Otani, and Aoyama 1991; Sakaruda, Morohashi, and Tanaka 1993; and Azizinamini et al. 1999a). Therefore, it is important to limit in design provisions the level of confinement provided by transverse reinforcement. The many factors affecting bond performance are presented in two main categories: member properties and material properties. Some of the factors are common to both strand and mild reinforcement while others are unique to one or the other.

Initially, in the testing of prestressing strand for bond to concrete, the simple pull-out tests were criticized because they did not include the wedging action, or Hoyer's effect, associated with pretensioned strands in real beams. However, subsequent testing with both the Moustafa Test and the NASP Bond Test have demonstrated that a direct correlation exists between results from these simple pull-out tests and strand performance in pretensioned beams. Therefore, in this testing program the NASP Bond Test was employed as an assessment tool to quantify the "bond-ability" of prestressing strands that will be employed. Testing sponsored by the NASP has demonstrated that the NASP Bond Test has superior repeatability and reproducibility when compared with the Moustafa Test.

2.3.1 Member Properties

2.3.1.1 Transfer Length of Prestressing Strand

In the specific case where prestressing strands are bonded to concrete, bond stresses are derived through a combination of adhesion, friction, and mechanical interlocking (Hanson

and Kaar 1959). It has been widely believed that a wedging effect, called Hoyer's Effect, unique to pretensioned strands, creates significant bond stresses in the transfer zone where the effective prestressing force is transferred from the pretensioned strand to the concrete. In those same regions, slip occurs between strand and concrete due to the difference in strain condition. Research has indicated that the strand end slip can be used as a quality control measure for the bond of prestressing strands (Rose and Russell 1997). Furthermore, the relative slip between strand and concrete virtually ensures that adhesion plays little or no role in the transfer of prestressing forces to concrete (Russell and Burns 1996).

2.3.1.2 Development and Splice Length

Bond forces are not uniformly distributed over the length of anchorage (see Figure 2.13). Thus, bond failures are incremental, initiating in the region of highest bond force per unit of

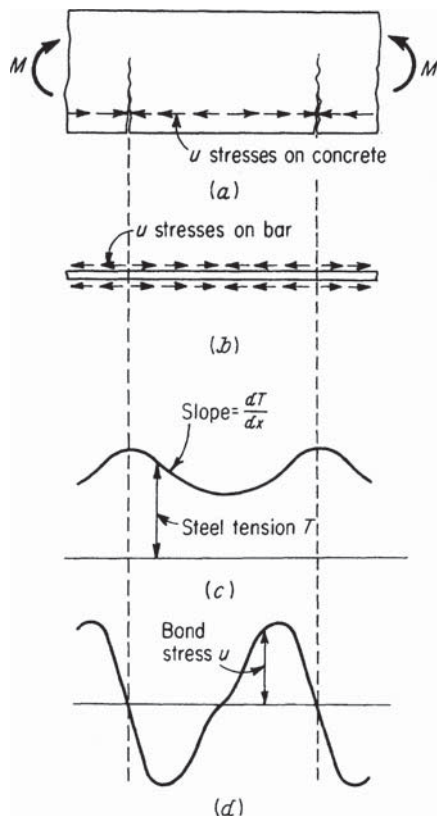


Figure 2.13. Variation of steel and bond forces in a reinforced concrete member subjected to pure bending: (a) cracked concrete region, (b) bond stresses acting on a reinforcing bar, (c) variation of tensile force in steel, and (d) variation of bond force along the bar (Nilson 1997).

length. In the case of anchored reinforcement by means of straight embedment, longitudinal splitting will initiate at either a free surface or at a flexural crack location. In the case of spliced bars, splitting will start at the ends of the splice and move toward the center. The mode of failure explains the fact that the non-loaded end of a developed/spliced bar is less effective than the loaded end in transferring forces between concrete and reinforcement. It can be concluded that there is a non-proportional relationship between development/splice length and bond strength. Thus, even though bond strengths have been measured for very short embedment lengths, it is not appropriate to linearly extrapolate such findings to code development lengths. This observation suggests the need for testing at appropriate scale for development of design provisions.

In beams tested for strand development, it is equally apparent that cracking causes the mobilization of the strand relative to concrete. Commonly, bond stresses that develop strand tension from the transfer zone to the point where flexural capacity is required are called "flexural bond stresses." Flexural bond results primarily from a combination of mechanical interlocking and friction. The mechanical interlocking bond stresses are derived by the helical windings of the 7-wire prestressing strand, which act similarly to the mechanical deformations found on rolled, mild reinforcement.

Development length testing of pretensioned beams indicates that splitting occurs less frequently than in conventionally reinforced beams (although splitting cracks have been observed in pretensioned bond failures). Issues for strand development are more related to the cracking patterns that occur as the pretensioned beams approach their ultimate strength. In testing on beams with debonded strands, it is clear that cracks that propagate through or near the transfer zone of pretensioned strands cause strands to slip. In many of those tests, cracking in the transfer zones of pretensioned strands caused bond failure of pretensioned strands (Russell, Burns, and ZumBrunnen 1994; Russell and Burns 1994).

Additionally, in pretensioned strands with fully bonded beams, it is important to note that sections with narrow webs, specifically I-shaped beams, have failed in bond in concert with web shear cracking that occurs near or through the transfer zones of pretensioned strands (Jacob 1998; Kaufman and Ramirez 1988; Russell and Burns 1993). In contrast, tests on rectangular prestressed beams will not produce web shear cracks, so the behavior of rectangular cross sections can be significantly different than cross sections with narrow webs. For that reason, the testing program includes testing of both rectangular and I-shaped sections.

2.3.1.3 Transverse Reinforcement

Orangun, Jirsa, and Breen (1977) indicated that transverse reinforcement confines the concrete around anchored bars

and limits the progression of splitting cracks. An additional beneficial effect of transverse reinforcement is that increases in transverse reinforcement lead eventually to pull-out failures rather than splitting-type failures. However, the Orangun, Jirsa, and Breen study also noted that transverse reinforcement in excess of the amount required to cause the change in mode of failure is not as effective and eventually leads to no further increase in bond strength. These observations and the observations by Maeda, Otani, and Aoyama 1991; Sakaruda, Morohashi, and Tanaka 1993; and Azizinamini et al. 1995 that the transverse reinforcement confining the anchored bar seldom yields in splitting failure indicates the need for an upper limit on the improvement in bond strength provided by the presence of transverse reinforcement.

2.3.1.4 Casting Position

It has been observed by various researchers that top cast bars have lower bond strengths than bottom cast bars. Clark (1946), using pull-out type specimens cast in a horizontal position, noted that in the top position, bars were two-thirds as effective in bond as in the bottom position. The depth of the concrete under the bar in the top position was 15 in., and the depth of the concrete under the bar in the bottom position was 2 in. The concrete slump was 4.25 in., and the compressive strength averaged 5.6 ksi. Ferguson and Thompson (1965) noted that with 12 in. of concrete below the bar, the strength dropped from 3 to 13 percent as the slump was increased. They noted that for the beam depths tested, from 13 to 22 in., the 1.4 factor used in the specifications was conservative. This observation is currently recognized in the 318 Code where a 1.3 factor is used to increase the development length or splice of bars cast horizontally with more than 12 in. of fresh concrete cast in the member below the bar (ACI 2005). A 1.4 factor is currently prescribed in the *AASHTO LRFD Bridge Design Specifications* to cover this case, and it is thus conservative if the effects of cover and transverse reinforcement are included in the specifications.

Additional research (Jirsa and Breen 1981) indicates that the concrete slump plays an important role in determining the effects of casting position, and this is most significant when very large depths of concrete are cast below the bars or splices. The 1981 study by Jirsa and Breen further indicated that the so-called top bar factor should vary with the depth of concrete cast below the reinforcement and recommended a maximum factor of 1.3 for slumps of less than 4 in. For slumps between 4 and 6 in., a maximum factor of 1.35 is recommended for depths below 24 in., and a maximum factor of up to 1.6 is recommended for depths greater than 48 in. For slumps greater than 6 in., a factor of 1.8 for depths below 24 in. is recommended, and a factor of 2.2 for depths below 48 in. is recommended. It is further stated that the basic bond

strength of vertical bars seems to be reduced only by 25 percent with respect to the bond strength of horizontal bars. A single factor of 1.3 is recommended for all vertical bars where the center of the splice or the development length has more than 24 in. of concrete cast below.

2.3.1.5 Concrete Cover and Spacing of Reinforcement

As shown in Figure 2.12, splitting failure is expected to control in the majority of structural applications. In this type of failure, the actual location of the splitting cracks in the case of bottom cast reinforcement depends on the relative values of the concrete bottom cover, concrete side cover, and one-half of the clear spacing between bars. If the bottom cover is less than the side cover and one-half the spacing between bars, splitting occurs through the cover to the bottom free surface. If either the side cover or one-half the bar spacing is smaller than the bottom cover, then splitting of the concrete occurs either through the side cover or between the reinforcement. This observation supports the need to modify the current *AASHTO LRFD Bridge Design Specifications* for bond and development length of mild reinforcement to incorporate the effects of cover, bar spacing, and transverse reinforcement.

2.3.2 Material Properties

2.3.2.1 Reinforcement Properties

For a given bonded length required to achieve a given steel stress level, reinforcement of different areas will achieve different levels of force at the onset of splitting failure, with the larger area reinforcement achieving higher forces. Therefore larger area reinforcement will require longer development/splice length than smaller area reinforcement for the same degree of confinement. The size of the reinforcement being developed also plays a role in the contribution of the confining reinforcement for the case of deformed bars. As large bars slip, higher strains are mobilized in the transverse reinforcement, thus the beneficial effect of transverse reinforcement on the bond strength of deformed bars increases as the area of the bar increases.

It is now customary to relate bond performance to bar geometry by means of the relative rib area factor, R_r , defined as:

$$R_r = \frac{\text{projected rib area normal to bar axis}}{(\text{nom. bar perimeter}) \times (\text{center-to-center rib spacing})} \quad (2.6)$$

Typical bars currently used in the United States have relative rib area factors ranging between 0.057 and 0.087 (Choi et al. 1990). Darwin and Graham (1993a, 1993b) concluded that the bond strength is independent of deformation pattern if the bar

is under small cover conditions and there is no transverse reinforcement. Darwin and Graham observed that under large cover or with transverse reinforcement, bond strength increased with an increase in relative rib area. They also found that deformations parallel to the splitting cracks were more effective.

The bond strength of epoxy-coated bars has been found to increase under all conditions of confinement as the relative rib area is increased. Zuo and Darwin (1998) recommended that for epoxy-coated bars with relative rib areas greater than or equal to 0.1 and concrete with compressive strength below 10 ksi, development and splice length should be increased by 20 percent instead of the 50-percent increase for cover less than $3d_b$ or clear spacing less than $6d_b$. For concrete strengths greater than 10 ksi, a 50-percent increase appeared warranted regardless of the value of R_r .

The surface condition is important from the standpoint of bond strength because it affects adhesion, friction, and bearing in the transfer of forces between steel and surrounding concrete. Items such as cleanliness, rust, and coatings affect the surface condition of the reinforcement. Specifications require that the reinforcement be free of mud and other substances capable of reducing bond strength. It is well established that the presence of epoxy coatings reduces the bond strength of reinforcement (Mathey and Clifton 1976; Johnston and Zia 1982; Treece and Jirsa 1989; Choi et al. 1990, 1991; Cleary and Ramirez 1993).

2.3.2.2 Concrete Properties

Compressive strength and lightweight aggregate are acknowledged in codes and specifications as influencing bond strength. In addition, tensile strength and fracture energy, mineral admixtures, and consolidation and vibration are also factors affecting bond strength of reinforcement.

Azizinamini et al. (1993, 1999a) noted that for higher strength concretes, the higher bearing capacity prevents crushing of the concrete in front of the ribs, thus reducing the local slip. These researchers further noted that the reduced slip also limited the number of ribs participating in the load transfer between concrete and reinforcement. The reduced participation of the ribs increases the local tension stresses and further leads to a non-uniform distribution of bond force. Although traditionally $\sqrt{f'_c}$ has been used to reflect the concrete compressive strength in bond calculations, Zuo and Darwin (1998, 2000) have postulated that $f'_c{}^{1/4}$ for members without stirrups and $f'_c{}^{3/4}$ for members with stirrups better reflect the effect of concrete strength on bond. These findings indicate that if bond strengths are normalized with respect to $f'_c{}^{1/2}$, the effect of concrete strength on the bond strength is severely overestimated. High-strength concrete has been shown to improve anchorage of prestressing strand, thus reducing the required transfer length and development length.

In unconfined bar bond tests, the use of basalt aggregates has been shown to increase bond strength by almost 13 percent over the bond strength of concretes with weaker aggregate such as limestone (Zuo and Darwin 1998, 2000). Tests on bars confined by transverse reinforcement (Darwin et al. 1996; Zuo and Darwin 1998) also indicate an increase in bond strength in the presence of stronger aggregates showing a significant effect on the contribution from the transverse reinforcement.

Lower strength aggregates, on the other hand, have a detrimental effect on the bond strength. Reports by ACI Committee 408 (1966, 1970) have emphasized the paucity of experimental data on the bond strength of reinforced concrete elements made with lightweight aggregate concrete. The *AASHTO LRFD Bridge Design Specifications* includes a factor of 1.3 for development length to reflect the lower tensile strength of lightweight aggregate concrete and allows that factor to be taken as $0.22 \sqrt{f'_c} / f_{ct} \geq 1.0$ if the average splitting strength, f_{ct} , of the lightweight aggregate concrete is specified. For lightweight sand, where f_{ct} is not specified, a factor of 1.2 is specified. Although design provisions, in general, require longer development lengths for lightweight aggregate concrete, test results from previous research are contradictory, in part, because of the different characteristics associated with the particular type of aggregate and mix design. The use of lightweight aggregate concrete is outside the scope of NCHRP Project 12-60.

It has been widely observed that as the concrete compressive strength increases, the bond strength of the same concrete also increases—albeit at a slower rate—leading to potentially more brittle failures (Azizinamini et al. 1993, 1999a). On the other hand, the tensile strength of the concrete is not the only factor controlling bond strength, as it has been noted by Zuo and Darwin (1998, 2000) for deformed bars. The Zuo and Darwin studies recommended the use of $f'_c{}^{1/4}$ instead of the traditional $f'_c{}^{1/2}$ to represent the effect of concrete compressive strength on bond strength for unconfined bars. They also noted that the presence of confinement influenced the power of the compressive strength and recommended the use of $f'_c{}^{3/4}$ as a good representation of the influence of compressive strength on bond strength.

Most of the work related to bond has focused on the effect of silica fume. The studies have shown increases of less than 10 percent on bond strength in the presence of the mineral admixture (DeVries, Moehle, and Hester 1991; Hamad and Itani 1998).

2.4 Issues Related to Testing Protocols

A review of testing protocols for determining bond characteristics was presented. From our review of available research, we recommended that the NASP Bond Test be employed

throughout the experimental program to quantify the bond characteristics of individual strand samples. The testing program includes “round robin” testing at both Purdue University and Oklahoma State University (OSU) to validate the repeatability of the test procedure. The NASP Bond Test procedure has been refined through this research and is now recommended for adoption into the AASHTO LRFD Bridge Code as the Standard Test Method for the Bond of Prestressing Strands. The testing protocols for splice/development lengths and bars terminated with standard hooks are also presented. The beam-splice test for splice/development length and the Marques and Jirsa (1975) and Hamad, Jirsa, and D’Abreu de Paulo (1993) exterior beam column joint setup for bars in tension anchored by means of standard hooks are recommended for use in this study.

2.4.1 Testing Protocols for Prestressing Strand

Since 1994, three new test procedures or protocols have been developed for assessing the bonding characteristics of prestressing strand: the Moustafa Bond Test, the Post-Tensioning Institute (PTI) Bond Test, and the NASP Bond Test. Testing has demonstrated that the NASP Bond Test delivers the greatest degree of repeatability and reproducibility of the three tests. Therefore, the testing program for NCHRP Project 12-60 employed the NASP Bond Test as the standard test to assess the relative “bond-ability” of prestressing strands. Previous experience with research on strand bond demonstrates the importance of quantifying the strand bonding properties prior to or concurrent with testing programs for transfer and development length of strands.

2.4.1.1 Prestressing Strand up to 0.6 in. in Diameter

Engineers and contractors concerned with the bond of prestressing strand used for rock anchors developed the PTI Bond Test. In conformance with standard practice for rock anchors, the test protocol indicates explicitly that testing should be conducted on 0.6-in. strand. The test protocol has been modified to accept 0.5-in. strand, but the acceptance value has not been adjusted or evaluated using 0.5-in. strand. Both the Moustafa Test and the NASP Bond Test were developed using 0.5-in. strand. In the experimental program, the NASP Bond Test was performed using 0.6-in. strand. The testing demonstrated that the Standard Test Method for the Bond of Prestressing Strands is suitable for 0.6-in. strands as well as 0.5-in. strands.

2.4.1.2 Influence of Concrete Strength

As noted in the literature review, concrete strength has long been described as an important variable affecting the

transfer and development of prestressing strands. Through the years, several researchers have included concrete strength as a variable in transfer and development length equations. However, the lack of consistency in the strand products themselves has worked against developing a consensus regarding the effect of concrete strength. By quantifying strand bond characteristics through the NASP Bond Test, this research has been able to assess the effects of concrete strength on transfer and development of pretensioned strands. Recommendations to include concrete strength in the design equations have been made.

2.4.1.3 Influence of Water-Reducing Admixtures

There is a lack of data available to assess what effect, if any, water-reducing admixtures have on the bond of pretensioned strands. This contrasts directly with the fact that more than 99 percent of the prestressing plants in North America use HRWRs (the source for this information is an informal, unpublished committee report on a survey of precast/prestressing plants done by the Prestressing Steel Committee of PCI circa 1998). For historical perspective, it is noted that the bulk of development regarding the Moustafa Test employed concrete that did not contain HRWRs. A majority of the Moustafa testing has been performed at Stresscon Corporation in Colorado Springs, where HRWRs are not commonly employed. Yet, others that have participated in Moustafa Testing have employed HRWRs as part of the standard casting procedures used in the local prestressing plants. Variations that result from the use of HRWR have not been measured or quantified. These data were compiled informally through the work of the Prestressing Steel Committee of the Precast/Prestressed Concrete Institute and are not available for publication.

2.4.1.4 Influence of Air Entrainment

There is a lack of data available to assess what effect, if any, air entrainment has on the bond of pretensioned strands. The experiences of the states are mixed with regard to whether air entrainment is required in pretensioned beams. The NASP Bond Test was employed to examine what effects, if any, air entrainment has on bond. Results indicate that concrete strength is more important to bond strength than air entrainment.

2.4.1.5 Top Bar Effects

There is a small database in existence available to examine the “top bar effect” on transfer and development of prestressing strands. This information is primarily available from testing programs on prestressed concrete piling. The top bar

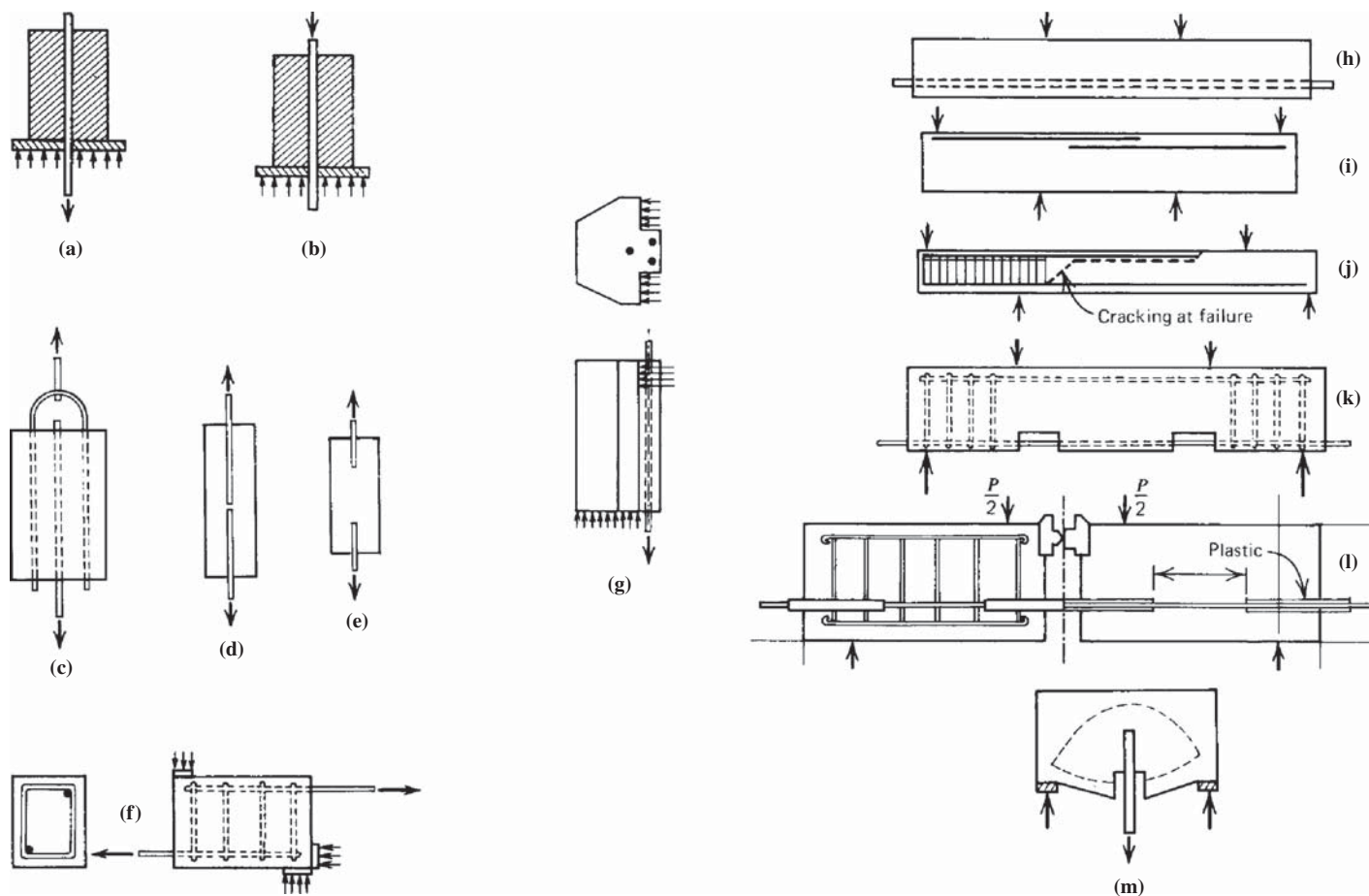
effect is expected to be assessed during casting of the scale model and full-sized specimens by including pretensioned strands in the top half of the cross section.

2.4.2 Testing Protocols for Mild Reinforcement

A review of testing protocols was conducted to determine the appropriate testing protocol(s) for addressing gaps in the experimental data. It is well established that testing protocols to evaluate development and splice length requirements for deformed bars and wire in tension must be of an appropriate scale, containing more than one bar or wire; testing protocols should also show due regard for a realistic transfer of force between concrete and steel reinforcement, as well as cover and bar spacing effects. The more commonly used testing configurations are shown in Figure 2.14. Although they are economically appealing, pull-out tests used by earlier researchers to evaluate bond performance of various reinforcing bars embedded in concrete of different strengths (Figures 2.14[a] through [e]) present the problem of introducing transverse compression, a compression not typical of

situations encountered in structures. Transverse compression has a beneficial effect on bond strength and yields an overly optimistic assessment of the actual performance of structures. For this reason, various testing schemes have been proposed to eliminate transverse compression (see Figure 2.14[f] and [g]). In the case of semi-beam specimens, such as those shown in Figure 2.14(f), it is critical to properly account for the increase in the length over which splitting resistance tends to be mobilized due to the confining pressure at the end of the bar (if the bar end is not shielded). ACI Committee 408 (1964) prepared a detailed guide for the determination of bond strength in beam specimens. The more popular variation, the so-called beam splice test with the splice located in the constant moment region (the most critical condition is one where both bars in the splice are subjected to high stresses), can be seen in Figure 2.14(i).

Splice tests have been realistic simulations of real conditions in structures, but development length tests have been conducted largely using pull-out tests in which splitting failures are purposely avoided. As a result, the bond stresses developed along splices are low compared with the bond along a bar in a pull-out test. This difference in test methods is responsible for



P = applied load.

Figure 2.14. Testing methods to evaluate bond strength.

large differences in code-required anchorage lengths for splices and development of single bars. Pull-out failures occur in cases of high confinement and short bonded lengths. In most structural applications, however, splitting failures tend to control. On this basis, the data developed for extending the current AASHTO LRFD specification for splice/development length had a minimum bonded length to bar diameter ratio of 15 in order to avoid unrealistically high values of bond strength. A similar concept of minimum embedment length should be included in any proposed specifications.

Splice specimens such as those shown in Figure 2.14(i) are deemed to represent larger-scale specimens designed to directly measure development and splice strength in full-scale members. Because of the relative ease of fabrication and the realistic state of stress achieved during testing, splice specimens were used in the development of experimental data on development/splice length of mild reinforcement in this research.

Review of experimental data on anchorage of bars terminated using standard hooks indicates the need for additional testing to extend the current AASHTO LRFD specifications to concrete strengths up to 15 ksi (see Section 2.2.2). Tests have shown that the bar force is transferred rapidly into the concrete, and the portion following a hook is generally ineffective and can potentially be limited by the tensile strength of the concrete. Further study of failures of hooked bars indicates that splitting of the concrete cover is the primary cause of failure and that splitting originates at the inside of the hook, where the local stress concentrations are higher. Thus, it has been determined that hook development is a direct function of bar diameter, d_b , which governs the magnitude of compressive stresses on the inside of the hook. The experimental work supporting the current requirements for development of standard hooks in tension was conducted using the test setup shown in Figure 2.15. In NCHRP Project 12-60, a similar specimen and test setup was used in the evaluation of uncoated and epoxy-coated bars terminated with standard hooks in tension to normal-weight concrete with compressive strength up to 15 ksi.

A useful test protocol to help understanding the bond strength of mild reinforcement in concrete members must define a minimum level of information to be provided. The recommended level of information is described in the following subsections.

2.4.2.1 Concrete Properties

The following information on concrete properties should be provided:

- the source of the concrete.
- the mix proportions, including identification of the components:
 - cement type;

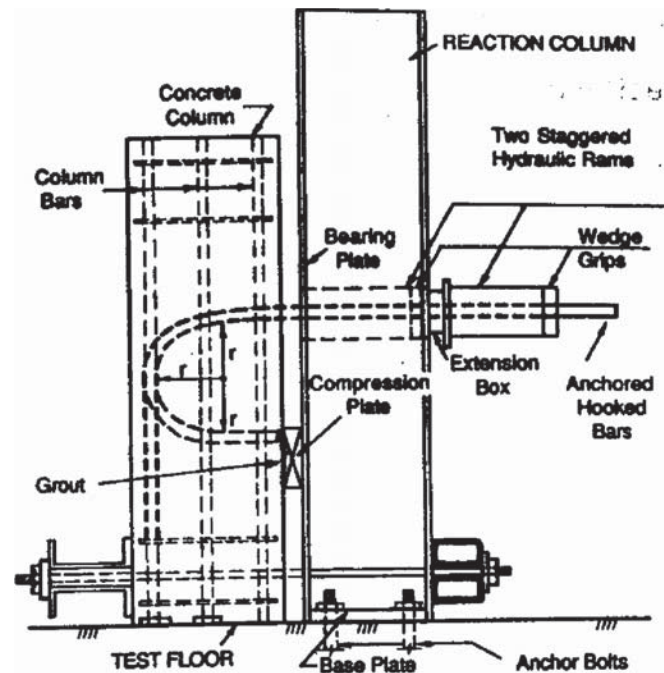


Figure 2.15. Exterior beam-to-column joint setup to evaluate bond performance of bars developed using standard hooks.

- mineral admixtures;
- chemical admixtures, including specific gravity and percent solids; and
- fine and coarse aggregates and their properties (e.g., specific gravity [SSD] and absorption).
- the concrete compressive strength, as obtained from a standard concrete cylinder (which should be cured side-by-side with, and in the same manner as, the bond/splice specimens), and including:
 - size of the compressive strength specimens,
 - type and thickness of the cylinder caps used on the specimens, and
 - age of the specimen at testing.
- the concrete flexural strength, including:
 - size of the flexural strength specimens,
 - age of specimen at testing, and
 - flexural test method used.

2.4.2.2 Reinforcement Properties

The properties of the reinforcing steel are required for basic identification and, in most cases, are needed to fully characterize the steel used in the tests. The following information should be provided for each heat or production run of reinforcing steel: the standard (ASTM) under which the bars were manufactured, the nominal diameter, bar designation, yield strength, tensile strength, proof strength (if applicable), elongation at failure, weight (mass) per unit length,

rib spacing and rib height (according to the standard under which the bar was manufactured as well as the average value), relative rib area, rib angle (the included angle between the rib and the bar axis), rib-face angle, and type of coating and coating thickness (if applicable).

2.4.2.3 Specimen Characteristics

The following specimen characteristics should be recorded: exterior dimensions, the location of structural/tensile reinforcement (including the effective depth), bottom/top cover, side cover, the clear spacing between bars, and the length of the specimen. These additional specimen characteristics should be recorded: the length of the developed/spliced bars, the number of developed/spliced bars, the number and average spacing of stirrups/ties used as transverse reinforcement in the region of the developed/spliced bars, the tensile strength of this reinforcement, and the load (tensile/bending) on the specimen at the time of failure (including the specimen self-weight and the weight of the test system). Specimen dimensions should be measured after casting. It is also recommended that the cover be measured after casting and/or testing.

2.4.2.4 Test Information

The following basic information should be recorded for each test: a description of the test system; the weight of the loading system; the rate of loading; the presence or absence of

strain gages on the developed/spliced reinforcing bars; location, type, and number of displacement transducers; the full load-deflection curves for the tests; and the number and location of load measurement devices. More information on the local behavior of the splice or development length can be obtained by placing strain gages on the bar itself. The strain gage instrumentation provides information on the changes in bar force along its length. In order to avoid excessive disturbances due to the presence of the gages, they are installed by splitting the bar in half, forming a channel along the centerline. Strain gages and wires are then placed in the channel, and the bar is welded together. An acceptable alternative is to place the wires and gages in grooves cut along the longitudinal ribs of the bar. Transverse reinforcement should be instrumented as well. Surface concrete strains should be monitored in the test region using strain gages and/or Zurich-type gages by means of a reference grid attached to the surface of the specimen.

2.5 Summary

Based on the results of the literature review conducted in this chapter, the experimental plan for NCHRP Project 12-60 was refined and carried out with the approval from the project panel. The results of the entire experimental program for both strand and mild steel are presented and discussed in Chapter 3 of this report.

CHAPTER 3

Experimental Program and Results

3.1 Introduction to the Experimental Program

Each section of this chapter focuses on a phase of the research program. Each section begins with a discussion of testing procedures for the phase of the research program covered and then discusses the test results. Prestressed sections are discussed in Sections 3.2 through 3.7. The mild steel phase is discussed in Section 3.8. The experimental thrust areas consist of the following:

- Refinement of the NASP Bond Test, culminating in the results from round robin testing by OSU and Purdue. Based on its repeatability and the reproducibility, the NASP Bond Test is presented as the Standard Test Method for the Bond of Prestressing Strands (Standard Test for Strand Bond). The Standard Test Method for the Bond of Prestressing Strands is recommended for adoption by AASHTO. The Standard Test Method for the Bond of Prestressing Strands was modified by testing strand in concrete of varying strengths. The tests demonstrate that the bond strength between strand and concrete is improved by increases in concrete strength. The results indicate that bond performance improves in proportion to the square root of the concrete strength. This relationship is subsequently used in the recommended code expressions for transfer length and development length.
- Transfer length measurements made on pretensioned concrete beams, both rectangular beams and I-shaped beams. The results show a direct correlation between decreasing transfer length and increasing concrete strength. Based on the results, a design expression for transfer length is recommended that includes a factor for concrete strength.
- Development length tests on the pretensioned concrete beams. The results show that strand development length requirements shorten with increased concrete strength. Additionally, the development length tests provide the data

to support the recommendation for minimum threshold values from the Standard Test Method for the Bond of Prestressing Strands. Based on the results, a design expression for development length is recommended that includes a factor for concrete strengths up to 15 ksi.

- The object of the mild steel phase of the experimental program was to evaluate the bond strength under monotonic loading of lap-spliced and hooked uncoated and coated bars in tension embedded in normal weight higher strength concrete. The 318 Code (ACI 2005) places an upper limit on the $\sqrt{f'_c}$ of 100 psi in the calculation of splice length/development length of bars as well as on the development length of standard hooks in tension in higher strength concretes. This limitation was first introduced in the 1989 edition of 318 Code (ACI 1989). Section 5.4.2.1 of the 2004 edition of the *AASHTO LRFD Bridge Design Specifications* states that design concrete strengths above 10 ksi shall be used only when allowed by specific articles or when physical tests are made to establish the relationships between the concrete strength and other properties. The object of this experimental program was to provide the information necessary to determine whether these limitations can be removed for concrete compressive strengths up to 15 ksi.

3.2 The Standard Test Method for the Bond of Prestressing Strands

In the past, testing programs intended to measure transfer and/or development length have instead highlighted the variation in bond-ability that resulted from the varying bonding properties of prestressing strands. So, rather than addressing the primary research focus, which was often to develop code equations for strand transfer and development lengths, the results of these testing programs were muddled and confus-

ing to transportation agencies and others. Therefore, as a first step in this research program, a Standard Test Method for the Bond of Prestressing Strands was refined from prior testing. The research reported herein continues and expands research begun by NASP. The focus of NASP's research has been to develop a standardized test for bond that would be repeatable at a testing site, reproducible among sites, and provide a reliable prediction of the performance of a pretensioned concrete product. With the development of a repeatable, reproducible standard test, design expressions for transfer and development length can be developed.

Figure 3.1 shows a NASP specimen mounted in the loading frame at OSU. Each test specimen is prepared by casting a single prestressing strand in a sand-cement mortar within a cylindrical steel casing. The sand-cement mortar is proportioned to produce a strength of 4750 ± 250 psi at 24 hr, after standard curing. Additionally, the sand-cement mortar is required to produce a flow in the range of 100 to 125 as measured by ASTM C 1437. The strand is pulled from the concrete mortar at a displacement rate of 0.10 in./min, 24 hr after casting. Pull-out force is measured in relation to the movement of the free end of the strand to the hardened mortar. The NASP Bond Test records the pull-out force that corresponds to 0.10 in. of free strand end slip. One single NASP Bond Test consists of six or more individual test specimens; the average value from the set of six becomes the "NASP Bond Test Value." The appendices to this report contain three separate bond test protocols; each protocol



Figure 3.1. NASP specimen on the loading frame at OSU.

represents a different stage in the development and refinement of the NASP Bond Test.

3.2.1 Refinement of the NASP Bond Test

The NASP Bond Test was originally developed in Round II and Round III research sponsored by NASP. The NASP research investigated the repeatability and reproducibility of the test method together and also compared the NASP Bond Test with other test methods. In Rounds II and III, the research showed that the NASP Bond Test was a better predictor for bond than the Moustafa Test or the PTI Bond Test. The NASP Bond Test also showed convincing results when compared with transfer lengths measured on prestressed concrete beams. Additionally, Round III testing showed evidence that the NASP Bond Test could be used to ensure adequate strand development. The early versions of the NASP Bond Test protocols are included in Appendix I. Appendix I contains two versions of the NASP Bond Test, the first dated August 2001 and the second dated May 2004. The earliest version of the NASP Bond Test was employed for Rounds II and III of the NASP-sponsored research. The May 2004 protocols were used for NCHRP Project 12-60 for the purpose of further refining the NASP Bond Test. Some refinements in protocol were made to develop the final version found in Appendix H and titled, "Standard Test Method for the Bond of Prestressing Strands."

For this research, minor changes were made to the NASP Test procedures that were used in NASP Round III research. Although the underlying methodology in the procedure was not changed significantly, changes in the sample preparation were made and test procedures were refined. The NASP protocols in 2001 specified a sample preparation in which the cement mortar had a sand-cement-water ratio of 2:1:0.45 and a target 1-day mortar cube strength of 3,500 to 5,000 psi. The wide range in the mortar cube strength proved to adversely affect the NASP Bond Test values. Weaker mortar produced lower pull-out strengths, whereas stronger mortar produced higher pull-out strengths. The May 2004 protocols used in the NCHRP research targeted a smaller range ($4,750 \pm 250$ psi) for mortar cube strength. Later, through refinement, the mortar proportions were not specified so that consistent mortar strengths could be produced despite possible variations in the constituent materials from site to site. Therefore, the August 2006 protocol for the Standard Test Method for the Bond of Prestressing Strands required mortar strength in the range of 4,500 and 5,000 psi, but did not specify the mixture proportions.

Additionally, the test methodology adopted a mortar flow requirement in the range of 100 to 125, whereas flow measurements were not made during the NASP Round III tests of the August 2001 protocols. The standardized flow rates help

ensure workability of the mortar and consistent consolidation of the mortar. The strand is centered in a steel casing with an outer diameter of 5 in. and a bond length of 16 in. The cement mortar is cast and consolidated in the steel casing.

The NASP Bond Test protocols in 2001 did not specify the frame used for loading the NASP specimen. The loading frames used in the Round III trials were more “flexible” when compared with the frame used in the current NCHRP research, which is more “rigid.” Because the NASP Bond Test protocols require a displacement rate, the rigidity of the test apparatus affects the loading rate. Therefore, the Standard Test Method for the Bond of Prestressing Strands limits the loading rate to 8,000 lb/min for 0.5 in. diameter strands and 9,600 lb/min for 0.6 in. diameter strands. In its recommended form, the Standard Test Method for the Bond of Prestressing

Strands requires a loading rate of 0.1 in./min, as before, and the NASP value is reported as the load at which the free strand end slip is 0.1 in. The average of six or more NASP specimens is reported as the NASP value for the strand. Studies conducted earlier in the NASP Round II concluded that the least variation in the NASP values is exhibited for the 0.1 in. of strand end slip. The largest variation in the NASP values was reported in the 0.01 in. of free strand end slip.

The Moustafa Test and the PTI Bond Test, which are used by some to identify the bonding properties of prestressing strands with concrete, were neither repeatable nor reproducible. The NASP Bond Test was convincingly superior to the others in its ability to reproduce results among sites.

Table 3.1 provides the results of NASP Bond Tests that were performed at OSU. Ten different 0.5 in. diameter

Table 3.1. Results of NASP Bond Tests at OSU.

Batch #	Water-to-Cement Ratio	Mortar Strength \bar{f}'_{ci} (psi)	NASP IV STRAND ID	NCHRP ID	Strand Diameter (in.)	NASP Test Results			LC/DC
						Pull-Out Force at 0.1" slip (lbs.)	N	S (lbs.)	
8N	0.45	4765	C	D	0.5	6,870	12	861	DC
11N	0.45	4730	G	A	0.5	20,710	11	1604	DC
14N	0.45	4953	G	A	0.5	20,010	12	3088	LC
15N	0.45	4815	G	A	0.5	21,930	6	1106	LC
15N	0.45	4815	G	A	0.5	21,190	6	1333	DC
17N	0.45	4484	C	D	0.5	8,710	5	432	LC
17N	0.45	4484	C	D	0.5	6,910	5	338	DC
21N	0.5	4043	G	A	0.5	20,060	12	1129	LC
22N	0.5	4117	C	D	0.5	6,110	12	421	DC
23N	0.5	3981	G	A	0.5	16,360	12	1629	DC
24N	0.4	5763	C	D	0.5	8,420	12	415	DC
27N	0.45	4933	K6		0.6	19,010	5	4311	DC
27N	0.45	4933	L6	A	0.6	17,960	6	1292	DC
28N	0.45	4843	K6		0.6	22,420	5	1964	DC
28N	0.45	4843	L6	A	0.6	18,610	6	717	DC
29N	0.45	4723	A	C	0.5	14,130	6	1144	DC
29N	0.45	4723	E		0.5	15,950	6	1266	DC
30N	0.45	4723	J	B	0.5	19,330	5	808	DC
30N	0.45	4723	E		0.5	17,210	6	823	DC
31N	0.45	4927	J	B	0.5	21,090	6	733	DC
31N	0.45	4927	A	C	0.5	13,300	6	1763	DC
34N	0.45	4659	H		0.5	15,940	6	1153	DC
34N	0.45	4659	F		0.5	13,570	6	968	DC
35N	0.45	4659	H		0.5	18,080	6	1202	DC
35N	0.45	4659	F		0.5	16,540	6	684	DC
36N	0.45	4451	I		0.5	12,100	6	1455	DC
36N	0.45	4451	B		0.5	13,440	6	1243	DC
37N	0.45	4724	I		0.5	14,710	6	1181	DC
37N	0.45	4724	B		0.5	15,600	6	1044	DC
38N	0.45	4153	K6		0.6	19,510	12	2079	DC
39N	0.45	4303	D	E	0.5	5,240	6	635	DC

strands were tested along with two different 0.6 in. strands. In Table 3.1, LC/DC refers to whether the test was conducted using load control (LC) or displacement control (DC). These tests were critical to refining the test protocols and also to determining which strand samples would provide high and low targets for NCHRP Project 12-60 transfer length and development length tests. Testing also included variations in water-to-cement ratio (w/c), which resulted in variations in mortar strength. W/c ratios of 0.40, 0.45, and 0.50 were tested. Additionally, some tests were performed using load-controlled protocols instead of displacement control. From these tests, it was determined that displacement control provides more data that can be valuable in evaluating strand bond performance. Therefore, the recommended Standard

Test Method for the Bond of Prestressing Strands requires displacement control instead of load control.

The Standard Test Method for the Bond of Prestressing Strands (see Appendix H) includes specific dimensions for the test specimens and the procedures for the test. Figure 3.2 shows a schematic of the Standard Test Method for the Bond of Prestressing Strands. Additional details for the NASP Bond Test are shown in Figure 3.3. Figure 3.4 shows detail for the methodology employed to measure the strand end slip on its “free” end, i.e., the end of the strand that is not loaded in tension. The photograph in Figure 3.5 shows the strand end slip measurement device. Finally, in Figure 3.6, the photograph shows an entire Strand Bond Test specimen placed within the loading frame and ready for testing.

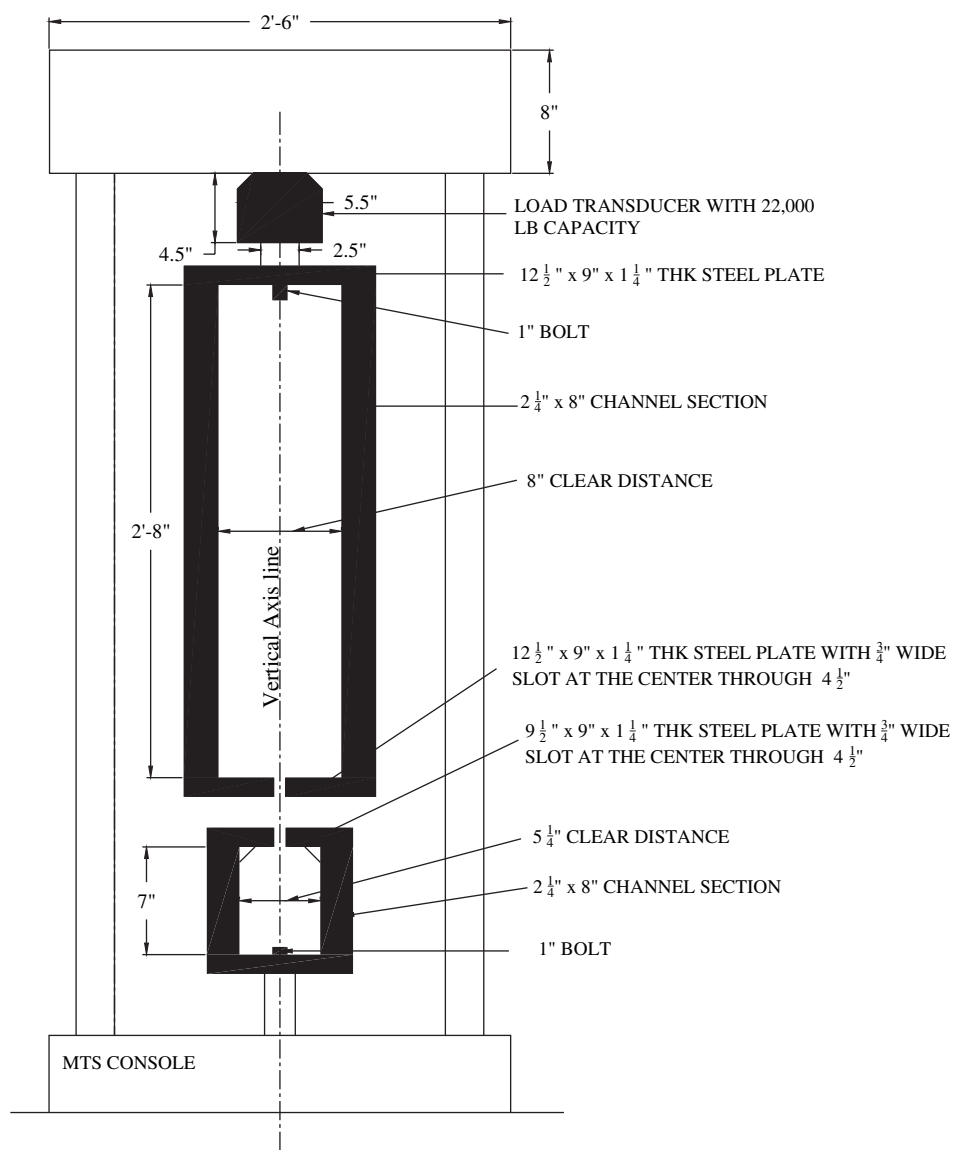


Figure 3.2. Schematic diagram of NASP Test setup.

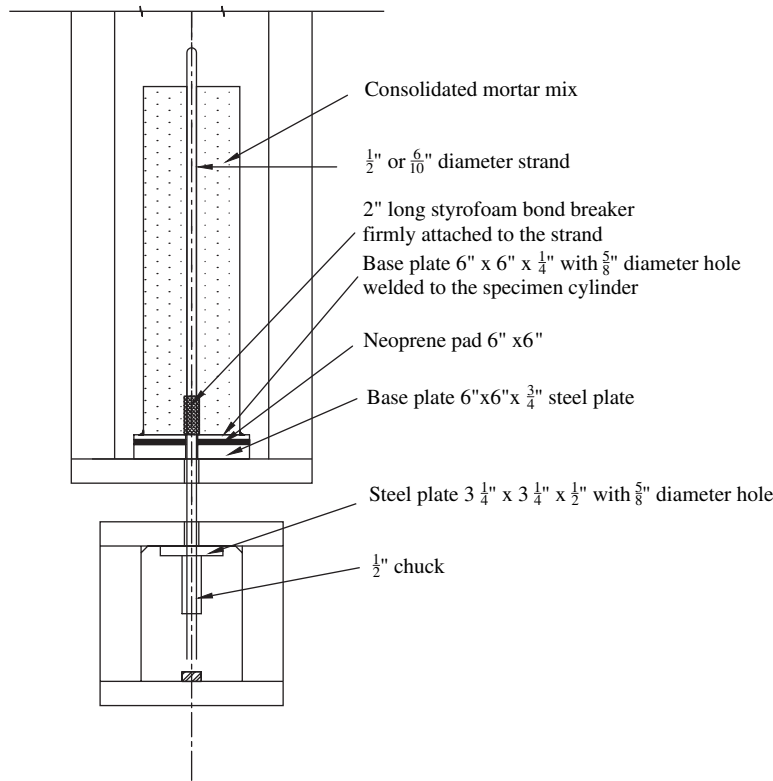


Figure 3.3. Details of the NASP Bond Test specimen.

3.2.2 Reproducibility of the NASP Bond Test Between Sites

The NASP Bond Test was performed on specific strand samples at Purdue and OSU. Round robin trials were performed on five 0.5 in. diameter and two 0.6 in. diameter, Grade 270, low-relaxation strands. The strands included in the round robin trials are shown in Table 3.2. Some of the

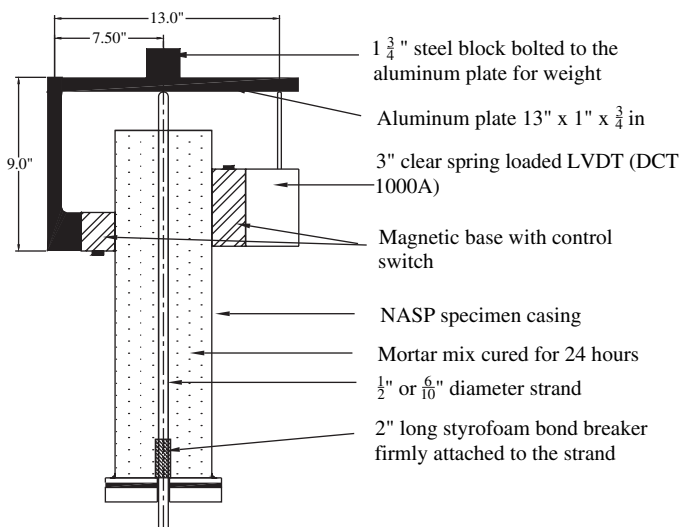


Figure 3.4. NASP Test specimen strand end slip measurement.

Strand Bond Test data from OSU was developed from tests with 12 samples. At Purdue, all of the tests had a sample size of six. Table 3.2 lists both the NASP identifiers (Round III and Round IV) and the NCHRP strand ID. Purdue performed the bond tests as completely blind trials—even the Purdue strand identifiers were changed from those used at OSU.

The results from the round robin testing are reported in Table 3.3. The five 0.5 in. diameter strand samples are Strand A, Strand B, Strand C, Strand D and Strand E. The two 0.6 in.



Figure 3.5. LVDT on NASP Test specimen.



Figure 3.6. NASP Test specimen inside loading frame.

diameter samples are labeled Strand A6 and Strand B6. For example, Strand E had the lowest reported results at both testing sites, 5240 lb at OSU and 6070 lb at Purdue. For Strand C, OSU reported an average of 13,715 lb, whereas Purdue reported an average of 14,710 lb. Note that the table reports results of testing with both 0.5 in. and 0.6 in. strands.

The results in Table 3.3 are illustrated in Figure 3.7. Figure 3.7 plots the average NASP values from OSU against the average NASP values from Purdue. A linear regression line and a “perfect fit” line are plotted in the figure. The test results

match the “perfect fit” line very closely, with an R^2 value of 0.92.

3.2.3 Recommendation for the Standard Test Method for the Bond of Prestressing Strands

The NASP Bond Test performed in this research program was conducted on ten 0.5 in. diameter and two 0.6 in. diameter strands. In the NCHRP testing, round robin tests were performed at Purdue and OSU. As shown in Figure 3.7, the results from the two testing sites closely match.

This research builds upon earlier work done by NASP to develop a standard test for bond. The NCHRP research further refined the testing protocols to the point where the test results are now demonstrably reproducible between testing sites. The refined test is recommended as a standard test method to evaluate the ability of a prestressing strand to bond with concrete.

3.3 The NASP Bond Test in Concrete

The NASP Bond Test protocol was modified to test the strand in concrete in place of mortar. This is important to the overall research because the NASP Bond Test modified for concrete demonstrates the relationship between bond strength and concrete strength. The overarching conclusion from this segment of the testing was that bond strength improves in proportion to the square root of the concrete strength. This conclusion stems from an examination of data from three of the 0.5 in. diameter strands and one of the 0.6 in. diameter strands. The concrete used for the modified NASP Bond Test had 1-day strengths varying from 4 ksi and to 10 ksi.

Table 3.2. Round-robin testing at OSU and Purdue.

STRAND DIAMETER (IN)	NASP ROUND III ID	NASP ROUND IV ID	NCHRP OSU ID	OSU	Purdue
0.5		A	C	x	
0.5		B		x	
0.5	FF	C	D	x	x
0.5	II	D	E	x	x
0.5		E		x	
0.5		F		x	
0.5	AA	G	A	x	x
0.5		H		x	
0.5		I		x	
0.5		J	B	x	x
0.6		K6	B6	x	x
0.6		L6	A6	x	x

Table 3.3. Results from round-robin testing—Standard Test for the Bond of Prestressing Strands in Concrete.

NCHRP STRAND ID	Strand Diameter (in)	NASP Test Results at OSU		NASP Test Results at Purdue	
		Mortar Strength \bar{f}'_{ci} (psi)	Pull-Out Force at 0.1" slip (lb)	Mortar Strength \bar{f}'_{ci} (psi)	Pull-Out Force at 0.1" slip (lb)
C	0.50	4,723	14,130	4,498	14,270
C	0.50	4,927	13,300	4,810	15,150
Avg.			13,715		14,710
D	0.50	4,765	6,870	4,665	7,280
D	0.50	4,484	6,910	4,365	9,770 ¹
D	0.50			4,767	9,970
Avg.			6,890		8,625
E	0.50	4,303	5,240	4,000	6,070
A	0.50	4,730	20,710	4,847	2,0880
A	0.50	4,815	21,190	4,318	16,470 ¹
A	0.50			4,638	18,880
Avg.			20,950		19,880
B	0.50	4,723	19,330	4,893	22,700
B	0.50	4,927	21,090	4,798	22,280
Avg.			20,210		22,490
B6	0.60	4,843	22,420	4,356	19,130
B6	0.60	4,933	19,010		
B6	0.60	4,153	19,510 ¹		
Avg.			20,715		19,130
A6	0.60	4,933	17,960	4,628	15,450
A6	0.60	4,843	18,610		
Avg.			18,285		15,450

¹Value omitted from average because the mortar strength was out of range.

The modified NASP Bond Test was conducted in concrete to understand the effects of varying concrete strengths on the bond of prestressing strands. The test procedure was identical to the NASP Bond Test protocols discussed in Section 3.2 except that concrete with varying strengths was used instead of the standard cement-sand mortar. The

NASP tests in concrete were conducted on three 0.5 in. diameter strands with NCHRP strand designations A, B, and D and on one 0.6 in. diameter strand with an NCHRP strand designation of A6. The number of NASP tests conducted on concrete for varying concrete strengths is reported in Table 3.4. Each test listed in Table 3.4 contains six

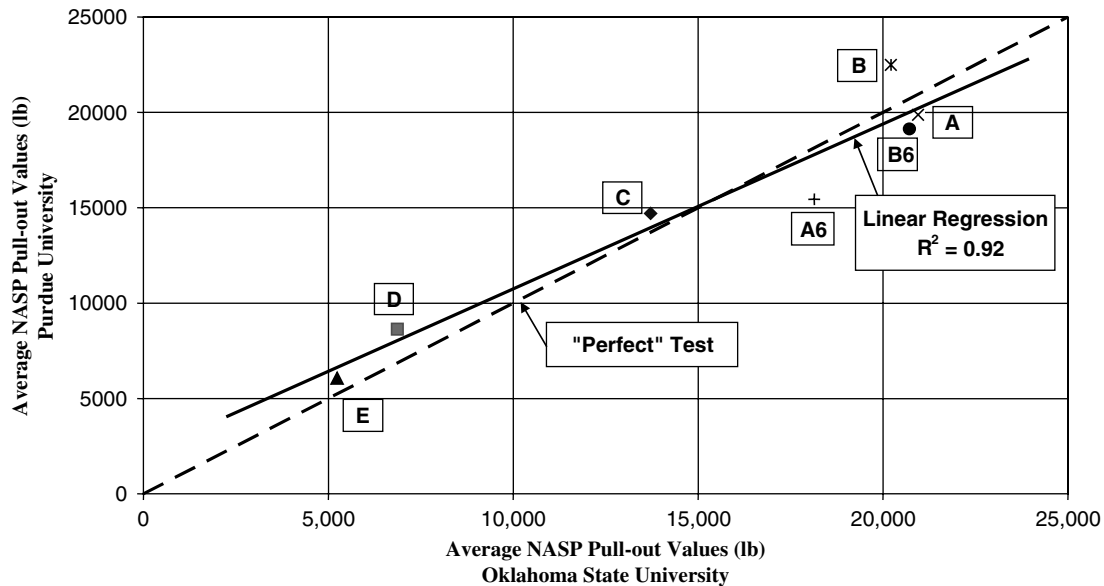


Figure 3.7. Comparison of NASP Bond Tests at OSU and Purdue.

Table 3.4. Number of NASP Bond Tests modified for concrete with varying concrete target strengths.

NASP Round ID	NCHRP ID	Strand Diameter (inches)	Target Id Concrete Strengths (ksi)			
			4	6	8	10
G	A	0.5	1	1	1	1
J	B	0.5	1	1	1	1
C	D	0.5	2	4	2	1
L	A6	0.6	1	1	1	1

or more NASP specimens. The target concrete strengths for each of the tests were 4, 6, 8, and 10 ksi. The concrete mixtures used for making the NASP specimens in concrete included Type III cement from Lafarge North America, coarse and fine aggregate from Dolese Bros. Co., cement slag from Lafarge North America, and admixtures from Degussa Admixtures, Inc. Admixtures used included HRWRs, normal range water reducers (NRWRs), and air entraining admixtures (AEAs). Table 3.5 gives the mix proportions and the target fresh and hardened properties for the concrete cast in the modified NASP specimens. The mix proportions were named based on the target 1-day strength. The mix C-0 targets a concrete strength of 4 ksi at release. Similarly, C-I, C-II, and C-III target strengths of 6, 8, and 10 ksi at release, respectively. The concrete mix C-IA has a target release strength of 6 ksi with AEA. Detailed trial batching

was performed (Tessema 2006) to arrive at the concrete mix proportions and the target fresh and hardened properties. The results and discussion on the concrete mix proportions are beyond the scope of this report. The mixture proportions reported in Table 3.5 were also employed to make the transfer length and development length beams.

The NASP Bond Test, modified to be tested in concrete, conforms to the same protocols for NASP Bond Testing that are found in Appendix I. The only variation is that concrete is used in place of the sand-cement mortar. Also, concrete slumps of 2 to 3 in. were achieved instead of the mortar flow rates of 100 to 125. The handling and preparation of the strands, the steel casing, and the bond breakers were identical to the NASP Bond Tests conducted in sand-cement mortar. The mixing procedures used for the NASP Bond Test conformed to ASTM C 192. The fresh concrete is placed in two layers; each layer is consolidated using a handheld electric vibrator. The slump, unit weight, and air content are measured per ASTM C 143, ASTM C 138, and ASTM C 231, respectively. The NASP specimens and the test cylinders were cured in conformance with ASTM C 192. The compressive strength testing was conducted during the time of the NASP Bond Test in concrete, in conformance with ASTM C 39. The NASP specimens are then kept in a laboratory curing room for 22 to 24 hr from the time of hydration. Curing conditions near 73.4 °F and 100-percent relative humidity were maintained. The modified NASP Bond Test is performed at 24 ± 2 hr after the hydration of the cement. The NASP specimen in

Table 3.5. Concrete mixture proportions for transfer and development length testing and for the NASP Bond Test in concrete.

Concrete Mixture Designations	C-0	C-I	C-IA	C-II	C-III
Cement (PCY)	650	800	800	800	900
Cement Slag (PCY)					100
Coarse Aggregates (PCY)	1,800	1,703	1,800	1,805	1,747
Fine Aggregates (PCY)	1,243	1,203	922	1,219	1,183
Water (PCY)	298	303	272	277	251
Glenium 3200 (fl oz/cm. wt)			10	14	7
Glenium 3400 (fl oz/cm. wt)	8	5			5.5
Polyheed 997 (fl oz/cm. wt)			3		
MB-AE 90 (fl oz/cm. wt)			1.88		
Target Properties for Fresh and Hardened Concrete					
1-Day Strength (ksi)	4	6	6	8	10
28-Day Strength (ksi)	6	8	8	10	14
56-Day Strength (ksi)	n/a	10	10	14	15
Slump (in)	8	8	8	8	9
Unit Weight (pcf)	145	148	148	150	157
Air Content (%)	2	2	6	2	2

concrete is mounted on a rigid steel frame in the same manner described for the NASP Bond Test (in mortar).

3.3.1 Results from the NASP Bond Tests in Concrete

The NASP Bond Test standardized in mortar was conducted in concrete to understand the effect of concrete strengths on the NASP Bond Test. The results from this experimental testing are reported in Table 3.6. Table 3.6 reports the NCHRP Strand ID, the NASP Strand ID (for comparison purposes), the 1-day concrete strength (f'_{ci}), the NASP Bond Test result (from the Standard Test for Strand Bond in mortar), and the NASP Bond Test when modified and performed in concrete. The table reports the w/cm (water–cementitious materials) ratio because there were pozzolanic materials added for some of the concrete mixtures reported in Table 3.5. The concrete strengths reported in Table 3.6 are averages of three or more concrete specimens tested during the NASP test. The number of NASP Bond Test specimens (N) that were included as part of the test and the standard deviation

(S) for each set of tests are reported for the modified NASP Bond Test in concrete.

3.3.2 Discussion of the Results from the NASP Bond Tests in Concrete

Figure 3.8 shows the pull-out values from the Modified NASP Bond Test for Strands A and B plotted versus the concrete strength. There are a total of 8 data points, also reported in Table 3.6, found in Figure 3.8. Both linear regression and the power regression curves are plotted on the figure. The coefficient of determination (R^2) value for both the regressions is 0.82. The linear and the power best-fit equations are reported in Figure 3.8. Figure 3.8 clearly shows that increases in concrete strength result in a higher NASP pull-out value for NCHRP Strands A and B. Note that the NASP Bond Test pull-out value for the standardized test in mortar is 20.95 kips for NCHRP Strand A and 20.21 kips for Strand B. Also, note that the regression plots cross the 4 ksi concrete strength at a corresponding NASP Bond Test (modified) value of about 23 kips.

Table 3.6. Results of NASP Bond Tests in concrete.

Strand ID			Concrete			NASP Test Results			
NCHRP ID	NASP STRAND ID	Strand Diameter (in.)	w/cm	\bar{f}'_{ci} (ksi)	$\sqrt{\frac{\bar{f}'_{ci}}{(\sqrt{\text{ksi}})}}$	NASP in Mortar (kips)	NASP Value (kips)	N	S (ksi)
A	G	0.5	0.425	4.52	2.13	20.95	23.58	6	0.66
A	G	0.5	0.38	7.02	2.65		26.35	6	1.44
A	G	0.5	0.36	8.05	2.84		30.68	6	1.77
A	G	0.5	0.235	11.79	3.43		35.29	6	2.33
B	J	0.5	0.46	3.56	1.89	20.21	22.55	6	5.57
B	J	0.5	0.4	5.58	2.36		30.8	6	1.04
B	J	0.5	0.32	7.11	2.67		28.78	6	4.55
B	J	0.5	0.24	10.06	3.17		34.33	6	4.17
D	C	0.5	0.45	4.71	2.17	6.89	7.48	6	2.76
D	C	0.5	0.46	4.56	2.13		6.66	6	2.52
D	C	0.5	0.36	6.99	2.64		8.96	6	2.23
D	C	0.5	0.38	7.34	2.71		9.51	6	2.64
D	C	0.5	0.4	6.13	2.48		6.74	6	0.25
D	C	0.5	0.3	8.67	2.94		10.26	6	0.26
D	C	0.5	0.32	8.34	2.89		9.97	6	1.06
D	C	0.5	0.26	9.95	3.15		11.56	6	0.84
A6	L	0.6	0.46	2.23	1.49	18.29	11.6	6	0.61
A6	L	0.6	0.38	5.02	2.24		23.13	6	1.24
A6	L	0.6	0.28	8.79	2.96		24.84	6	0.82
A6	L	0.6	0.235	10.42	3.23		28.74	6	1.39

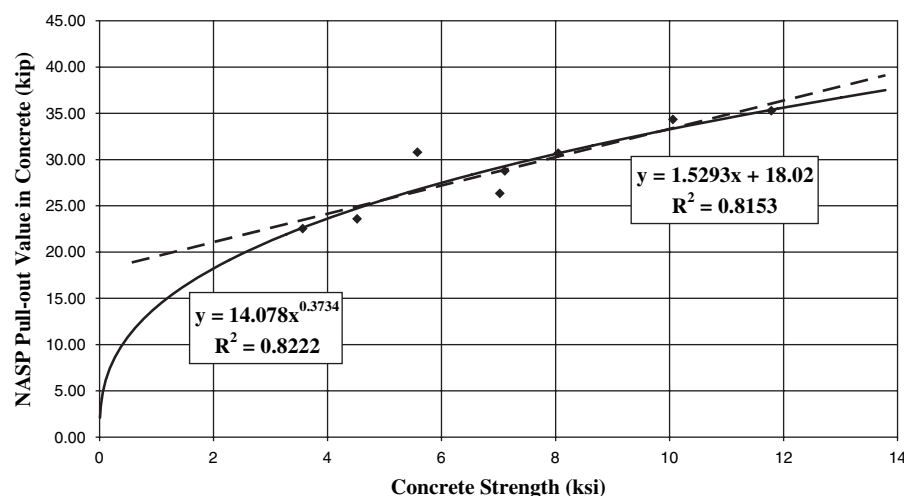


Figure 3.8. Pull-out values from the modified NASP Bond Test for Strands A/B versus concrete strength.

Figure 3.9 illustrates the pull-out values from the Modified NASP Bond Test for NCHRP Strand D plotted against concrete strength. NCHRP Strand D had a NASP Bond Test value of 6.89 kips in the standardized test, which was lower than the standardized NASP Bond Test values of Strands A and B. There are a total of 8 data points for Strand D, and the data shown in Figure 3.9 correspond to data reported in Table 3.6. Linear regression and the power regression curves are plotted on Figure 3.9 for Strand D. The coefficient of determination (R^2) values are 0.89 for the linear regression and 0.84 for the power regression. The linear and the power best-fit equations are also reported in the figure. Figure 3.9 clearly shows that increases in concrete strength result in a higher NASP pull-out value for NCHRP Strand D. Please note that the NASP Bond Test pull-out value for the standardized test in mortar is 6.89 kips for the NCHRP Strand D. Also, note

that the regression plots cross the 4 ksi concrete strength at a corresponding NASP Bond Test (modified) value of about 6 kips.

Figure 3.10 makes the same comparison as Figures 3.8 and 3.9, but for 0.6 in. diameter strand, NCHRP A6. The data shown in Figure 3.10 are also reported in Table 3.6. Both linear regression and the power regression curves are plotted on Figure 3.10 for NCHRP Strand A6. Please note that the exponent in the best-fit power curve is approximately 0.56. As in Figures 3.8 and 3.9, Figure 3.10 clearly shows that increases in concrete strength result in higher NASP pull-out values for NCHRP Strand A6. Please note that the NASP Bond Test pull-out value for the standardized test in mortar is 18.29 kips for the NCHRP Strand A6, and that the regression plots cross the 4 ksi concrete strength at a corresponding NASP Bond Test (modified) value of about 17.5 kips.

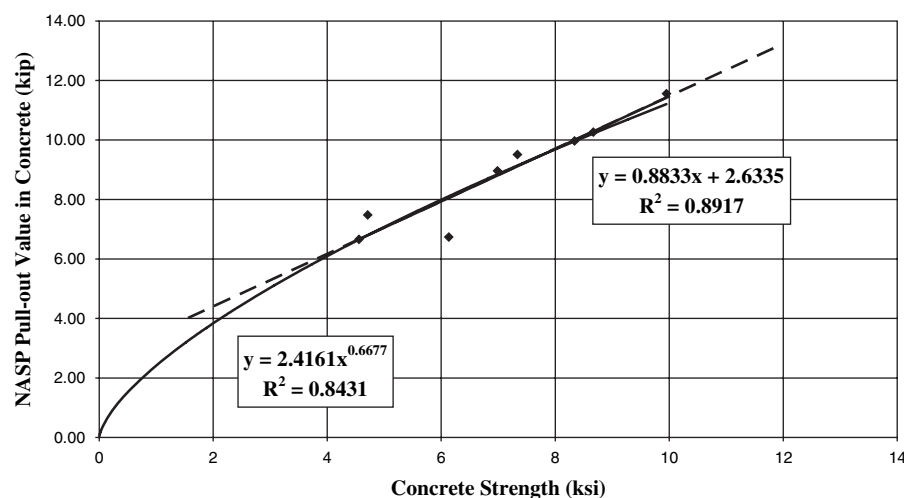


Figure 3.9. Pull-out values from the modified NASP Bond Test for Strand D versus concrete strength.

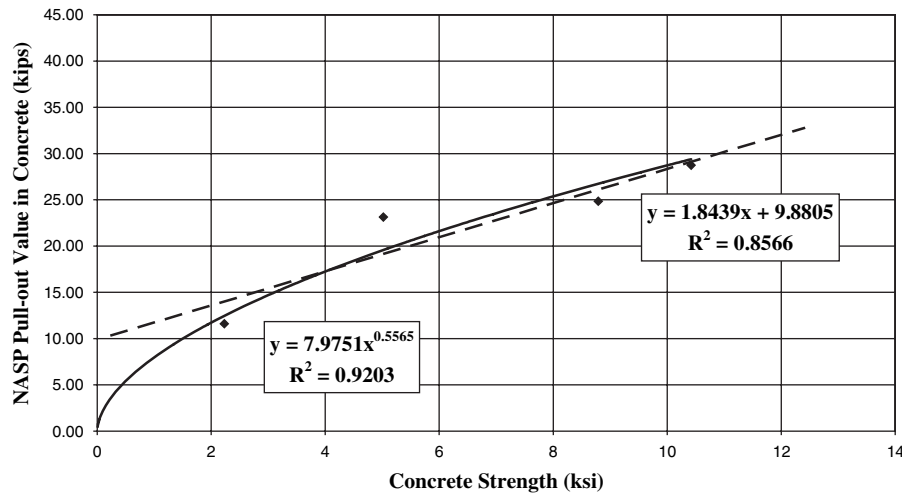


Figure 3.10. Pull-out values from the modified NASP Bond Test for Strand A6 versus concrete strength.

Table 3.6 also reports values for the square of the 1-day concrete strength. The NASP pull-out values and the square root of the concrete strength are presented for all the strands tested in concrete in Figure 3.11. The linear best fit-lines are plotted in the figure with the corresponding R^2 values for the four strands tested in the modified NASP test in concrete. In Figure 3.11, the best-fit curves tend to have a steeper slope for strands with higher NASP values in the same range of concrete strengths. The NASP value increases with increases in concrete strength, and the high-performing strands have a steeper best-fit line. Thus, for a given change in the concrete strength, the NASP results can have a higher variation for the high-performing strands (strands with higher NASP values) when compared with the moderately performing strands (strands with lower NASP values).

The data presented in Table 3.6 are normalized and presented all together in Figure 3.12. The NASP Bond Test values were normalized by dividing by the NASP Bond Values in concrete by the Standard NASP Bond Test (in mortar) values. Figure 3.12 includes data from all three 0.5 in. diameter strands and the one 0.6 in. diameter strand. Concrete strength at 24 hr from the modified NASP Bond Test is plotted against normalized NASP values. The data are plotted against a best-fit power regression curve, also shown in Figure 3.12. The R^2 value for the test data is 0.80, indicating that the power regression equation closely agrees with the test data. The best-fit equation is given in Equation 3.1.

$$\frac{(NASP_{\text{concrete}})}{NASP} = 0.49139 \bar{f}'_c^{0.51702} \quad (3.1)$$

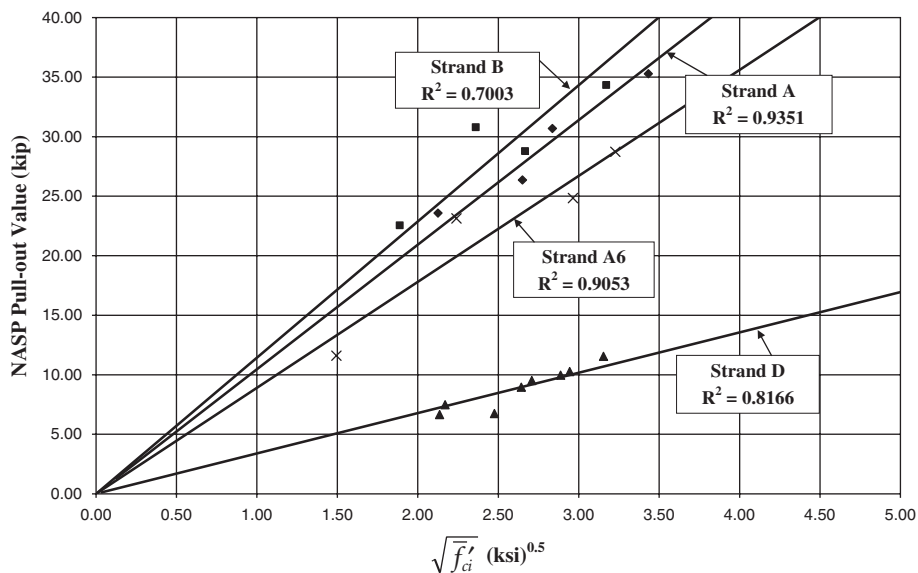


Figure 3.11. NASP pull-out values versus $\sqrt{f'_c}$ for all strands.

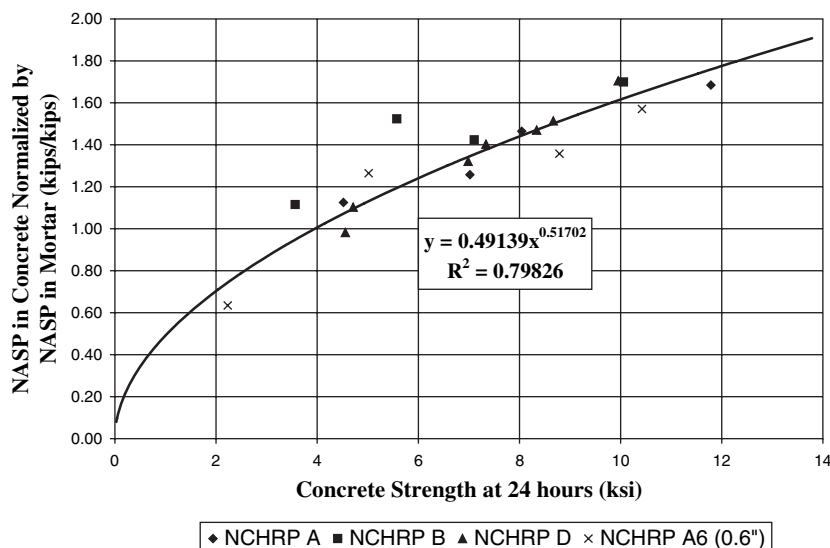


Figure 3.12. Normalized NASP pull-out values versus concrete strength for all strands.

where

$NASP_{\text{concrete}}$ = the value obtained from the NASP Bond Test in concrete, and

$NASP$ = the value obtained from the Standard NASP Bond Test (NASP Bond Test in mortar).

The equation is modified to fit the NASP values as a function of the square root of concrete strengths. In Figure 3.13, the normalized NASP pull-out values are plotted against the square root of the concrete strength. The linear regression results in the following equation:

$$\frac{(NASP_{\text{concrete}})}{NASP} = 0.51\sqrt{f'_{ci}} \quad (3.2)$$

The result of the regression is remarkable for two reasons. One, the data's best fit regression demonstrates a coefficient of determination of 0.79, illustrating that the data set is fairly well predicted by the regression; two, the data demonstrate that bond improvements are directly proportional to the concrete strength at 1 day of age. Furthermore, the normalized value of 1.0 is achieved at an f'_{ci} of 4 ksi. These significant results are used later in the recommendation for transfer and development length code expressions. Also note that the modified NASP Bond Test in concrete nearly matches the Standard NASP Bond Test if the concrete strength is only 4 ksi, as compared to the requirement for mortar strength of 4,500 to 5,000 psi.

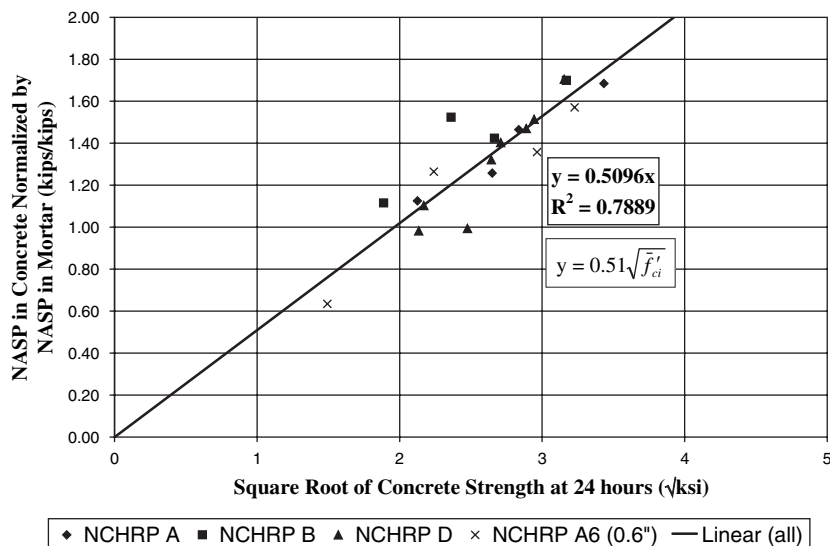


Figure 3.13. Normalized NASP pull-out values versus $\sqrt{f'_{ci}}$.

3.4 Measured Transfer Lengths versus Varying Concrete Strengths and Varying NASP Bond Test Values

The research aims at assessing the effects that varying concrete strength can have on strand bond. This section deals primarily with transfer lengths measured on pretensioned beams. Variables included strand with varying bond quality and concrete strengths varying between 4 ksi at release and 10 ksi at release. Beams were either rectangular in shape or I-shaped. A total of 43 rectangular-shaped beams and 8 I-shaped beams were cast using 4 different strand sources. The number of beams made and the corresponding research variables are reported in Table 3.7. Two-strand rectangular beams included two strands placed near the bottom of the cross section. The four-strand rectangular beams had two strands placed near the bottom and two strands placed near the top. Beams were cast using both 0.5 in. and 0.6 in. diameter strands. Figure 3.14 illustrates the beam numbering system that describes the variables that are contained within each beam specimen. Cross section details for the rectangular beams are found in Figures 3.15 and 3.16.

Figure 3.17 depicts some of the rectangular beams during fabrication, prior to release of the prestressing strands. Beams were made with a target 1-day concrete strength of 4,000, 6,000, 8,000 and 10,000 psi. The 6,000-psi release strength concrete beams were made using both air-entrained and non-air-entrained concrete to study the effects of air entrainment

on transfer lengths. Three different sources for 0.5 in. diameter strand and one source for 0.6 in. diameter strand were employed in this research program.

Figure 3.18 shows the details of the I-shaped cross section. In the I-shaped beams made with 0.5 in. diameter strands, four strands were located within the bottom bulb of the cross section with a fifth strand located 2 in. from the top of the cross section. In the I-beams made with 0.6 in. diameter strands, three strands were located within the bottom bulb of the cross section with a fourth strand located 2 in. from the top of the cross section.

3.4.1 Fabrication of Beams

Transfer lengths were measured at release on all the beams using strand end slips. On some of the beams, transfer lengths were measured using a detachable mechanical strain gage (DEMEC gage), which effectively measures changes in concrete surface strains. The transfer lengths measured from strand end slips are compared with those measured using the DEMEC gage.

The rectangular beams were 17 ft in length with a cross section that was 6.5 in. wide by 12 in. high. Two #6 bars were placed within 1 in. of the top of the cross section in all rectangular beams to ensure ductile flexural failures. The cross section for the I-shaped beams is shown in Figure 3.18. The beams were fabricated 24 ft in length. The beams cast had 0.5 in. diameter strands and 0.6 in. diameter strands. All of the I-beams contained horizontal web rein-

Table 3.7. Number of transfer length beams and research variables employed.

Target Release Strength (ksi)	Concrete Design Strength (ksi)	Target Air Content (%)	0.5 in Diameter Strands			0.6 in Diameter Strands
			Strand A	Strand B	Strand D	Strand A6
Two-Strand Rectangular Beams						
4	6	2	0	2	2	2
6	10	2	2	0	2	3
6	10	6	2	0	2	0
8	14	2	2	0	2	3
10	15	2	2	0	2	3
Four-Strand Rectangular Beams						
6	10	2	2	0	2	0
8	14	2	2	0	2	0
10	16	2	2	0	2	0
I-Shaped Beams						
6	10	2	1	0	1	2
10	15	2	1	0	1	2

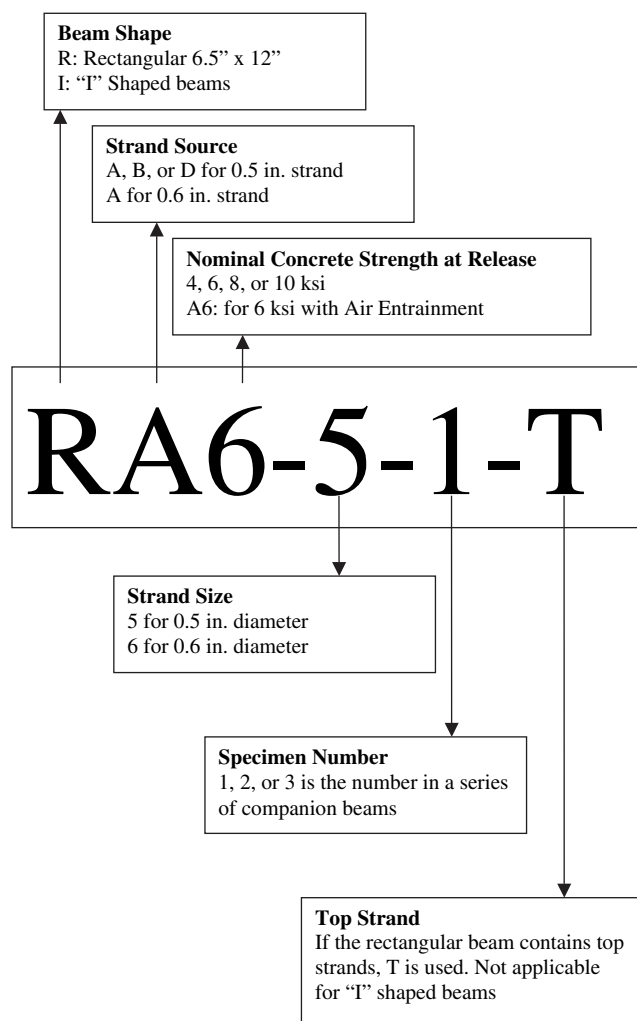


Figure 3.14. Beam number identification.

forcement consisting of four or two #4 bars, 96 in. long, located near the ends of the beams and anchored with standard hooks. Two horizontal #4 bars were placed at the south end of every beam, and four horizontal #4 bars were placed at the north end. The deck slab contained two #3 straight bars in the longitudinal direction in the deck slab.

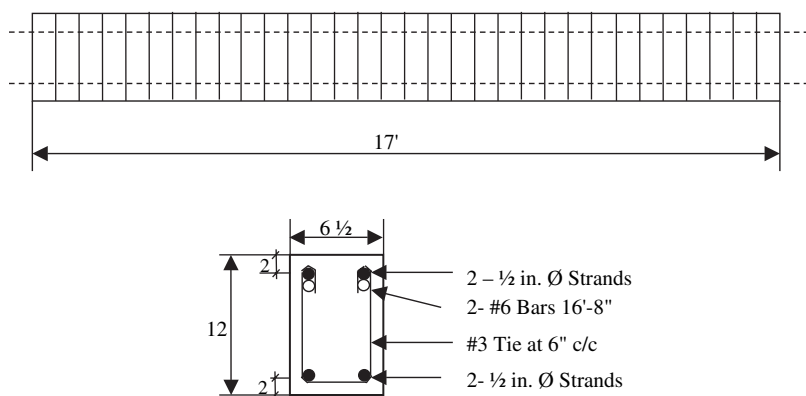


Figure 3.15. Details of four-strand beams.

Internal hoop reinforcements were placed in the form of triangular cages at both ends of the beam.

Strands were tensioned to 75 percent of f_{pu} (the guaranteed breaking strength) or 202.5 ksi. The expected elongations were calculated and compared with the measured elongations to ensure proper stressing. The strands were stressed to an initial level of 2,000 lb. Once the force on the strand reached 2,000 lb, the strand was marked with a permanent marker coinciding with the datum level marking on the prestressing bed. The strand was then stressed to 202.5 ksi. The elongation was then measured as the distance the mark on the strand moved from the datum marking on the prestressing bed.

Concrete was batched onsite at Coreslab's batch plant. Fresh properties of concrete, slump, unit weight, and air content were checked before casting the concrete. Extensive trial batching was performed (Tessema 2006) to determine the fresh and hardened properties of the concrete mix designs. If the fresh properties of unit weight, slump, or air content did not meet with the design expectations, the concrete was not used. Concrete cylinders were made at the site and placed in the same prestressing bed as the test beams until transfer. Steam curing was used if the ambient temperatures were low. The test beams together with the concrete cylinders were kept under cover if steam curing was used.

3.4.2 Measuring Transfer Lengths

Transfer lengths were measured on all strands by measuring the distance each strand slipped into the concrete after prestress release. A depth micrometer was used in combination with specially made clamps to measure the strand end slip. Figure 3.19 shows the depth micrometer measuring strand end slips immediately after prestress release.

Strand end slips are directly related to measured transfer lengths, as shown in Figure 3.20. In Figure 3.20, stresses are used to indicate the loss of prestress caused by elastic shortening (ES). After release, ES is the primary prestress loss. The transfer length of the strand is directly related to the area of

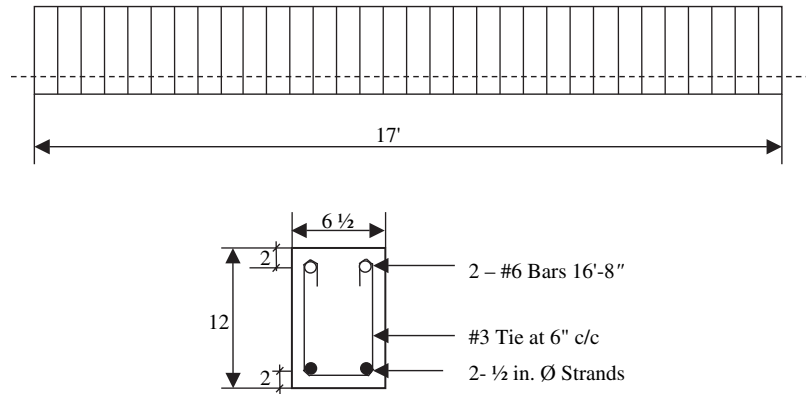


Figure 3.16. Details of two-strand beams.



Figure 3.17. Fabrication of rectangular beams.

the shaded triangle shown in Figure 3.20. The shaded area divided by the elastic modulus of the strand gives the strand end slip measurement. Thus, by measuring the strand end slip, the transfer length can be calculated directly. Over time, the beam experiences additional losses and a lengthening of the transfer length. The transfer length over time is illustrated in Figure 3.20 by the larger, unshaded triangle. In Figure 3.20, f_{si} is the stress in the prestressing strand just prior to release, and f_{se} is the strand stress after all losses. ES is the elastic shortening loss that occurs immediately upon release of the prestressing force.

Changes in concrete surface strains were measured on some of the specimens using a DEMEC gage. The DEMEC gage is pictured in Figure 3.21. DEMEC target points were set at 100-mm spacings. The DEMEC gage spans 200 mm, so readings were taken over a 200-mm gage length. The procedure

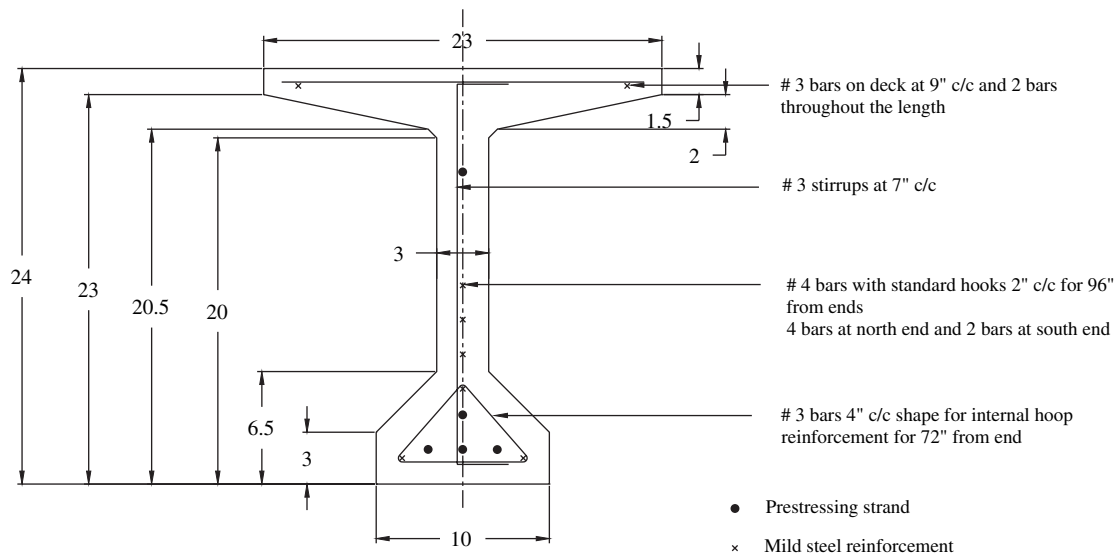


Figure 3.18. Details of I-shaped beams.

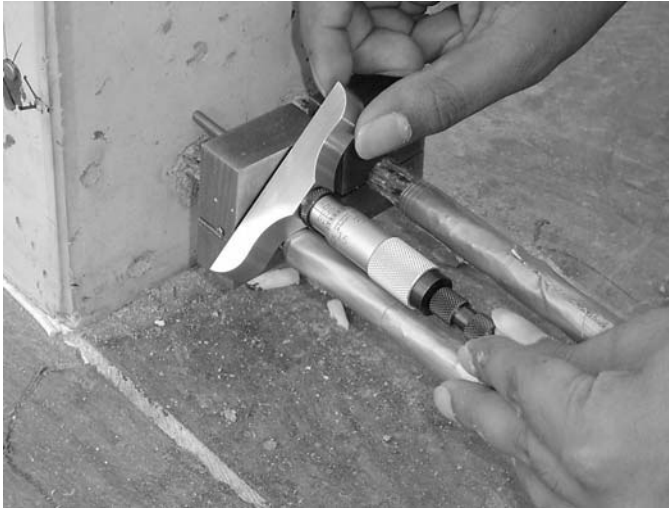


Figure 3.19. Strand end slip measurement using a micrometer.

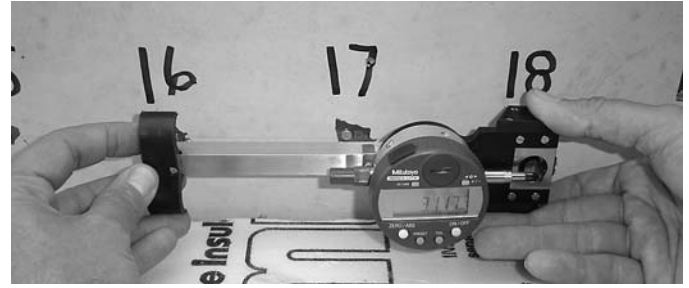


Figure 3.21. Concrete surface strain measurements with DEMEC gage.

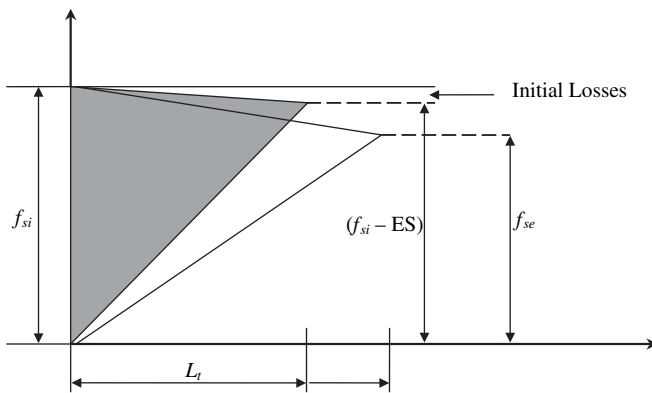


Figure 3.20. Variation in strand stress variations with length and relation to strand end slip measurements.

requires initial readings to be made prior to strand cutting. After release, the measurements are repeated, and the differences can be plotted as a strain profile, such as the one shown in Figure 3.22. As shown, concrete strains on the north end and the south end are plotted along the length of the beam. The strain profile is “smoothed” by averaging three measurement points. The Average Mean Strain (AMS) is found out by averaging the points on the strain plateau on the north and the south sides independently. The measured transfer length obtained from the DEMEC readings is the location where the 95-percent AMS line intersects the Smoothed Strain profile.

3.4.3 Results of the Transfer Length Measurements

Results of the transfer length measurements are reported in several tables, generally organized by strand type. Table 3.8 reports the transfer lengths computed from measured strand end slips on Strands A and B. Table 3.8 reports transfer lengths only on strands located at the bottom of the cross sections. Table 3.8 reports a transfer length for each

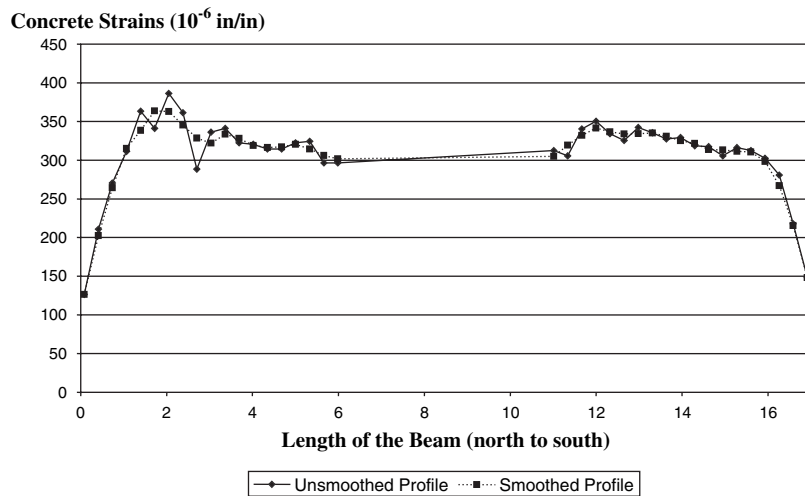


Figure 3.22. Concrete strain profile highlighting strand transfer lengths.

Table 3.8. Summary of transfer lengths at release for bottom Strands A/B.

Beam Number	Location	North	South	\bar{X} (kips)	S (kips)	\bar{f}'_c (psi)	$\bar{f}'_c(56d)$ (psi)
RB4-5-1	East	17.06	18.31	20.12	2.56	4,033	7,050
	West	19.78	18.66				
RB4-5-2	East	24.13	22.47	20.12	2.56	4,033	7,050
	West	18.1	22.45				
RA6-5-1	East	20.66	20.24	18.02	2.23	6,183	8,500
	West	17.68	16.16				
RA6-5-2	East	15.94	11.78	18.02	2.23	6,183	8,500
	West	17.12	18.23				
RA6-5-1T	East	19.39	18.7	18.02	2.23	6,183	8,500
	West	20.62	18.93				
RA6-5-2T	East	18.7	18.84	18.02	2.23	6,183	8,500
	West	19.07	16.27				
RA8-5-1	East	12.01	13.09	13.63	1.32	8,570	13,490
	West	14.58	13.9				
RA8-5-2	East	13.9	11.74	13.63	1.32	8,570	13,490
	West	15.93	12.42				
RA8-5-1T	East	(a)	12.51	13.63	1.32	8,570	13,490
	West	(b)	14.71				
RA8-5-2T	East	14.52	15.6	13.63	1.32	8,570	13,490
	West	12.55	13.36				
RA10-5-1	East	(c)	(d)	13.72	2.27	9,711	14,470
	West	(e)	13.57				
RA10-5-2	East	12.75	15.25	13.72	2.27	9,711	14,470
	West	12.75	14.8				
RA10-5-1T	East	17.74	12.06	13.72	2.27	9,711	14,470
	West	18.16	11.32				
RA10-5-2T	East	12.2	11.78	13.72	2.27	9,711	14,470
	West	11.46	14.53				

(a) L_t of 1.48 in. not included (c) L_t of 25.65 in. not included
(b) L_t of 5.26 in. not included (d) L_t of 5.82 in. not included
(e) L_t of 22.89 in. not included

strand, two at each end of the beam, with each end of the beam designated as either north or south; thus, all together, four transfer length measurements are reported for each beam.

Table 3.8 also reports the average transfer length for all of the transfer length measurements on beams for a particular concrete strength, \bar{X} . The standard deviation, S is reported in inches for the data set. The release strength, \bar{f}'_c (psi), is the average of at least three 4 in. by 8 in. cylinders. The 56-day strength, $\bar{f}'_c(56d)$, is the average of three cylinders placed in laboratory curing conditions.

Table 3.9 reports the measured transfer lengths on beams that contained air-entrained concrete. Only Strand A was used for this set of beams. While the transfer lengths measured in air-entrained concrete appear to be longer than the transfer lengths measured in the companion beams without air entrainment, no clear pattern emerges with the limited data.

Table 3.10 reports the measured transfer lengths for Strand A, placed near the tops of cross sections in the respective beams. Again, no clear pattern emerges of the top strands having longer transfer lengths than the bottom strands.

Table 3.11 reports the measured transfer lengths for 0.5 in diameter Strand D. Table 3.11 includes the beam number, the measured transfer length for each strand, the average transfer length for Strand D by concrete strength, the standard deviation of the transfer lengths, and 1-day and 56-day concrete strengths.

Table 3.12 reports transfer lengths measured on Strand D placed in top locations of four-strand beams. Again, there is no clear pattern of top strands having longer transfer lengths than bottom strands.

Table 3.13 reports transfer lengths measured on I-shaped beams, including data from both 0.5 in. diameter strands—Strand A and Strand D—and data from the 0.6 in. diameter

Table 3.9. Summary of transfer lengths at release of bottom Strands A/B in air-entrained concrete.

Beam Number	Location	North	South	\bar{X} (kips)	S (kips)	\bar{f}'_{ci} (psi)	$\bar{f}'_c(56d)$ (psi)
RA6A-5-1	East	19.26	17.47	20.49	3.39	7,960	11,420
	West	16.22	17.88				
RA6A-5-2	East	26.41	22.63	26.26	6.93	7,960	11,420
	West	22.6	21.42				
RD6A-5-1	East	36.25	30.04	26.26	6.93	7,960	11,420
	West	34.55	28.15				
RD6A-5-2	East	21.16	21.79	26.26	6.93	7,960	11,420
	West	19.79	18.36				

strand, Strand A6. As in Tables 3.8 through 3.12, measured transfer lengths are reported for each strand, the average and standard deviation are reported for each beam, along with concrete strengths at release and at 56 days. Table 3.13 includes data collected from strands located in the bottom bulbs on the I-shaped beams only.

Table 3.14 reports the measured transfer lengths on top strands from the I-shaped beams. The data are erratic, so no conclusions can be drawn from these measurements. All of the transfer lengths reported in Tables 3.8 through 3.14 report transfer lengths measured immediately after release.

Tables 3.15, 3.16 and 3.17 all include both transfer length measurements made with the DEMEC gage and transfer length measurements made from strand end slips for comparison. Approximately 43 percent of the beam ends had

transfer length measured using both methods. Figure 3.23 presents the data from Tables 3.15 through 3.17 graphically and shows that generally the transfer lengths measured by the DEMEC gage are approximately the same as the transfer lengths obtained from strand end slip measurements.

Tables 3.18 through 3.22 provide the transfer length measurements over time, from release through 240 days after release. Strand end slips can be measured individually for each strand. In the tables reporting measured transfer lengths from strand end slips, the east strand is represented in the column headed by "E" whereas the west strand is reported in the columns headed by "W." Transfer lengths were not measured beyond release for beams RB4-5-1 and RB4-5-2. As the data indicate, transfer lengths grow over time, and the 240-day transfer lengths are considerably longer than the transfer lengths measured at release. All of the transfer

Table 3.10. Summary of transfer lengths at release of Strand A in top locations.

Beam Number	Location	North	South	\bar{X} (kips)	S (kips)	\bar{f}'_{ci} (psi)	$\bar{f}'_c(56d)$ (psi)
RA6-5-1T	East	21.03	19.11	19.04	2.07	6,183	8,500
	West	19.47	20.58				
RA6-5-2T	East	17.07	16.52	14.55	1.96	8,570	13,490
	West	21.82	16.71				
RA8-5-1T	East	13.38	14.88	14.55	1.96	8,570	13,490
	West	10.74	14.42				
RA8-5-2T	East	17.61	15.7	14.55	1.96	8,570	13,490
	West	15.12	14.56				
RA10-5-1T	East	14.93	13.5	12.90	1.65	9,711	14,470
	West	14.53	11.32				
RA10-5-2T	East	10.63	11.2	12.90	1.65	9,711	14,470
	West	14.11	12.99				

Table 3.11. Summary of transfer lengths at release for bottom Strand D.

Beam Number	Location	North	South	\bar{X} (kips)	S (kips)	\bar{f}'_{ci} (psi)	$\bar{f}'_c(56d)$ (psi)				
RD4-5-1	East	31.69	32.11	32.90	2.64	4,033	7,050				
	West	33.88	29.93								
RD4-5-2	East	36.9	(a)	32.90	2.64	4,033	7,050				
	West	(b)	(c)								
RD6-5-1	East	29.88	30.42	26.19	2.99	6,183	8,500				
	West	30.6	25.71								
RD6-5-2	East	25.35	30.15								
	West	25.84	28.29								
RD6-5-1T	East	23.89	25.12								
	West	23.43	26.59								
RD6-5-2T	East	25.53	19.93								
	West	24.67	23.71								
RD8-5-1	East	21.16	20.89					20.94	6.05	8,570	13,490
	West	19.13	19.41								
RD8-5-2	East	16.79	21.43								
	West	10.54	13.17								
RD8-5-1T	East	35.63	29.78								
	West	15.94	26.34								
RD8-5-2T	East	20.87	21.99								
	West	18.99	23.01								
RD10-5-1	East	23.48	16.16	18.36	3.72	9,711	14,470				
	West	28.59	17.54								
RD10-5-2	East	13.95	19.33								
	West	15.74	17.12								
RD10-5-1T	East	21.76	16.22								
	West	21.1	17.4								
RD10-5-2T	East	16.36	15.25								
	West	17.13	16.58								

(a) Excessive movement of the beams during flame cutting, L_t observed as 50.43 in.
(b) Excessive movement of the beams during flame cutting, L_t observed as 47.48 in.
(c) Excessive movement of the beams during flame cutting, L_t observed as 48.98 in.

length measurements over time were made using the strand end slip method.

3.4.4 Discussion of Transfer Length Measurements

The discussion on transfer lengths focuses on two essential elements: (1) what effects, if any, concrete strength has on transfer length and (2) whether the NASP Bond Test provides an indicator regarding transfer length. Another objective of this discussion is to present to the industry a reasonable code equation to adequately predict the transfer lengths of pre-tensioned strands.

Figure 3.24 illustrates the transfer length measurements at release plotted against the concrete strengths at 1 day of age for Strands A/B. (Although Strand A and Strand B represent two different sources of strand, their NASP Bond Test values were very similar; therefore, the data from the two strands are treated as part of one data set.) Two regression curves are shown in Figure 3.24; one shows the best fit for data derived from the DEMEC gage, and the other shows the best fit for the data derived from strand end slip measurements. Both regression curves in Figure 3.24 show that transfer lengths shorten as concrete strengths increase.

Figure 3.25 shows the transfer length measurements at release plotted against the concrete strengths at 1-day of age for

Table 3.12. Summary of transfer lengths at release for Strand D in top locations.

Beam Number	Location	North	South	X_{\parallel} (kips)	S (kips)	\bar{f}'_{ci} (psi)	$\bar{f}'_c(56d)$ (psi)
RD6-5-1T	East	27.91	21.46	23.76	3.03	6,183	8,500
	West	27.52	20.26				
RD6-5-2T	East	23.7	20.2	22.64	4.68	8,570	13,490
	West	23.61	25.43				
RD8-5-1T	East	22.06	16.45	15.93	2.22	9,711	14,470
	West	17.61	18.84				
RD8-5-2T	East	27.82	23.71	10.77	5.43	5,810	9,350
	West	28.67	25.94				
RD10-5-1T	East	16.79	15.56	10.59	2.15	7,615	13,490
	West	17.27	16.32				
RD10-5-2T	East	18.98	15.02	18.49	9.88	5,492	9,840
	West	16.19	11.29				

Table 3.13. Summary of transfer lengths at release for I-shaped beams—bottom Strands B and D (0.5 in.) and Strand A6 (0.6 in.).

Beam Number	Location	North	South	X_{\parallel} (kips)	S (kips)	\bar{f}'_{ci} (psi)	$\bar{f}'_c(56d)$ (psi)
IB6-5-1	East	16.12	6.42	10.77	5.43	5,810	9,350
	West	17.82	2.9				
	Cent.	10.93	9.45				
	Midd.	16	6.48				
IB10-5-1	East	11.14	12.45	10.59	2.15	7,615	13,490
	West	10.03	5.8				
	Cent.	11.6	12.45				
	Midd.	11.31	9.9				
ID6-5-1	East	24.47	12.23	18.49	9.88	5,492	9,840
	West	23.47	2.56				
	Cent.	26.69	(a)				
	Midd.	28.96	11.04				
ID10-5-1	East	19.03	19.03	20.82	2.8	8,225	14,160
	West	20.34	23.61				
	Cent.	15.99	21.13				
	Midd.	23.51	23.94				
IA6-6-1	East	18.36	16.33	21.17	4.68	4,381	8,990
	West	29.83	22.21				
	Cent.	20.15	20.15				
IA6-6-2	East	9.62	14.18	16.04	4.49	10,480	14,990
	West	15.48	19.47				
	Cent.	22.58	14.92				
IA10-6-1	East	9.4	21.15	13.29	5.91	10,590	14,930
	West	14.35	5.81				
	Cent.	10.19	18.85				
IA10-6-2	East	17.94	10.64	14.72	3.46	10,590	14,930
	West	13.85	10.76				
	Cent.	17.83	17.32				

(a) Spalling of concrete surface during flame cutting

Table 3.14. Summary of transfer lengths at release for top strands in I-shaped beams.

Beam Number	Location	North	South	\bar{X} (kips)	S (kips)	\bar{f}'_{ci} (psi)	$\bar{f}'_{c(56d)}$ (psi)
IA6-6-1	Top	22.84	9.36	18.57	6.23	4,381	8,990
IA6-6-2	Top	20.22	21.84				
IA10-6-1	Top	3.82	1.91	2.87	1.35	10,480	14,990
IA10-6-2	Top	9.3	9.04	9.17	0.18	10,590	14,930
IB6-5-1	Top	21.43	6.16	13.80	10.80	5,810	9,350
ID6-5-1	Top	36.25	29.99	33.12	4.4	5,492	9,840
ID10-5-1	Top	(a)	16.86	16.86	-	8,225	14,160

(a) End clamp loosened during detensioning

Table 3.15. Transfer length at release measured by DEMEC gage and strand end slip for 0.5-in. Strands A/B.

Beam	Strand End Slips		DEMEC	
	North (in.)	South (in.)	North (in.)	South (in.)
RB4-5-1	18.4	18.5	24.2	27.1
RB4-5-2	21.1	22.5	-	-
RA6A-5-1	17.7	17.7	16.0	17.5
RA6A-5-2	24.5	22.0	-	-
RA6-5-1	19.2	18.2	-	-
RA6-5-2	16.5	15.0	-	-
RA6-5-1-T	20.3	19.8	-	-
RA6-5-2-T	19.4	16.6	-	-
RA8-5-1	13.3	13.5	14.3	12.0
RA8-5-2	14.9	12.1	-	-
RA8-5-1-T	12.1	14.7	12.0	15.6
RA8-5-2-T	16.4	15.1	-	-
RA10-5-1	24.3	9.7	24.3	14.4
RA10-5-2	12.8	15.0	-	-
RA10-5-1-T	14.7	12.4	12.5	11.7
RA10-5-2-T	12.4	12.1	-	-
IB6-5-1	12.2	Not available	15.2	-
IB10-5-1	11.1	Not available	11.0	-

- measurements were not taken.

Table 3.16. Transfer length at release measured by DEMEC gage and strand end slip for 0.5-in. Strand D.

Beam	Strand End Slips		DEMEC	
	North (in.)	South (in.)	North (in.)	South (in.)
RD4-5-1	32.8	31.0	25.6	24.8
RD4-5-2	36.9	Not available	–	–
RD6A-5-1	35.4	29.1	39.0	26.4
RD6A-5-2	20.5	20.1	–	–
RD6-5-1	30.2	28.1	–	–
RD6-5-2	25.6	29.2	–	–
RD6-5-1-T	27.7	20.9	–	–
RD6-5-2-T	23.7	22.8	–	–
RD8-5-1	20.2	20.2	11.3	18.5
RD8-5-2	13.7	17.3	–	–
RD8-5-1-T	19.8	17.6	12.4	12.0
RD8-5-2-T	28.2	24.8	–	–
RD10-5-1	26.0	16.9	23.4	19.4
RD10-5-2	14.8	18.2	–	–
RD10-5-1-T	17.0	15.9	16.1	15.7
RD10-5-2-T	17.6	13.2	–	–
ID6-5-1	25.2	Not available	25.9	–
ID10-5-1	17.5	Not available	19.7	–

– measurements were not taken.

Table 3.17. Transfer Length at release measured by DEMEC gage and strand end slip for 0.6-in. Strand A6.

Beam	Strand End Slips		DEMEC	
	North (in.)	South (in.)	North (in.)	South (in.)
RA4-6-1	33.4	25.0	31.4	30.3
RA4-6-2	30.2	29.3	–	–
RA6-6-1	29.7	28.2	22.4	21.1
RA6-6-2	31.7	30.1	–	–
RA6-6-3	25.8	33.6	–	–
RA8-6-1	28.2	29.2	19.5	22.0
RA8-6-2	28.2	25.7	–	–
RA8-6-3	22.8	28.3	–	–
RA10-6-1	20.0	21.9	16.6	15.0
RA10-6-2	15.6	21.8	–	–
RA10-6-3	16.3	22.7	–	–
IA6-6-2	24.3	26.1	15.9	16.2
IA10-6-1	18.0	Not available	11.3	–
IA10-6-2	16.0	Not available	16.5	–

– measurements were not taken.

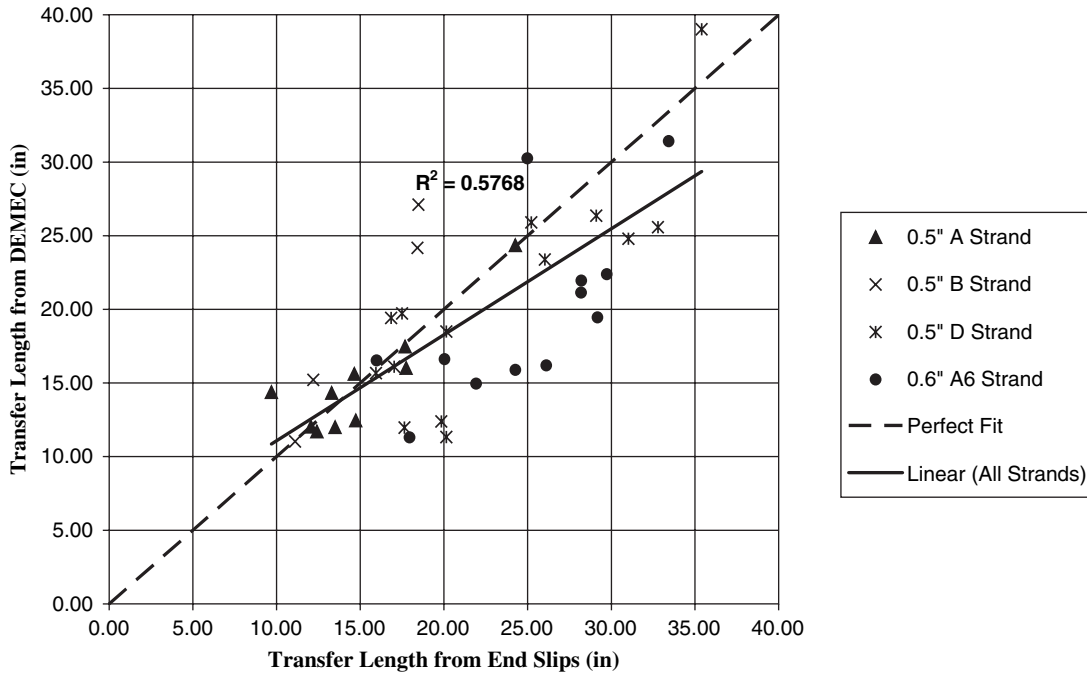


Figure 3.23. Transfer lengths measured by DEMEC gage versus transfer lengths measured by strand end slip.

Table 3.18. Change in transfer lengths over time for bottom 0.5 in. diameter Strands A/B in two-strand rectangular beams.

Beam Number	Transfer Length at Release from Strand End Slips (in.)		Transfer Length after 60 Days from Strand End Slips (in.)		Transfer Length after 90 Days from Strand End Slips (in.)		Transfer Length from 240 Days from Strand End Slips (in.)	
	North	South	North	South	North	South	North	South
	Average W & E		Average W & E		Average W & E		Average W & E	
RB4-5-1	18.42	18.48						
RB4-5-2	21.11	22.46						
RA6-5-1	19.17	18.20	33.07	28.86	33.07	29.55	33.69	30.03
RA6-5-2	16.53	15.01	26.57	20.82	26.56	23.38	27.95	23.52
RA6A-5-1	17.74	17.68	25.23	26.62	26.33	28.14	26.54	28.55
RA6A-5-2	24.50	22.02	28.92	27.72	31.41	29.03	31.75	29.38
RA8-5-1	13.30	13.50	15.59	21.13	17.68	21.46	24.91	22.54
RA8-5-2	14.92	12.08	22.07	19.24	23.69	19.71	35.23	19.98
RA10-5-1	24.27	9.69	23.92	9.83	24.13	12.11	24.34	13.14
RA10-5-2	12.75	15.02	16.47	16.67	18.05	17.23	19.15	17.30

Table 3.19. Change in transfer lengths over time for bottom 0.5-in. diameter Strand D in two-strand rectangular beams.

Beam Number	Transfer Length at Release from Strand End Slips (in.)		Transfer Length after 60 Days from Strand End Slips (in.)		Transfer Length after 90 Days from Strand End Slips (in.)		Transfer Length from 240 Days from Strand End Slips (in.)	
	North	South	North	South	North	South	North	South
	Average W & E		Average W & E		Average W & E		Average W & E	
RD4-5-1	32.78	31.02						
RD4-5-2	42.19	49.70						
RD6-5-1	30.24	28.07	43.00	38.57	46.82	44.37	49.75	45.26
RD6-5-2	25.60	29.22	36.79	39.87	41.99	44.72	44.24	48.27
RD6A-5-1	35.40	29.10	37.39	34.47	39.40	36.41	39.94	37.16
RD6A-5-2	20.48	20.08	26.26	35.24	30.73	39.37	32.39	40.07
RD8-5-1	20.15	20.15	28.34	26.55	32.66	30.33	39.08	34.54
RD8-5-2	13.66	17.30	34.14	46.08	36.82	47.73	37.38	50.41
RD10-5-1	26.03	16.85	26.31	25.27	26.45	26.51	30.24	27.14
RD10-5-2	14.85	18.23	17.47	20.16	18.71	22.30	22.30	22.03

Table 3.20. Change in transfer lengths over time for 0.6-in. Strand A6 in two-strand rectangular beams.

Beam Number	Transfer Length at Release from Strand End Slips (in.)		Transfer Length after 60 Days from Strand End Slips (in.)		Transfer Length after 90 Days from Strand End Slips (in.)		Transfer Length from 240 Days from Strand End Slips (in.)	
	North	South	North	South	North	South	North	South
	Average W & E		Average W & E		Average W & E		Average W & E	
RA4-6-1	33.42	24.98						
RA4-6-2	30.24	29.35						
RA6-6-1	29.73	28.19	36.87	41.73	39.00	44.45	40.85	55.13
RA6-6-2	31.65	30.10	47.03	46.36	49.24	48.20	52.18	49.37
RA6-6-3	25.83	33.63	39.73	44.60	44.08	44.82	44.96	45.93
RA8-6-1	28.21	29.17	42.46	41.87	43.87	43.26	45.48	43.41
RA8-6-2	28.20	25.70	42.68	38.55	46.28	42.35	46.35	42.37
RA8-6-3	22.80	28.26	36.85	44.00	41.17	46.93	43.00	49.22
RA10-6-1	20.03	21.92	25.69	25.77	28.08	28.82	29.98	32.15
RA10-6-2	15.62	21.78	20.99	25.99	26.14	29.47	26.79	30.70
RA10-6-3	16.34	22.73	24.46	28.82	26.13	32.30	27.73	33.32

Table 3.21. Change in transfer length over time for 0.5-in. Strand A in four-strand rectangular beams.

Beam Number and Location	Transfer Length at Release from Strand End Slips (in.)		Transfer Length after 60 Days from Strand End Slips (in.)		Transfer Length after 90 Days from Strand End Slips (in.)		Transfer Length after 240 Days from Strand End Slips (in.)	
	North	South	North	South	North	South	North	South
	Average W & E		Average W & E		Average W & E		Average W & E	
RA8-5-1-T (Top)	12.06	14.65	24.27	24.67	24.96	26.18	25.16	27.21
(Bottom)	3.37	13.61	11.59	21.29	11.66	25.11	12.80	27.27
RA8-5-2-T (Top)	16.37	15.13	27.30	27.30	28.20	28.68	28.96	29.44
(Bottom)	13.54	14.48	22.03	24.25	23.31	25.40	24.05	25.33
RA6-5-1-T (Top)	20.25	19.84	33.01	32.69	34.46	34.96	34.60	34.89
(Bottom)	20.00	18.82	31.92	26.29	34.06	28.36	34.06	28.56
RA6-5-2-T (Top)	19.44	16.61	37.07	35.15	39.33	37.28	40.64	37.49
(Bottom)	18.89	17.55	45.33	35.77	47.82	42.71	49.55	43.34
RA10-5-1-T (Top)	14.73	12.41	21.59	18.79	22.16	19.43	22.16	19.70
(Bottom)	17.95	11.69	19.00	14.40	19.07	15.30	19.62	15.93
RA10-5-2-T (Top)	12.37	12.10	14.29	22.15	15.42	22.22	15.63	22.36
(Bottom)	11.83	13.16	16.28	16.01	16.56	16.29	17.33	16.43

Table 3.22. Change in transfer length over time for 0.5-in. Strand D in four-strand rectangular beams.

Beam Number and Location	Transfer Length at Release from Strand End Slips (in.)		Transfer Length after 60 Days from Strand End Slips (in.)		Transfer Length after 90 Days from Strand End Slips (in.)		Transfer Length from 240 Days from Strand End Slips (in.)	
	North	South	North	South	North	South	North	South
	Average W & E		Average W & E		Average W & E		Average W & E	
RD8-5-1-T (Top)	19.84	17.64	35.57	35.90	40.15	39.59	41.18	42.47
(Bottom)	25.78	28.06	23.98	38.41	30.63	41.05	27.73	44.59
RD8-5-2-T (Top)	28.25	24.82	65.51	67.04	67.56	68.62	68.52	68.62
(Bottom)	19.93	22.50	49.52	32.36	50.91	33.26	52.86	35.00
RD6-5-1-T (Top)	27.71	20.86	53.89	56.65	57.32	59.03	58.79	60.29
(Bottom)	23.66	25.85	38.10	38.09	40.76	42.20	42.89	45.27
RD6-5-2-T (Top)	23.66	22.81	49.07	48.64	57.90	53.33	63.27	54.49
(Bottom)	25.10	21.82	65.45	39.67	69.56	44.05		
RD10-5-1-T (Top)	17.03	15.94	26.10	24.12	27.87	26.36	30.19	27.11
(Bottom)	21.43	16.81	23.51	19.77	23.51	21.63		23.77
RD10-5-2-T (Top)	17.58	13.15	24.81	23.58	26.30	24.95	26.58	26.99
(Bottom)	16.74	15.92	24.05	23.01	25.98	23.01	28.18	23.01

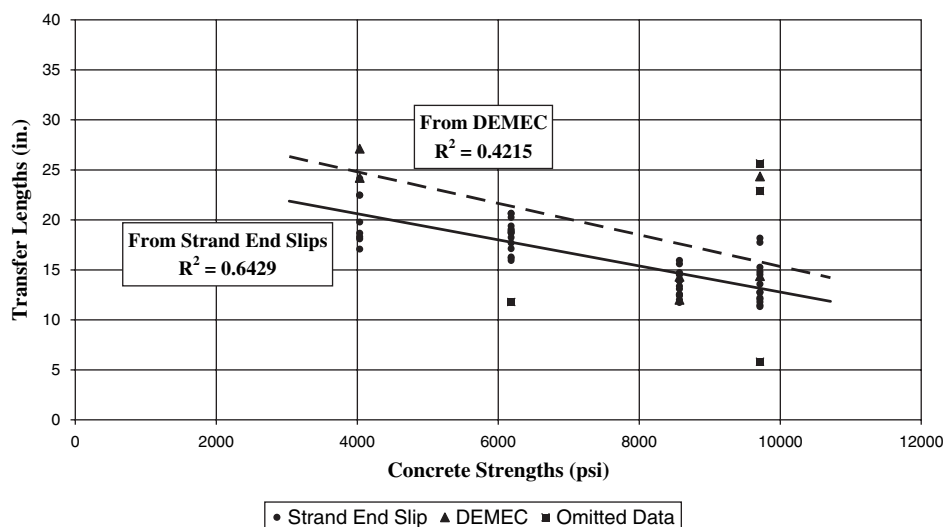


Figure 3.24. Transfer length versus \bar{f}'_d for Strands A/B in rectangular beams.

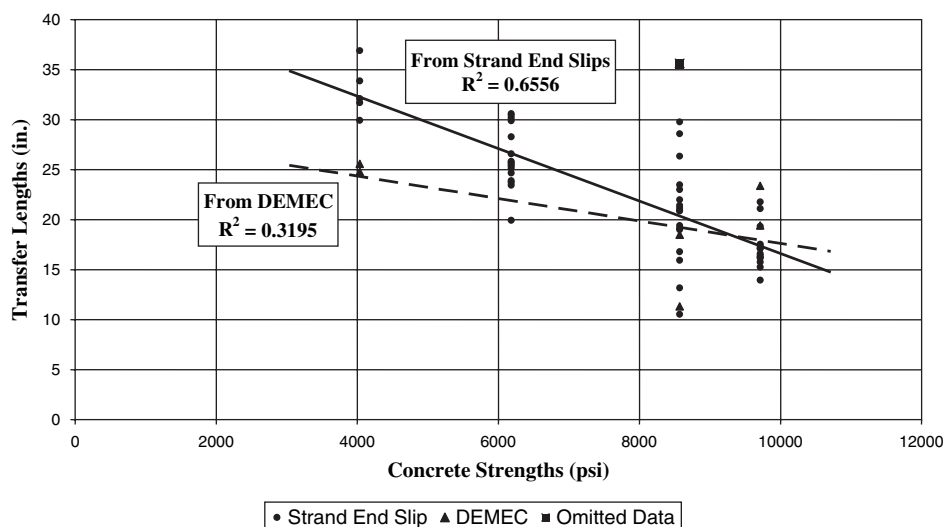


Figure 3.25. Transfer length versus \bar{f}'_d for Strand D in rectangular beams.

Strand D. Again, it is clear that the transfer length decreases with increasing concrete strength.

Finally, Figure 3.26 illustrates the transfer length measurements taken on beams made with the 0.6 in. diameter strand, Strand A6. Again, the data clearly show the inverse relationship between transfer lengths and concrete strength. The data from all three of the strand sources are illustrated in Figure 3.27, where the transfer lengths for each strand are plotted against the concrete strengths at release.

Figures 3.24 through 3.27 show the relation between transfer length data and linear regression models. Linear regression is often used because the methodology is less abstract than others and perhaps more easily understood. However, there is a direct relationship between the NASP Bond Test values in concrete and the square root of concrete strengths. Figures 3.12 and 3.13 show a strong correlation between the NASP

Bond Test value and the square root of concrete strength. The coefficient of determination in those comparisons is a very robust 0.8. If the NASP Bond Test value, which is a direct measure of bond between the strand and concrete, varies with the square root of concrete strength, then it is logical that the transfer length would also vary with the square root of concrete strength.

Figure 3.28 plots the same data as Figure 3.27, but does a best-fit curve from power regressions. The coefficients of determination for these power curves are nearly as good as the coefficients of determination for the linear regressions. Furthermore, the best-fit regressions provide an exponent in the equation of -0.56 , -0.83 and -0.56 . As a reminder, the inverse of the square root would be an exponent of -0.50 .

Figure 3.29 plots the transfer lengths for Strands A/B at release and at 240 days after release. The data are fitted to a

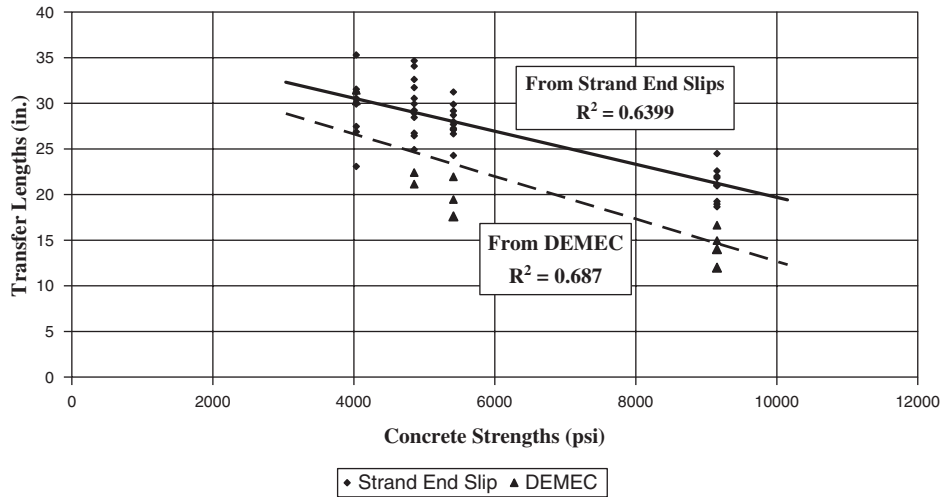


Figure 3.26. Transfer length versus \bar{f}'_{ci} for Strand A6 (0.6 in) in rectangular beams.

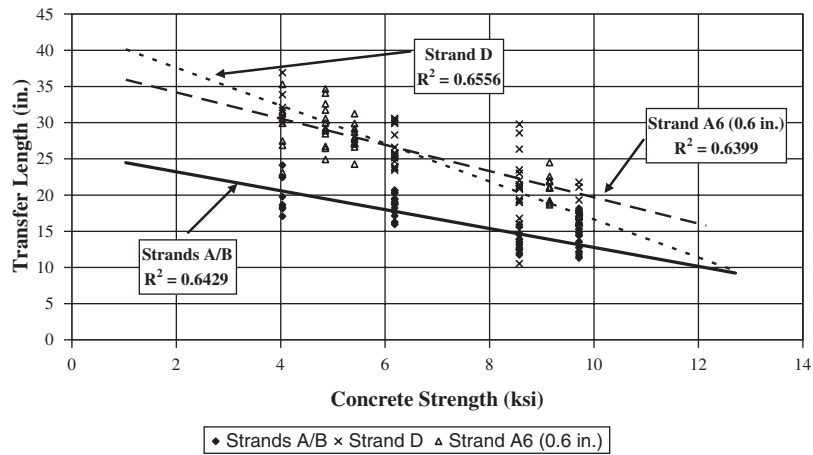


Figure 3.27. Linear regression for transfer lengths and f'_{ci} .

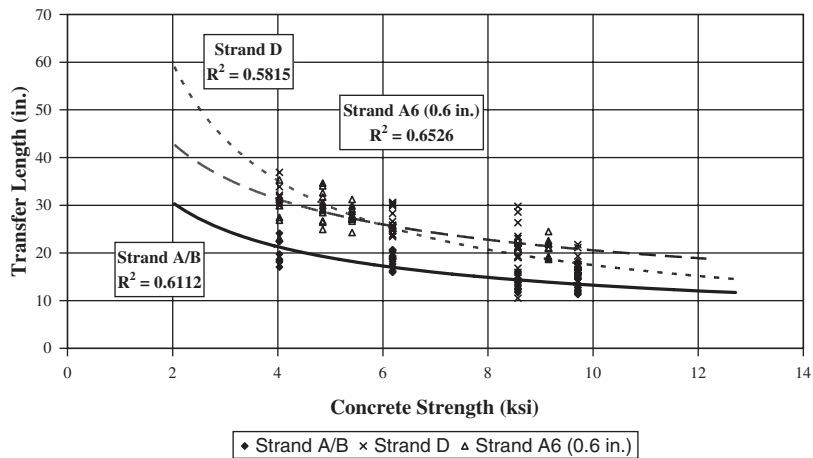


Figure 3.28. Power regression for transfer lengths and f'_{ci} .

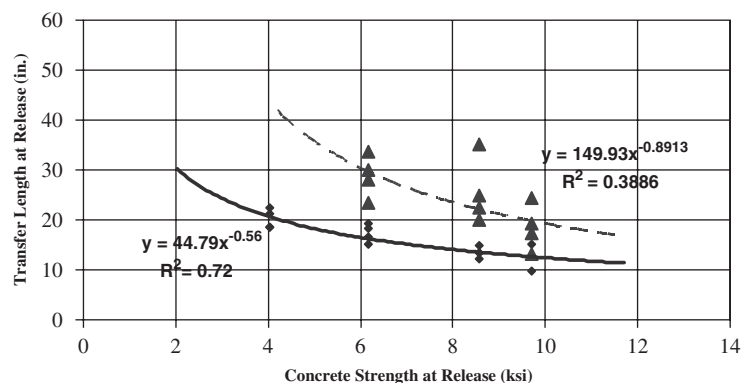


Figure 3.29. Transfer lengths versus concrete strengths for 0.5-in. Strands A/B at release and at 240 days.

power regression curve. The best-fit equations are also shown in Figure 3.29. In Figures 3.29 through 3.32, transfer length data obtained immediately after release are represented by diamond-shaped data points and the solid regression curve. Transfer lengths measured at 240 days are represented by triangular-shaped data points and the dashed regression curve.

Figure 3.30 plots the transfer lengths for Strand D at both release and at 240 days after release. Again, these data are fitted to a power regression curve. Note that the transfer lengths

for Strand D are considerably longer than those for Strands A/B. Recall that Strand D had a NASP Bond Test value of 6,890 lb, whereas both Strands A and B had NASP Bond Test values in excess of 20,000 lb (see Table 3.3). These data would support the idea that higher NASP Bond Test values will result in shorter transfer lengths.

Figure 3.31 plots the same data but for the 0.6 in. diameter strand, Strand A6. Again, the data clearly show that transfer lengths decrease with increasing concrete strength.

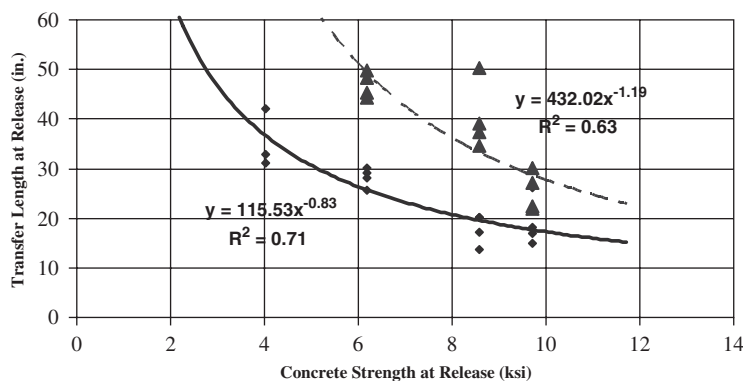


Figure 3.30. Transfer lengths versus concrete strengths for 0.5-in. Strand D at release and at 240 days.

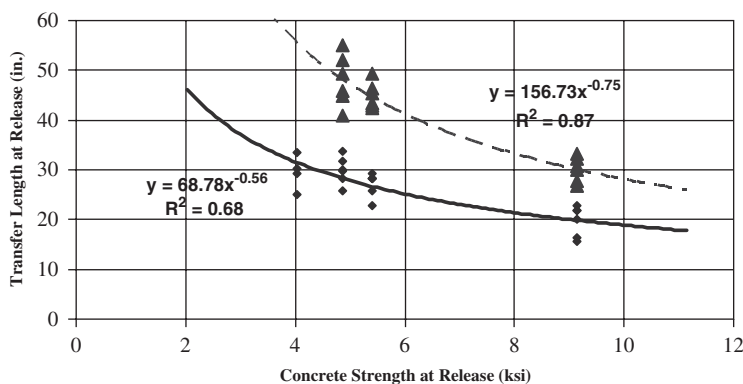


Figure 3.31. Transfer lengths versus concrete strengths for 0.6-in. Strand A6 at release and at 240 days.

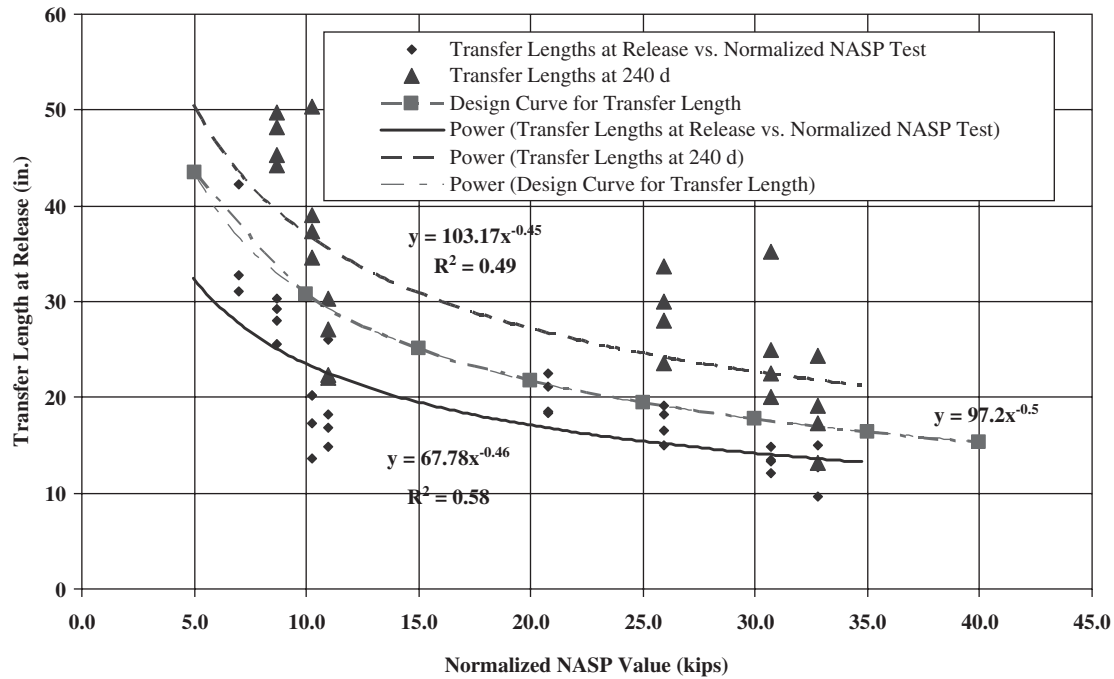


Figure 3.32. Transfer lengths versus normalized NASP bond values for Strands A/B and plotted together at release and at 240 days.

Finally, in Figure 3.32, the transfer lengths at release and at 240 days after release are plotted against the normalized NASP Bond Test value. The normalized NASP Bond Test value is obtained from Equation 3.1. In Equation 3.1, the normalized value can be obtained because the ratio of the NASP Bond Test Value in concrete to the standard NASP Bond Test value (in mortar) is essentially equal to one-half of the square root of the concrete strength at 1 day. In this manner, data from strands with widely dissimilar NASP Bond Test values can be plotted on the same chart and the results compared. In Figure 3.32, we see that the power regression curve fits through both sets of data. The data set shown with lower NASP Bond Test values, toward the left side of the chart, are the data derived from Strand D; data with higher NASP Bond Test values, toward the right side of the chart, are obtained from Strands A/B. The power regression curve shows a best fit with an exponent of -0.46 .

Also plotted on Figure 3.32 is the curve that corresponds to the proposed equation for transfer length. The normalized NASP Bond Test value is obtained from Equation 3.1. For example, for a concrete strength of 4 ksi, the transfer length should be 60 strand diameters. For 0.5 in. diameter strand, the transfer length would be 30 in. The data illustrated in Figure 3.32 show that transfer lengths are shortened with increasing NASP Bond Test values. However, it is not proposed to shorten the transfer length equation as a function of NASP Bond Test values. It is worth noting, however, that the data illustrated in Figures 3.12, 3.13, and 3.32 clearly show that increases in concrete strength have a similar effect in

improving bond, as do the increasing NASP Bond Test values. The proposed design equation shown indicates that transfer length can be obtained by dividing 97.2 in. by the square root of the normalized NASP Bond Test value. The normalized NASP Bond Test value factors in the same factor for the square root of the concrete strength. The proposed design equation will provide a transfer length of 60 strand diameters for concrete strength of 4 ksi. Increasing concrete strengths will reduce the proposed transfer length in proportion to the square root of the concrete strength.

3.5 Development Length Tests

Measured transfer and development lengths of prestressing strands are indications of the quality of bond between the strand and concrete. The research conducted as part of NCHRP Project 12-60 and described earlier resulted in five overarching conclusions:

1. The Standard NASP Bond Test method provides a reliable and repeatable method to test for the bond performance of prestressing strands. Results were found to be repeatable at different testing sites.
2. The Standard NASP Bond Test is able to determine acceptable quality levels for bond of prestressing strands. This ability is demonstrated by the correlation of NASP Bond Test results with measured transfer lengths. Increases in measured transfer lengths correlate directly with decreases in bond performance, as measured by the NASP

Bond Test. The development length tests reported in this chapter supplement the findings from the NASP Bond Tests and transfer length measurements.

3. The NASP Bond Test can be modified by testing strand bond performance in concrete instead of mortar. The modified NASP Bond Tests in concrete demonstrate that increases in concrete strength result in improving bond performance. The results develop a strong statistical correlation, and the best fit indicates that bond strength improves in proportion to the square root of concrete strength.
4. Concrete strength influences the bond of prestressing steel with concrete. In the NASP Bond Tests (modified), increasing concrete strengths resulted in increasing bond strength between strand and concrete. In beams where transfer lengths were measured, increasing concrete strength correlated to shortening transfer lengths. The measured pull-out forces from the NASP Bond Tests established that bond strength improves in proportion to the square root of concrete strength at release.
5. The transfer length data further establish that measured transfer lengths decrease in inverse proportion (approximately) to the square root of concrete strength. The influence of concrete strength and NASP Bond Test value correlates with the inverse of strand end slip measurement, which is a direct indicator of transfer lengths.

The development length tests are necessary to determine the following:

- Whether the NASP Bond Test can be used as a predictor of strand bond performance in flexural applications,
- The minimum acceptable level of bond performance as measured by the NASP Bond Test, and
- What modifications are necessary to the LRFD development length equation to account for variations in concrete strength.

3.5.1 Testing Program

The experimental program consisted of the flexural tests on two types of beam specimens:

- **Rectangular beam specimens.** In all, 43 rectangular beam specimens were fabricated with target release concrete strengths varying from 4 ksi to 10 ksi. Rectangular beams were cast with two prestressing strands at a depth of 10 in. in a beam 12-in. deep. Both 0.5 in and 0.6 in diameter strands were used. The rectangular beams were 7 ft in length and designed to be tested independently at each end to assess the development length of embedded strands. Prior to development length testing, transfer lengths were

measured on each beam end, either directly by measuring concrete surface strain or indirectly by measuring strand end slip before release.

- **I-shaped beam specimens.** In all, eight I-shaped beam specimens were fabricated with target concrete release strengths of 6 ksi and 10 ksi. These beams were 24 ft in length and designed to be tested at each end. Transfer lengths were also measured on these beams prior to development length testing.

3.5.1.1 Terminology

The testing program terminology was as follows.

Embedment length, l_e . For the purposes of this research and generally in the broader literature, the embedment length is the length of bond provided from the beginning of bond (usually at the end of the beam) to the critical section of the beam. The critical section in these tests is generally understood to be the section where maximum moment occurs. In this testing program, the embedment length is the distance from the end of the beam to the point of loading, which corresponds to the point of maximum moment.

Development length, l_d . Development length of prestressing strands is the minimum distance from the free end of the strand over which the strand should be bonded to concrete so that the section under consideration achieves its full nominal capacity.

Flexural bond length. The flexural bond length is measured from the section where the prestressed force is fully effective (at the end of the transfer length) to the critical section. In these tests, the flexural bond length is equivalent to the embedment length minus the transfer length. Often, the flexural bond length is used in conjunction with the development length, l_d . In that case, the embedment length is the development length minus the transfer length.

3.5.1.2 Beam Identification System and Section Properties

Each beam carries a unique identifying name. The system for identification is described in Figure 3.14. The identification system indicates the following beam characteristics: shape (rectangular [R] or I-shaped [I]), strand source, strand size, nominal concrete strength at release, and specimen number in a series. The section properties and materials are described in the sections under transfer length.

Rectangular beams 17 ft in length were fabricated with two strands in each beam. Longitudinal top steel was included in the cross section to provide additional compression reinforcement and to ensure under-reinforced flexural

conditions at capacity. As shown in Figures 3.15 and 3.16, #3 stirrups, or “ties,” were provided on 6-in. centers. The nominal flexural capacity, M_n , of the rectangular beams varied from about 700 k-in. for the lower strength concrete (nominal 4 ksi at release) to approximately 754 k-in. for the 10 ksi (release) concrete.

Four-strand beams were cast for transfer length measurements with two strands in the bottom of the cross section and two strands at the top of the cross section. Four-strand beams were not tested for development length and are not discussed in this chapter.

Figure 3.18 shows the cross-section of the I-shaped beam with the reinforcement details. Each I-shaped beam was cast with a length of 24 ft. Top flanges were reinforced longitudinally with two #3 bars that ran the length of the beam. Transverse reinforcement in the top flange consisted of #3 bars at 9-in. centers over the beam length. Stirrups were made from #3 bars with standard 90° hooks and spaced at 7-in. centers. Stirrups were arranged so that the legs alternated directions. Horizontal reinforcement was placed in the webs of each end of each I-shaped beam.

3.5.1.3 Loading Geometry

Both rectangular and I-shaped beams were designed to be tested on both ends, enabling a distinct development length test at each beam end. The loading geometry varied from end to end so that a different embedment length was tested at each end. Embedment lengths varied for each test and were chosen depending upon results from prior tests.

The typical loading geometries for rectangular beams with 0.5-in. strands are shown in Figure 3.33. The geometry shown for the south end corresponds with an embedment length of 58 in., which is approximately 80 percent of the computed development length requirement. The geometry shown for the north end corresponds with an embedment length of 73 in., which is approximately equivalent to the AASHTO LRFD and ACI requirements for development length. Rectangular beams with 0.6-in. strands required longer embedment lengths than those shown in Figure 3.33. The two testing lengths, 73 in. and 58 in., were established through testing programs conducted by Rose and Russell (1997) and Logan (1997).

The typical loading geometries for the I-shaped beams are shown in Figure 3.34. The geometry illustrated is typical for

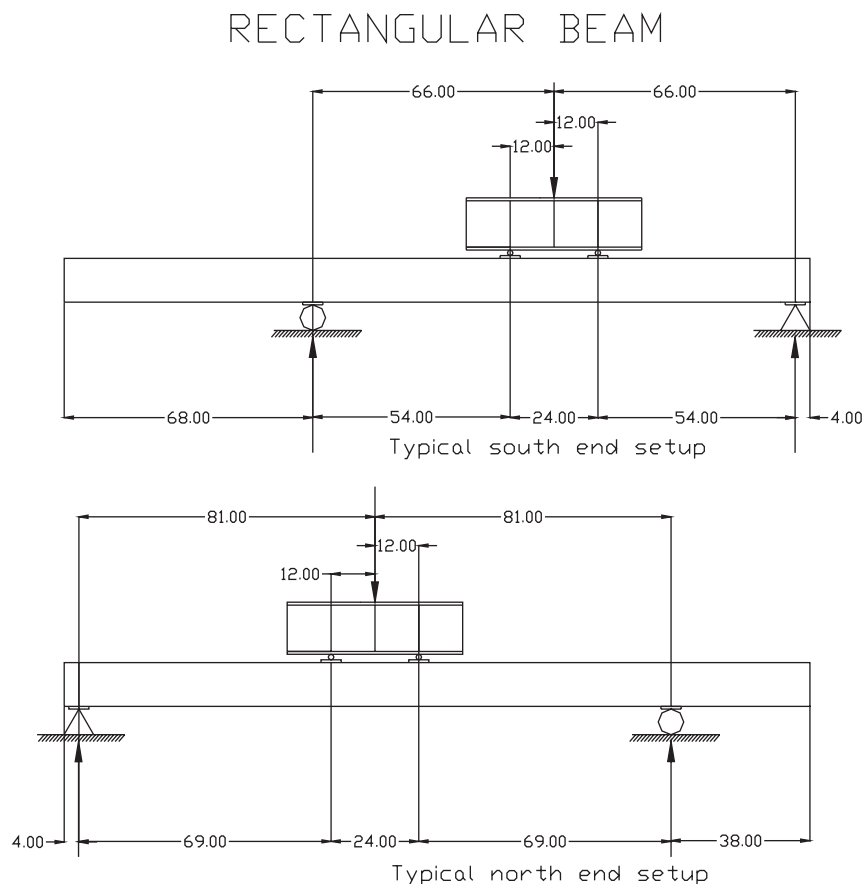


Figure 3.33. Typical loading geometry for rectangular beams.

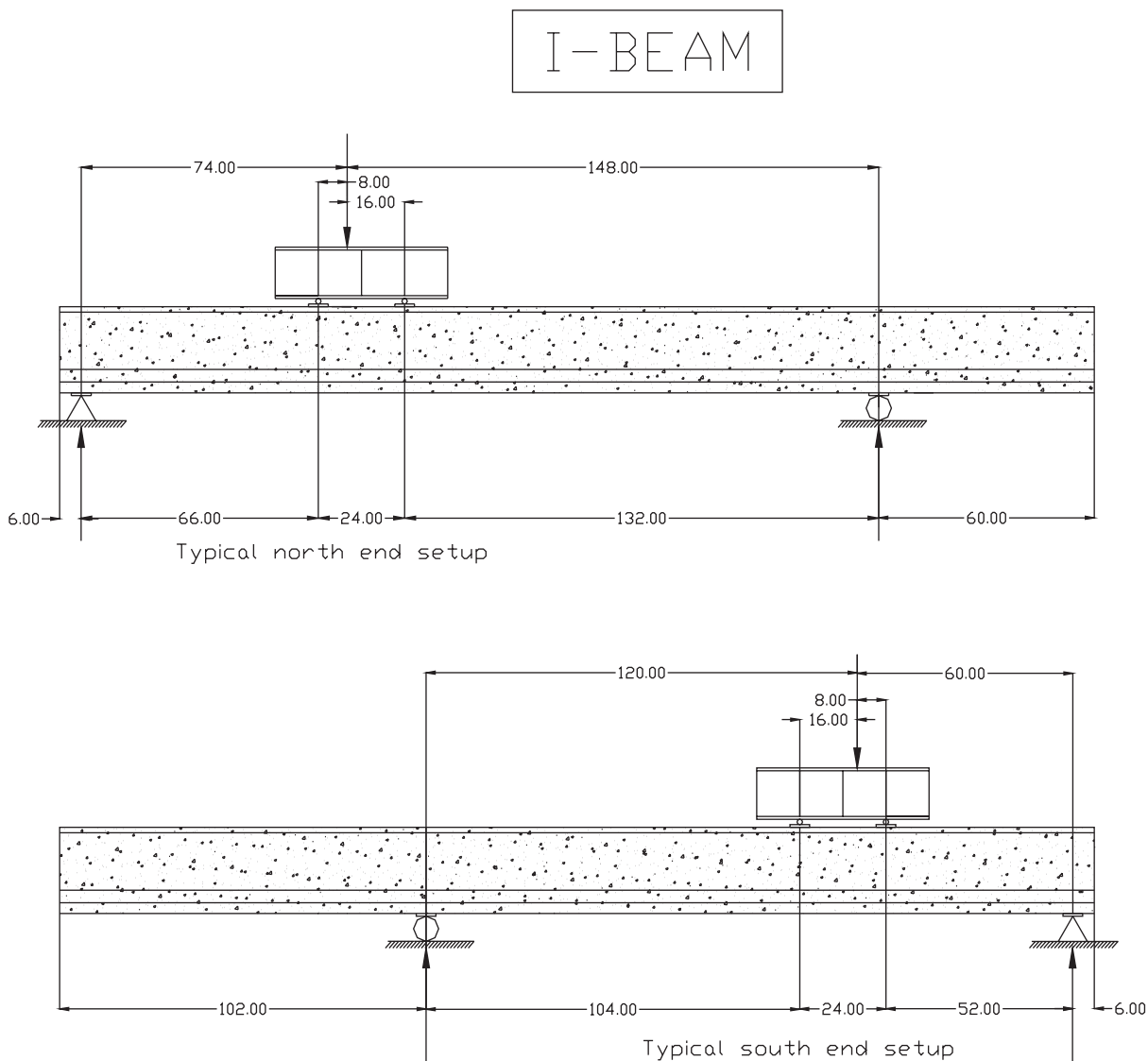


Figure 3.34. Typical loading geometry for I-shaped beams.

beams made with 0.5 in. strands. The test on the south end shows an embedment length of 58 in. The north end shows development length test geometry for an embedment length approximately equal to the LRFD and ACI requirements, 72 in. As with the rectangular beam series, tests on I-shaped beams with 0.6 in. diameter strands required longer embedment lengths than those shown in Figure 3.34.

3.5.1.4 Test Frame

The test frame was designed to perform flexural tests on both rectangular beams and I-beams. The photograph in Figure 3.35 shows the test frame with a beam in position for testing. The test frame has four sides that form a rectangular “frame.” Load is applied through a hydraulic actuator (attached to the top horizontal beam in the frame) to a spreader beam (attached to the bottom of the actuator). The spreader beam distributes loading

to the pretensioned concrete test beam. The loading geometry was arranged so that constant bending moment is applied between the two load points. In this picture, the beam that is being tested is a rectangular beam. It is supported by a pin on the near end and a roller at the far end.

3.5.1.5 Instrumentation

The following instrumentation was used.

Electronic data acquisition. Load, hydraulic pressure, beam deflection, and strand end slips were measured and recorded by an electronic data acquisition system. Data were sampled and recorded at regular intervals without manual prompting. The rate of sampling was fixed at 1.0 Hz, which provided smooth transition of load, displacement, and strand end slip values. The data were stored on a laptop computer

and were then available for analysis. During each development length test, data were also recorded manually in the event that electronic data were corrupted by unforeseen circumstance.

Load. Load was measured electronically with a load cell placed between a spherical head under the hydraulic actuator and the spreader beam. The load cell can be seen in Figure 3.35 just above the steel loading beam. Load was applied hydraulically, and the hydraulic pressure was also monitored electronically by a pressure transducer. The pressure transducer also sent electronic signals to the data acquisition system for monitoring and recording. A hydraulic pressure gage was employed during the test for visual observations and manual recording.

Deflection. Wire transducers with a range of 30 in. and accuracy ± 0.005 in. were used to determine the vertical deflection. Deflection was measured below the center of the loading point. Two wire transducers were used to measure deflection, one on each side of the beam, so that any twisting of the beam would be taken out when computing the average between the two sides. Data from the wire transducers were recorded and stored electronically. In addition to the electronic data, a dial gage with a precision of one one-thousandth of an inch was used to manually record deflection readings. The dial gage was also used to monitor displacements when the testing switched from load-controlled testing to displacement controls. The wire transducers and the dial gage are shown in Figure 3.36.

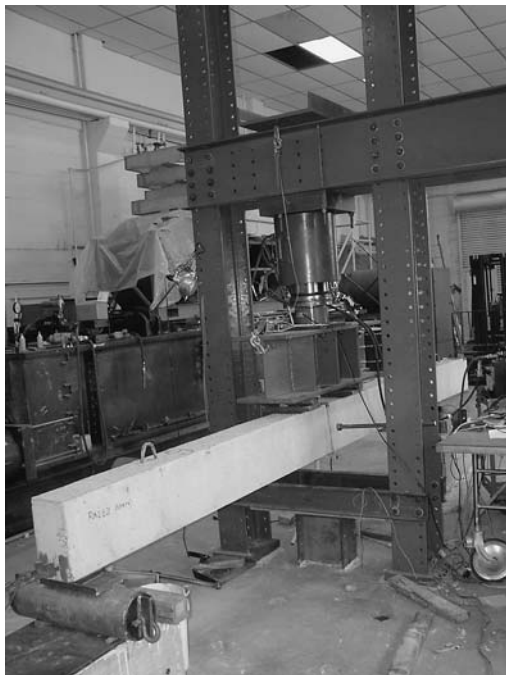


Figure 3.35. Test frame with a rectangular beam readied for testing rupture.

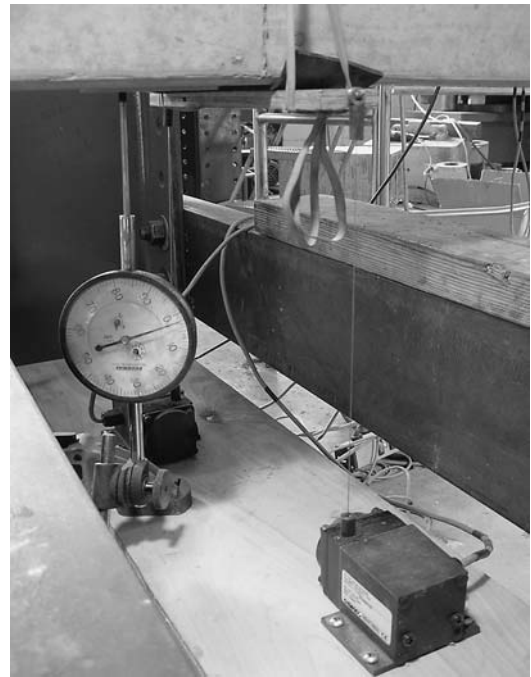


Figure 3.36. Wire transducers (foreground) and a dial gage.

Strand end slip. Linear voltage displacement transducers (LVDTs) were used to measure strand movement relative to the concrete. The LVDTs had a stroke limit of 1.0 in. and recorded strand end slips to one one-thousandth of an inch. Clamps were attached to the strands, and LVDTs were mounted on these clamps at a location providing an initial reading of approximately 0.9 in. with an error of (± 0.003 in. Strand end slips were measured and recorded for each strand on the “test” end. The photograph in Figure 3.37 shows the LVDTs clamped to strands to measure strand end slip relative to concrete.

At the far end of the beam, or at the end of the beam opposite the end being tested, strand end slips were measured by a mechanical deflection gage with an electronic readout. The device and arrangement are shown in Figure 3.38. Measurements with a precision of ± 0.005 in. were possible using this technique.

3.5.1.6 Testing Procedure

For each test, the instrument readings were initialized prior to the application of external load. Load was then applied to beams in regular load increments. Load was applied manually by a hydraulic pump. At all load increments, values of load, displacement, and strand end slips, as well as DEMEC readings (wherever applicable) were noted and recorded manually. In addition to electronic data being stored at the 1-Hz refresh rate on the data acquisition system, data were recorded manually. Once cracking began, cracks were marked with perma-

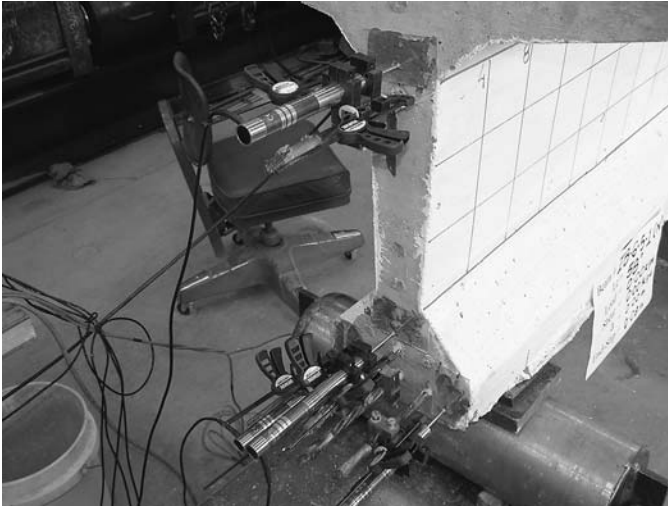


Figure 3.37. LVDTs clamped to strands to measure strand end slip relative to concrete.

ment markers as soon as they were observed. The loads at which the cracks first appeared were noted alongside of the cracks. Photographs were taken at regular intervals to record cracking patterns.

As displacements became larger with smaller increments in load, the manual system of loading switched from regular load increments to regular displacement increments. This was done arbitrarily by the researchers conducting the test. At each load or displacement increment, manual readings of hydraulic pressure and beam displacements were made. Additionally, manual and electronic instruments were checked to determine whether strand end slip had occurred during the prior loading increment. Loading was continued



Figure 3.38. Mechanical deflection gage arrangement for measuring strand end slips at the beam end opposite to the test end.

until failure. Failure was defined by the beam's inability to sustain or maintain load with increasing deflections or by abrupt failures of the concrete or strand.

Throughout the test, manual readings at every load increment were noted along with any significant development such as first flexural crack, first shear crack, appearance of flexure-shear crack, first strand end slip, concrete spalling, concrete crushing, and any audible developments. Written summaries of each development length test appear in the appendices. Detailed progress of each test was documented and is included along with significant photographs and data plots in Appendices C through G. Also, plots of moment versus deflection, strand end slip versus deflection, and shear versus average shear strain were plotted from the acquired data. Shear strains were measured from DEMEC target points attached to the webs of I-shaped beams. Shear stress was determined by dividing the shear force applied by the product of the web width and the beam depth.

3.5.2 Experimental Results from Development Length Testing

All together, 50 flexural tests were performed on rectangular beams and 14 tests on I-shaped beams. All of these tests were carried out at the Civil Engineering Laboratory at OSU. Most of the beams were tested on both ends. For each beam test, the embedment length was determined on the basis of various factors, including the AASHTO development length equation with changes to account for prior results, concrete strength, or strand bond strength. In this section, Tables 3.23 through 3.27 report the results from development length testing. These tables report on the following parameters:

- Concrete strength at release;
- Concrete strength at 56 days;
- Average NASP Bond Test value for the strands contained in the beams;
- Embedment length for each individual test;
- Test span;
- Failure Moment, which is the maximum applied moment measured during the test;
- Percentage of the Failure Moment to the nominal flexural capacity, M_n , as determined by strain compatibility. The calculation for M_n assumes that the strands are fully developed; no reduction in flexural capacity was assumed for embedment lengths provided that are less than the calculated development length;
- Maximum beam deflection;
- Maximum strand end slip; and
- Classification for each type of failure.

Table 3.23. Development length test results on rectangular beams containing Strand D.

Beam End	f'_c @ Release (psi)	f'_c 56 Days (psi)	Avg. NASP Pull-Out Value (lb)	Avg. L_d @ Release (in)	Avg. L_d (56-Day or @ Test) (in)	Actual L_e (in)	Span (in)	Failure Moment (kip-in)	$\%M_n$	Deflection @ Failure (in)	Max. End Slip (in)	Failure Mode
RD-4-5-1-N	4,033	7,050	6,890	32.79	38.54	73	162	804	115	3.4	0.00	Flexure
RD-4-5-1-S	4,033	7,050	6,890	31.02	42.28	58	132	759	108	1.6	0.35	Bond
RD-4-5-2-N	4,033	7,050	6,890	42.19	63.05	73	162	831	119	2.7	0.40	Flexure
RD-4-5-2-S	4,033	7,050	6,890	49.71	51.81	58	132	513	73	2.5	0.57	Bond
RD-6-5-1-N	6,183	8,500	6,890	30.24	49.75	73	162	797	111	2.5	0.06	Flexure
RD-6-5-1-S	6,183	8,500	6,890	28.07	45.26	58	132	788	109	2.0	0.18	Flexure
RD-6-5-2-N	6,183	8,500	6,890	25.60	44.24	73	162	735	102	2.0	0.01	Flexure
RD-6-5-2-S	6,183	8,500	6,890	29.22	48.27	58	132	724	100	2.0	0.25	Bond
RD-6A-5-1-N	7,960	11,420	6,890	35.4	39.94	73	162	794	106	2.3	0.00	Flexure
RD-6A-5-1-S	7,960	11,420	6,890	29.1	37.16	58	132	805	108	2.5	0.08	Flexure
RD-6A-5-2-S	7,960	11,420	6,890	20.08	40.07	58	132	778	104	1.9	0.02	Flexure
RD-8-5-1-N	8,570	13,490	6,890	20.15	39.08	73	162	811	107	2.6	0.00	Flexure
RD-8-5-1-S	8,570	13,490	6,890	20.15	34.54	58	132	805	106	2.6	0.08	Flexure
RD-8-5-2-N	8,570	13,490	6,890	13.67	37.38	58	132	775	102	2.2	0.08	Flexure
RD-8-5-2-S	8,570	13,490	6,890	17.30	50.41	58	132	813	107	2.0	0.00	Flexure
RD-10-5-1-N	9,711	14,470	6,890	26	30.24	58	132	821	108	2.1	0.00	Flexure
RD-10-5-1-S	9,711	14,470	6,890	13.57	27.14	46	120	819	107	2.6	0.00	Flexure
RD-10-5-2-N	9,711	14,470	6,890	14.85	22.30	58	132	788	103	1.9	0.00	Flexure
RD-10-5-2-S	9,711	14,470	6,890	18.23	22.03	46	120	794	104	1.9	0.01	Flexure

3.5.2.1 Tabulated Beam Test Results—Rectangular Beams

Table 3.23 reports the results from development length tests on rectangular beams made with Strand D. Strand D was the 0.5 in. strand with the lower NASP pull-out value, 6,890 lb. Concrete strengths at release varied from a target of 4 ksi to a target of 10 ksi. 56-day concrete strengths ranged from 7.05 ksi to 14.47 ksi. Table 3.23 reports only three bond failures, all occurring with lower strength concretes. Also, all of the bond failures occurred at an embedment length of only 58 in., which is approximately 80 percent of the ACI- and AASHTO-prescribed development lengths. Of the three bond failures, two occurred at an applied moment that matched or exceeded M_n , the nominal flexural capacity for the beams. Table 3.23 also shows that at higher strengths, in general, flexural failures were observed in all tests. For example, two ends of the beams with 14.47 ksi concrete were tested with an embedment length of only 46 in., or approximately 63 percent of l_d . In these cases, the development length test resulted in flexural failures without bond slip (beams RD-10-5-1-S and RD-10-5-2-S).

Table 3.23 also reports the maximum strand end slip that occurred during testing, which corresponds to the maximum strand end slip measured at the time the beam failed, whether a flexural failure or a bond failure. Note that it is not uncommon for strand end slips to be measured even though a beam fails in flexure. For example, RD-4-5-2-N failed in flexure at a load that exceeded its nominal capacity by 19 percent. Further, the beam achieved adequate ductility as demonstrated by 2.7 in. of overall deflection while sustaining capacity. However, the measured strand end slip was 0.40 in. This finding is consistent with other research that has been performed to date. More notably, the results in Table 3.23 demonstrate that the measured strand end slips decrease measurably with increasing concrete strengths. At higher concrete strengths, strand end slips did not occur. Overall, the results support a conclusion that higher concrete strengths result in increasing bond strength and reducing the required development lengths. Detailed testing summaries on each development length test are found in Appendix C.

Table 3.24 reports the results from development length tests on rectangular beams made with Strands A/B. Strands A

Table 3.24. Development length test results on rectangular beams containing Strands A/B.

Beam End	f'_c @ Release (psi)	f'_c 56 Days (psi)	Avg. NASP Pull-Out Value (lb)	Avg. L_t @ Release (in)	Avg. L_t (56-Day or @ Test) (in)	Actual L_e (in)	Span (in)	Failure Moment (kip-in)	$\%M_n$	Deflection @ Failure (in)	Max. End- Slip (in)	Failure Mode
RA-6-5-1-N	6,183	8,500	20,950	19.2	33.70	73	162	790	110	2.1	0.00	Flexure
RA-6-5-1-S	6,183	8,500	20,950	18.2	30.03	58	132	800	111	2.1	0.00	Flexure
RA-6-5-2-N	6,183	8,500	20,950	16.5	28.00	58	120	772	107	1.5	0.00	Flexure
RA-6-5-2-S	6,183	8,500	20,950	15.01	23.50	46	120	777	108	1.5	0.00	Flexure
RA-6A-5-1-N	7960	11,420	20,950	17.74	26.54	73	162	769	103	2.4	0.00	Flexure
RA-6A-5-1-S	7,960	11,420	20,950	17.68	28.55	58	132	770	103	1.7	0.00	Flexure
RA-6A-5-2-N	7,960	11,420	20,950	24.51	31.75	58	132	788	105	1.9	0.00	Flexure
RA-6A-5-2-S	7,960	11,420	20,950	22.03	29.38	46	120	788	105	1.7	0.01	Flexure
RA-8-5-1-N	8,570	13,490	20,950	13.3	24.91	58	132	829	109	1.7	0.01	Flexure
RA-8-5-1-S	8,570	13,490	20,950	13.5	22.54	46	120	832	110	1.9	0.00	Flexure
RA-10-5-1-N	9,711	14,470	20,950	24.27	24.34	58	132	788	103	1.7	0.00	Flexure
RA-10-5-1-S	9,711	14,470	20,950	9.69	13.14	46	120	796	104	1.7	0.00	Flexure
RB-4-5-1-N	4,033	7,050	20,210	18.42	22.10	73	162	776	111	1.9	0.00	Flexure
RB-4-5-1-S	4,033	7,050	20,210	18.49	20.51	58	132	802	114	2.0	0.00	Flexure
RB-4-5-2-N	4,033	7,050	20,210	21.12	22.52	73	162	721	103	2.4	0.00	Flexure
RB-4-5-2-S	4,033	7,050	20,210	22.46	23.75	58	132	748	107	1.7	0.00	Flexure

Table 3.25. Development length test results on rectangular beams containing Strand A6 (0.6-in. diameter).

Beam End	f'_c @ Release (psi)	f'_c 56 Days (psi)	Avg. NASP Pull-Out Value (lb)	Avg. L_t @ Release (in)	Avg. L_t (56-Day or @ Test) (in)	Actual L_e (in)	Span (in)	Failure Moment (kip-in)	$\%M_n$	Deflection @ Failure (in)	Max. End- Slip (in)	Failure Mode
RA-4-6-1-N	4,033	7,050	18,290	33.42	41.82	88	192	1084	114	3.0	0.00	Flexure
RA-4-6-1-S	4,033	7,050	18,290	24.96	28.87	70	156	964	102	2.7	0.00	Flexure
RA-4-6-2-N	4,033	7,050	18,290	30.24	37.66	73	162	1011	107	2.4	0.13	Flexure
RA-4-6-2-S	4,033	7,050	18,290	29.35	33.19	58	148	921	97	3.0	0.33	Bond
RA-6-6-1-N	4,855	8,040	18,290	29.73	40.85	88	192	1012	104	2.5	0.00	Flexure
RA-6-6-2-N	4,855	8,040	18,290	31.65	52.18	73	162	1001	103	2.1	0.02	Flexure
RA-6-6-2-S	4,855	8,040	18,290	30.1	49.37	58	148	913	94	2.7	0.41	Bond
RA-6-6-3-N	4,855	8,040	18,290	25.83	44.96	88	192	1046	108	2.6	0.00	Flexure
RA-8-6-1-N	5,413	8,220	18,290	28.21	45.48	88	192	1008	103	2.4	0.00	Flexure
RA-8-6-2-N	5,413	8,220	18,290	28.2	46.35	73	162	1007	103	2.0	0.01	Flexure
RA-8-6-2-S	5,413	8,220	18,290	25.7	42.37	58	132	988	~101	2.5	0.14	Bond
RA-10-6-1-N	9,150	14,610	18,290	20.03	29.98	88	192	1084	102	2.8	0.00	Flexure
RA-10-6-2-N	9,150	14,610	18,290	15.62	26.79	73	162	1070	101	2.5	0.00	Flexure
RA-10-6-2-S	9,150	14,610	18,290	21.78	30.70	58	148	1083	102	2.4	0.00	Flexure

Table 3.26. Development length test results on I-shaped beams containing 0.5 in. diameter strands.

Beam End	Measured Overall Depth (h) (in)	f'_c @ Release (psi)	f'_c 56 Days (psi)	Avg. NASP Pull-Out Value (lb)	L_e (in)	Span (in)	Maximum Moment (kip-in)	$\%M_n$	Maximum Deflection (in)	Max. End-Slip (in)	Failure Mode
IB-6-5-1-N	24	5,810	9,350	20,210	58	166	3,526	82	1.1	0.04	Shear
IB-6-5-1-S	24	5,810	9,350	20,210	72	222	3,980	98	3.1	0.03	Flexure
IB-10-5-1-N	24	7,615	13,490	20,210	54	168	4,282	102	2.0	0.03	Flexure
IB-10-5-1-S	24	7,615	13,490	20,210	58	180	4,196	100	1.6	0.02	Flexure
ID-6-5-1-N	24	5,492	9,840	6,890	72	222	3,538	82	2.5	0.80	Bond
ID-6-5-1-S	24	5,492	9,840	6,890	88	270	3,280	81	3.5	0.75	Bond
ID-10-5-1-N	24	8,225	14,160	6,890	88	270	4,026	92	5.2	0.08	Flexure
ID-10-5-1-S	24	8,225	14,160	6,890	72	222	4,039	92	3.7	0.75	Bond

and B were used interchangeably in this beam series as the two strand samples tested with approximately the same NASP Bond Test value. Concrete strengths at release varied from a target of 4 ksi to a target of 10 ksi. 56-day concrete strengths ranged from 7.05 ksi to 14.47 ksi. Table 3.24 reports no bond failures. These results demonstrate that the NASP Bond Test is a good predictor of the ability of strands to perform in pre-tensioned applications. At concrete strengths above 4 ksi, embedment lengths as short as 46 in. were tested. All of these tests also resulted in flexural failures without any strand end slip. All of the flexural failures occurred at an applied moment that matched or exceeded M_n , the nominal flexural capacity for the beams. Detailed testing summaries on each develop-

ment length test are found in Appendix D, for Rectangular Beams Made with Strands A and B.

Both Tables 3.23 and 3.24 report results on beams made with air-entrained concrete. The development length test results on the air-entrained beams closely match from beams made with 6-ksi concrete without air entrainment. In other words, all of the ends tested with air-entrained concrete failed in flexure, with strand end slip in only a few cases. These results mirrored the results of the development length tests without air entrainment.

Table 3.25 reports the results from development length tests on rectangular beams made with 0.6 in. diameter strand. The strand is called Strand A6. Strand A6 had an NASP Bond

Table 3.27. Development length test results on I-shaped beams containing 0.6 in. diameter Strand A6.

Beam End	Measured Overall Depth (h) (in)	f'_c @ Release (psi)	f'_c 56 Days (psi)	Avg. NASP Pull-Out Value (lb)	L_e (in)	Span (in)	Maximum Moment (kip-in)	$\%M_n$	Maximum Deflection (in)	Max. End-Slip (in)	Failure Mode
IA-6-6-1-N	24.125	4,381	8,990	18,290	75	156	3,267	81	1.7	0.05	Shear @ opposite end
IA-6-6-1-S	24.125	4,381	8,990	18,290	91	188	4,387	109	2.8	0.12	Flexure
IA-6-6-2-N	24.125	4,381	8,990	18,290	88	270	4,125	102	3.2	0.13	Shear
IA-10-6-1-N	24.25	10,480	14,990	18,290	58	166	4,243	103	1.2	0.05	Shear @ opposite end
IA-10-6-1-S	24.25	10,480	14,990	18,290	72	222	4,620	112	2.5	0.03	Flexure w/ Strand Rupture
IA-10-6-2-N	24.375	10,590	14,930	18,290	72	222	2,983	73	0.9	0.00	Shear @ opposite end
IA-10-6-2-S	24.375	10,590	14,930	18,290	88	270	4,559	111	5.7	0.00	Flexure

Test value of 18,290 lb, which is interesting as it falls between the higher and lower NASP Bond Test values for the 0.5 in. strands tested. Concrete strengths at release varied from a target of 4 ksi to a target of 10 ksi. The range for 56-day concrete strengths was 7.05 ksi to 14.61 ksi.

For 0.6 in. strands, the ACI and AASHTO development length provision would require a development length of approximately 88 in. From Table 3.25, it can be seen that several of the tests were performed at an embedment length of 88 in., which roughly corresponds to 100 percent of the AASHTO required development length. At the embedment length equal to the required development length of 88 in., all of the beam specimens failed in flexure, regardless of concrete strength. This would indicate that the strand performance was adequate and suitable for making pretensioned concrete beams.

Other tests on beams made with Strand A6 were conducted at an embedment length of 72 in., which roughly corresponds to 80 percent of l_d . This was done intentionally to mirror the 80 percent of l_d that was tested for 0.5 in. strands. Additionally, note that some tests were conducted at an embedment length of 58 in., which is about 55 percent of l_d .

Three bond failures occurred in the tests on rectangular beams made with Strand A6. Notably, all three bond failures occurred at embedment lengths of 58 in., which is considerably shorter than the required development length. The three bond failures occurred in beams made with the three lower concrete strengths, with nominal release strengths of 4 ksi, 6 ksi, and 8 ksi. In contrast, the fourth beam, made from concrete with a nominal release strength of 10 ksi, failed in flexure when tested at an embedment length of 58 in. The results of these tests would support the conclusion that increasing concrete strength improves the bond performance of prestressing strands. Detailed testing summaries on each development length test are found in Appendix N, for Rectangular Beams Made with 0.6 in. Strands A, or Strand A6.

3.5.2.2 Tabulated Beam Test Results—I-Shaped Beams

Table 3.26 reports the results from development length tests on I-shaped beams made with 0.5 in. strands. Strand D was the 0.5 in. strand with the lower NASP pull-out value, 6,890 lb, and Strand B possessed the higher NASP Test value of 20,210 lb. Two different concrete strengths were employed, concrete with a target release strength of 6 ksi and concrete with a target release strength of 10 ksi. The beams were made in pairs, and the release strength of 10 ksi was not achieved. 56-day concrete strengths ranged from 9.35 ksi to 14.16 ksi, which is very near the target design strengths of 10 and 15 ksi. Detailed testing summaries on each development length test are found in Appendix F, for I-Shaped Beams Made with 0.5 in. strands, including both Strand B and Strand D.

Strand D. Table 3.26 reports three bond failures out of four tests on I-shaped beams made with the lower bond performer, Strand D. The fourth flexural test resulted in a flexural failure; this beam was made with the higher strength concrete. Bond failures occurred at both the lower concrete strength and the higher concrete strength. Unlike the rectangular beams, bond failures of Strand D occurred at lengths equal to and exceeding the ACI and AASHTO development length design equation. At the lower concrete strength, 9.48 ksi, bond failures occurred at embedment lengths of 72 and 88 in. At the higher concrete strength, 14.16 ksi, one bond failure occurred at an embedment length of 72 in. The flexural failure had an embedment length of 88 in. These results support two primary conclusions:

1. The strand with an NASP Bond Test value of 6,890 lb is inadequate to develop the tension necessary to support flexural failures as intended, and
2. Higher concrete strength can improve the bond between prestressing steel and concrete.

Strand B. Table 3.26 reports results of four tests done on beams made with Strand B. In the four tests, none of the beams failed in bond. The highest strand end slip measured was 0.04 in. Of the four failures, one was a shear failure and the other three were flexural failures. Three of the four tests were conducted with embedment lengths of 52, 54, and 58 in., lengths which are significantly less than the development length prescribed by ACI and AASHTO. These results support one of the primary conclusions, i.e., that strand with a high NASP Bond Test value, in this case 20,210 lb, will provide bond that exceeds the implicit requirement of the development length design equations.

Strand A6. Table 3.27 reports the results from development length tests on I-shaped beams made with 0.6 in. strands. Strand A6 was the only 0.6 in. strand cast in beams. It has an NASP pull-out value of 18,290 lb. Four beams were made, two with a target release strength of 6 ksi and two with a target release strength of 10 ksi. These casts achieved the target release strength of 10 ksi, and 1-day strengths measured 10,590 lb. The range for 56-day strengths was 8,990 and 14,910 lb. Of the seven beam ends tested, three ends failed in shear at the end opposite the “test” end. The larger diameter strands required longer testing spans, and the beams were not able to overcome the damage sustained during tests on the south end when tests were performed on the north end.

Of the four tests that would qualify as development length tests, one resulted in shear failure whereas the other three tests resulted in a flexural failure. None of the failures resulted from bond failure. At the lower strength, some strand end slips were measured and observed; however, these strand end

slips were consistent with behavior that was noted in previous testing and did not prevent the strands from development tension adequate to support flexural failures at, or exceeding, the nominal flexural capacity. Detailed testing summaries on each development length test are found in Appendix G, for I-Shaped Beams Made with 0.6 in. strand, Strand A6.

3.5.3 Discussion of Development Length Test Results

Development length tests must be conducted to failure, and the type of failure observed determines whether the embedment length provided was adequate to ensure proper strand development. Three distinct types of beam failures were observed in the conduct of the development length tests: (1) flexural failure, (2) bond failure, or (3) shear failure.

3.5.3.1 Types of Failure—Flexure

Flexural failures are characterized by two primary criteria:

1. The beam is able to resist a flexural moment that approaches and often exceeds the nominal flexural capacity (strength), and
2. The beam is able to undergo large deformations while sustaining its capacity for resistance (ductility).

Flexural failures of the beam specimens were typically characterized by the crushing of concrete at the top of the cross section where the compression zone exists. The beams were designed to be under-reinforced, which ensures that the strands themselves will experience large strains at flexural failure. Even so, crushing of the concrete is the most common failure mode. In one or two specimens of this test series, strands ruptured in tension. It should be noted that some strand end slip can be observed even during a flexural failure. The strands consistently exhibit an ability to develop strand tension even with small amounts of slip. However, when larger amounts of slip are observed, often the result is a bond failure. When strand end slips are observed, the determination of whether the failure is a flexural failure with adequate strand bond or a bond failure is based on whether the beam meets the two criteria listed above for a flexural failure.

Beams that failed in flexure also showed considerable ductility, with deflection increasing dramatically with sustained loads or with some incremental load increases. In some flexural failures, strand fractures occurred. Typically, strand fractures occurred in beams made with higher strength concrete. In these cases, failures did not cause crushing of concrete at the top surface; rather, the applied moments were large enough to cause the strands to rupture in tension.

Flexural failures of rectangular beams. A typical flexural failure is observed from the test on the south end of Beam RB-4-5-1. The rectangular beam contained two 0.5 in. strands, with a Strand B designation and a 56-day concrete strength of 7.05 ksi. The embedment length for this test was 58 in., or about 80 percent of the AASHTO design requirement for 0.5 in. strands. Strand B had a relatively high NASP Bond Test value of 20,120 lb.

The moment versus deflection curve is found in Figure 3.39. Note that the beam achieves its nominal flexural capacity, M_n , and that it also displays the ability to sustain the moment under large deflections. Additionally, for this beam, strand end slips remained small or the strand did not slip at all. The beam failed in flexure as the concrete in the compression zone crushed. A photograph of the beam at failure is shown in Figure 3.40.

Flexural failures of I-shaped beams. The test on the south end of I-shaped beam IA-10-6-1 provides a good example of a flexural failure. In this test, one of the strands ruptured in tension, an obvious indicator that the strand was able to fully develop the tension necessary to resist the flexural capacity. The embedment length for this test was 72 in., which is approximately 80 percent of the ACI and AASHTO required development length for 0.6 in. strands. The NASP Bond Test value for Strand A6 was 18,290 lb.

The moment versus deflection curve is found in Figure 3.41. Note that the beam achieves its nominal flexural capacity, M_n , and that it also displays the ability to sustain the load under large deflections. The beam failed at a moment of 4,620 kip-in., which exceeded the calculated M_n by about 12 percent. In this beam, the strands slipped a small amount as loads increased to capacity; the maximum strand end slip measured was 0.03 in. This small amount of strand end slip is also consistent with many of the flexural failures that occur during development length testing.

The beam failed when one of the strands ruptured in tension. Strand rupture was accompanied by a loud noise. The cracking pattern at failure is shown in the photograph shown in Figure 3.42. The cracking pattern is typical for I-shaped beams. There are two distinct regions of cracking. Flexural cracking is predominant in the regions of maximum moment. These cracks are distinguished by a vertical propagation near the bottom fibers of the beam. Web shear cracking occurs in the webs within the shear span of the tested end. These cracks are distinguished by their diagonal nature. It was uniformly observed that web crack propagation was limited to the webs of the I-shaped beams until loads approaching flexural capacity were applied. As loading increased, the web cracks would propagate into the bottom “bulb” of the I-shaped beam. Additionally, the photograph in Figure 3.42 shows inclined flexural cracks that propagate vertically from

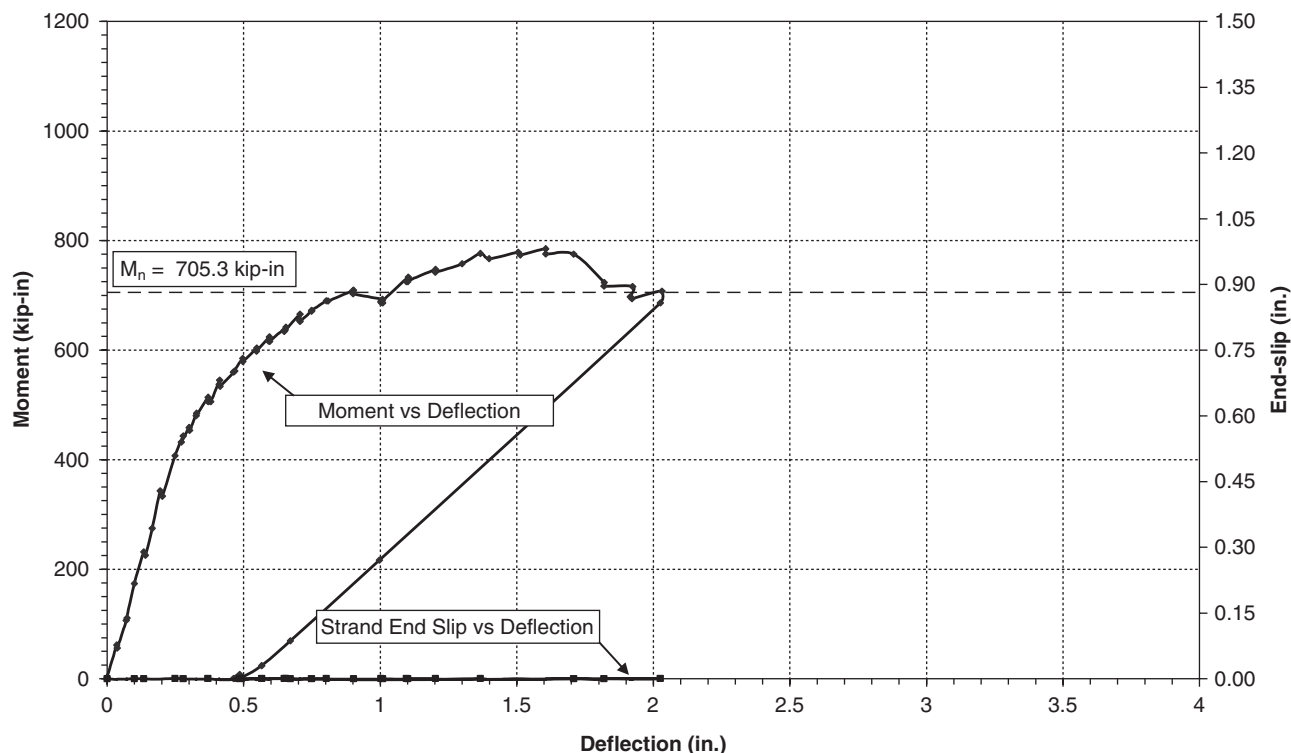


Figure 3.39. Moment versus deflection and strand end slip for Beam RB-4-5-1-S.

the bottom of the beam, but then incline as the crack approaches and enters the webs.

3.5.3.2 Types of Failure—Bond

Failures of pretensioned bond are characterized by the following two primary markers: (1) an inability to develop resistance to meet its design capacity and (2) excessive strand end slip.

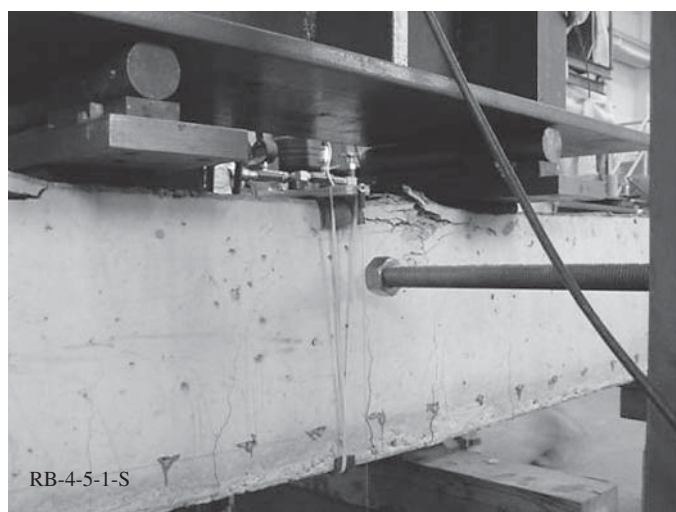


Figure 3.40. Concrete crushing in the compression zone of Beam RB-4-5-1-S.

Oftentimes, although not always, bond failures can be abrupt and occur without warning. However, it is generally noted that test beams failing in bond demonstrate some measure of gradual failure; that is, they possess an ability to sustain some load through large deformations. However, bond failures nearly always occur at loads less than the calculated nominal flexural capacity, M_n .

Bond failures in rectangular beams. A typical bond failure is observed from the test on the south end of Beam RD-4-5-2. The rectangular beam contained two 0.5 in. strands. The concrete strength at 56 days was 7.05 ksi. The embedment length for this test was 58 in., or about 80 percent of the AASHTO design requirement for 0.5 in. strands. The beam contained strands from the sample Strand D, which possessed a relatively low NASP Bond Test value of 6,890 lb.

The moment versus deflection curve is shown in Figure 3.43. The moment versus deflection curve illustrates that the beam was unable to reach its nominal flexural capacity, M_n . M_n for this beam was 705 kip-in., and the beam's actual capacity was 513 kip-in., as measured during the test. In reviewing the load versus deflection curve and the strand end slip curve, it is apparent that the strand started slipping very soon after flexural cracking first occurred. The beam was unable to resist loads that were much larger than the cracking moment, and strand end slips continued to increase with additional beam deflections. At a total deflection of about 3 in., the compression block at the top of the beam exhibited

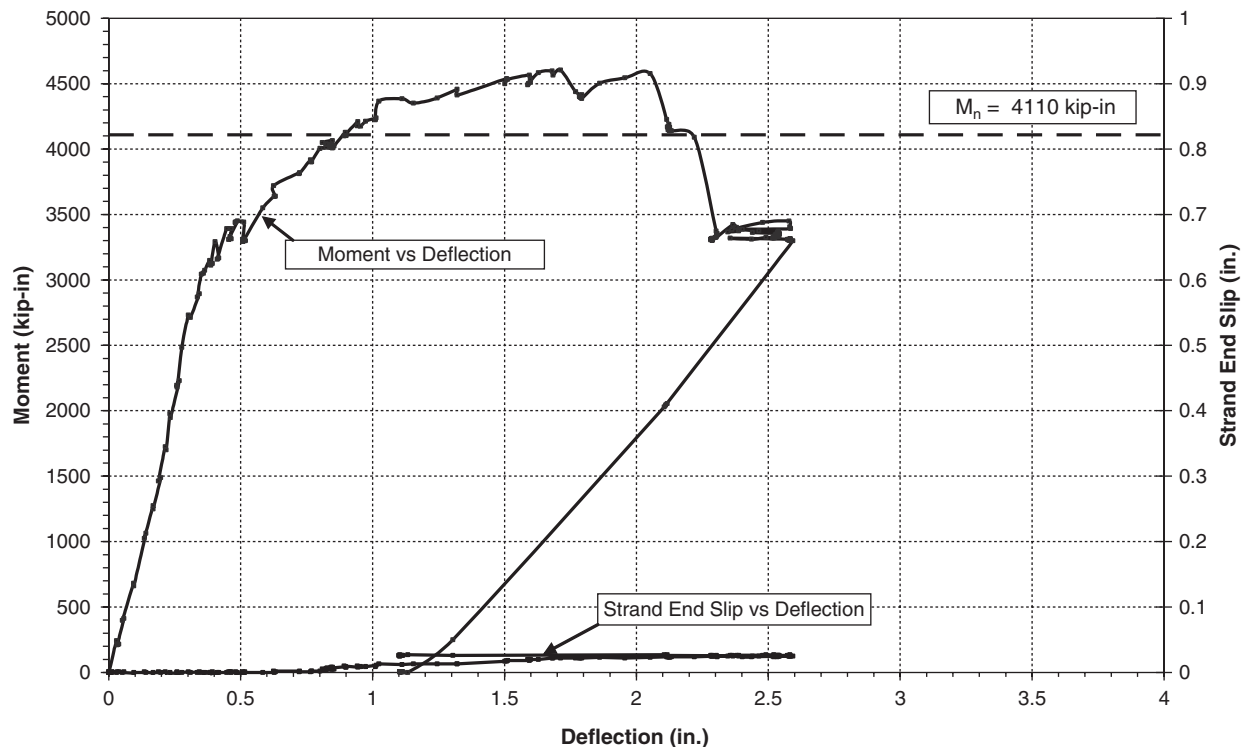


Figure 3.41. Load versus deflection and strand end slip for IA-10-6-1 South.

crushing failure. The cracking pattern and the crushing failure of the beam can be viewed in Figure 3.44. Note the one wide flexural crack, which is often a characteristic of bond failures. Because the beam was unable to achieve its nominal flexural capacity and because the beam exhibited excessive strand end slips, this test was classified as a bond failure.

It should be noted that two rectangular beams were constructed with Strand D and a targeted release strength of 4 ksi. These beams are the RD-4-5-1 and RD-4-5-2 beams. Of the

four ends tested, bond failures occurred on the beams where the embedment length was only 58 in. The companion beam to Beam RD-4-5-2 (south end), described above, was Beam RD-4-5-1 (south end). It also failed in bond but at a load equal to the nominal flexural capacity. Still, the beam exhibited excessive strand end slip during the test, and the failure was not particularly ductile in that the beam was unable to sustain its resistance through large deformations. A description of that test and all other development length tests can be found in the appendices to this report.

Bond failures in I-shaped beams. In development length tests on I-shaped beams made with 0.5 in. strands, three bond failures occurred. All of the bond failures occurred in beams made with Strand D, the strand with the lower NASP Bond Test value of 6,890 lb. Of the three tests that failed in bond, two ends failed at embedment lengths of 72 in. and 88 in. These were two ends of the same beam that had a release strength of 5,490 psi and a 56-day strength of 9,840 psi. On the higher strength beam, with a 56-day concrete strength of 14.16 ksi, a bond failure occurred at an embedment length of 72 in., and a flexural failure occurred at an embedment length of 88 in. These tests demonstrated that Strand D, with an NASP Bond Test value of 6,890 lb, was inadequate in its ability to bond with concrete and satisfy the design requirements implied in the ACI and AASHTO expressions for development length.

Beam ID-6-5-1 (south end) shows a typical bond failure. This I-shaped beam contained five 0.5 in. strands; the con-

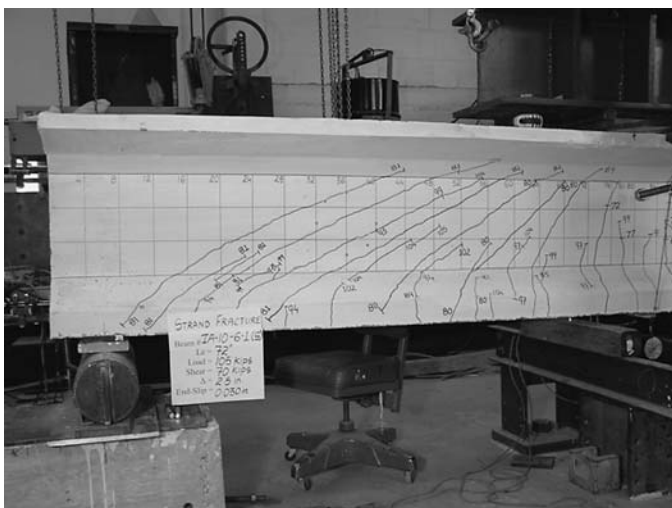


Figure 3.42. Cracking pattern for Beam Test IA-10-6-1 South, at strand.

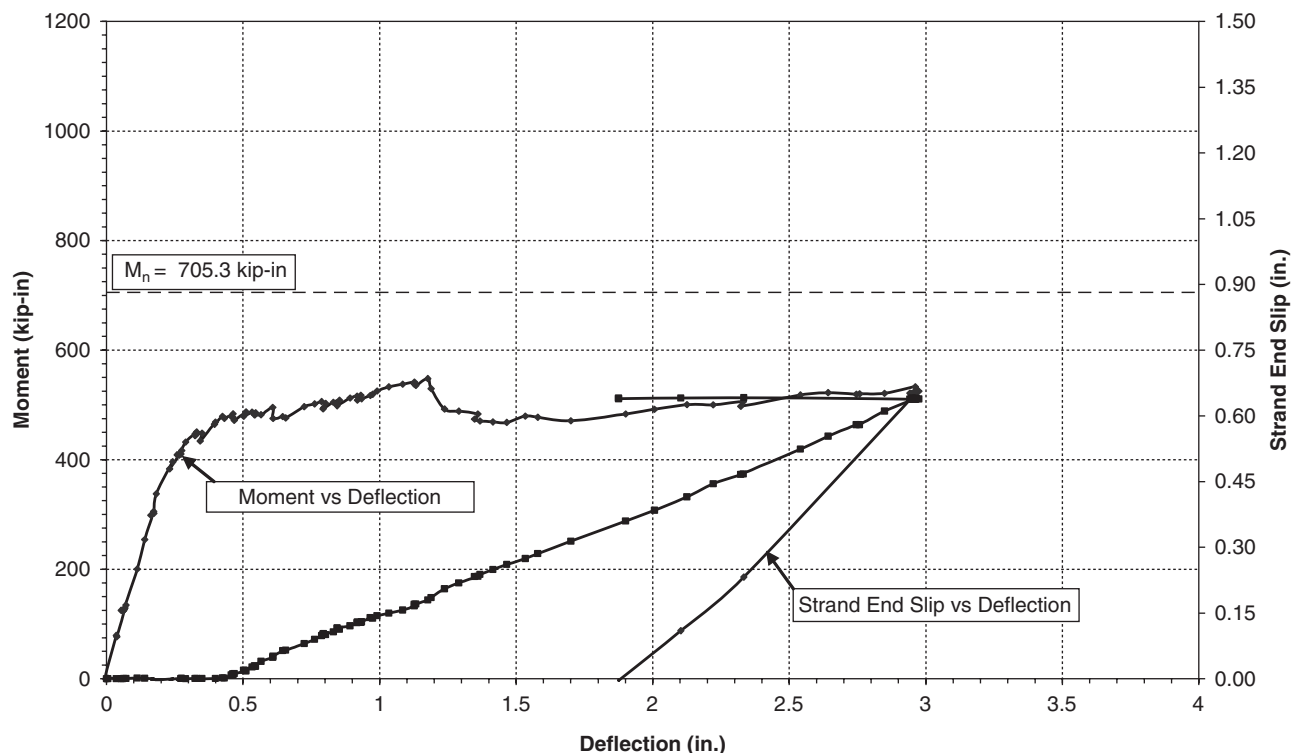


Figure 3.43. Applied moment versus deflection and strand end slip for Beam RD-4-5-2-South.

crete strength at 56 days was 9.84 ksi. The embedment length for this test was 88 in., or about 120 percent of the AASHTO design requirement for 0.5 in. strands. The beam contained strands from the sample Strand D, which possessed a relatively low NASP Bond Test value of 6,890 lb.

The moment versus deflection curve is found in Figure 3.45. The moment versus deflection curve illustrates that the beam was unable to reach its nominal flexural capacity, M_n . The results indicate that the beam's flexural capacity of 3,280

kip-in. was only about 81 percent of its calculated nominal flexural capacity. In reviewing the results from the test, it is apparent that the incidence of web shear cracking coincided with the initial strand end slips. Strand end slips continued to increase with increased beam loadings and increased beam deflections. The test was concluded at a total deflection of about 3.5 in., when it was apparent that deflections were increasing without further increase in beam capacity. The cracking pattern and the crushing failure of the beam can be viewed in Figure 3.46. The photograph shows one flexural crack under the loading point that became very wide under load. The excessive width of the crack is further evidence of bond failure in the prestressing strand. Because the beam was unable to achieve its nominal flexural capacity and because the beam exhibited excessive strand end slips, this test was classified as a bond failure.

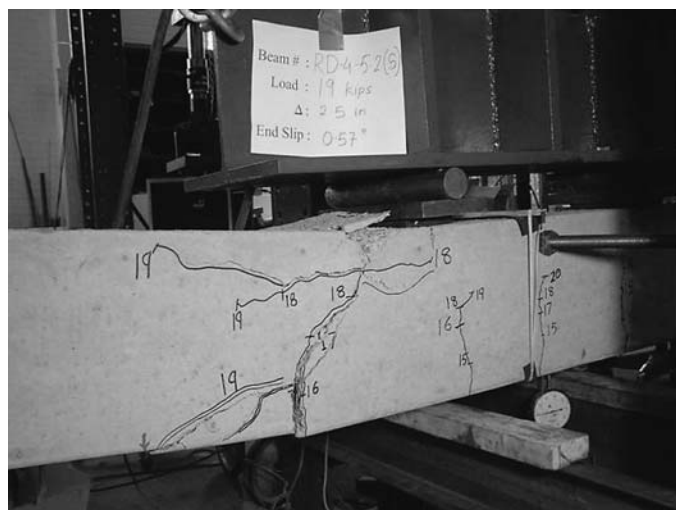


Figure 3.44. Cracking pattern of bond failure for Beam RD-4-5-2 (South).

3.5.3.3 Types of Failure—Shear Failure

Two shear failures occurred in I-shaped beams; no shear failures occurred in the rectangular beams. Prior research has shown that significant interaction can exist between shear and bond behaviors, especially in I-shaped beams with narrow webs (Kaufman and Ramirez 1988). In these beams, shear behavior is improved considerably by the inclusion of horizontal mild reinforcement within the webs and extending for the first 96 in. from each end of the I-shaped beam.

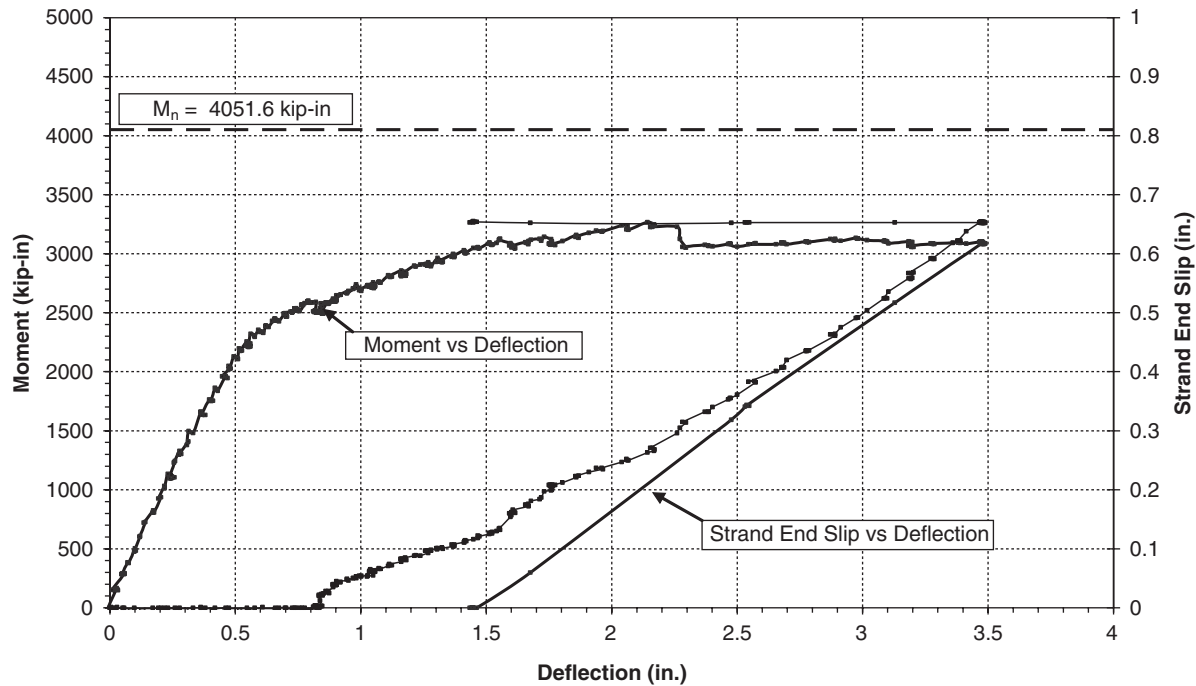


Figure 3.45. Applied moment versus deflection and strand end slip for Beam ID-6-5-1 (South).

An example shear failure is observed from the test on Beam IA-6-6-2 (north end). This I-shaped beam contained four 0.6 in. strands; the concrete strength at 56 days was 8.99 ksi. The embedment length for this test was 88 in., or approximately equal to the AASHTO design requirement development length for 0.6 in. strands. The beam contained strands from the sample Strand A6, which possessed a NASP Bond Test value of 18,290 lb. Also, this beam was dropped and damaged during handling at the prestressing plant. Several cracks resulted from the dropping of the beam.

The moment versus deflection curve and the strand end slip versus deflection curve are shown in Figure 3.47. The

moment versus deflection curve follows a pattern indicative of a flexural failure. The curve also shows that the beam was unloaded and then reloaded a second time. Web shear cracking and flexural cracking occurred at the same load increment, corresponding to a moment of about 2,400 kip-in. Strand end slips did not occur with the initial web crack, but soon followed.

One of the interesting things about this test is that the shear failure occurred as the beam had reached its nominal flexural capacity. The large deformations also suggest that strand yielding was probably occurring, and, as the test on the beam was being conducted, a flexural failure was indicated. However, as one can view in the photograph shown in Figure 3.48, the beam failed suddenly and violently with a diagonal compression failure of the web. The shear failure shows that even though the beam is failing in shear, the strand possesses bond adequate to develop the beam's capacity.

3.5.3.4 Summary of Development Length Tests

There are three key issues:

1. Whether the NASP Bond Test can be used as a predictor of strand bond performance in flexural applications,
2. What the minimum acceptable level of bond performance is as measured by the NASP Bond Test, and
3. What modifications are necessary to the LRFD development length equation to account for variations in concrete strength.

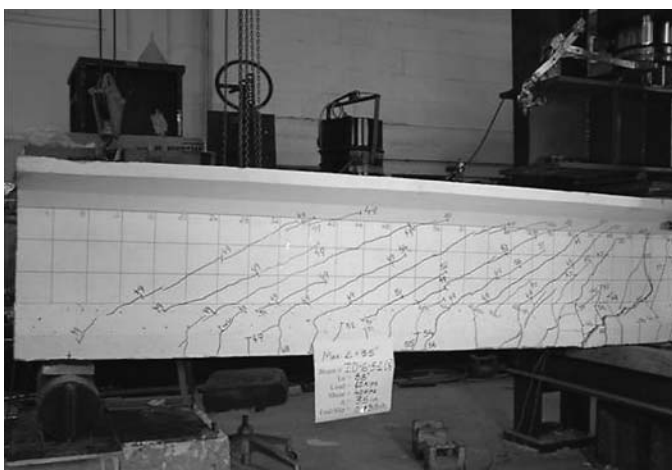


Figure 3.46. Cracking patterns at the maximum load (failure) of Beam ID-6-5-1 (South).

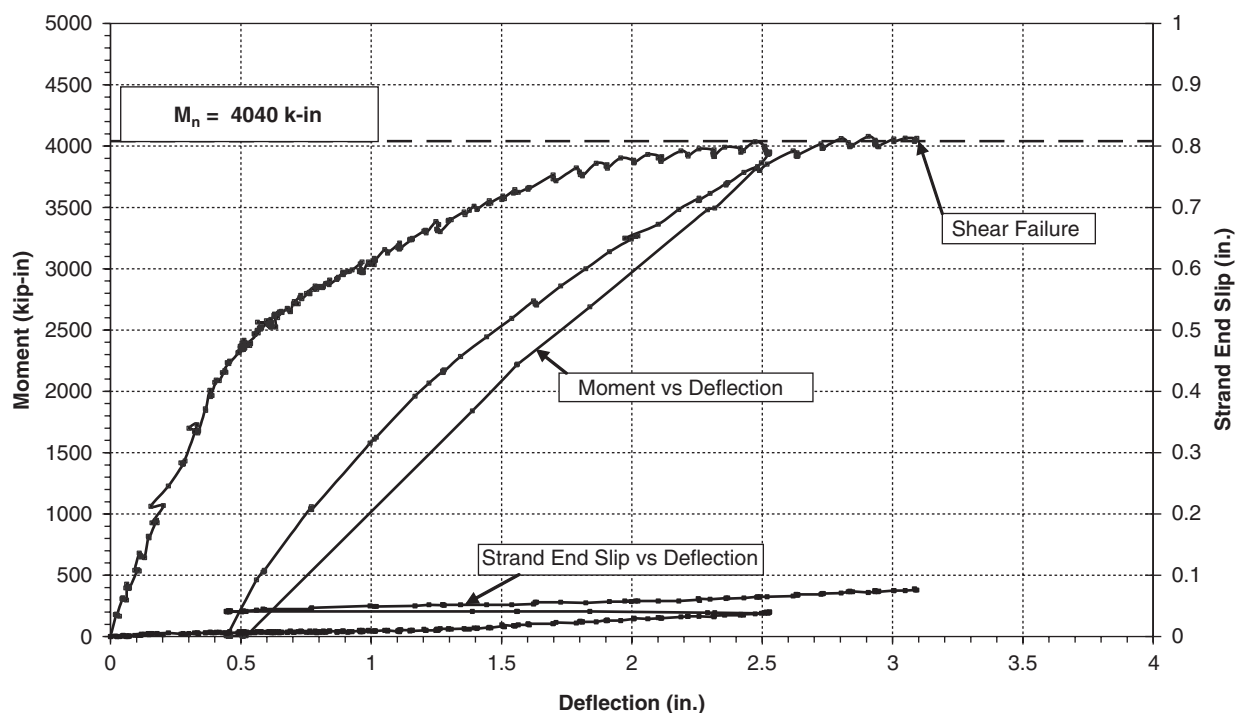


Figure 3.47. Applied moment versus deflection and strand end slip for Beam Test IA-6-6-2 (North).

The NASP Bond Test as a predictor of strand bond performance in flexural applications. Two 0.5 in. strands were tested in beams. Strand D had an NASP Bond Test value of 6,890 lb and Strands A and B had an NASP Bond Test value exceeding 20,000 lb. In the rectangular beams made with Strands A or B, no bond failures were experienced, even at relatively short embedment lengths. In I-shaped beams made with Strand B, no bond failures were experienced, even at embedment lengths shorter than the AASHTO design requirement for development length. In contrast, both rectangular beams and I-shaped beams made with Strand D experienced

bond failures at shorter embedment lengths. In I-shaped beams made with Strand D, the strand failed in bond even at lengths in excess of the ACI and AASHTO design requirements for development length. In other words, Strands A and B, which have relatively high NASP Bond Test values, demonstrated excellent bond characteristics. In contrast, Strand D, with a relatively low NASP Bond Test value, demonstrated poor bond characteristics. The results clearly show that the NASP Bond Test can distinguish between strands with good bonding behavior and strands with poor bonding behavior.

The minimum acceptable level of bond performance as measured by the NASP Bond Test. To determine a minimum level of bond performance as measured by the NASP Bond Test, results from the testing program conducted in the NASP Round III testing program are required. However, the results from the testing described in this chapter clearly indicate that the minimum value for the NASP Bond Test should be greater than the value measured on Strand D, 6,890 lb, but need not be as strong as the bond value measured on Strands A and B, which exceeded 20,000 lb.

Modifications necessary to the LRFD development length equation to account for variations in concrete strength. The results clearly show that increases in concrete strength bring about improvements in strand development. Strand D, which failed in bond at lower concrete strengths, was still able to fully develop adequate tension at the higher concrete strengths.

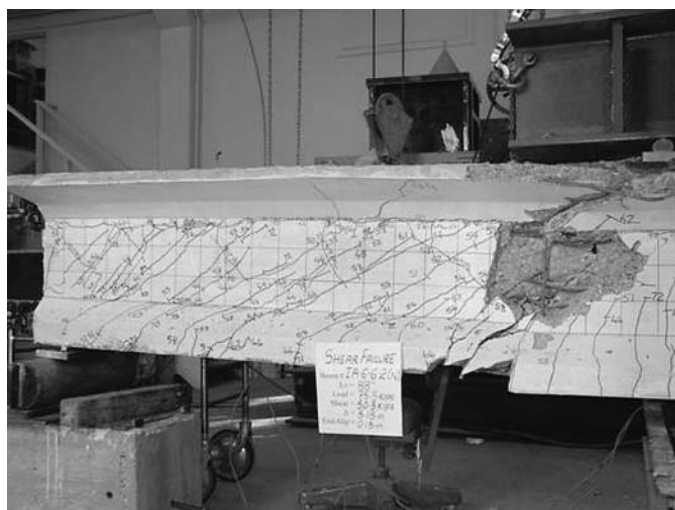


Figure 3.48. IA-6-6-2 (North) at shear failure.

3.5.4 Discussion of Test Results

This section includes analysis in three primary areas:

1. What influence does concrete strength have on the development length for pretensioned prestressing strands?
2. What is the proper expression for development length?
3. What should be the minimum NASP Bond Test Value of the prestressing strand for achieving adequate anchorage?

The NASP Bond Tests in concrete clearly demonstrate that concrete strength can exert great influence over the bond of strand with concrete. This trend was also demonstrated in measured transfer lengths as the transfer length for a given strand was shortened as concrete strength increased. In this section, the results from development length tests are analyzed to determine the influence of concrete strength. Based on the analysis, certain modifications to the current AASHTO equation for development length are recommended. Comparisons among flexural test results are used to assess the validity of such recommendations.

3.5.4.1 Evaluating Development Length from the Flexural Tests

The development length is the length for which the strand must be fully bonded to ensure strand anchorage adequate to develop the tension stress necessary to support the nominal flexural capacity of the cross section. The development length is distinguished from the embedment length, which is the length of bond that is actually provided. In the course of testing, a specific embedment length may be longer or shorter than the strand's development length. If a beam test results in a bond failure, then one must conclude that the embedment length provided was shorter than the required development length. Conversely, if a beam test results in a flexural failure, then one can conclude that the embedment length provided was longer than the required development length. Each independent beam test therefore becomes a single data point that can indicate whether the embedment was sufficient. In most cases, it is difficult to discern from a single test what the "true" development length must be.

Ideally, the "true" value of development would be when the flexural test results in simultaneous flexural, shear, and bond failures (Meyer 2002). Research that varies the embedment length between the values corresponding to complete flexural failure and the values corresponding to complete bond failure can get closer to identifying the "true" development length. Based on prior test results, the embedment length can be systematically lengthened or shortened for the purpose of bracketing the test results. In this manner, an accurate picture for development length may be obtained through multiple beam tests.

The variables for development length tests in this research were embedment length, concrete strength, and the type of strand. These parameters were changed for flexural tests on both rectangular and I-shaped beam specimens.

The current ACI/AASHTO equation does not include the concrete strength parameter for calculating transfer and development length. However, results obtained during the flexural tests strongly suggest that the anchorage ability of the strands is improved as concrete strength increases. The next section reports on the effects of increasing concrete strength on the results obtained during the flexural tests.

3.5.4.2 Direct Tabular Method

Table 3.28 summarizes the results from development length tests performed on Strand D cast in rectangular beams. In the Tables 3.28 through Table 3.30, the letter "F" denotes a flexural failure, and the letter "B" denotes a bond failure. In Table 3.28, the results indicate that for embedment lengths of 73 in. and concrete release strengths of about 4 ksi (56-day strength of 7 ksi), Strand D was able to develop the necessary tension to achieve a flexural failure in the beam. However, at an embedment length of 58 in. and tested at the opposite ends of the same beams, Strand D failed in bond.

The embedment length of 73 in. corresponds to 100 percent of the development length prescribed in the AASHTO

Table 3.28. Development length tests on rectangular beams with 0.5-in. Strand D (average NASP pull-out value = 6,870 lb).

Beam No.	f'_c @ Release (psi)	f'_c 56 Days (psi)	Embedment Length (in)		
			46	58	73
RD-4-5-1	4,033	7,050		B	F
RD-4-5-2	4,033	7,050		B	F
RD-6-5-1	6,183	8,500		F	F
RD-6-5-2	6,183	8,500		B	F
RD-6A-5-1	7,960	11,420		F	F
RD-6A-5-2	7,960	11,420		F	F
RD-8-5-1	8,570	13,490		F	F
RD-8-5-2	8,570	13,490		F, F*	-
RD-10-5-1	9,711	14,470	F	F	-
RD-10-5-2	9,711	14,470	F	F	-
F = Flexural failures					
B = Bond failures					
* Both ends were tested at an embedment length of 58 in. Both ends failed in flexure.					

Table 3.29. Development length tests on rectangular beams with 0.5-in. Strands A/B (average NASP pull-out value for A = 20,210 lb and for B = 20,950 lb).

Beam No.	f'_c RLS (psi)	f'_c 56 Days (psi)	Embedment Length (in)		
			46	58	73
RB-4-5-1	4,033	7,050		F	F
RB-4-5-2	4,033	7,050		F	F
RA-6-5-1	6,183	8,500		F	F
RA-6-5-2	6,183	8,500	F	F	
RA-6A-5-1	7,960	11,420		F	F
RA-6A-5-2	7,960	11,420	F	F	
RA-8-5-1	8,570	13,490	F	F	
RA-10-5-1	9,711	14,470	F	F	
F = Flexural failures					
B = Bond failures					

LRFD Bridge Design Specifications, while the embedment length of 58 in. corresponds to 80 percent of the code-specified value. Important to the purposes of this research, the bond of Strand D demonstrates marked improvement as concrete strengths increase. At a concrete strength of 11 ksi, Strand D was able to develop the necessary tension at embedment lengths of either 58 in. or 73 in. The test results indicate that for Strand D, cast in 11 ksi concrete, the development length required is equal to or less than 58 in. Further, in Beams RD-10-5-1 and RD-10-5-2, Strand D was able to develop its tensile force in only 46 in. of bonded length. These tests indicate that for Strand D cast in 14 ksi concrete, the development length required is equal to or less than 46 in.

The tests demonstrate that, had the concrete strength been 7 ksi, the development length required for Strand D would be less than 73 in. but greater than 58 in. The dark line in the table separates the zone of bond failures from the zone of flexural failures. The test results clearly show that the strand bond improves in development length applications with increases in concrete strength.

Table 3.29 shows the results from development length tests performed on beams made with Strands A/B. The results show that (1) Strands A/B bonded better with concrete than Strand D, and (2) the bond of Strands A/B improved as concrete strength increased. The dark line in the table separates the zone of bond failures from the zone of flexural failures.

Table 3.30 summarizes the results of beam tests on rectangular beams made with 0.6 in. strands. The current AASHTO expression gives a development length requirement equal to 88 in. for 0.6 inch diameter strands. Test results show that flexural failures occurred at lengths of 88 in. and 73 in. for all concrete strengths. The results also show that bond failures occurred for the three concrete strengths when an embedment length of 58 in. was tested. However, when Strand A6 was cast in concrete with a release strength of 10 ksi and a 56-day strength of over 14 ksi, the strand was able to develop the required tension force at an embedment length of 58 in. The dark line in the table separates the zone of bond failures from the zone of flexural failures. These results show clear improvements in strand bond behavior with increasing concrete strength.

The current ACI/AASHTO equation does not include the concrete strength parameter for calculating transfer and development length. However, results obtained during the

Table 3-30. Development length tests on rectangular beams with 0.6-in. Strand A6 (average NASP pull-out value = 18,920).

Beam End	f'_c RLS (psi)	f'_c 56 Days (psi)	Embedment Length (in)			
			58	70	73	88
RA-4-6-1	4,033	7,050		F		F
RA-4-6-2	4,033	7,050	B		F	
RA-6-6-1	4,855	8,040				F
RA-6-6-2	4,855	8,040	B		F	
RA-6-6-3	4,855	8,040				F
RA-8-6-1	5,413	8,220				F
RA-8-6-2	5,413	8,220	B		F	
RA-10-6-1	9,150	14,610				F
RA-10-6-2	9,150	14,610	F		F	
F = Flexural failures						
B = Bond failures						

flexural tests demonstrate that the anchorage ability of the strands is improved as concrete strength increases.

3.6 Discussion of Design Recommendations

The current AASHTO code provisions do not include the effects of concrete strength when calculating the required development length of prestressing strands. As a result, the development length for strands is the same regardless of concrete strength. However, the results of this research clearly demonstrate that the required transfer and development lengths are shortened as concrete strength increases.

The approach develops from the findings of the research:

1. The current AASHTO transfer length of $60d_b$ is adequate to predict the transfer length of prestressing strands in “normal strength concrete” (4-ksi release strength).
2. The data support modification of the AASHTO transfer length to account for variations in concrete release strength and in recognition of the finding that bond strength improves in proportion to the square root of the concrete strength.
3. The current AASHTO development length equation can be used to adequately predict required development lengths for “normal strength concrete” with a release strength in the range of 4 ksi and a design strength of 6 ksi.
4. The data demonstrate that shorter development lengths are required as concrete strength increases.

3.6.1 Discussion of Transfer Length Recommendations

The standard NASP Bond Test is a test where a prestressing strand is pulled from sand-cement mortar. The mortar is made from sand, cement, and water and possesses a 1-day compressive strength of 4,500 to 5,000 psi. The NASP Bond Test can be modified to perform the test in concretes with varying concrete strengths. However, the NASP Bond Test values used in the discussions regarding minimum Bond Values are pull-out strengths obtained from the standardized NASP Bond Test performed in mortar.

The results from NASP pull-out tests in concrete are presented and compared in this section. Figure 3.12 presents normalized NASP values (obtained by dividing the NASP pull-out values in concrete by the NASP standardized test values [from tests conducted in mortar]) versus the concrete strengths for the NASP tests in concrete. The tests demonstrate remarkable correlation between the bond-ability of prestressing strand and the concrete strength. Compared with a power regression, the chart in Figure 3.12 shows the

following relationship between NASP values in concrete and NASP values in mortar (standard NASP values):

$$\frac{(NASP_{\text{concrete}})}{NASP} = 0.49139 \bar{f}'_c^{0.51702} \quad (3.3)$$

The equation was further modified to fit the NASP values as a function of square root of concrete strengths. Figure 3.13 is a plot of normalized NASP values against the square roots of corresponding concrete strengths. Following is the relationship shown in Figure 3.13:

$$\frac{(NASP_{\text{concrete}})}{NASP} = 0.51 \sqrt{\bar{f}'_c} \quad (3.4)$$

With the help of this relationship, it was possible to use the Standardized NASP Bond Test, conducted in mortar, to estimate the bond strength as if the test were conducted in concrete with various strengths. The graphs in Figures 3.9 through 3.13 demonstrate that the NASP Bond Test pull-out value in concrete is inversely proportional to the square root of the concrete strength. From these data, one can further assert that the average bond stress, taken as the pull-out force divided by the bonded length, is also inversely proportional to the concrete strength at release. Further evidence for this same relationship between bond strength and pull-out force is found in Figures 3.24 through 3.32, which chart measured transfer lengths versus concrete strengths. The transfer length data demonstrate that transfer lengths change inversely with concrete release strength. Figure 3.32, which charts transfer length measured on three different strand samples, shows that transfer lengths are approximately inversely proportionate to the square root of the concrete strength. The best fit power regression indicates an exponent of -0.46 for measured concrete strengths at release. This is approximately equal to the inverse of the square root. It can therefore be concluded that transfer length is inversely proportional to the square root of concrete strength. Therefore, a transfer length expression is recommended that is equivalent to the current design expression of 60 strand diameters at a release strength of 4 ksi, but that shortens in proportion to the square root of the concrete strength at release. The recommended code provision also provides a minimum transfer length of $40 d_b$. The $40 d_b$ value corresponds to 10-ksi concrete, which was the highest 1-day strength tested.

The transfer length equation is modified by the square root of the concrete release strength, as follows:

$$l_t = \frac{120d_b}{\sqrt{f'_c}} \quad (3.5)$$

where

- l_t = transfer length (in.),
- f'_c = release concrete strength (ksi), and
- d_b = diameter or prestressing strand (in.).

Using concrete release strength of 4 ksi, this equation results in a transfer length equal to $60 d_b$. The recommendation for transfer length is only modified so that a minimum length for transfer length is used, regardless of concrete strength. The recommendation effectively limits improvements in transfer length based on a concrete release strength of 9 ksi, which is less than the maximum release strength obtained in the beams cast for this research (9.7 ksi on rectangular beams). Therefore, the final recommended expression for transfer length is the following:

$$l_t = \frac{120}{\sqrt{f'_c}} d_b \geq 40d_b \quad (3.6)$$

3.6.2 Development Length Recommendations

Since the inception of the pretensioned, prestressed concrete industry in the United States, the development length equation has been made from the sum of two components: (1) transfer length and (2) “flexural bond length,” which is the additional length of bond beyond the transfer length required for development. This approach has been utilized in the industry for decades. Research continues to demonstrate that the approach is adequate to explain observed behavior and predict results. Thus, the same approach is followed, but with modifications to include the effects of varying concrete strengths:

- The results demonstrate that for all types of 0.5 in. strands—Strands A/B and Strand D—flexural failures occurred at embedment lengths of 73 in. The embedment length of 73 in. corresponds to 100 percent of the current code provision for development length for these specimens. The results included tests on beams made with concrete strength of approximately 4 ksi at release and approximately 6 ksi at the time of the beam test.
- The results uniformly indicate that the development length requirements diminish with increasing concrete strength.
- The required development length calculated from the current code provisions is approximately $150 d_b$, although some variations will exist due to variations in strand stressing, beam geometry and subsequent variations in computed prestress losses.
- If the transfer length is approximately $60 d_b$, and the development length is approximately $150 d_b$, then the flexural bond length must be approximately $90 d_b$.

The development length expression can then be written as follows:

$$l_d = l_t + \frac{225d_b}{\sqrt{f'_c}} \quad (3.7)$$

where

- l_d = development length,
- l_t = transfer length,
- d_b = diameter of the prestressing strand, and
- f'_c = design concrete strength.

Using concrete design strength of 6 ksi, which roughly corresponds to a “normal” concrete strength within the industry and forms the base case from the experimental results, the coefficient of 225 corresponds to flexural bond length of 90 strand diameters.

Like the transfer length expression, the development length expression is limited by a minimum value. The recommended expression for development length, therefore, is based on a limiting concrete strength of approximately 14 ksi, which is slightly less than the maximum concrete strength attained in beams tested in the research program (14.9 ksi). Thus, the recommended development length equation is as follows:

$$l_d = \left[\frac{120}{\sqrt{f'_c}} + \frac{225}{\sqrt{f'_c}} \right] d_b \geq 100d_b \quad (3.8)$$

3.6.3 Distribution of Failure Types in Beams Tested

This section presents the development length test results in graphical fashion. The result of each beam test, whether flexural failure or bond failure, is plotted on a chart showing concrete strength versus embedment length. The recommended design equation for development length is also shown on each of the charts. Note that the development length varies with concrete strength. For the purpose of plotting the values while using the equation, release strength is taken as 66.7 percent of the design strength. This is a reasonable ratio of release strength to design strength, borne out by years of experience in prestressed concrete.

Figure 3.49 shows the results of development length tests on Strand D. Strand D demonstrated below average to poor bond performance with a relatively low NASP Bond Test result (6,890 lb), longer transfer lengths, and longer development length requirements than Strands A/B. Figure 3.49 shows that bond failures occurred in rectangular beams with embedment lengths of 58 in. at the lower concrete strengths. More importantly, the figure shows improvement in strand bond behavior as concrete strengths increased.

Note, however, that bond failures occurred in I-shaped beams cast with Strand D. Results of the tests demonstrate that the Strand D, with an NASP Bond Test value of only 6,890 lb, does not provide adequate bond-ability with concrete. Figure 3.50 shows the results of development length tests on Strands

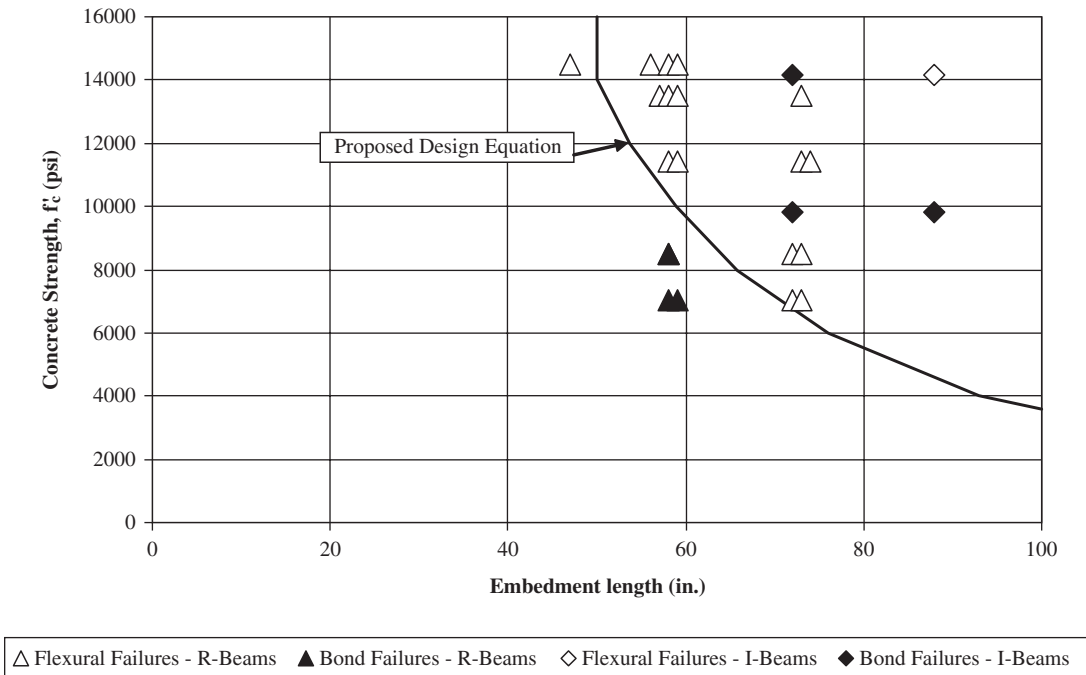


Figure 3.49. Distribution of bond and flexural failures for Strand D (0.5 in.).

A and B. Both of these strands can be considered “high bonding,” since the NASP Bond Test value was so high. Strand B was cast in the 4 ksi rectangular beams and I-shaped beams, and Strand A was used in the higher strength rectangular beams. The chart shows that the high-bonding strand was developed in all concrete strengths, even in embedment lengths as short as 46 in. The proposed design equation is shown on the chart along with the beam test results.

Figure 3.51 shows the distribution of bond and flexural failures for 0.6 in. strand, Strand A6, with respect to concrete strength and embedment lengths. As in Figure 3.50, the proposed design equation is shown in Figure 3.51 along with the beam test results. There are no bond failures occurring in the region where embedment length exceeds the calculated development length using the proposed equation. The tests support the proposed equation for development length.

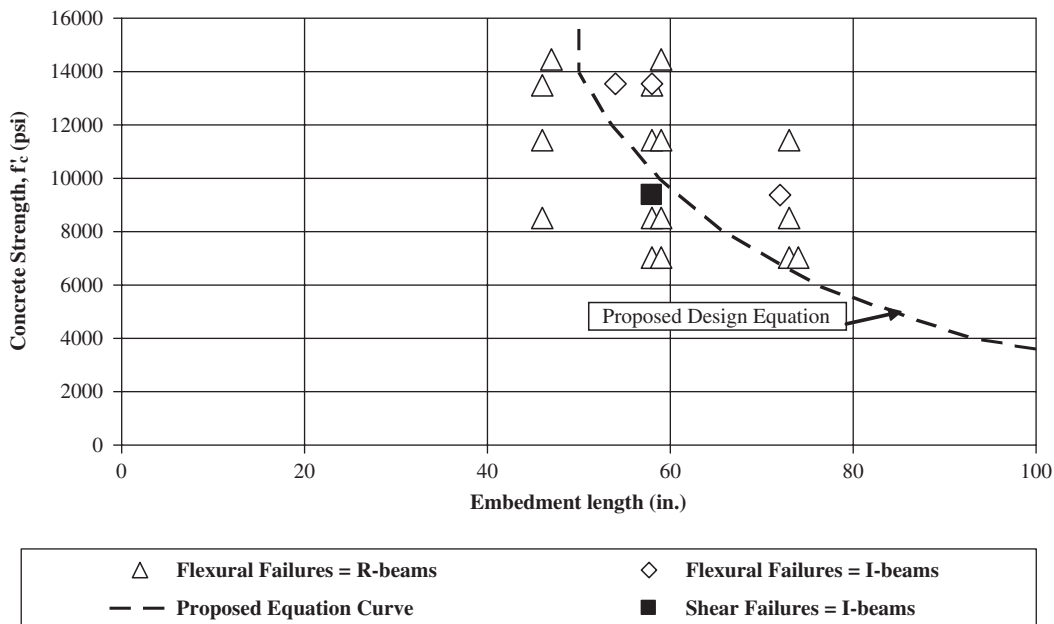


Figure 3.50. Distribution of bond and flexural failures for Strands A/B (0.5 in.).

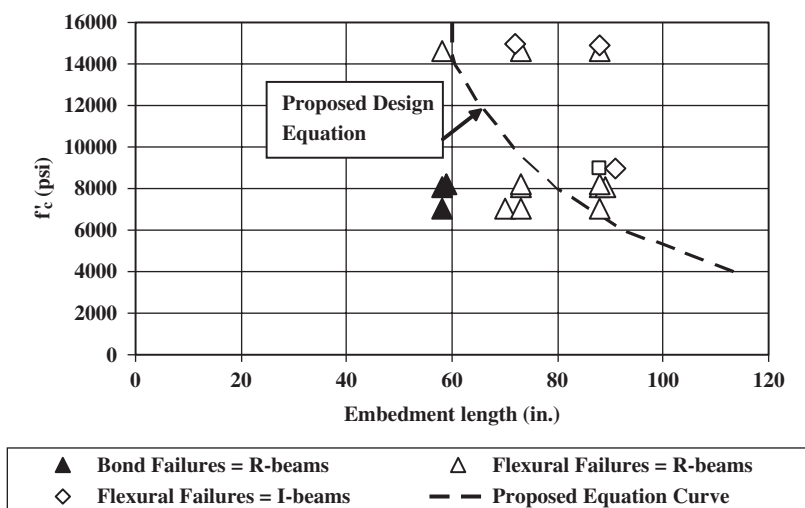


Figure 3.51. Distribution of bond and flexural failures for Strand A6 (0.6 in.).

3.6.4 NASP Value and Bond Performance

Along with the recommendation for the development length design expression, it is important to recommend a minimum value from the NASP Bond Test. First of all, however, it was important to establish a correlation between the NASP pull-out test values and the bond performance of the same strands in transfer and in development length tests. Russell and Brown (2004) measured transfer lengths and performed flexural tests on rectangular-shaped beams. Table 3.31 and Table 3.32 summarize the test results and the failure modes obtained from flexural tests performed by Russell and Brown (2004). The NASP pull-out test values are also given.

Strand II had the lowest NASP Bond Test value, only 4,140 lb. Strand II is the same strand as that labeled Strand E in the NCHRP research. One can see also that Strand II was the

worst performer of the four strands in both single strand and double strand beams, with bond failures at the AASHTO development length of 73 in.

Strand FF from Russell and Brown's research (2004) is the same strand labeled Strand D in the NCHRP research. As seen in Tables 3.31 and 3.32, Russell and Brown reported a NASP Bond Test value of 7,300 lb for Strand FF. This compares with a NASP Bond Test value of 6,890 lb in the NCHRP testing. Strand FF demonstrated the ability to develop adequate tension in an embedment length of 73 in. in the rectangular beams. However, if one looks at the results of the I-shaped beams in Table 3.27, one can see that Strand D or Strand FF was unable to develop adequate strand tension at the development length of 73 in.

Table 3.31. Failure modes on single-strand beams (Russell and Brown 2004).

Beam No.	f'_c 56 Days (psi)	Average NASP Pull-Out Value (lb)	Embedment Length (in)	
			58	73
II11	6,290	4,140	B	F
II12	6,280	4,140	B	B
FF11	6,260	7,300	V	F
FF12	6,070	7,300	B	F
HH11	6,330	10,700	F	F
HH12	6,300	10,700	B	F
AA11	6,220	14,950	F	F
AA12	6,160	14,950	F	F

F = Flexural Failure
 V = Shear Failure
 B = Bond Failure

Table 3.32. Failure mode on beams made with two strands (Russell and Brown 2004).

Beam No.	f'_c 56 Days (psi)	Average NASP Pull-Out Value (lb)	Embedment Length (in)	
			58	73
II21	6,290	4,140	B	F
II22	6,280	4,140	B	B
FF21	6,260	7,300	F	F
FF22	6,070	7,300	F	F
HH21	6,330	10,700	F	F
HH22	6,300	10,700	F	F
AA21	6,220	14,950	F	F
AA22	6,160	14,950	F	F

F = Flexural Failure
 V = Shear Failure
 B = Bond Failure

Also, in Russell and Brown's research (2004), NASP Round IV testing, Strand HH demonstrated the ability to develop adequate strand tension at the development length of 73 in. The NASP Bond Test value was 10,700 lb. One bond failure occurred at an embedment length of 58 in. This occurred in a single strand beam. The results from NASP Round IV testing reported by Russell and Brown (2004) indicate that the bond performance of Strand HH was adequate.

Figure 3.52 shows the distribution of bond and flexural failures for Strand HH (0.5 in.) with respect to the concrete strength and the provided embedment lengths. There are no bond failures occurring in the region where provided embedment length exceeds the calculated development length using the proposed equation. The tests support the proposed equation for development length and also indicate that bond performance of strand HH was adequate.

No bond failure was recorded on the beams with Strand AA. Comparing the NASP values of these strands, the following observation can be made: as the NASP value increases, chances of bond failure at provided embedment length decrease. In other words, Strand II had the lowest NASP value and the highest number of bond failures, Strand FF and Strand HH had NASP values lying between those of Strand II and Strand AA, and bond failures were noted on fewer occasions for Strand FF and Strand HH than for Strand II. Strand AA had the highest NASP value and no bond failures, suggesting that it was capable of developing enough anchorage to achieve flexural failures. A higher NASP value seems to indicate better bonding qualities for the strand.

Table 3.33 presents the number of failures obtained for all types of strands (0.5 in.) including NASP Round III Strands. In Table 3.33, strands are arranged in the order of increasing NASP pull-out values. The number of bond failures obtained at 58-in. and 73-in. embedment lengths is shown.

Table 3.33. Bond failures at 58 in. and 73 in. for all 0.5 in. strands—I-shaped beams and rectangular beams.

Strand Name	NASP Value (lb)	Number of Bond Failures	
		58-in Embedment Length	73-in Embedment Length
II	4,140	4	2
D	6,590	3	2*
FF	7,300	1	0
HH	10,700	1	0
AA	14,950	0	0
B	20,210	0	0
A	20,950	0	0

* Embedment lengths were 72 in. instead of 73 in.

The number of bond failures is lower for strands with higher NASP pull-out values. Strand HH, with NASP pull-out value of 10,700 lb, lies at a critical position (boldfaced in Table 3.33): strands with NASP pull-out values lower than Strand HH's pull-out value sustained bond failures, but no strands with NASP pull-out values higher than Strand HH's pull-out value suffered bond failure. Embedment lengths of 58 in. and 73 in. correspond to 80 percent and 100 percent, respectively, of the code provision for development length. Strand HH suffered a bond failure at an embedment length of 58 in., but none at 73 in. These data show that a NASP pull-out value of 10,700 lb is adequate to develop enough anchorage for achieving flexural failures at the code-specified development length.

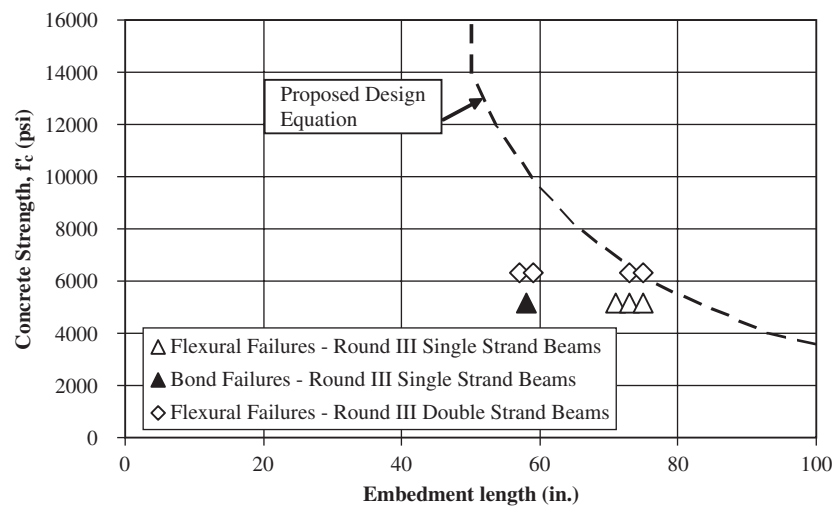


Figure 3.52. Distribution of bond and flexural failures for Strand HH (Russell and Brown 2004).

3.7 The Effect of Concrete Strength on Bond Performance— Summary, Conclusions, and Recommendations

The research program involved development length tests on two types of beam specimens. Four types of strands were employed to cast 43 rectangular-shaped beams and 8 I-shaped beams. Both 0.5 in. and 0.6 in. diameter strands were included in the testing program. The beam specimens had concrete release strengths varying between 4 ksi and 10 ksi for both types of beams. Transfer lengths were measured on all beam specimens using the strand end slip of the strands with the help of clamps attached to the strands. Transfer lengths were also measured using the concrete surface strain measurements. Fifty flexural tests were carried out on the rectangular beams, and 14 flexural tests were carried out on the I-shaped beams. Values of load, deflection, and strand end slip were recorded electronically and manually along with photographic records of failure stages and crack patterns. I-shaped beam specimen concrete surface strains were measured at 36 in. from the end of the beam and vertically at the center of the web.

Prestressing strand anchorage requirements were assessed using the data collected from the development length tests. Results from the development length tests were compared with the NASP pull-out values of corresponding strands. Based on the failure modes during the development length tests, the effect of concrete strength on bond performance was analyzed. The current AASHTO code requirements for development length of prestressing strands were assessed for their effectiveness in predicting accurate anchorage requirements. The conclusions from this research are the following:

- Development length tests can be used to assess the bond performance of prestressing strands.
- The ability of a prestressing strand to bond with concrete is affected by concrete strength. Increasing concrete strength improves the bond-ability of a given prestressing strand.
- The development length requirement for a particular strand is reduced if cast in higher strength concrete.
- The NASP Bond Test provides a good indicator of strand bond performance in a pretensioned concrete beam.
- The required development length shows a clear relationship with the NASP Bond Test values of the prestressing strand. Higher NASP Bond Test values result in shorter development lengths.
- Rectangular beams with all types of strands were able to achieve flexural failures at embedment lengths less than or equal to the AASHTO-specified development length.
- With increased concrete strength, it is possible to achieve flexural failures at an embedment length less than the AASHTO-specified value.

- Current AASHTO code provisions may overestimate the required development length of prestressing strands in higher strength concretes.
- I-shaped beams were more susceptible to bond failures than rectangular beams because of the higher incidence of web shear cracks developing in I-shaped beams.

Finally, on the basis of the study findings, the following recommendations are made:

- AASHTO code equations for transfer length should include a parameter reflecting the reduced transfer length with increasing concrete release strength. The recommended equation for transfer length, l_t (in.), is

$$l_t = \left[\frac{120d_b}{\sqrt{f'_{ci}}} \right] \leq 40d_b \quad (3.9)$$

where

f'_{ci} = release concrete strength in ksi, and
 d_b = diameter of prestressing strands in inches.

- AASHTO code equations for development length should include a parameter reflecting the reduced transfer length with increasing concrete release strength. Further, the flexural bond length is reduced by higher strength concrete as well. The recommended equation for development length is the following:

$$l_d = \left[\frac{120}{\sqrt{f'_{ci}}} + \frac{225}{\sqrt{f'_c}} \right] d_b \geq 100d_b \quad (3.10)$$

where

l_d = development length (in.),
 f'_{ci} = release concrete strength in ksi,
 f'_c = design concrete strength in ksi, and
 d_b = diameter of prestressing strands in inches.

- A relatively large database has been collected during the course of this research project. The data include crack patterns, crack spacing, and surface strain measurements on I-shaped beams. A more detailed analysis should be made using the information embedded in the summary reports for a better understanding of the failure mechanisms. It is recommended that the Standardized Test for Strand Bond be adopted into the *AASHTO LRFD Bridge Design Specifications*. The Standard Test for Strand Bond, formerly known as the NASP Bond Test, requires an average pull-out value of 10,500 lb with no single test out of a sample of six tests falling below 9,000 lb. These values are established from the review of the data obtained from the testing reported herein. Supporting data is found in the NASP Round III test report, which is incorporated into this report via discussion in previous sections. The Standard Test Method for the Bond of Prestressing Strands is recommended to ensure adequate

anchorage at embedment lengths equal to or higher than AASHTO code development length provision for normal-strength concretes.

- The effect of admixtures on the transfer and development length tests should be studied, with more development length tests carried out while changing the proportions of different admixtures in the concrete.

3.8 Experimental Program—Mild Steel Anchorage of Uncoated Bars in Tension

An extensive literature review of test data was conducted, and the results were reported in Chapter 2. The findings of the literature review indicated the need to supplement the data with six additional tests of top cast uncoated bar splices in order to extend the use of the *AASHTO LRFD Bridge Design Specifications* for development and splice length of uncoated bars to higher strength concretes. The variables considered were bar size (#6, #8, and #11) and amount of transverse reinforcement over the splice length. All six specimens tested had clear concrete cover of d_b .

3.8.1 Specimen Design

Six beam splice specimens were tested. The specimen dimensions and variables are shown in Table 3.34. The test variables were bar size and the presence of transverse reinforcements in the splice region in higher strength concretes. The cover value given in Column 3 of Table 3.34 is for both

top and side clear cover to the bar being developed or spliced. Details of typical specimens are shown in Table 3.34 and Figure 3.53. In Specimens I-4, I-5, and I-6, transverse reinforcement was used in the splice region to confine the concrete as shown in Figure 3.54(b). The splice length shown in Column 7 of Table 3.34 was selected to provide a direct link with companion test specimens containing epoxy-coated bars, which were reported on in a separate paper and other tests in the literature. The same splice lengths were used for the specimens with transverse reinforcement so that the confining effect of this reinforcement could be evaluated. Rearranging Equation 12-1 of the 318 Code (ACI 2005) with appropriate modification factors and with a splice class factor of 1.0, it was possible to estimate a design stress and force in the bars for various anchorage conditions, as shown in Equation 3.11. To determine the calculated stress, f_y (specified yield strength of reinforcing bars [psi]) is replaced with f_s and l_d is replaced by the splice length provided, 16, 24, and 36 in. for specimens with #6 (#19M) bars, specimens with #8 bars, and specimens with #11 bars, respectively. Note that all the specimens had more than 12 in. of concrete cast below the splice. As shown in Table 3.34, all the bars in the specimens with transverse reinforcement had a calculated stress over the design stress of 60 ksi. These values are shown in Column 8 of Table 3.34 next to the yield design value.

$$f_s = \frac{l_d}{d_b} \left[\frac{40\sqrt{f'_c} \left(\frac{c_b + K_{tr}}{d_b} \right)}{3(1.3)\psi_e\psi_s} \right] \quad (3.11)$$

Table 3.34. Specimen dimensions and variables.

(1) Specimen	(2) Bar Size	(3) Cover (in.)	(4) Beam Size (B x H) (in.)	(5) Effective Depth (in.)	(6) Number of Spliced Bars	(7) Splice Length (in.)	(8) 318-05 Cal. Stress (ksi)	(9) Test Date Compressive Strength (f'_c , ksi)
I-1	#6	0.75	9 x 18	16.88	3	16	52.10	16.2
I-2	#8	1.00	12 x 18	16.50	3	24	44.68	14.6
I-3	#11	1.50	18 x 18	15.75	3	36	49.89	16.2
I-4*	#6	0.75	9 x 18	16.88	3	16	60 (66.91)	15.1
I-5*	#8	1.00	12 x 18	16.50	3	24	60 (64.54)	14.6
I-6*	#11	1.50	18 x 18	15.75	3	36	60 (63.55)	15.1

1 in. = 25.4 mm; 1 ksi = 6.89 MPa.
 B = specimen width. H = specimen height.
 (* shows specimens with transverse reinforcement in the splice region)

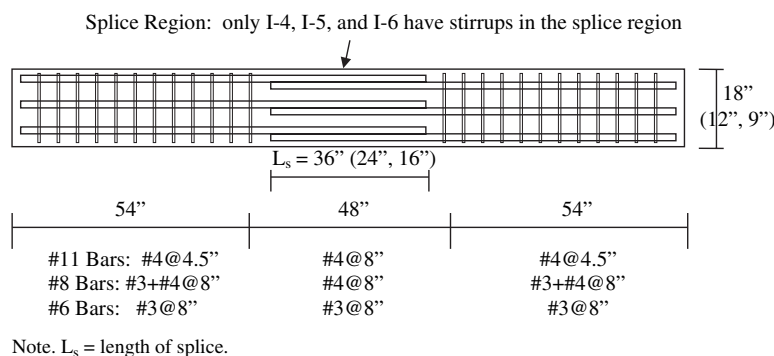


Figure 3.53. Specimen details (1 in. = 25.4 mm).

The factor representing the contribution of confining reinforcement across potential splitting planes is K_{tr} . The variable c_b represents the spacing or cover dimension, calculated using either the distance from the center of the bar (or wire) to the nearest concrete surface or one-half the distance of the center-to-center spacing of the bars being developed. ψ_e is a coating factor of 1.5 for cases with cover less than $3d_b$, or clear spacing less than $6d_b$, and 1.2 for all other cases. The parameter ψ_s is a reinforcement size factor: 0.8 for #6 bars and smaller and 1.0 for all other cases.

The specimens were checked and reinforced in the overhang region to prevent premature shear failures outside of the test region. To prevent shear failure, a stress of 1.25 times the yield strength of the bar was assumed in the overhang for purposes of estimating the required shear reinforcement to resist the maximum shear associated with the moment capacity of the section at the support. The shear reinforcement in the overhang region consisted of #3 @8 in., #3 + #4 @8 in., and #4 @4.5 in., in Specimens I-1 and I-4, I-2 and I-5, and I-3 and I-6, respectively. The shear reinforcement in the splice region consisted of #3 @8 in. on centers in I-4 and #4 @8 in. on cen-

ters in both I-5 and I-6. Figure 3.54 shows the specimen reinforcing cages.

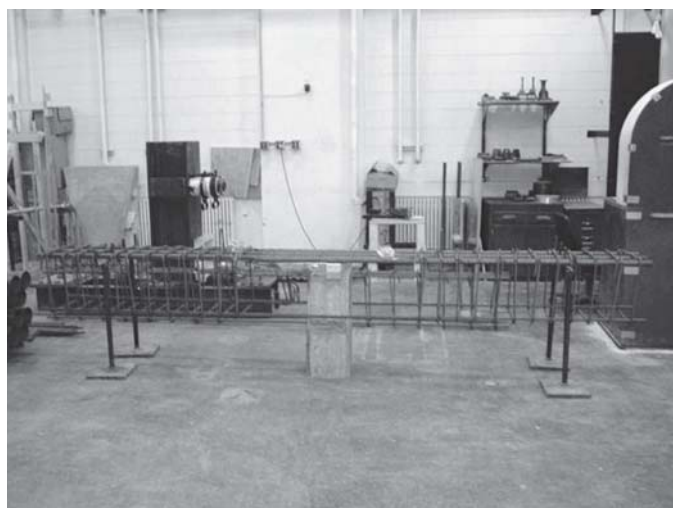
3.8.2 Test Set-Up

The beam splice setup used in this investigation is shown in Figure 3.55. In all specimens, the distance between the loading points and the support was 48 in. The constant moment region was also 48 in. Splices were located within the constant moment region. To investigate the characteristics of spliced beams, the applied loads, the resulting deflections at each beam end and midspan, and strains developed in longitudinal bars and stirrups were monitored using load cells, linear variable differential transducers (LVDTs) anchored to a reference frame, and electrical resistance strain gages attached to the bars, as shown in Figure 3.55 (b) and (c).

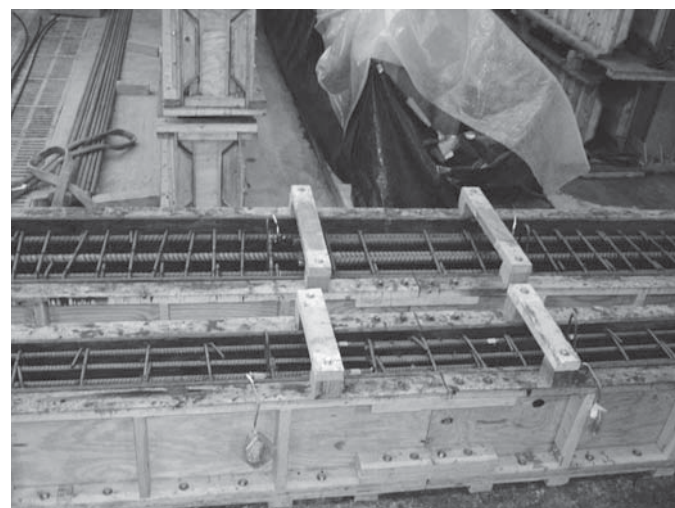
3.8.3 Materials

Concrete and reinforcing steel were the materials used.

Table 3.35 shows a typical concrete mix for the specimens. This mix was designed for a compressive strength of at least

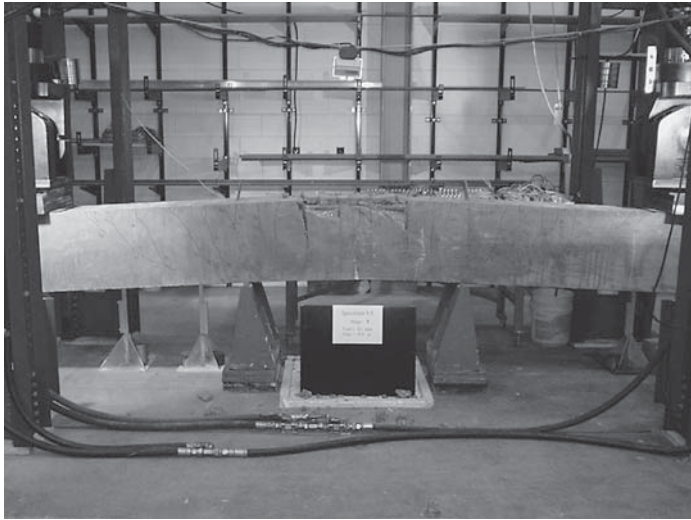


(a) Specimen I-1



(b) Specimens I-4 & I-6

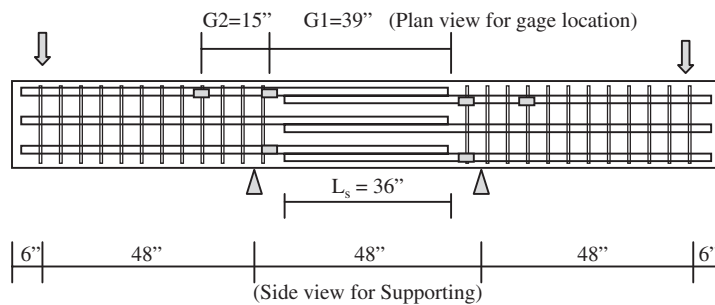
Figure 3.54. Specimen fabrication.



(a) Loading & Supporting



(b) Measuring by LVDT



(c) Location of gages and support (Specimen I-3)

Specimen	Bar Size	L_s (in.)	G1 (in.)	G2 (in.)
I-1, I-4	#6 (#19M)	16	19	13
I-2, I-5	#8 (#25M)	24	27	9
I-3, I-6	#11 (#35M)	36	39	15

Note: G1 = Gage 1. G2 = Gage 2.

Figure 3.55. Test setup (1 in. = 25.4 mm).

Table 3.35. Typical concrete mix ratio (per 1 cubic yard).

Contents	15-ksi Mix
Cement (lb)	900
Silica fume (lb)	200
Water (lb)	220
Coarse aggregate (lb)	1800 (1/2" crushed limestone)
Fine aggregate (lb)	1000
High-range water reducer (oz)	520
Normal-range water reducer (oz)	38
1 lb = 0.454 kg; 1 oz = 28.35 gr; 1 yd ³ = 0.765 m ³ ; 1 ksi = 6.89 MPa	

15 ksi. The water to cement ratio was 0.20. The average modulus of rupture was 834 psi at 28 days. Typical maximum compressive stress versus age data are shown in Figure 3.56. The concrete strength continued to increase after 28 days and achieved a strength of 17 ksi at 56 days. The specimens began to be tested after they reached a 15-ksi uniaxial compressive strength.

The reinforcing bars were ASTM A615 Grade 60 steel and had a yield strength based on tests of samples of the reinforcing bars of 78.3 ksi, 70.3 ksi, and 66 ksi for the #6, #8, and #11 bars, respectively. Stress versus strain curves for #6, #8 and #11 bars are shown in Figure 3.57.

3.8.4 Cracking and Failure Mode

In nearly all tests, the cracking sequence was similar. First, a flexural crack appeared in the constant moment region.

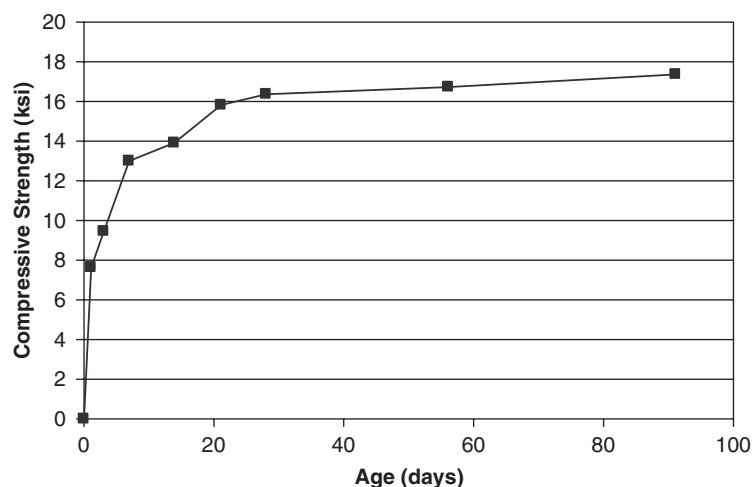


Figure 3.56. Concrete stress versus age relationship (1 ksi = 6.89 MPa).

With the increase of beam end loads, a shear crack appeared in the overhang region and was arrested by the presence of the shear reinforcement. Near the peak load, horizontal cracks appeared along the longitudinal bars within the splice region. Finally, the deformations pushed the concrete away from the bar by wedge action. Failure crack patterns of all the specimens are shown in Figure 3.58. All the specimens failed in splitting mode following yielding of the spliced bars in the constant moment region.

3.8.5 Beam End Displacement

The applied load versus deflection at the tip of the overhang response for Specimens I-1 to I-6 is shown in Figure 3.59. Load represents the average of the two values from the actuators. Deflections were calculated by averaging displacements at both ends of the beam. The test results are summarized in Table 3.36. In the specimens without transverse reinforcement in the splice region (Specimens I-1, I-2, and I-3), the end

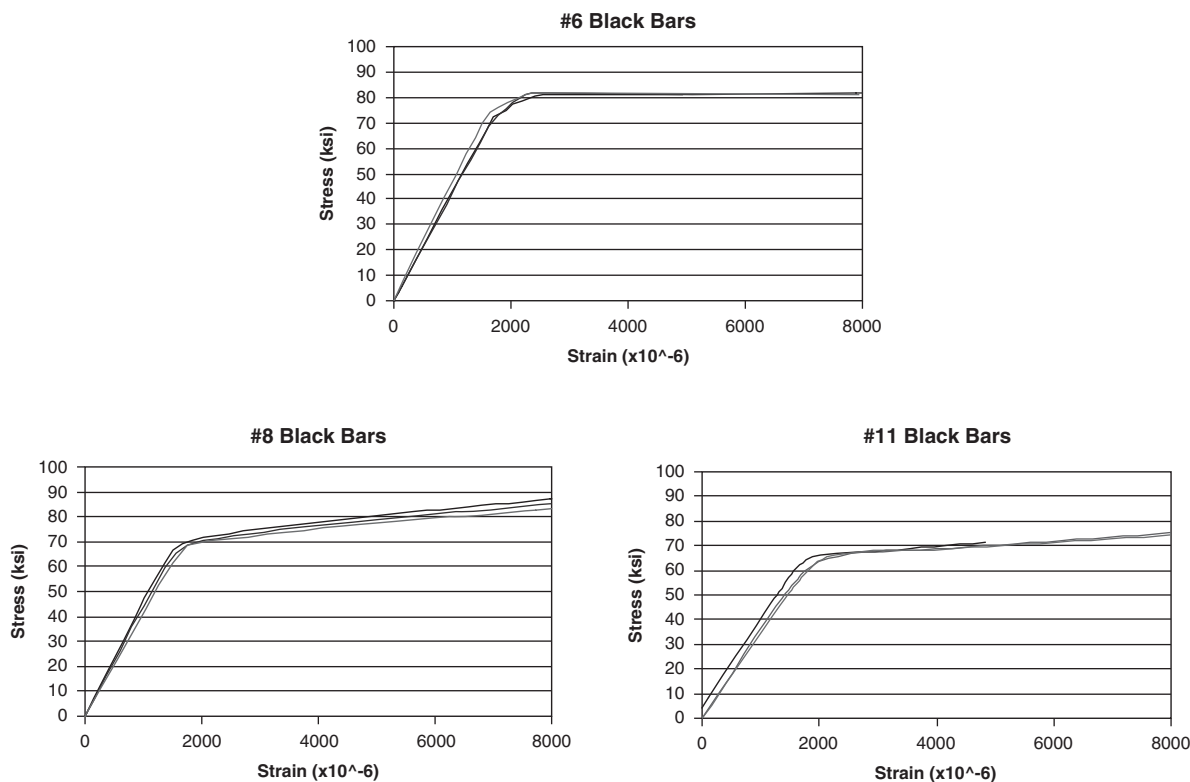
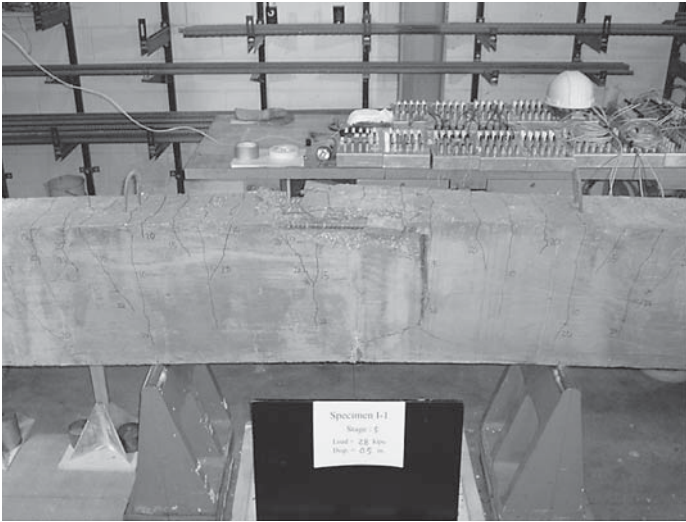
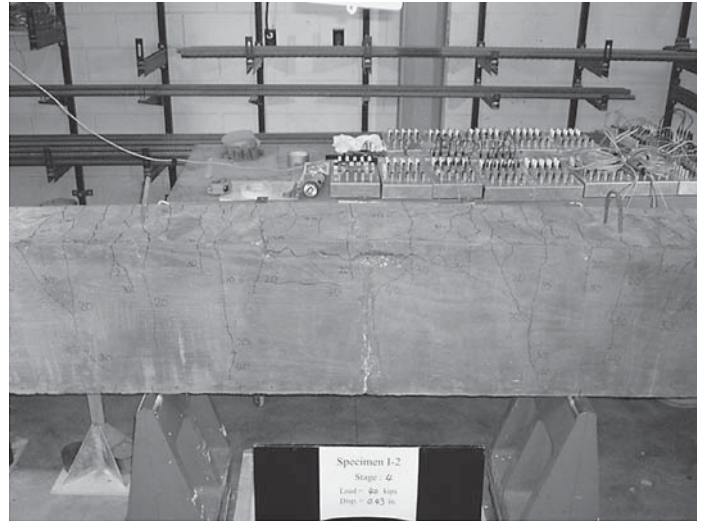


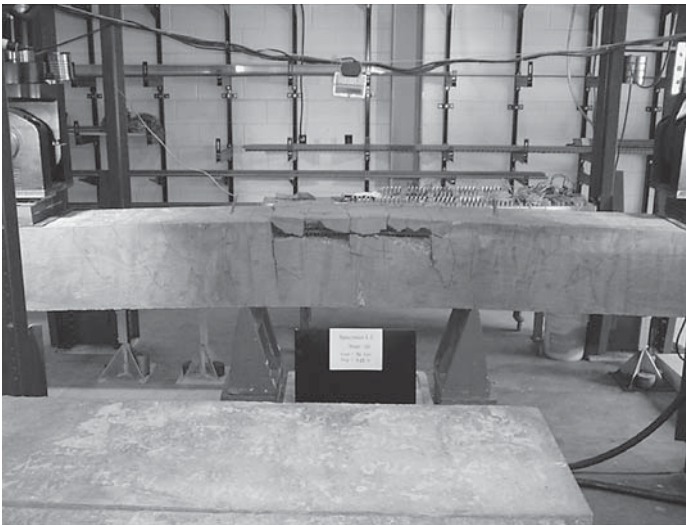
Figure 3.57. Tensile stress versus strain relationship (1 ksi = 6.89 MPa).



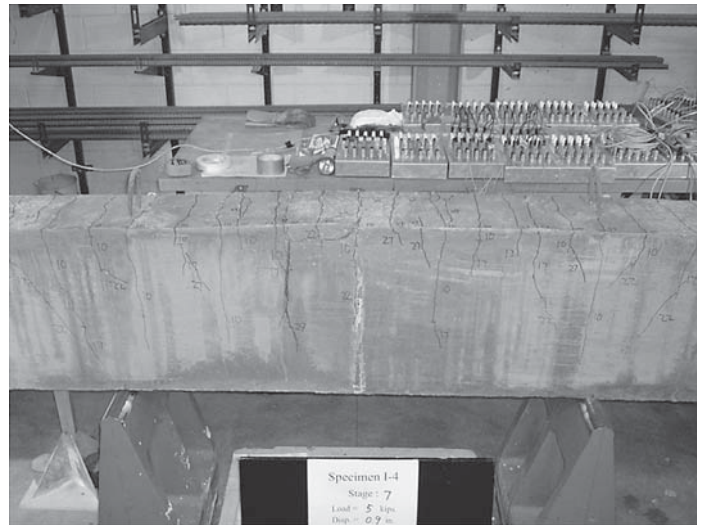
(a) Specimen I-1



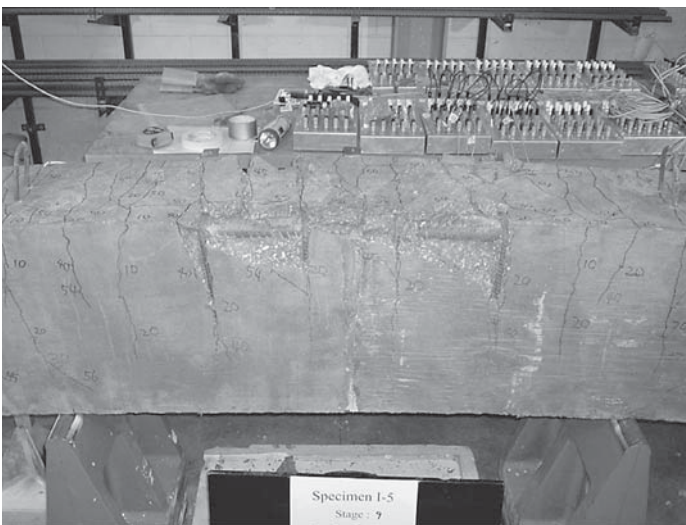
(b) Specimen I-2



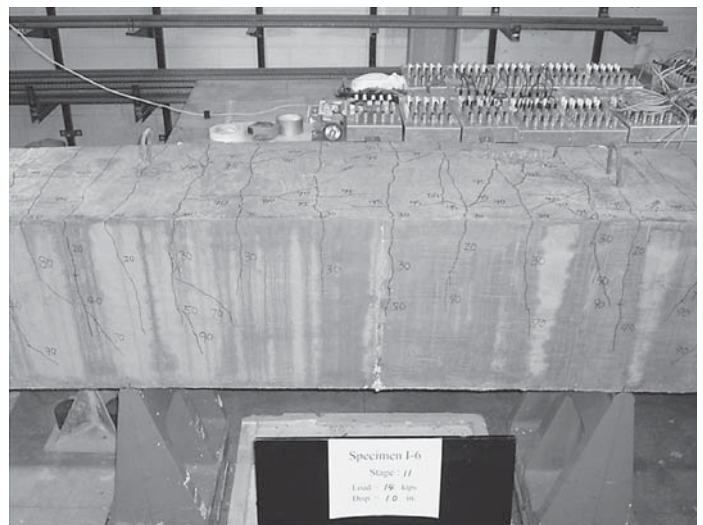
(c) Specimen I-3



(d) Specimen I-4



(e) Specimen I-5



(f) Specimen I-6

Figure 3.58. Failure crack patterns for all the specimens for the #6, #8, and #11 bars.

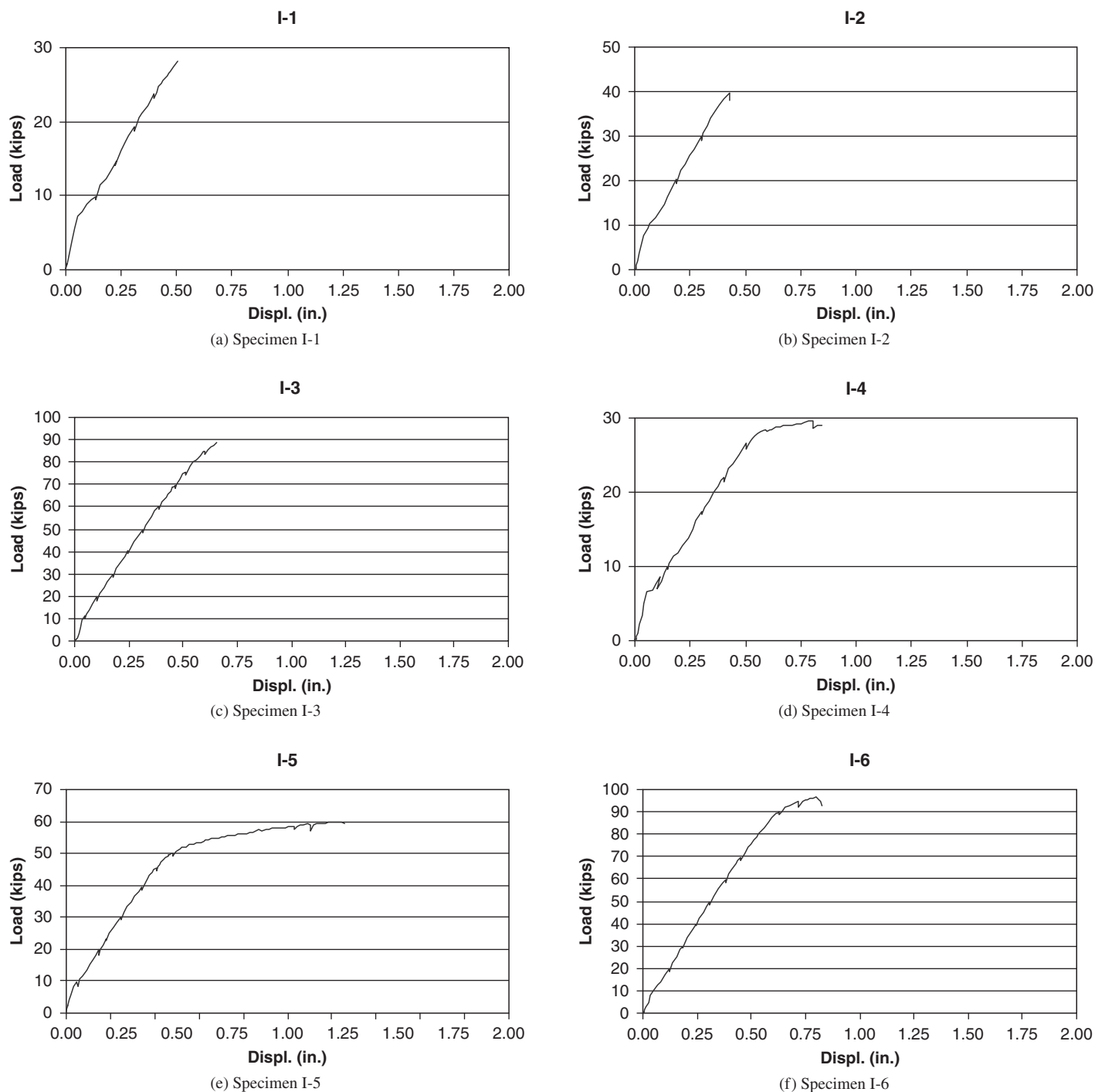


Figure 3.59. End load—end displacement curves for Specimens I-1 through I-6 (1 in. = 25.4 mm; 1 kip = 4.448 kN).

displacements at the peak load were 0.5 to 0.7 in. In the specimens with transverse reinforcement over the splice region (Specimens I-4, I-5, and I-6), the end displacements at the peak load were 0.8, 1.6 and 0.8 in., respectively.

3.8.6 Bar Strains

In Figure 3.60, the typical end concentrated load versus measured longitudinal bar and transverse bar strains in the

constant moment region of Specimen I-6 are shown. Yield strain in the longitudinal reinforcement was first recorded at around one-third of the peak load. Table 3.37 shows the measured maximum strains on all of the specimens. All the gages on the longitudinal reinforcement showed strains in excess of the bar yield strain before reaching peak load. In the gages placed on the stirrups in the constant moment region, the measured maximum strain was around half of the bar yield strain in Specimens I-4 and I-5 and almost equal to the

Table 3.36. Summary of test results for uncoated bar specimens.

(1) Spec.	(2) Max. Load (kips)	(3) Displ. at Peak (in)	(4) 318-05 Cal. Stress (ksi)	(5) 318-05* Cal. Stress (ksi)	(6) AASHTO Cal. Stress (ksi)	(7) Test Max. Stress (ksi)	(8) (7)/(4)	(9) (7)/(5)	(10) (7)/(6)
I-1	28.2	0.506	52.10	41.68	38.10	78.55	1.51	1.88	2.06
I-2	39.6	0.429	44.68	44.68	42.86	70.93	1.59	1.59	1.65
I-3	88.6	0.654	49.89	49.89	45.59	67.65	1.36	1.36	1.48
I-4**	29.5	0.805	60 (66.91)	53.54	38.10	81.24	1.21	1.52	2.13
I-5**	59.4	1.572	60 (64.54)	60 (64.54)	42.86	91.88	1.42	1.42	2.14
I-6**	96.4	0.800	60 (63.55)	60 (63.55)	45.59	71.94	1.13	1.13	1.58

1 in. = 25.4 mm; 1 kip = 4.448 kN; 1 ksi = 6.89 MPa
 * Shows stress calculated by removing bar size factor
 ** Shows specimens with transverse reinforcement in the splice region

bar yield strain in Specimen I-6. The use of stirrups in the splice region of Specimens I-4, I-5, and I-6 resulted in an increase in the displacement capacity when compared with companion specimens I-1, I-2, and I-3, respectively.

3.8.7 U.S. Design Specifications

3.8.7.1 318 Code (ACI 2005)

Orangun, Jirsa, and Breen (1977) evaluated the results of a large number of bond and splice tests. The evaluation highlighted the importance of parameters such as bar diameter, stress in the bar to be developed ($\sqrt{f'_c}$), cover or bar spacing, and the amount of transverse reinforcement. The Orangun,

Jirsa, and Breen study—together with contributions on bond of reinforcement from ACI Committee 318 and ACI Committee 408 that were meant to simplify the provisions for calculating development length of straight bars in tension—led to Equation 12-1 in the 318 Code (ACI 2005), which is Equation 3.12 herein:

$$l_d = \left[\frac{3 f_y \Psi_t \Psi_e \Psi_s \lambda}{40 \sqrt{f'_c} \left(\frac{c_b + K_{tr}}{d_b} \right)} \right] d_b \quad (3.12)$$

In Equation 3.12, f_y is the specified yield strength of reinforcing bars (psi), Ψ_t is the reinforcement location factor of

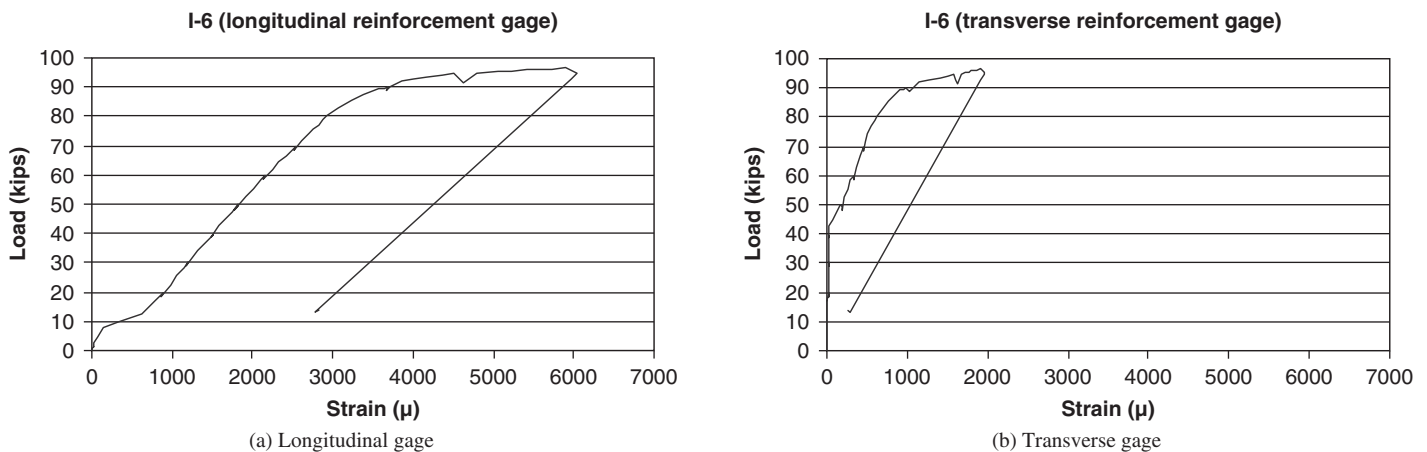


Figure 3.60. Beam end load versus measured strain relationship in Specimen I-6 (1 kip = 4.448 kN).

Table 3.37. Measured maximum strains (μ) in specimens I-1 through I-6.

Gage Location	I-1	I-2	I-3	I-4	I-5	I-6
Longitudinal Bar	3,405	2,370	3,100	10,300	10,750	5,960
Transverse Reinforcement	N/A	N/A	N/A	1100	875	1,910

1.3 to reflect the adverse effects on top casting position on the bond strength of the reinforcement. The parameter ψ_e is a coating factor of 1.5 for cases with cover less than $3d_b$, or clear spacing less than $6d_b$, and 1.2 for all other cases. These factors are consistent with a ratio of bond strength of coated bars to bond strength of uncoated bars observed in the literature of $1/1.5 = 0.67$ and $1/1.2 = 0.82$. However, the product of ψ_t and ψ_e need not be taken greater than 1.7. The parameter ψ_s is a reinforcement size factor: 0.8 for #6 bars and smaller and 1.0 for all other cases. The factor reflecting the lower tensile strength of lightweight concrete is λ . Bar diameter is d_b . The factor representing the contribution of confining reinforcement across potential splitting planes is K_{tr} . The variable c_b represents the spacing or cover dimension, calculated using either the distance from the center of the bar (or wire) to the nearest concrete surface or one-half the distance of the center-to-center spacing of the bars being developed. The ratio of $(c_b + K_{tr})/d_b$ should not be taken greater than 2.5.

However, the development length, l_d , so calculated, cannot be less than 12 in. In addition, when calculating anchorage length requirements for tension lap splices, these should be as required for a Class A or B splice, but not less than 12 in., where

Class A splice.....1.0 l_d
 Class B splice.....1.3 l_d

It must be noted that this factor is associated with the potential mode of failure when multiple bars are spliced at the same location and does not speak to the actual strength of the spliced bar.

3.8.7.2 2004 AASHTO Specifications (Section 5.11: Development and Splices of Reinforcement)

The bond provisions for mild reinforcement in the *AASHTO LRFD Bridge Design Specifications* mirrored the 318 Code provisions first introduced in the 1963 edition of the ACI Standard (ACI 1963). At the end of the last decade, the ACI 318 provisions for development and splices of reinforcement were extensively modified; however, the AASHTO provisions for development and splices of reinforcement continued to mirror the ACI provisions first introduced in

1963. A brief description of the background of the 1963 ACI specifications is provided below.

The 1963 edition of the 318 Code provisions for bond and anchorage for ultimate strength design were stated on the basis of the ultimate flexural bond stress at the sections of interest (ACI 1963), μ_u

$$\mu_u = \frac{V_u}{\phi \sum_o j_d} \quad (3.13)$$

Critical sections were stated to occur at the face of support, at each point of inflection, and at each point where tension bars were terminated within a span. V_u was the factored shear at the section, \sum_o , which represented the sum of bar perimeter(s) at the same section, and j_d was the flexural lever arm.

To prevent bond failure or splitting, the calculated tension or compression force in any bar at any section had to be developed on each side of that section by proper embedment length or end anchorage, or, for tension only, by hooks. Anchorage, or development bond stress (μ_u), was to be determined as the bar force, computed from M (moment at the section due to factored loads) / ϕ , divided by the product of \sum_o times the embedment length. The two values so calculated—ultimate flexural bond stress and anchorage bond stress—were not to exceed the limits given below, except that flexural bond stress did not have to be considered in compression or in those cases of tension where anchorage bond was less than 0.8 of the permissible stress given below. For tension, there were two equations given for each of the two types of steel included: ASTM A 305 and ASTM A 408. For instance, for ASTM A 408, the permissible values were the following:

- Top bars (more than 12 in. of concrete below the bar)— $4.2\sqrt{f'_c}$;
- Bars other than top bars— $6\sqrt{f'_c}$; and
- For all deformed bars in compression— $13\sqrt{f'_c}$ or 800 psi.

In 1971, there was a complete revamping of the bond specifications in ACI's 318 Code. In the new format, a basic development length, l_{db} , was determined and then modified by appropriate factors to obtain the required anchorage length, l_d .

$$l_d = l_{db} * f_1 * f_2 \dots \quad (3.14)$$

The development length concept replaced the dual system contained in the 1963 ACI Code. It was no longer necessary to use the flexural bond concept, which placed an emphasis on the computation of nominal peak bond stresses. The average bond resistance over the full development length of the bar is more meaningful in part because of the highly empirical nature of the design provisions and because bond tests involve averaging of bond resistance. The current minimum development length for bars in tension and in compression is based on the attainable average bond stress over this length. The various l_d lengths in the 1971 ACI Code were based directly on the 1963 ACI Code permissible bond stresses. Slightly modified versions of the 1971 provisions in ACI's 318 Code (due to the fact that f_y and f'_c are stated in terms of ksi) are the current provisions for these design situations in the *AASHTO LRFD Bridge Design Specifications*.

The basic tension development length, l_{db} (in.), for #11 bar and smaller bars shall be taken as Equation 3.15:

$$l_{db} = 1.25 A_b f_y / \sqrt{f'_c} \text{ but not less than } \dots 0.4 d_b f_y$$

$$\text{For \#14 bars: } l_{db} = 2.7 f_y / \sqrt{f'_c}$$

$$\text{For \#18 bars: } l_{db} = 3.5 f_y / \sqrt{f'_c} \quad (3.15)$$

$$\text{and for deformed wire: } l_{db} = 0.95 d_b f_y / \sqrt{f'_c}$$

In Equation 3.15, A_b is the area of bar or wire (in.²), f_y is the specified yield strength of reinforcing bars (ksi), f'_c is the specified compressive strength at 28 days unless another age is specified (ksi), and d_b is the diameter of bar or wire (in.).

The tension development length, l_d , shall not be less than the product of the basic tension development length, l_{db} , and modification factor specified in Article 5.11.2.1.2 (for epoxy-coated bars with cover less than $3d_b$ or with clear spacing between bars less than $6d_b$. . . 1.5, For epoxy-coated bars not covered above . . . 1.2). The tension development length shall not be less than 12.0 in., except for lap splices specified in Article 5.11.5.3.1 (Class A splice . . . 1.0 l_d , Class B splice . . . 1.3 l_d , Class C splice . . . 1.7 l_d).

In the 1989 ACI Code, major changes were made in the procedures for calculating development lengths for deformed bars and deformed wire in tension. *This represented a major departure in approach between the ACI Code and the current AASHTO LRFD Bridge Design Specifications*. These changes resulted in an increase in the development lengths for closely spaced bars and bars with small covers. The basic development length was modified to reflect the influence of cover, spacing, transverse reinforcement, casting position, type of aggregate, and epoxy coating. The basic development lengths remained essentially the same as in the 1971 edition of the ACI Code and the current *AASHTO LRFD Bridge Design Specifications* with the exception of the equation for #18 bars,

which was revised on the basis of a review of available test results on large bars. The revised version for #18 bars was the following:

$$l_{db} = 0.125 * f_y / \sqrt{f'_c} \quad (3.16)$$

with f_y and f'_c in psi. If put in ksi units,

$$l_{db} = 3.95 * f_y / \sqrt{f'_c} \quad (3.17)$$

This is an increase of 12 percent over the values given by the current *AASHTO LRFD Bridge Design Specifications* for the same size bars. Another important change introduced in the 1989 ACI Code was the limitation that $\sqrt{f'_c}$ cannot be taken greater than 100 psi. This limitation meant that development lengths would no longer decrease with concrete strengths greater than 10,000 psi. It was noted that research on development of bars in high-strength concretes was not sufficient to substantiate a reduction beyond the limit imposed.

While these provisions were based on extensive research and professional judgment, many found them overly complex in application. In 1999, Committee 318 of the ACI re-examined these procedures with the goal of formulating a more user-friendly format while maintaining general agreement with the research results and professional judgment that produced the changed provisions. The revision was based on the same general equation for development length that served as the basis for the 1989 provisions. This equation was Equation 12-1 in the 2005 version of the 318 Code (ACI 2005) and Equation 3.11 in this report.

In 1977, provisions for tension lap splices of deformed bars and deformed wire encouraged the location of splices away from regions of high tensile stresses to locations where the area of steel provided at the splice location is at least twice that required by analysis. A lap splice of any portion of the total area of steel in regions where (A_s provided/ A_s required) was less than 2.0 had to be at least 1.3 times the development length of the individual bar in tension (Class B splice) in length. If more than one-half of the reinforcement was spliced in such regions, lap splices had to be at least 1.7 times the development length of the individual bar (Class C splice) in length. Class A splices where the length of bar was equal to the development length of the individual bar were only permitted in regions where (A_s provided/ A_s required) was less than 2.0 and no more than 25 percent of the total area was spliced within one lap length. These same provisions are in the current *AASHTO LRFD Bridge Design Specifications*. When the changes in development in tension that eliminated many concerns regarding tension splice due to closely spaced bars were introduced in the 1989 version of the 318 Code (ACI 1989), Class C splices were eliminated.

In summary, there are a few major differences between the ACI Code and the *AASHTO LRFD Bridge Design Specifica-*

tions with respect to development and splice length of tension reinforcement:

- The *AASHTO LRFD Bridge Design Specifications* don't have bar size factor for smaller bars.
- The *AASHTO LRFD Bridge Design Specifications* don't consider the role of confining reinforcement over the splice region; however, in the ACI Code, the K_{tr} factor represents the contribution of confining reinforcement across potential splitting planes in the case of closely spaced bars with small covers.
- The *AASHTO LRFD Bridge Design Specifications* still contain Class C splices. The second and third differences are, of course, related. This parameter is especially important because bars are being developed in higher strength concretes.

3.8.8 Bond Strength Comparisons

Table 3.36 shows the comparison of calculated stress in the bar using Equations 3.12 and 3.15 and test results. In the specimens with transverse reinforcement (Specimens I-4 through I-6), the 318 Code (ACI 2005) calculated stress was higher than the calculated stress in specimens without transverse reinforcement (Specimens I-1 to I-3). Also, the use of transverse reinforcement over the splice region increased deflection at failure. The ratio of test maximum stress to ACI-calculated stress in the bar ranged from 1.13 to 1.59. The ratio of test maximum stress to AASHTO-calculated stress in the bar ranged from 1.48 to 2.14. It should be noted that the second part of Equation 3.15 controlled the basic development length in the entire specimen, and the calculated flexural capacity was greater than the moment at failure. The failure moment ranged between 60 and 98 percent of the flexural capacity.

Column 5 in Table 3.36 shows the calculated stress with the bar size factor removed. Even though the test results of NCHRP Project 12-60 do not result in ratios of test maximum stress to calculated stress less than 1.0, on the basis of the analysis of the entire database, it is proposed that the 0.8 bar size factor not be used for smaller bars. In Figure 3.61(a), the comparison of test maximum stress to the stress calculated using 318 Code (ACI 2005) for uncoated bottom bars (reported by ACI Committee 408 [2003] and discussed in Chapter 2) is shown. It can be seen that many of the specimens had ratios less than 1.

Figure 3.61(b) and (c) show the comparison of test maximum stress to calculated stress in the bar using Equation 3.11 without bar size factor for test results on uncoated bars reported by ACI Committee 408 (2003). In these figures, the specimens are divided by casting position. The bond efficiency (the ratio of test maximum stress to stress calculated using 318 Code [ACI 2005] without bar size factor) of

specimens with bottom bars (478 specimens) was 0.51 to 3.02, and some specimens had a ratio of less than 1, which means the test bond strength was lower than the strength calculated using the 318 Code (ACI 2005) without bar size factor. The bond strength of specimens with top bars (111 specimens) was 1.04 to 3.27. In tests for this study, the ratio of test result to calculated result was 1.13 to 1.88. The design equation without the bar size factor conservatively estimated bar stress for the specimens with top bars. However, it overestimated the bar stress in many specimens with bottom bars, especially for specimens with concrete compressive strength higher than 10 ksi. These are tests with values greater than 100 psi along the horizontal axis. Figure 3.61(d) shows the comparison of test maximum stress to calculated stress in the bar using Equation 3.15 (*AASHTO LRFD Bridge Design Specifications*) on uncoated bars for the specimens reported by ACI Committee 408 (2003). The bond efficiency (the ratio of test stress to calculated stress using *AASHTO LRFD Bridge Design Specifications*) of specimens with bottom bars (478 specimens) was 0.50 to 2.63, and 85 specimens had less than 1, which means the test bond strength was lower than the strength calculated by Equation 3.15.

ACI Committee 408 (ACI 408R-03) proposed a new design equation for the bond and development of straight reinforcing bars in tension based on research by Zuo and Darwin (2000). Figure 3.61(e) shows the comparison of stress in the bar calculated using Equation 3.18 and the previous test results reported by ACI Committee 408 (2003). The result shows that the ratio of bond efficiency of specimens with bottom bars was 0.79 to 2.26, and only 12 specimens showed a ratio of less than 1.

$$l_d = \left[\frac{\left(\frac{f_y}{f_c^{1/4}} - 2200\omega \right) \alpha \beta \lambda}{70 \left(\frac{c\omega + K_{tr}}{d_b} \right)} \right] d_b \quad (3.18)$$

In Equation 3.18, α is a factor reflecting the lower tensile strength of lightweight concrete, β is 1.2 for all epoxy-coated bars, λ is a factor reflecting the lower tensile strength of lightweight concrete, and c , ω , and K_{tr} are defined as follows:

$$c = c_{\min} + 0.5d_b \quad (3.19)$$

where

c = spacing or cover dimension

= $c_{\min} + d_b/2$;

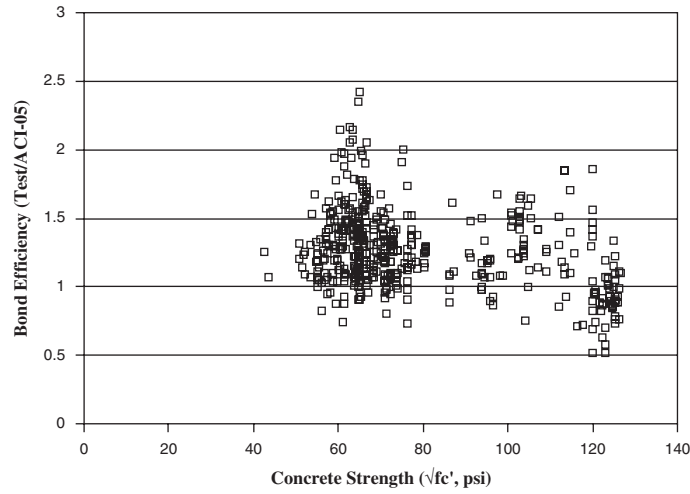
c_{\min} = minimum concrete cover or one-half of the clear spacing between bars, whichever is smaller,

= minimum (c_b , c_s);

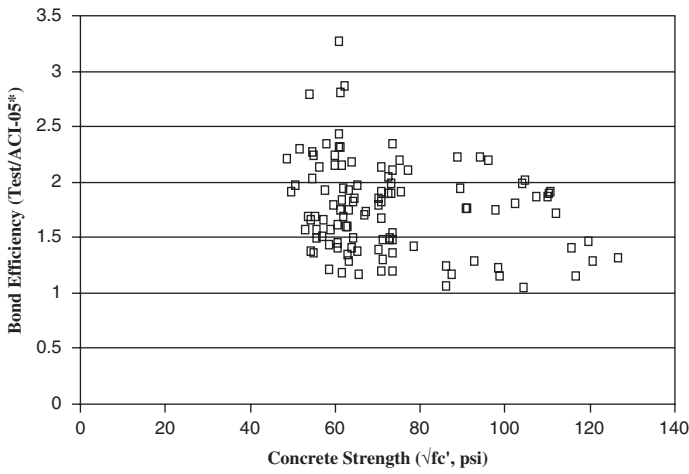
c_b = bottom concrete cover for reinforcing bar being developed or spliced;

c_s = minimum [c_{s0} , $c_{si} + 0.25$ in.];

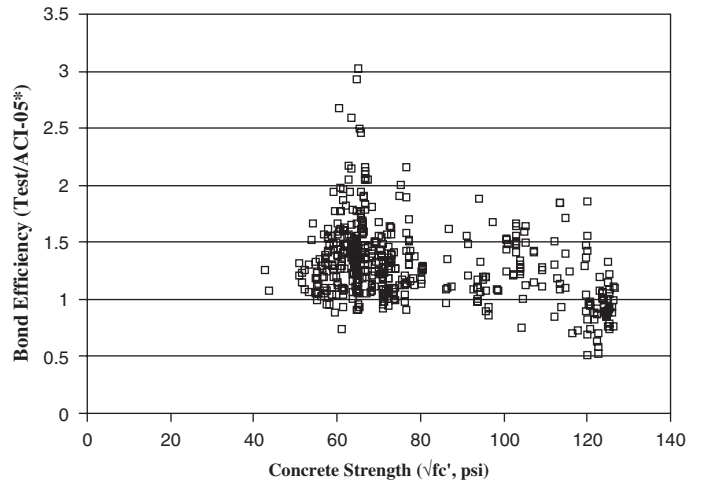
c_{s0} = side concrete cover for reinforcing bar;



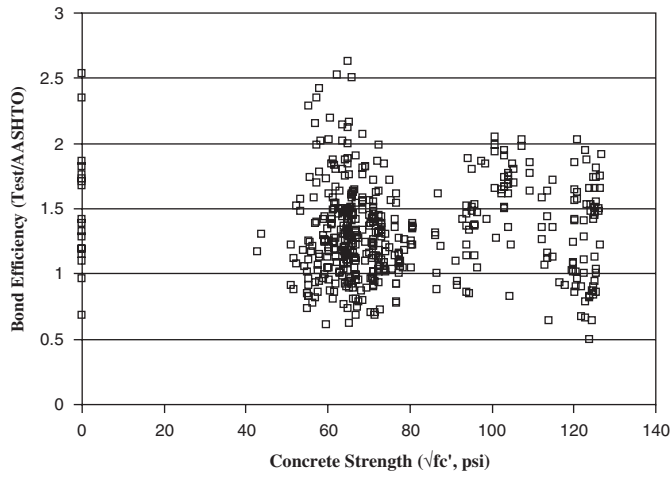
(a) Specimens with Bottom Bars (ACI-05)



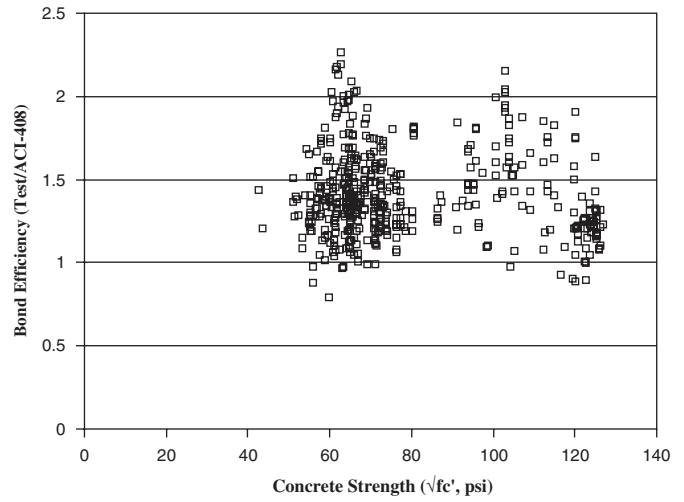
(b) Specimens with Top Bars (ACI-05*)



(c) Specimens with Bottom Bars (ACI-05*)



(d) Specimens with Bottom Bars (AASHTO)



(e) Specimens with Bottom Bars (ACI-408)

(*shows stress calculated by removing bar size factor, 1 psi = 6.89 kPa)

Figure 3.61. Comparison of bond efficiency with concrete strength.

c_{st} = one-half of the bar clear spacing; and
 d_b = diameter of bar.

$$\omega = 0.1 \frac{c_{\max}}{c_{\min}} + 0.9 \leq 1.25 \quad (3.20)$$

where c_{\max} = maximum (c_b, c_s)

$$K_{tr} = (0.52 t_r t_d A_{tr} / s n) f_c^{n/2} \quad (3.21)$$

where

$$t_r = 9.6 R_r + 0.28 \text{ " } 1.72;$$

R_r = relative rib area of the reinforcement;

$$t_d = 0.78 d_b + 0.22;$$

A_{tr} = area of each stirrup or tie crossing the potential plane of splitting adjacent to the reinforcement being developed, spliced, or anchored;

n = number of bars being developed or spliced; and

s = spacing of transverse reinforcement.

3.8.9 Summary and Conclusions

On the basis of the analysis of results from the tests of six beam specimens with lap-spliced uncoated bars embedded in higher strength concretes conducted as part of NCHRP Project 12-60 and the evaluation of an extensive database of test results compiled by ACI Committee 408, the following conclusions can be drawn:

- The ratios of test maximum stress on the top spliced bars to the stress calculated from the design equation in the 318 Code (ACI 2005) ranged from 1.13 to 1.59. A similar ratio of test maximum stress to stress calculated from the AASHTO specifications ranged from 1.48 to 2.14. Thus, the procedure in the 318 Code (ACI 2005) and the AASHTO specifications for top bar uncoated splice and development length in tension can be extended to normal-weight concrete with uniaxial cylinder strength up to 16 ksi.
- The design equation in the 318 Code (ACI 2005) and the design equation in the *AASHTO LRFD Bridge Design Specifications*, Equations 3.11 and 3.15, respectively, overestimated the bar stress in several of the bottom cast specimens in the ACI 408 Committee Database, especially for specimens with concrete compressive strength higher than 10 ksi. However, the calculated result proposed by ACI 408 Committee, Equation 3.18, resulted in fewer cases where the ratio of test to calculated stress was less than 1.0. It also resulted in more conservative estimates of the bond strength defined by the stress of spliced bars embedded in higher strength concrete beams.
- Based on the maximum bar stress and beam end displacement at peak load in all the specimens, the use of stirrups in the amount of K_{tr} from 0.37 to 0.67 in the splice region resulted in increases in both maximum bar stress and maximum displacement capacity of the beam end at failure for higher strength concretes.

3.9 Anchorage of Epoxy-Coated Bars in Tension

The object of this phase of NCHRP Project 12-60 was to evaluate the bond strength of epoxy-coated bar lap splices in concrete with strengths up to 15 ksi. An extensive literature review of test data was supplemented with 12 additional tests of top cast epoxy-coated bar splices. The variables considered in the experimental program included bar size (#6 and #11), concrete strength (12 to 17 ksi), and the amount of transverse reinforcement over the splice length.

3.9.1 Literature Review

Epoxy-coated bars have been used as an economical method of protection against deterioration of reinforced concrete structures associated with corrosion of steel reinforcement. Treece and Jirsa (1989) tested 21 beams in 9 series. The variables were bar size (#6 and #11), concrete strength (4, 8, and 12 ksi), casting position, and coating thickness (5 and 12 mils). The splice lengths were selected so that the bars would fail in bond before reaching yield, and no transverse reinforcement was provided in the splice region. Test results showed that epoxy-coated bars with an average coating thickness above 5 mils developed 67 percent of the bond strength of black bars.

DeVries, Moehle, and Hester (1991) reported the test results of 36 beams. The variables were casting position, bar size (#6 and #9), and the presence of an antibleeding agent in the concrete. The range of concrete strengths was 8 to 15 ksi. Test results indicated that the ratio of bond strength of epoxy-coated bars to black bars was 0.84. Based on the test results, De Vries and Moehle indicated that the effects of casting position and epoxy coating were not cumulative and that the modification for top cast epoxy-coated bars relative to bottom cast epoxy-coated bars was not needed. Also, the results showed that the presence of an antibleeding agent in the concrete did not significantly alter the bond stress of the splice for either top cast or bottom cast bars.

Choi et al. (1991) reported on the tests of 15 beams. The variables were bar size (#5, #6, #8, and #11), average coating thickness (3 to 17 mils), and deformation patterns (three patterns designated S, C, and N). The concrete strength was around 6 ksi. Test results indicated that the ratio of the bond strength of epoxy-coated bar splices to that of black bar splices varied from 0.71 to 0.94 with an average value of 0.82. They reported that all splice specimens exhibited extensive longitudinal and transverse cracking in the region of the splices at failure. The salient conclusion was that differences

in coating thickness have little effect on the amount of the bond strength reduction for #6 bars and larger with coating thicknesses between 5 and 12 mils.

Hamad and Jirsa (1993) reported on an experimental study in which 12 beams were tested. The main variables were bar size, bar spacing, and the amount of transverse reinforcement in the splice region. The concrete strength was around 4 ksi. Failure of all beams was governed by splitting of the concrete cover in the splice region. Test results indicated that the presence of transverse reinforcement in the splice region increased the deformation capacity of the beams and improved anchorage strength of epoxy-coated bar splices relative to black bar splices more than 10 percent.

Cleary and Ramirez (1993) reported on an experimental study in which 23 beam splice tests were subjected to repeated loadings and then tested to failure to compare the service and ultimate load behavior of beams with coated and uncoated reinforcement. The range of concrete strengths was 4 to 7 ksi. They reported that the differences in crack widths, deflections, and reinforcement stresses in beams with coated and uncoated reinforcement were reduced with repeated loading. The ratio of the average bond stress at failure for a beam containing epoxy-coated bars to its companion specimen containing uncoated reinforcement ranged from 0.82 to 0.96, with an average of 0.88.

Hester et al. (1993) tested 65 beam and slab splice specimens containing #6 and #8 bars. The average coating thickness ranged from 6 to 11 mils, and concrete strength ranged from 5 to 6.5 ksi. The Hester et al. study concluded that transverse reinforcement improved the strength of splices containing both coated and uncoated bars, and the percentage increase in strength was approximately the same for both coated and uncoated bars with an equal amount of transverse reinforcement. A maximum development length modification factor of 1.35 was proposed for design with epoxy-coated reinforcement.

Grundhoffer et al. (1998) reported on a series of 94 inverted half-beam specimens. The variables were bar size (#6, #8, and #11), bar surface (epoxy and uncoated), concrete strength (6, 10, 12, and 14 ksi), and the addition of microsilica to concrete. A comprehensive review of the effect of epoxy-coating on bond strength was conducted using the results of this study and 151 test results from seven other research studies. They concluded that ACI's 1989 318 Code was more conservative than the 1995 318 Code for all the test results based on the comparison between experimental results and the values of design bond strength calculated using ACI's 1989 and 1995 318 Code equations.

The review of past work shows that only two specimens of Treece and Jirsa (1989), eight specimens of DeVries, Moehle, and Hester (1991) and some specimens of two groups out of eight groups in Grundhoffer et al. (1998) used concrete strengths greater than 10 ksi. Other researchers' concrete

strengths vary from 4 to 10 ksi. The relationship between the bond efficiency (the ratio of test stress to stress calculated using 318 Code [ACI 2005]) of the spliced bars and the square root of concrete compressive strength in this literature review is shown in Figure 3.62. Note that the upper limit on the $\sqrt{f'_c}$ of 100 psi was removed in this calculation. Generally, the calculated stress was conservative in the range of higher strength concretes.

3.9.2 U.S. Design Specifications

3.9.2.1 318 Code (ACI 2005)

318 Equation 12-1 (ACI 2005) for estimating tension splice and development length requirements, Equation 3.12 in this report, contains several factors. One of these is ψ_b , the traditional reinforcement location factor of 1.3 to reflect the adverse effects of the top reinforcement casting position. Parameter ψ_c is the specific coating factor to deal with epoxy-coated bars. It is 1.5 with cover less than $3d_b$ or clear spacing less than $6d_b$, and it is 1.2 for all other cases. These factors are consistent with the ratio of bond strength of coated bars to bond strength of uncoated bars reported in the literature of $1/1.5 = 0.67$ and $1/1.2 = 0.82$. However, the product of ψ_t and ψ_c need not be taken greater than 1.7. All other factors are the same as for uncoated bars. In addition, as for uncoated bars, when calculating anchorage length requirements for tension lap splices, these should be as required for Class A or B splice but not less than 12 in., where

$$\begin{aligned} \text{Class A splice} & \dots\dots\dots 1.0 l_d \\ \text{Class B splice} & \dots\dots\dots 1.3 l_d \end{aligned}$$

3.9.2.2 2004 AASHTO Specifications (Section 5.11 Development and Splices of Reinforcement)

In 1989, on the basis of several test programs that showed that the bond strength of epoxy-coated bars is reduced

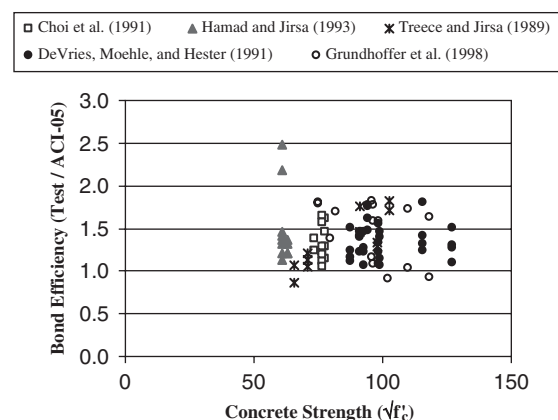


Figure 3.62. Bond efficiency of the spliced bars with concrete strength relationship (1 psi-6.89 kPa).

because coating prevents adhesion between the bar and the concrete, two factors—1.5 and 1.2 (function of the amount of concrete cover or bar spacing)—were introduced in the 318 Code provisions for development length of bars in tension. No factors were stated for similar bars in compression or epoxy-coated bars terminated by means of standard hooks anchored to resist tension. Similar factors are currently employed in the *AASHTO LRFD Bridge Design Specifications*. The rest of the approach is the same as for uncoated bars. No factors were stated for similar bars in compression or epoxy-coated bars terminated by means of standard hooks anchored to resist tension.

The tension development length, l_d , shall not be less than the product of the basic tension development length, l_{db} (see Equation 3.15), and the modification factor specified in Article 5.11.2.1.2 (1.5 for epoxy-coated bars with cover less than $3d_b$ or with clear spacing between bars less than $6d$ and 1.2 for epoxy-coated bars not covered above). The tension development length shall not be less than 12.0 in., except for lap splices specified in Article 5.11.5.3.1 (Class A splice . . . 1.0 l_{db} , Class B splice . . . 1.3 l_{db} , Class C splice . . . 1.7 l_d). When the changes that eliminated many concerns regarding development length of tension lap splices due to closely spaced bars were introduced in the 1989 version of the 318 Code, Class C splices were eliminated.

In summary, although the factors are the same in both the ACI Code and *AASHTO LRFD Bridge Design Specifications* with respect to development and splice length of tension of epoxy-coated reinforcement, the same differences observed in the case of uncoated bars for the calculation of tension development length remain.

3.9.3 Experimental Program

3.9.3.1 Test Specimens

The experimental program covers the testing of 12 beam splice specimens reinforced with epoxy-coated bars. The specimen dimensions and variables are shown in Table 3.38. The test variables are bar size, concrete cover, concrete strength, and transverse reinforcements in the splice region in higher strength concretes. The cover value given in Column 3 is both top and side clear cover to the bar being developed or spliced. Details of typical specimen are shown in Figure 3.63. In Specimens II-15 through II-18, transverse reinforcement was used in the splice region to confine the concrete as shown in Figure 3.64(b). In the splice region, the transverse reinforcement consisted of #3 @8 in. for Specimens II-15 and II-17 and #4 @8 in. for Specimens II-16 and II-18, respectively.

The splice length shown in Column 7 of Table 3.38 was selected to provide a direct link with previous tests in order to

Table 3.38. Specimen dimensions and variables.

(1) Specimen	(2) Bar Size	(3) Cover (in.)	(4) Beam Size (B x H) (in.)	(5) Effective Depth (in.)	(6) Number of Spliced Bars	(7) Splice Length (in.)	(8) 318-05 Cal. Stress (ksi)	(9) Compressive Strength (f'_c , ksi)
II-7	#6	0.75	9 x 18	16.875	3	16	34.82	12.4
II-8	#11	1.50	18 x 18	15.750	3	36	33.34	12.3
II-9	#6	2.25	18 x 18	15.375	3	16	66.67	13.6
II-10	#11	4.50	24 x 18	12.750	2	36	63.83	13.6
II-11	#6	0.75	9 x 18	16.875	3	16	40.78	16.8
II-12	#11	1.50	18 x 18	15.750	3	36	39.05	16.8
II-13	#6	2.25	18 x 18	15.375	3	16	73.50	16.6
II-14	#11	4.50	24 x 18	12.750	2	36	70.38	16.6
II-15*	#6	0.75	9 x 18	16.875	3	16	54.51	17.2
II-16*	#11	1.50	18 x 18	15.750	3	36	51.76	17.2
II-17*	#6	2.25	18 x 18	15.375	3	16	72.93	16.4
II-18*	#11	4.50	24 x 18	12.750	2	36	69.83	16.4

1 in. = 25.4 mm; 1 ksi = 6.89 MPa (* denotes specimens with transverse reinforcement in the splice region). B = specimen width. H = specimen height.

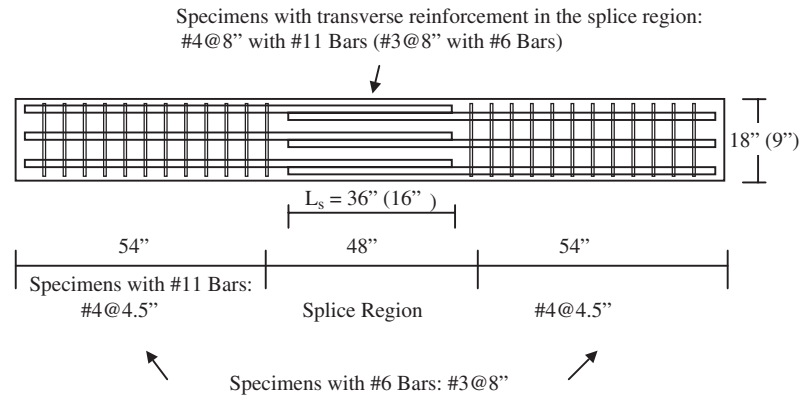


Figure 3.63. Typical beam-splice specimen reinforced with epoxy-coated bars (1 in. = 25.4 mm).

extend the specifications to higher strength concretes for epoxy-coated bars and to permit a more straightforward cover effect evaluation among specimens. The splice lengths have been selected to get a yielding stress in the basic specimens with $3d_b$ concrete cover (II-9 and II-10) as shown in Column 8 of Table 3.38. Using Equation 3.11 with appropriate modification factors, including the epoxy-coated bar factor, and with a splice class factor of 1.0, it was possible to calculate stress and force in the bar for various anchorage conditions. To determine the calculated stress, f_s , l_d is replaced by the splice length provided, 16 and 36 in. Note that all the specimens were cast with more than 12 in. below the splice. As shown in Table 3.38, all the bars in specimens with $3d_b$ concrete cover had a calculated stress greater than 60 ksi.

The specimens were reinforced in the overhang region to prevent premature shear failures outside of the test region. For safety against shear failure, a stress of 1.25 times the yield strength of the longitudinal bar was assumed in the overhang

for purposes of estimating the required shear reinforcement to resist the maximum shear associated with reaching the moment capacity of the section at the support. In the overhang region, the spacing of shear reinforcement was #3 @8 in. on centers and #4 @4.5 in. on centers for specimens with #6 bars and specimens with #11 bars, respectively. Figure 3.64 depicts the construction of the specimens.

3.9.3.2 Test Setup and Loading Protocol

The test setup is shown in Figure 3.65(a). In all specimens, the distance between the loading points and the support was 48 in., and the distance between supports was also 48 in. To investigate the characteristics of spliced beams, the applied loads, resulting deflections at each beam end and midspan, and strains developed in longitudinal bars and stirrups were monitored using load cells, LVDTs attached to an external reference frame, and electrical

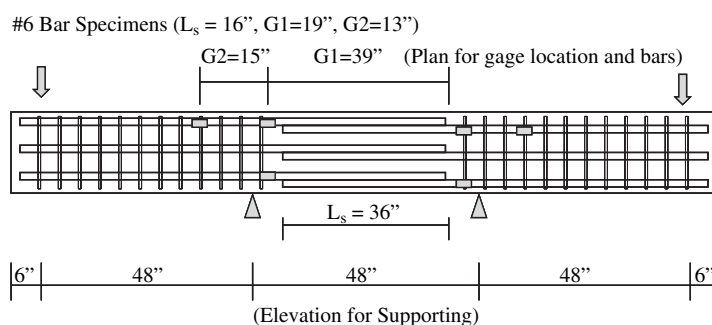
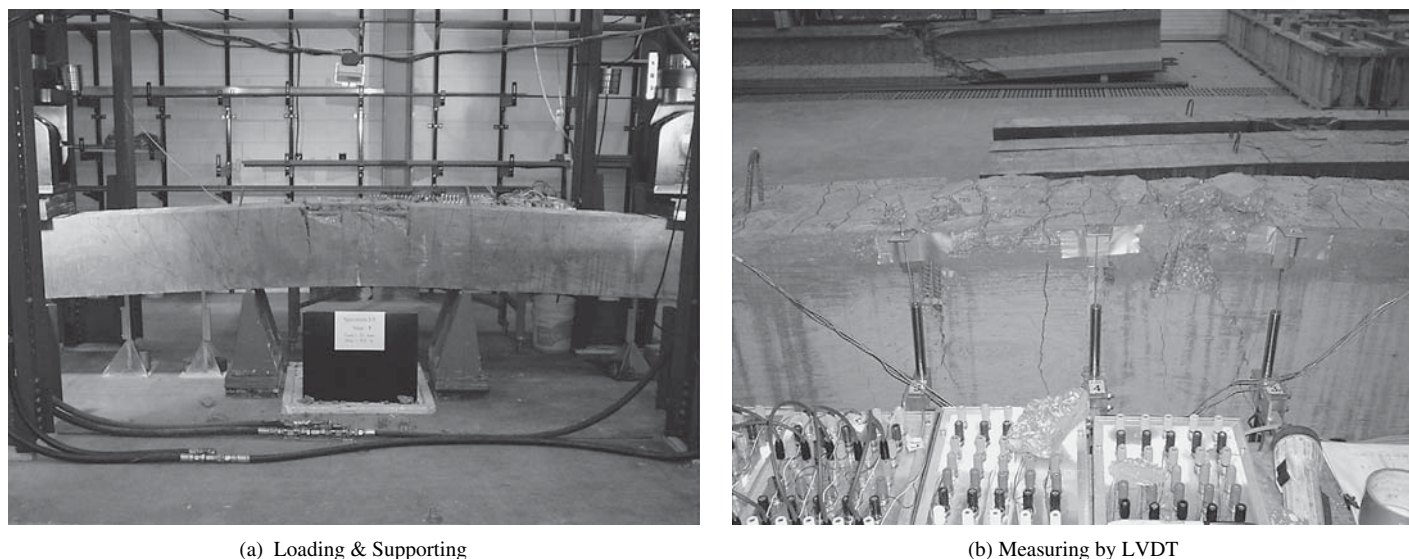


(a) Specimens II-7 & II-8



(b) Specimens II-17 & II-18

Figure 3.64. Construction of beam-splice specimen with epoxy-coated bars.



(c) Location of gages and support (Specimen II-8)

Figure 3.65. Test setup for beam-splice specimens reinforced with epoxy-coated bars (1 in. = 25.4 mm).

resistance strain gages affixed to the bars as shown in Figure 3.65 (b) and (c).

3.9.3.3 Materials

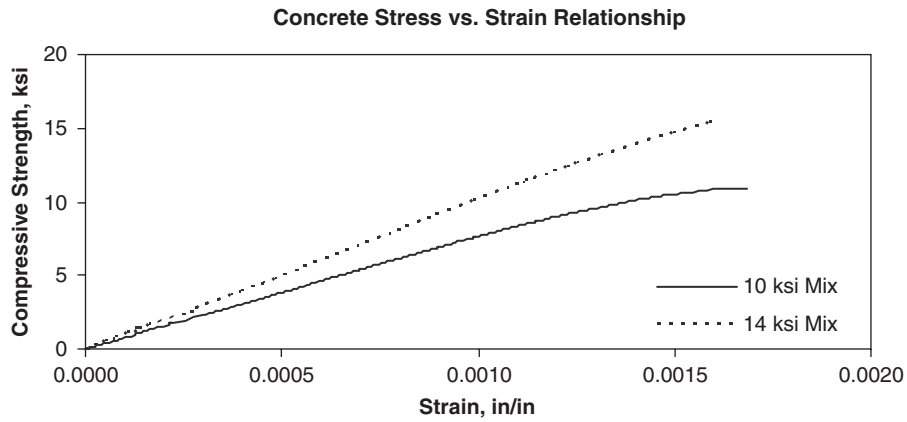
Table 3.39 shows the design concrete mixes. The water-to-cement ratio was 0.32 for the 10-ksi Mix I and 0.20 for the 14-ksi Mix II. A sample of the uniaxial stress versus strain relationship for the concrete is shown in Figure 3.66(a). The average modulus of rupture was 566 psi and 834 psi at 28 days for Mix I and Mix II, respectively. Also, typical data for

uniaxial compressive stress by age are shown in Figure 3.66(b). As shown, the strength of Mix II continued to increase after 28 days and achieved a strength of 17 ksi at 56 days.

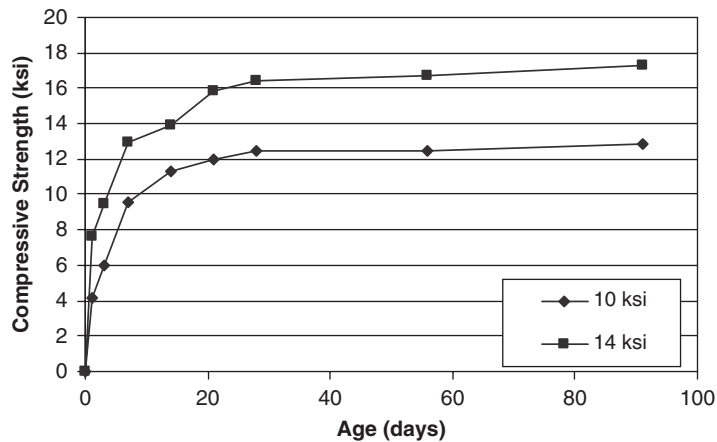
ASTM A615 Grade 60 reinforcing bars were used for both longitudinal and transverse reinforcement. The yield strength, calculated by a 0.2-percent offset from tensile tests of samples of the reinforcing bars, was 70.3 ksi and 74 ksi for the #6 and #11 bars, respectively. The average thickness of epoxy coating was 12.5 mils and 11.5 mils for the #6 and #11 bars, respectively. The relative rib area was 0.091 and 0.135 for the #6 and #11 bars, respectively. The measured tensile

Table 3.39. Concrete mix (per cubic yard).

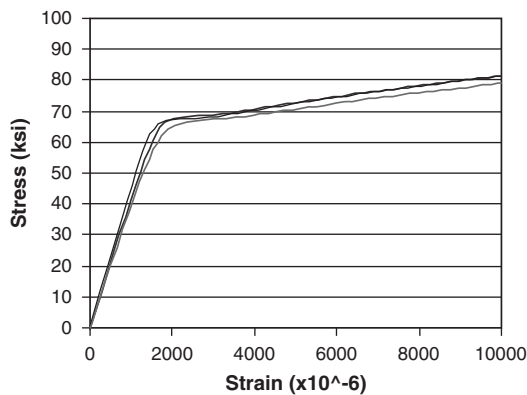
Contents	Mix I: 10 ksi	Mix II: 14 ksi
Cement (lb)	780	900
Silica fume (lb)	50	200
Water (lb)	265	220
Coarse aggregate (lb)	1,600 (3/8" pea gravel)	1,800 (1/2" crushed limestone)
Fine aggregate (lb)	1,240	1,000
High-range water reducer (oz)	190	520
Normal-range water reducer (oz)	35	38
1 lb = 0.454 kg; 1 oz = 28.35 gr; 1 yd ³ = 0.765 m ³ ; 1 ksi = 6.89 MPa		



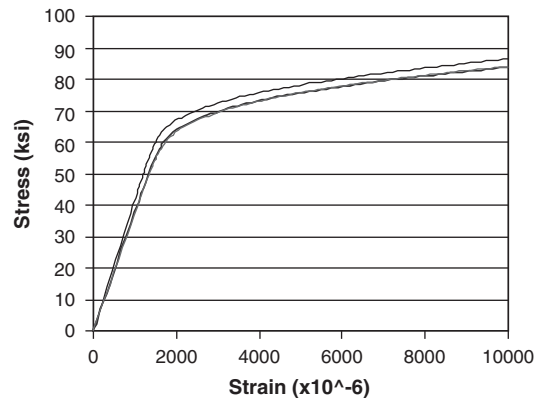
(a) Concrete Stress vs. Strain Relationship



(b) Concrete Strength vs. Age Relationship



(c) # 6 (#19M) Bars



(d) #11 (#35M) Bars

Figure 3.66. Material properties for beam-splice specimens reinforced with epoxy-coated bars (1 in. = 25.4 mm; 1 ksi = 6.89 MPa).

stress versus strain curves for #6 and #11 bars are shown in Figure 3.66(c) and (d).

3.9.4 Experiment Results

3.9.4.1 Cracking Pattern and Mode of Failure

In nearly all tests, the cracking sequence was similar. First, a flexural crack appeared in the constant moment region.

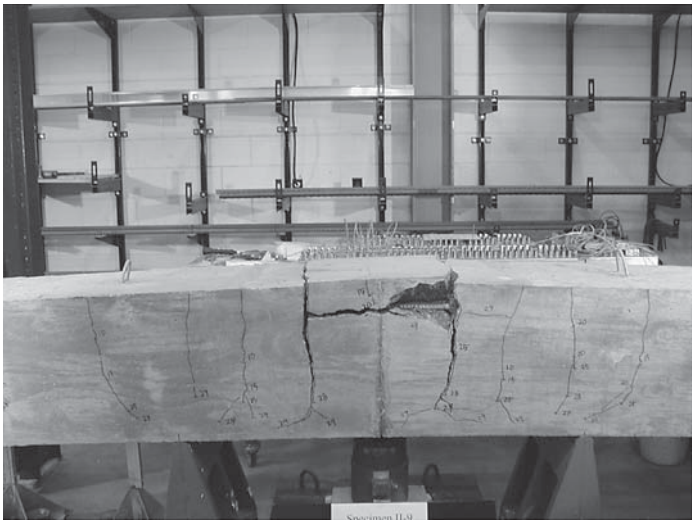
With the increase of beam end loads, a shear crack appeared in the overhang region. Near the peak load, splitting horizontal cracks appeared along the longitudinal bars in the splice region. Finally, the deformations pushed the concrete away from the bar by wedge action. Typical failure crack patterns are shown in Figure 3.67. All the specimens failed in splitting mode after yielding of the spliced bars in the constant moment region.



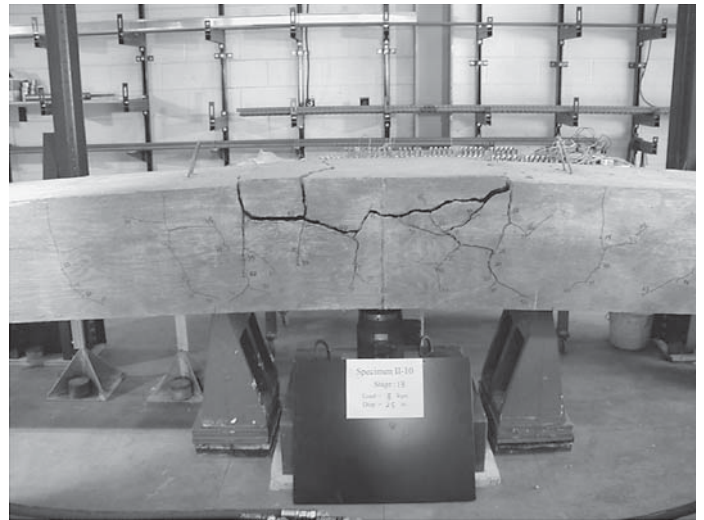
(a) Specimen II-7



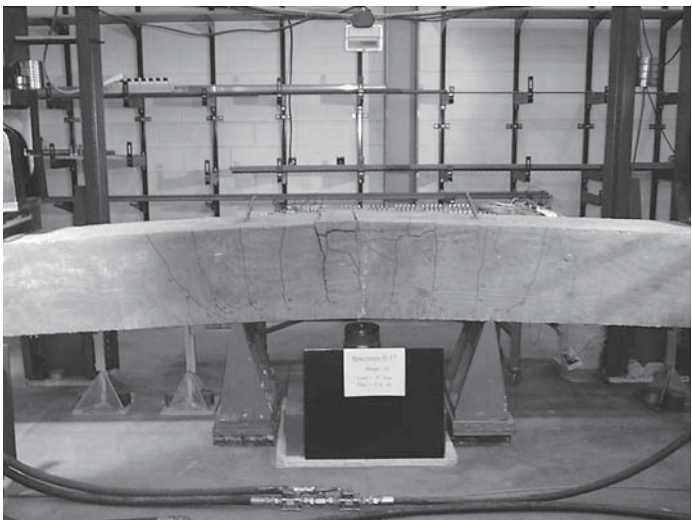
(b) Specimen II-8



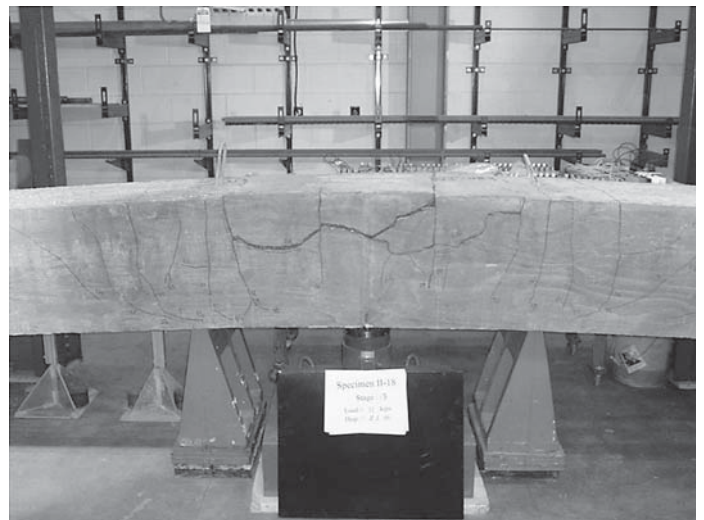
(c) Specimen II-9



(d) Specimen II-10



(e) Specimen II-17



(f) Specimen II-18

Figure 3.67. Typical failure crack pattern for beam-splice specimens reinforced with epoxy-coated bars.

3.9.4.2 Load versus End Displacement Characteristics

The applied load versus deflection at the tip of the overhang response for Specimens II-7 to II-10 and II-17 and II-18 is shown in Figure 3.68. Load was calculated by averaging the two values from the actuators, and deflection was obtained averaging displacements at both ends of the beam.

3.9.4.3 Summary of Test Results

The test results are summarized in Table 3.40 and findings from these results are presented on the basis of three main parameters.

Concrete Cover (d_b). Comparison of Specimens II-7 and II-9 (#6 bars) and comparison of Specimens II-11 and II-13

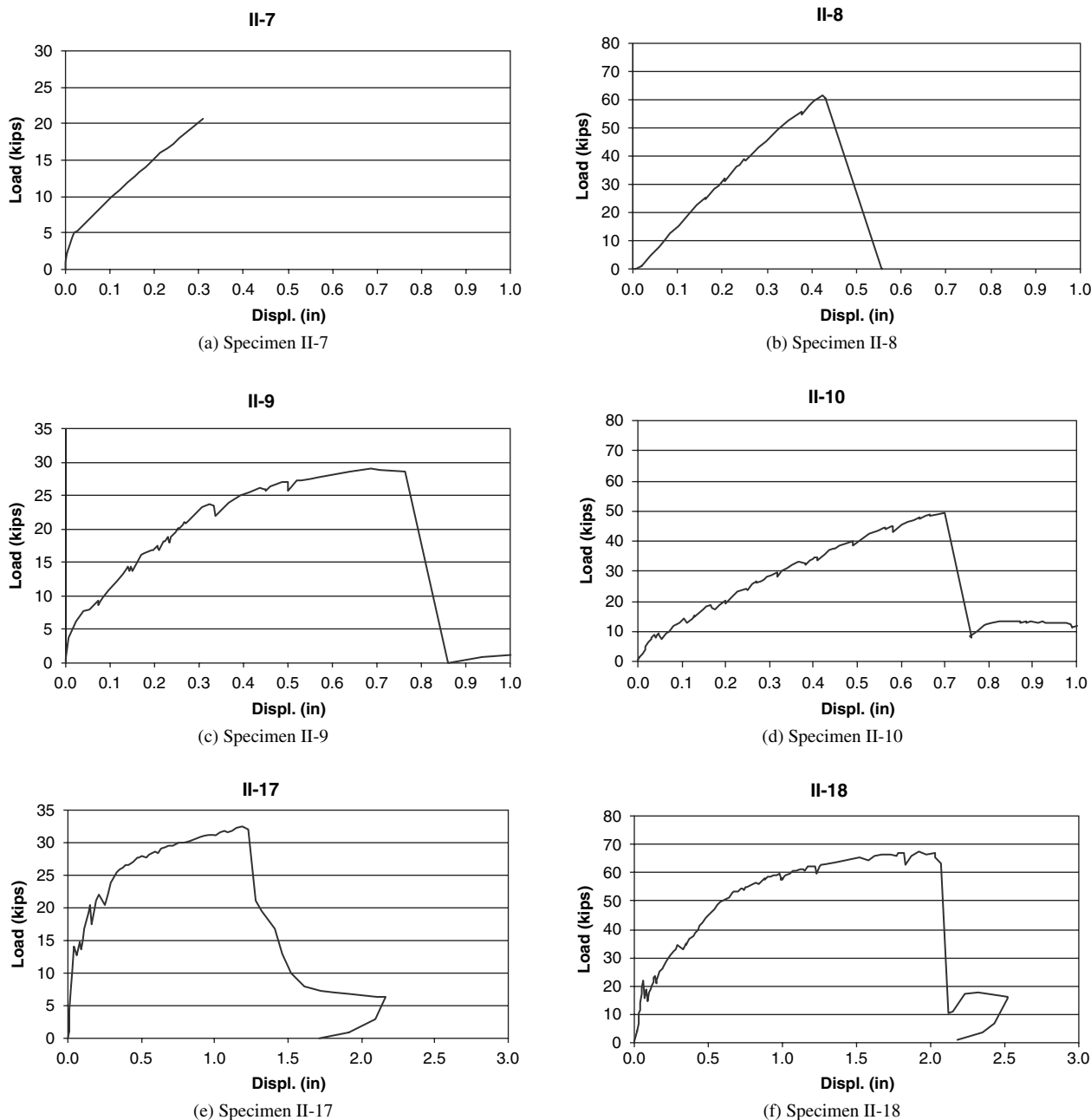


Figure 3.68. Applied load versus deflection at the tip of the overhang response (Specimens II-7 through II-10 and II-17 through II-18).

Table 3.40. Summary of test results.

(1) Specimen	(2) Max. Load (kips)	(3) Displ. at Peak Load (in)	(4) 318-05 Cal. Stress (ksi)	(5) 318-05* Cal. Stress (ksi)	(6) AASHTO Cal. Stress (ksi)	(7) Test Max. Stress (ksi)	(8) (7)/(4)	(9) (7)/(5)	(10) (7)/(6)
II-7(d_b)	20.7	0.311	34.82	27.86	31.37	63.81	1.83	2.29	2.03
II-8(d_b)	61.5	0.423	33.34	33.34	37.55	65.50	1.96	1.96	1.74
II-9 ($3d_b$)	29.0	0.687	66.67	48.94	31.75	78.39	1.18	1.60	2.47
II-10 ($3d_b$)	49.4	0.701	63.83	58.57	37.99	66.19	1.04	1.13	1.74
II-11 (d_b)	21.0	0.315	40.78	32.63	31.37	65.50	1.61	2.01	2.09
II-12 (d_b)	64.5	0.395	39.05	39.05	37.55	65.00	1.66	1.66	1.73
II-13 ($3d_b$)	32.1	1.161	73.50	53.96	31.75	83.45	1.14	1.55	2.63
II-14 ($3d_b$)	52.9	0.793	70.38	64.58	37.99	69.31	0.98	1.07	1.82
II-15** (d_b)	28.8	0.602	54.51	43.60	31.37	65.34	1.20	1.50	2.08
II-16** (d_b)	92.0	0.662	51.76	51.76	37.55	65.96	1.27	1.27	1.76
II-17** ($3d_b$)	32.4	1.185	72.93	53.54	31.75	84.80	1.16	1.58	2.67
II-18** ($3d_b$)	67.4	1.924	69.83	64.08	37.99	86.41	1.24	1.35	2.27

1 in. = 25.4 mm; 1 kip = 4.448 kN; 1 ksi = 6.89 MPa
* shows stress calculated by removing bar size factor and using one epoxy-coated bar factor of 1.5.
** shows specimens with transverse reinforcement in the splice region.

(#6 bars) show that increasing the concrete cover increased both maximum stress and deflection at failure. This result can also be seen in comparison of Specimens II-8 and II-10 (#11 bars) and comparison of Specimens II-12 and II-14 (#11 bars). However, the increase in maximum stress for #11 bar specimens was less than the increase in maximum stress for #6 bar specimens.

Effect of Concrete Strength. For Specimens II-7 and II-11 (#6 bars) with small cover (equal to d_b), increasing the concrete strength led to an increase in maximum stress, but did not significantly increase the maximum deflection at failure. When larger cover ($3d_b$) was used, increasing the concrete strength increased both maximum stress and deflection at failure as can be seen by comparing Specimens II-9 and II-13. For Specimens II-8 and II-12 (#11 bars) with small cover (d_b), an increase in concrete strength did not increase the

maximum stress or deflection at failure. In Specimens II-10 and II-14 with larger cover ($3d_b$), increasing the concrete strength resulted in increases in both maximum stress and deflection at failure.

Effect of Minimum Amount of Transverse Reinforcement in Higher Strength Concretes. A comparison of Specimens II-11 and II-15 (#6 bars) shows that the use of transverse reinforcement over the splice region did not result in an increase in the maximum stress but more than doubled the deflection at failure when the small cover (d_b) was used. When the large cover ($3d_b$) was used, it resulted in increases to both maximum stress and deflection at failure, as can be seen by comparing Specimens II-13 and II-17. Comparison of Specimens II-12 and II-16 (#11 bars) and comparison of Specimens II-14 and II-18 (#11 bars) show that the use of transverse reinforcement over the splice

region resulted in increases to both maximum stress and deflection at failure.

3.9.5 Comparison of Calculated Stress and Test Results

The comparison of stress in the bar calculated using Equations 3.11 and 3.15 with appropriate modification factors and test maximum stress is also shown in Table 3.40. The ratios of test maximum stress to ACI-calculated stress in the bar ranged from 0.98 to 1.96, as shown in Column 8. The ratios of test maximum stress to AASHTO-calculated stress in the bar ranged from 1.73 to 2.67, as given in Column 10. It should be noted that the second part of Equation 3.15 controlled the basic development length. The findings from these comparisons are discussed on the basis of three main parameters studied: effect of concrete cover, effect of concrete strength, and effect of minimum amount of transverse reinforcement in higher strength concretes.

Effect of Concrete Cover. In the specimens without transverse reinforcement, the ratio of test maximum stress to ACI-calculated stress (see Column 8 in Table 3.40) in the specimens with $3d_b$ concrete cover was 0.98 to 1.18. The ratio of test maximum stress to ACI-calculated stress in the specimens with d_b concrete cover was 1.61 to 1.96, much higher than in the specimens with $3d_b$ concrete cover. This tendency was consistent regardless of other parameters, such as concrete strength and bar size.

Effect of Concrete Strength. In higher strength concrete specimens without transverse reinforcement, the average ratio of test maximum stress to ACI-calculated stress for the specimens with d_b and $3d_b$ concrete cover was near 1.64 and 1.06, respectively (see Column 8 in Table 3.40). These observations point to the possibility that the current cover contribution in the code may be overestimated in the case of higher strength concrete specimens for larger covers.

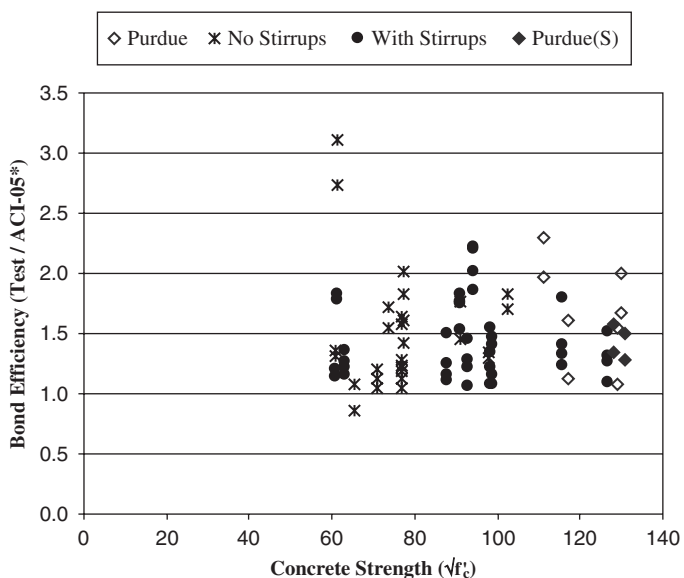
Effect of Minimum Amount of Transverse Reinforcement in Higher Strength Concretes. The ratios of test maximum stress to ACI-calculated stress for Specimens II-11 and II-14 are 1.61 and 0.98, respectively; the ratios of test maximum stress to ACI-calculated stress for Specimens II-15 and II-18 are 1.20 and 1.24, respectively. These data show that for specimens with transverse reinforcement over the splice region the difference between ratios of test maximum stress to ACI-calculated stress was smaller than the difference between ratios for specimens without transverse reinforcement (see Column 8, Table 3.40). The lower ratios in Specimens II-15 and II-16, with small covers, came from higher calculated stress, considering the contribution factor of confining reinforcement. However, the similarity of the ratios for Specimens II-17 and II-18 (with larger covers and transverse reinforcement) to the ratios for Specimens II-13 and II-14 (with larger covers but no transverse reinforcement) is due to the requirement that the ratio of $(c_b + K_{tr})/d_b$ in Equation 3.11 should not be taken greater than 2.5.

mens II-17 and II-18 (with larger covers and transverse reinforcement) to the ratios for Specimens II-13 and II-14 (with larger covers but no transverse reinforcement) is due to the requirement that the ratio of $(c_b + K_{tr})/d_b$ in Equation 3.11 should not be taken greater than 2.5.

3.9.6 Design Recommendation

When the spliced bar stress was calculated using 318 Code (ACI 2005), without a limitation on the square root of the compressive concrete strength, only Specimen II-14 with $3d_b$ concrete cover had a ratio of test maximum stress to calculated stress of less than 1. However, the average ratio of test maximum stress to 318 Code (ACI 2005) calculated stress for the specimens with $3d_b$ cover was less than average of the same ratio for the specimens with d_b cover. Therefore, it is possible to conclude that the current cover contribution may be overestimated in the case of higher strength concrete specimens with large covers. Using only one coating factor of 1.5 may be the simplest way to handle the possible overestimation of cover contribution.

Regarding bar size factor, no stress ratios less than 1 were obtained when the calculated stress included the 0.8 bar size factor within the range of specimens covered in this study. The three specimens shown in Figure 3.62 with a ratio of test maximum stress to calculated stress (defined in Figure 3.62 as “bond efficiency”) of less than 1 were specimens reinforced with #11 (#35M) bars. However, following the position of ACI Committee 408, the authors of this report also suggest not using the 0.8 bar size factor. Column 5 of Table 3.40 shows the calculated stress without the bar size modification factor. Figure 3.69 shows a comparison of bond efficiency (defined as the ratio of



*Stress calculated by removing bar size factor and the epoxy-coated bar factor of 1.5

Figure 3.69. Comparison of bond efficiency with concrete strength.

test maximum stress to calculated stress) using 318 Code (ACI 2005) without a limit on the square root of the concrete compressive strength, without a bar size factor, and with a single epoxy-coated bar factor of 1.5 with concrete strength (defined as the square root of the concrete compressive strength). In Figure 3.69, the specimens of Hamad, Jirsa, and D'Abreu de Paulo (1993), Treece and Jirsa (1989), Choi et al. (1991), DeVries, Moehle, and Hester (1991), and the tests on epoxy-coated bar splice specimens carried out under NCHRP Project 12-60 (Purdue [S]) were separated into two groups: test results from specimens with stirrups and test results from specimens without stirrups over the splice region. As can be seen from Figure 3.69, the bond efficiency values ranged from 0.86 to 3.11 for the specimens without stirrups and from 1.07 to 2.20 for the specimens with stirrups. The ranges for each of the studies, except for NCHRP Project 12-60, are listed in Table 3.41. The use of transverse reinforcement over the splice region increased the ACI-calculated stress, causing a decrease in the ratio of test maximum stress to ACI-calculated stress, and this tendency was consistent with the tendency of the tests conducted under NCHRP Project 12-60. It is interesting to note as well that for the studies in the literature, the range of stress ratios in the specimens with epoxy-coated bars and companion specimens with uncoated bars was similar, as shown in Table 3.41. Thus, on the basis of the maximum concrete compressive strength included in the experimental evaluation and the evaluation of the data in the literature, the procedure in Chapter 12 of the 318 Code (ACI 2005) for splice and development length of epoxy-coated bars in tension could potentially be extended up to 17 ksi without a limit of 100 psi to the square root of the concrete compressive strength and with these two modifications—removal of the bar size factor and use of a single epoxy-coated bar factor of 1.5.

3.9.7 Summary and Conclusions

From the test results of 12 beam splice specimens reinforced with epoxy-coated bars, the following conclusions can be drawn:

- The ratios of measured maximum stress on the spliced bars to stress calculated using 318 Code (ACI 2005) ranged from 0.98 to 1.96. Ratios calculated using 318 Code (ACI 2005) with these two proposed modifications—no bar size factor and a single epoxy-coated bar factor of 1.5—ranged from 1.07 to 2.29. Thus, the procedure in Chapter 12 of the 318 Code (ACI 2005) for splice and development length of epoxy-coated bars in tension can be extended up to 17 ksi with the modifications suggested in this section.
- The ratios of measured maximum stress on the spliced bars to the stress calculated using the AASHTO specification ranged from 1.73 to 2.67.
- The use of transverse reinforcement over the splice region resulted in increases both in the test maximum stress and deflection at failure.
- The current contribution of the cover in the 318 Code (ACI 2005) can be overestimated in the case of higher strength concrete specimens with large covers.

3.10 Anchorage of Bars Terminated with Standard Hooks in Tension

This section deals with the tensile strength of black and epoxy-coated reinforcing bars terminated in 90-deg hooks with and without transverse reinforcement under monotonic loading in normal-weight concrete with uniaxial compressive strength up to 16 ksi. As part of this examination, in addition to 43 previous tests, the test results of 21 beam-column joint type specimens are reported. Variables in the tests conducted under NCHRP Project 12-60 included bar size (#6 and #11), concrete strength (10, 14, and 16 ksi), and amount of transverse reinforcement in the anchorage region. Codes and specifications have limits to their applicability to higher strength concretes (ACI 2005, AASHTO 2004). These limits are justified on the basis of the empirical nature of code and specification requirements. The requirements for bars in tension

Table 3.41. Comparison of test results to calculated results.

Research Study	Without Stirrups	With Stirrups
Hamad and Jirsa (1993) (Black)	1.37 to 3.11	1.14 to 1.83
Hamad and Jirsa (1993) (Epoxy)	1.31 to 2.73	1.20 to 1.77
Treece and Jirsa (1989) (Black)	1.07 to 1.82	—
Treece and Jirsa (1989) (Epoxy)	0.86 to 1.71	—
Choi et al. (1991) (Black)	1.05 to 1.61	—
Choi et al. (1991) (Epoxy)	1.19 to 2.01	—
DeVries, Moehle, and Hester (1991) (Black)	—	1.07 to 2.21
DeVries, Moehle, and Hester (1991) (Epoxy)	—	1.22 to 2.20

—no data available.

anchored by means of a standard hook are an example of such specifications.

In 1975, Marques and Jirsa reported a series of tests to determine capacities of uncoated hooked bars. Twenty-two specimens simulating exterior beam-column joints were tested to evaluate the capacity of uncoated anchorage beam reinforcements subjected to varying degrees of confinement at the joint. The types of confinement included vertical column reinforcement, lateral reinforcement through the joint, side concrete cover, and column axial load. To simulate beam moment acting on the column, tension was applied to anchored bars and a reaction assembly transferred compression load to the specimen. Failure in most tests was sudden and resulted in the entire side cover of the column spalling away to the level of the hooked anchorage. The maximum concrete compressive strength in these tests, which served as the basis for the current anchorage requirements, was 5.1 ksi.

Anchorage of epoxy-coated hooked bars was evaluated by Hamad, Jirsa, and D'Abreu de Paulo (1993) in a series of tests. Twenty-four hooked-bar specimens simulating exterior beam-column joints were tested. It was reported that #11 hooked bars (coated or uncoated) were consistently less stiff than #7 hooked bars. Epoxy-coated hooked bars consistently developed lower anchorage capacities and load-slip stiffness than companion uncoated hooked bars. The companion hooked-bar specimens that had ties in the beam-column joint region improved both the anchorage capacity and load-slip behavior of both coated and uncoated bars.

To date, there has been little work on the anchorage performance of hooked bars, black and epoxy-coated, in high-strength concrete. In the 2005 ACI Building Code, the equation for the basic development length (l_{db}) of a hooked bar is limited to concrete strength of 10 ksi. Therefore, further investigation on anchorage strength of hooked bars in high-strength concrete is needed.

3.10.1 U.S. Design Specifications

3.10.1.1 318 Code (ACI 2005)

Development length for deformed bars in tension terminating in a standard hook, l_{dh} , is determined using Section 12.5.2 and applicable modification factors of 12.5.3, as shown in Equation 3.22. However, l_{dh} shall not be less than the larger of $8d_b$ and 6 in. as indicated in Section 12.5.1 of the 318 Code (ACI 2005).

$$l_{dh} = \left(0.02 \psi_e \lambda f_y / \sqrt{f'_c} \right) d_b \quad (3.22)$$

In Equation 3.22, ψ_e is the coating factor, taken as 1.2 for epoxy-coated reinforcement; λ is the factor reflecting the lower tensile strength of lightweight concrete, which is 1.3. In

other cases, these two factors are taken equal to 1.0. Other parameters are d_b , which is the bar diameter of the hooked bar; f'_c , which is the concrete compressive strength in psi; and the square root of the concrete compressive strength, which shall not exceed 100 psi as per Section 12.1.2 of the 318 Code (ACI 2005). The modification factors of Section 12.5.3 of the 318 Code (ACI 2005) are all less than 1.0 and thus reduce the calculated length on the basis of cover, presence of ties where the first tie encloses the bent portion of the hook within $2d_b$ of the outside of the bend, and where anchorage or development for specified minimum yield strength, f_y , is not specifically required. These modification factors are the following.

For #11 bar and smaller hooks with side cover (normal to the plane of the hook) not less than 2.5 in. and for 90-deg hooks with cover on the bar extension beyond the hooks that are not less than 2 in.:	0.7
For 90-deg hooks of #11 and smaller bars that are enclosed within ties or stirrups perpendicular to the bar being developed, spaced not greater than $3d_b$ along l_{dh} ; or enclosed within ties or stirrups parallel to the bar being developed, spaced not greater than $3d_b$ along the length of the tail extension of the hook plus bend:	0.8
For 180-deg hooks of #11 and smaller bars that are enclosed within ties or stirrups perpendicular to the bar being developed, spaced not greater than $3d_b$ along l_{dh} :	0.8
Where anchorage or development for f_y is not specifically required, reinforcement in (A_s required / excess of that required by analysis:	A_s provided)

The factor A_s required/ A_s provided, also referred to as the factor for excess reinforcement, applies only where anchorage for full f_y is not specifically required because the area of steel required to resist the factored flexural moment at the section, A_s required, is less than the area of steel provided, A_s provided, at the same section.

3.10.1.2 2004 AASHTO Specifications (Section 5.11.2.4 Standard Hooks in Tension)

The 1995 318 Code provisions for anchorage of bars terminated in a standard hook in tension are the current procedure in the *AASHTO LRFD Bridge Design Specifications* (ACI 1995). The 1983 provisions for development of standard hooks in tension in the 318 Code were a major departure from the 1977 318 Code in that they uncoupled hooked bar anchorages from

straight bar development provisions and measured the hooked bar embedment length from the critical section to the outside end or edge of the hook. The development length of the hooked bar is represented by the product of a basic development length and appropriate modification factors. In the 1995 edition of the 318 Code, a factor of 1.2 was introduced in the calculation of development lengths of epoxy-coated bars terminated in a standard hook (ACI 1995).

The development length, l_{dh} (in.), for deformed bars in tension terminating in a standard hook specified in Article 5.10.2.1 shall not be less than the following:

- The product of the basic development length and the applicable modification factor or factors, as specified in Article 5.11.2.4.2;
- 8.0 bar diameters; or
- 6.0 in.

Basic development length, l_{hb} , for a hooked-bar with yield strength, f_y , not exceeding 60.0 ksi shall be taken as:

$$l_{hb} = \frac{38.0d_b}{\sqrt{f'_c}} \quad (3.23)$$

where

d_b = diameter of the hooked bar (in.) and
 f'_c = specified compressive strength of concrete at 28 days, unless another age is specified (ksi).

Below, cases in which basic hook development length, l_{hb} , should be multiplied by a factor are given, as well as the applicable factor.

Reinforcement has a yield strength exceeding 60 ksi:	$f_y/60$
Side cover for #11 bar and smaller, normal to the plane of the hook, is not less than 2.5 in., and cover on bar extension beyond 90-deg hooks is not less than 2 in.:	0.7
Hooks for #11 bar and smaller that are enclosed vertically within ties or stirrup ties spaced along the full development length, l_{dh} , at a spacing not exceeding $3d_b$.	0.8
Anchorage or development of full yield strength is not required, or reinforcement is provided in excess of that required by analysis:	$(A_s \text{ required} / A_s \text{ provided})$
Lightweight concrete is used:	1.3
Epoxy-coated reinforcement is used:	1.2

3.10.2 Experimental Program

3.10.2.1 Test Specimens

The experimental program reported in this research consisted of the monotonic loading in tension only (see Figures 3.70 and 3.71) of 20 specimens with two bars terminated in 90-deg standard hooks (see Figure 3.72).

Key test parameters are given in Table 3.42. The test specimens were cast using normal-weight concrete (see

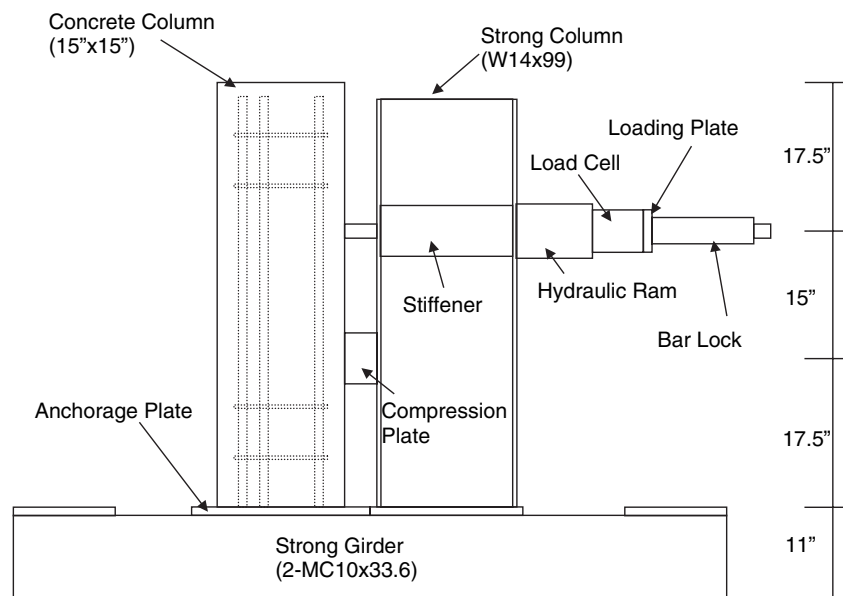


Figure 3.70. Test setup for beam-column-type specimens (1 in. = 25.4 mm).

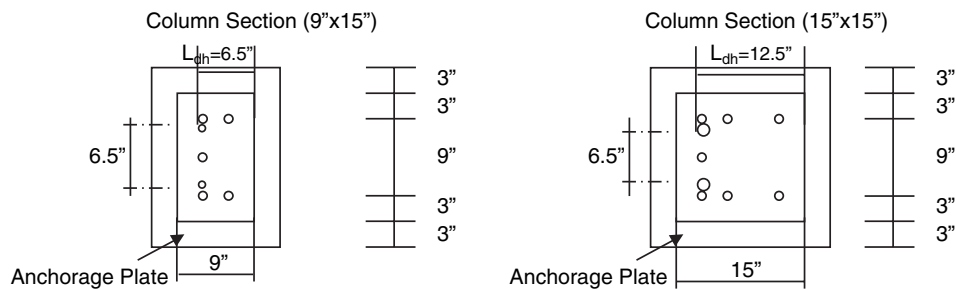


Figure 3.71. Specimen details for anchorage tests of bars terminated with standard hooks (1 in. = 25.4 mm).

Table 3.43). Specimens I-1 to I-6 contained black hooked bars. Specimens II-7 to II-12 had epoxy-coated hooked bars. In Specimens III-13 to III-20, transverse reinforcement was provided in the joint area to confine the concrete along the anchorage length of the hooked bars. The specimens were provided with an anchorage length, l_{dh} , as per 318 Code (ACI 2005) (see Table 3.42).

Test specimens contained two #6 hooked bars or two #11 hooked bars. The concrete column size of the specimens with the #6 hooked bars was 9 by 15 in. The column cross section of the specimens reinforced with the #11 bars (such as I-2) was 15 by 15 in. The width of the column was kept the same in all specimens, but the depth was changed to accommodate the different development lengths. In both types of specimens, concrete cover was 2.5 in. Each concrete column was reinforced with five or seven #8 main vertical bars and 4 stirrups spaced at 6 in.—two at the top and two at the bottom of the column as shown in Figure 3.72. The 318 Code (ACI 2005) anchorage requirements for uncoated bars anchored by a combination of standard hook and straight embedment length were based on the test results of Marques and Jirsa (1975). These provisions were later extended by Hamad, Jirsa, and D’Abreu de Paulo (1993) to

epoxy-coated bars. In NCHRP Project 12-60, a similar test setup was used in the evaluation of these provisions in higher strength concretes.

3.10.2.2 Test Setup and Procedure

The test setup used in this investigation is shown in Figures 3.70 and 3.73. A force couple consisting of a tensile force in the test bars (applied by two center-hole hydraulic rams) and a compressive force concentrated at a distance of 15 in. below the centerline of the bars was applied. The compression force at the face of test specimen was applied through two plates (3 in. and 3/4 in. thick) attached to the reaction column simulating a 6 in. deep compression zone of the assumed beam.

The reaction column consisted of a W14x99 column welded to a base plate 1 in. thick and bolted to the strong girder on the floor. Pull-out load was applied in 3.5-kip increments to the #6 bar specimens and in 10-kip increments to the #11 bar specimens until failure occurred. Two strain gages were affixed to each bar, and the slip of the anchored reinforcing bar relative to the concrete surface was measured using LVDTs.

3.10.2.3 Materials

The two concrete mixes ordered from a concrete ready-mix company were proportioned to yield a concrete compressive strength of 10 ksi (Mix I) and at least 14 ksi (Mix II). Table 3.43 shows a typical concrete mix. The water-to-cement ratio was 0.32 for Mix I and 0.20 for Mix II. A stress versus age relationship is shown in Figure 3.74. The modulus of rupture was 566 psi and 834 psi at 28 days for Mix I and Mix II, respectively.

Each size of reinforcing bar was from the same heat of steel, and all bars had the same deformation pattern. The relative rib area of #6 and #11 bars was 0.091 and 0.135, respectively. Grade 60 steel was used for both black and epoxy-coated bars. The yield strength obtained from tensile tests was 81.9 ksi and 63.1 ksi for the #6 and #11 black bars, respectively. For the epoxy-coated bars, the yield strength calculated by 0.2-

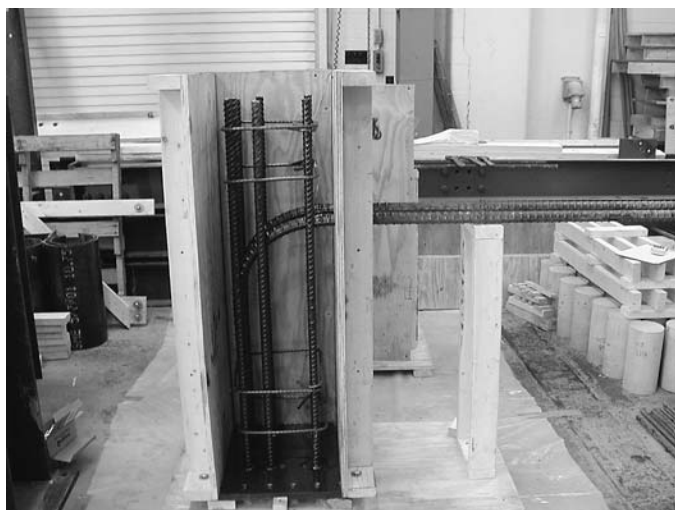


Figure 3.72. Detail of Specimen I-2.

Table 3.42. Description of key test parameters.

Name	Bar Size	Concrete Strength (psi)	Bar Type	l_{dh} (in.)	Concrete Cover (in.)	Stirrup Spacing
I-1	#6	8,905	Black	6.5	2.5	None
I-2	#11	8,905	Black	12.5	2.5	None
I-2'	#11	9,535	Black	15.5	2.5	None
I-3	#6	12,455	Black	6.5	2.5	None
I-4	#11	12,455	Black	12.5	2.5	None
I-5	#6	12,845	Black	6.5	2.5	None
I-6	#11	12,845	Black	12.5	2.5	None
II-7	#6	9,535	Epoxy-coated	6.5	2.5	None
II-8	#11	9,535	Epoxy-coated	12.5	2.5	None
II-9	#6	13,670	Epoxy-coated	6.5	2.5	None
II-10	#11	13,670	Epoxy-coated	12.5	2.5	None
II-11	#6	14,800	Epoxy-coated	6.5	2.5	None
II-12	#11	14,800	Epoxy-coated	12.5	2.5	None
III-13	#6	13,980	Black	6.5	d_b	$3d_b$
III-14	#11	13,980	Black	12.5	d_b	$3d_b$
III-15	#6	16,350	Black	6.5	d_b	$3d_b$
III-16	#11	16,500	Black	12.5	d_b	$3d_b$
III-17	#6	13,670	Epoxy-coated	6.5	d_b	$3d_b$
III-18	#11	13,670	Epoxy-coated	12.5	d_b	$3d_b$
III-19	#6	16,350	Epoxy-coated	6.5	d_b	$3d_b$
III-20	#11	16,500	Epoxy-coated	12.5	d_b	$3d_b$

1 in. = 25.4 mm; 1 psi = 6.89 kPa

percent offset from tensile tests was 72.5 ksi and 74.7 ksi for the #6 and #11 bars, respectively. The average coating thickness measured with a dry film thickness gage for all epoxy-coated bars was around 12 mils.

3.10.3 Experimental Results

3.10.3.1 Load versus Slip Behavior and Cracking Pattern

Pull-out load versus slip responses for Specimens II-9, II-10, III-17, and III-18 are shown in Figure 3.75. The pull-out load versus slip responses for Specimen III-19 and III-20 are given

in Figure 3.76. Load was measured using a load cell attached to each bar terminated with a 90- deg standard hook.

In almost all the specimens, the gages placed on the bar at a distance of 2 in. from the column surface showed yielding before reaching the maximum pull-out load, with less than 0.05-in. slip between hooked bar and concrete surface on the loaded side. As can be seen from Figure 3.75(a) and (b), specimens without shear reinforcement in the test region, II-9 and II-10, had a significant decrease in load at a 0.2-in. relative slip between hooked bar and concrete surface. However, in the specimens with shear reinforcement in the test region, III-17 and III-18 (see Figure 3.75[c] and [d]), the load decrease (20

Table 3.43. Typical concrete mix ratio (per 1 cubic yard).

Contents	10-ksi Mix	14-ksi Mix
Cement (lb)	780	900
Silica fume (lb)	50	200
Water (lb)	265	220
Coarse aggregate (lb)	1,600 (3/8" pea gravel)	1,800 (1/2" crushed limestone)
Fine aggregate (lb)	1,240	1,000
High-range water reducer (oz)	190	520
Normal-range water reducer (oz)	35	38

1 lb = 0.454 kg. 1 oz = 28.35 gr. 1 yd³ = 0.765 m³. 1 ksi = 6.89 MPa.

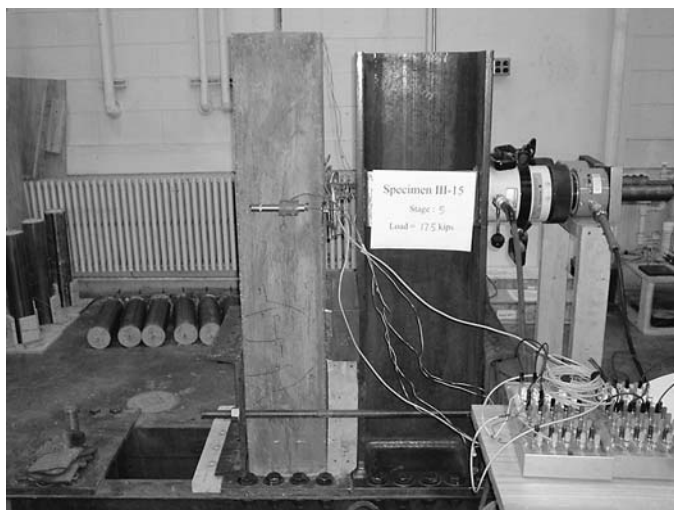


Figure 3.73. Beam-column-type specimen test setup and instrumentation.

percent of the peak load) was not as severe as the load decrease observed in the specimens without shear reinforcement (almost 50 percent of the peak load). In Specimens III-17 and III-18, at 0.2-in. slip, the sustained anchorage force was more than 80 percent of the maximum pull-out force. It can be concluded that the #6 epoxy-coated bar specimen with shear reinforcement in the test region and smaller cover was able to reach a higher peak load than its companion specimen without shear reinforcement but with a larger cover (see Figure 3.75[a] and [c]). This was not the case for specimens with #11 epoxy-coated bars anchored by standard hooks (Figure 3.75[b] and [d]). However, the specimens with shear reinforcement (Figure 3.75[c] and [d]) were able to sustain almost 80 percent of the peak load at a slip of 0.2 in. regardless of the bar size.

The load versus slip behavior of Specimens III-19 and III-20 are shown in Figure 3.76(a) and (b), respectively. Comparing

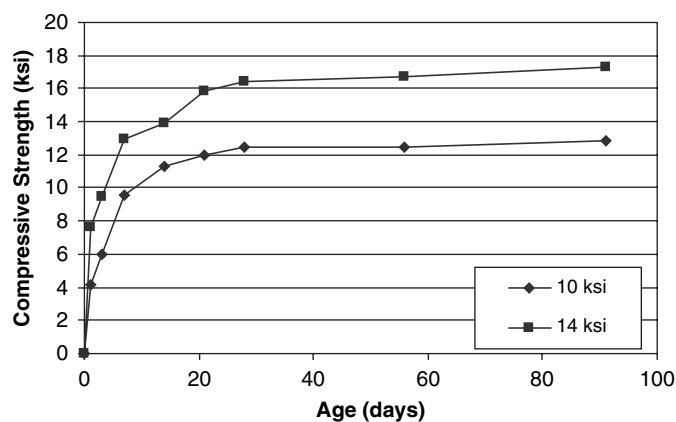


Figure 3.74. Concrete compressive strength versus age relationship in standard hook tests (1 ksi = 6.89 MPa).

the behavior for the #6 bar specimens, III-17 and III-19, recorded in Figure 3.75(c) and Figure 3.76(a), respectively, it can be observed that the increase in concrete compressive strength from about 13.5 ksi to 16.5 ksi resulted in an increase in pull-out strength. The same increase in concrete strength in the case of the specimens anchoring #11 bars, III-18 and III-20, also resulted in an increase in pull-out strength (see Figure 3.75[d] and Figure 3.76[b]). The same type of finding was observed for the specimens anchoring uncoated bars.

In almost all of the tests, the cracking sequence was similar. The first flexural (horizontal) crack occurred on the back face of the specimens at a load of 20 kips for the #6 bar specimens and 60 kips for the #11 bar specimens. The crack appeared near the tail end of the hook. After the initial flexural crack, a shear crack appeared on the side of the specimen as shown in Figure 3.77. With the increase in the pull-out load, the gage near the hook showed signs of yielding. At 90 percent of the peak load, the vertical cracks appeared along the column main bar. Finally, the concrete block near the hooked bar pushed out in Type I and II specimens that had no stirrups in the joint (see Figure 3.78). In the Type III specimens containing stirrups over the anchorage length, with the failure of the concrete near the hook, some of the side concrete cover spalled off (see Figure 3.79). Within the range of these tests, there was no significant difference on the pull-out characteristics of the hooked bars with different concrete compressive strength up to 16 ksi. It must be noted that with large slips and with the tendency of the bar to straighten under tension, the tail end of the hook tended to kick out, thus splitting the concrete behind the hook. However, these cracks were very small, implying that a cover of 2.5 in. over the tail end of the hook used was sufficient for design purposes in the range of concrete strengths considered in this study.

3.10.3.2 Maximum Pull-Out Stress and Failure Mode

Table 3.44 shows a comparison of maximum pull-out stress and the calculated stress on the basis of Equation 3.22. This equation gives the straight embedment length calculated in accordance with the 318 Code (ACI 2005) and measured from the critical section to the outside portion of the hook. In this equation, f_y is the yield strength of hooked bar, ψ_e is the coating factor (epoxy-coated reinforcement = 1.2, uncoated reinforcement = 1.0), λ is the lightweight aggregate concrete factor (for lightweight concrete = 1.3, for normal concrete = 1.0), and f'_c represents the concrete compressive strength. Substituting f_s in place of f_y , stress in the bar for a given anchorage length, and solving for s , with a given design anchorage length, as in Equation 3.24, it is possible to obtain the calculated stress shown in Table 3.44. The maximum stress corresponding to the peak pull-out load is obtained by

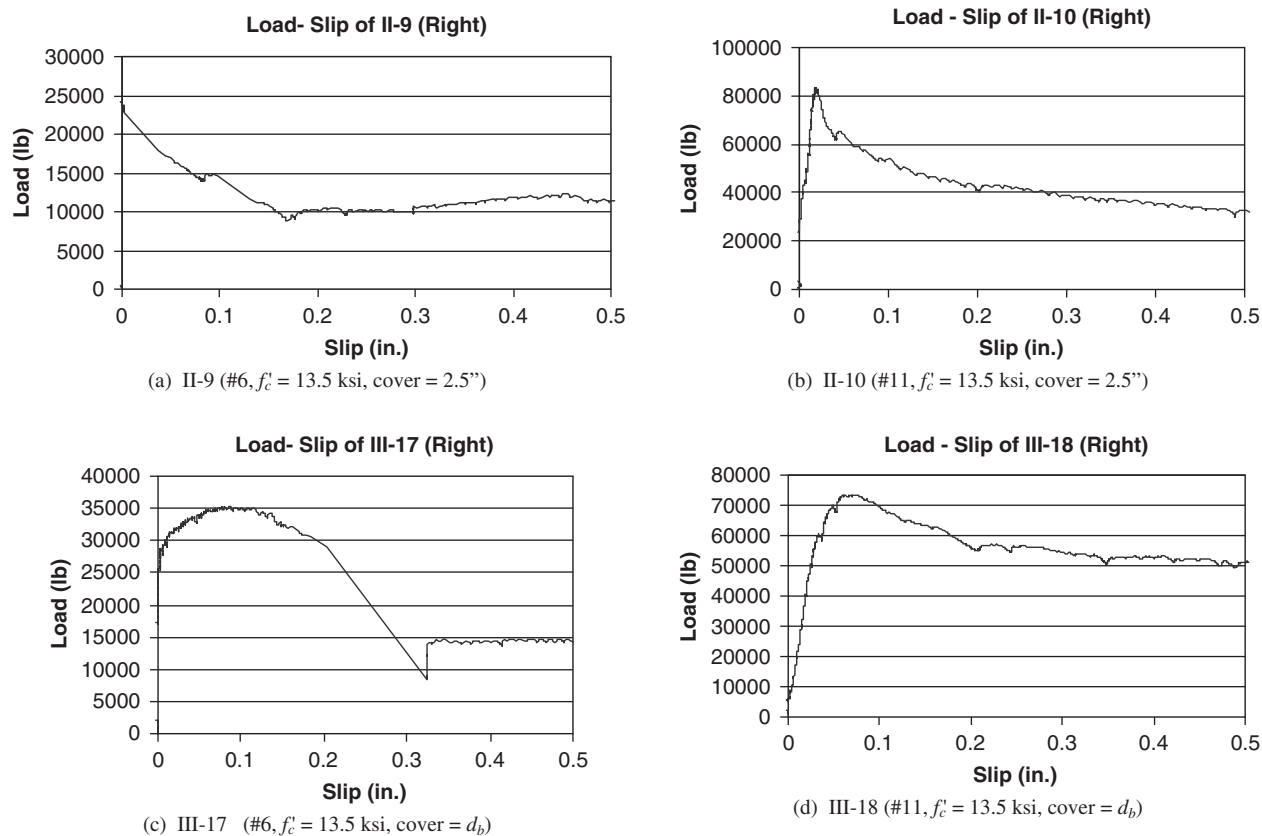


Figure 3.75. Effect of transverse reinforcement in the anchorage region on the pull-out load versus slip response (1 in. = 25.4 mm; 1 kip = 4.448 kN).

averaging the values from the two load cells attached to each hooked bar divided by the area of the bar.

$$f_s = \frac{\left[\left(\frac{l_{dh}}{d_b} \right)^* \sqrt{f'_c} \right]}{0.02 \psi_e} \quad (3.24)$$

Specimens with #6 bars, except Specimens II-9 and III-15, at failure reached a stress equal to or greater than the calculated stress (ratio of test result to calculated value of 0.99 to

1.23). However, most of the specimens anchoring # 11 bars at failure reached a stress less than or equal to the calculated stress (ratio of test result to calculated result of 0.83 to 1.02). In the case of specimens anchoring epoxy-coated bars (Series II), the tendency was the same as in Series I specimens reinforced with black bars. In Series III, the specimens anchoring #11 bars reached failure stress levels less than or equal to the calculated stress values, yielding a ratio of test to calculated stress ranging from 0.83 to 0.98 while the specimens

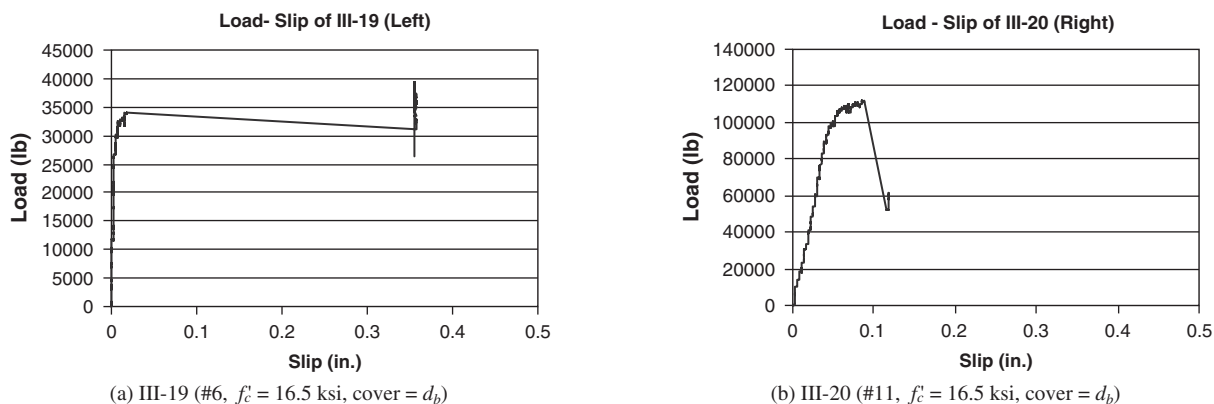


Figure 3.76. Effect of high-strength concrete in the anchorage region on the pull-out load versus slip response (1 in. = 25.4 mm; 1 kip = 4.448 kN).



(a) Specimen I-1



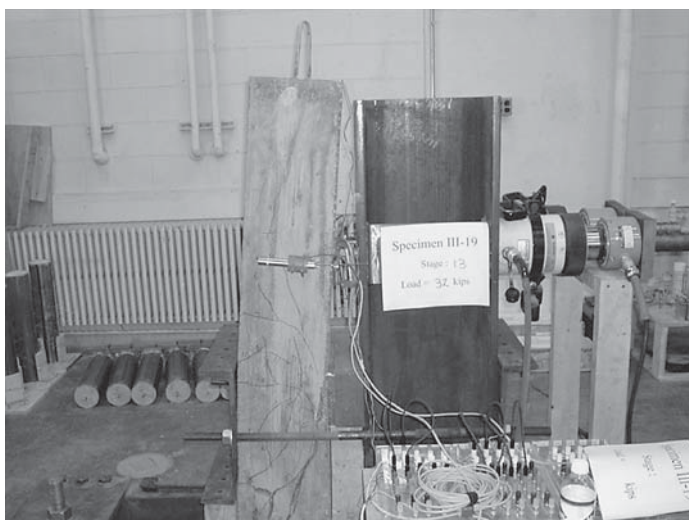
(b) Specimen I-2



(c) Specimen III-13



(d) Specimen III-14



(e) Specimen III-19



(f) Specimen III-20

Figure 3.77. Crack patterns.



Figure 3.78. Concrete block push off in specimens without stirrups in the anchored hooked bar specimens.



Figure 3.79. Failure region in the case of Specimen III-13 with stirrups.

anchoring #6 bars reached failure stresses greater than the calculated values, i.e., ratios ranging from 1.01 to 1.14, except Specimen III-15, which failed at a lower level. A similar comparison was conducted in terms of force developed in the bar. Comparison of the results of Specimens II-9 and II-10 with Specimens III-17 and III-18 indicated that the use of ties over the joint region developed 56 percent more force in the bar in

the case of #6 bars, and 15 percent more force in the case of #11 bars. Each pair of specimens had the same dimensions and material properties, but had different details, such as having ties, having no ties, or having different concrete cover. Taking into account these similarities and differences in the specimens, it can be concluded that the confinement (with ties) of the anchorage region produced stronger bond char-

Table 3.44. Comparison of maximum pull-out bar stress compared with calculated stress using the 318 Code (ACI 2005) method with a modification factor of 0.7 (ksi).

Specimen	d_b (in.)	f'_c (psi)	l_{dh} (in.)	Calculated	Test	Ratio (T/C)	Force (kips)
I-1-9	0.75	8905	6.5	58.4	68.2	1.17	30.0
I-2-9	1.41	8905	12.5	59.8	56.4	0.94	88.0
I-2'-10	1.41	9535	15.5	76.7	67.3	0.88	105.0
I-3-12	0.75	12455	6.5	69.1	68.2	0.99	30.0
I-4-12	1.41	12455	12.5	70.7	63.5	0.90	99.1
I-5-13	0.75	12845	6.5	70.2	69.3	0.99	30.5
I-6-13	1.41	12845	12.5	71.8	73.1	1.02	114.0
II-7-10	0.75	9535	9.5	73.6	90.9	1.23	40.0
II-8-10	1.41	9535	15.5	63.9	56.4	0.88	88.0
II-9-14	0.75	13670	6.5	60.3	56.1	0.93	24.7
II-10-14	1.41	13670	12.5	61.7	53.5	0.87	83.5
II-11-15	0.75	14800	6.5	62.8	64.8	1.03	28.5
II-12-15	1.41	14800	12.5	64.2	54.5	0.85	85.0
III-13-14	0.75	13980	8.3	92.9	93.8	1.01	41.3
III-14-14	1.41	13980	13.5	80.9	67.3	0.83	105.0
III-15-16	0.75	16350	8.3	100.5	87.5	0.87	38.5
III-16-16	1.41	16500	13.5	87.8	76.9	0.88	120.0
III-17-14	0.75	13670	8.3	76.6	87.5	1.14	38.5
III-18-14	1.41	13670	13.5	66.6	61.5	0.92	95.9
III-19-16	0.75	16350	8.3	83.7	89.8	1.07	39.5
III-20-16	1.41	16500	13.5	73.2	71.8	0.98	112.0

1 in. = 25.4 mm; 1 kip = 4.448 kN; 1 psi = 6.89 kPa; 1 KSI = 6.89 MPa

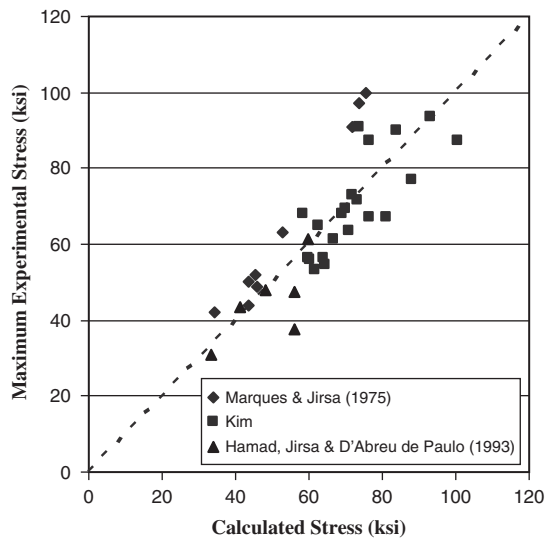


Figure 3.80. Maximum experimental stress versus 318 Code calculated stress (1 ksi = 6.89 MPa).

acteristics in hooked bars than no ties with a 2.5 in. cover. This tendency is observed with both the epoxy-coated bars and black bars.

3.10.3.3 Comparison with Other Tests and Recommendations

The comparison of the stress calculated using Equation 3.24 for NCHRP Project 12-60 tests (Kim) and test results reported by Hamad, Jirsa, and D'Abreu de Paulo (1993) and Marques and Jirsa (1975) are plotted against the experimental values in Figure 3.80. The comparison shows that NCHRP

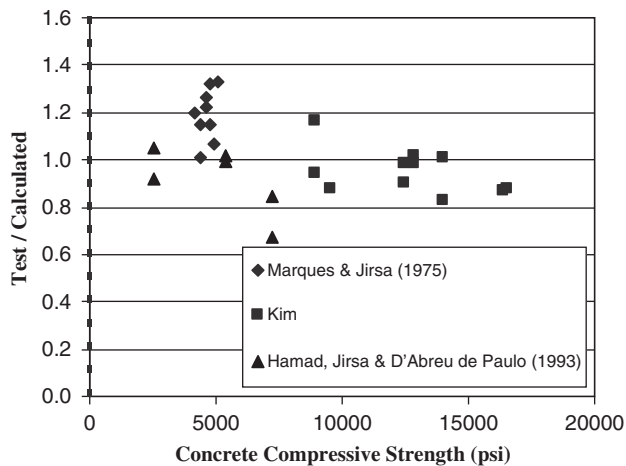
Project 12-60 test results follow in general the same trend as those of previous researchers. Thus, it is plausible to propose to extend the current ACI procedure for hooked bars up to 16 ksi without a limit on the $\sqrt{f_c}$ term.

In Figure 3.81, the ratio of test to calculated stress for hooked bars is shown versus the concrete compressive strength of the specimen. It can be seen that the ratio decreases as the concrete compressive strength is increased in both black and epoxy-coated bars terminated with a standard hook and subjected to direct tension. To increase the values of the ratio of test to calculated stress in specimens with higher concrete strengths, it is proposed that a 0.8 modification factor be used instead of the current factor of 0.7 [for hooks with side cover not less than 2-1/2 in. and for 90-deg hooks with cover on bar extension beyond hook not less than 2 in. in ACI Code 12.5.3(a) in concrete strengths above 10 ksi]. The calculated results using the proposed modification factor and current factor are shown in Figure 3.82.

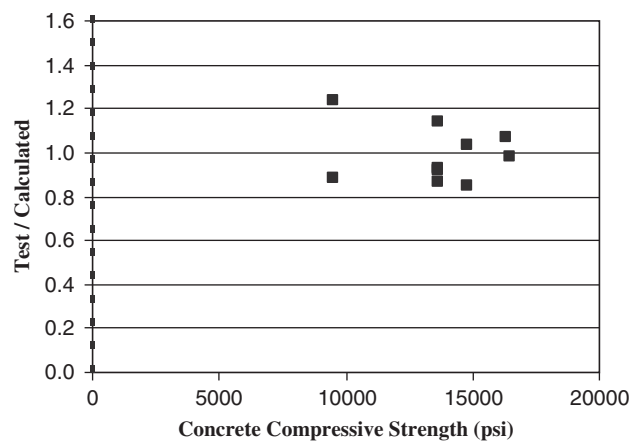
3.10.4 Summary and Conclusions

Based on the review of over 40 specimens in the literature and the results from 21 tests of hooked bar anchorages in beam-column specimens with normal-weight concrete strengths up to 16 ksi, the following conclusions can be drawn:

- The approach in the 318 Code (ACI 2005) provision for anchorage of bars terminated in standard hooks in tension, black and epoxy-coated, can be extended to concrete compressive strengths up to 15 ksi. However, a minimum transverse reinforcement ($3d_b$ spacing) should be provided in higher strength concretes to improve the bond characteristics of both epoxy-coated and black #11 hooked bars.



(a) Black Bar Specimens



(b) Epoxy-Coated Bar Specimens

Figure 3.81. Test to calculated stress ratio versus concrete compressive strength (1 psi = 6.89 KPa).

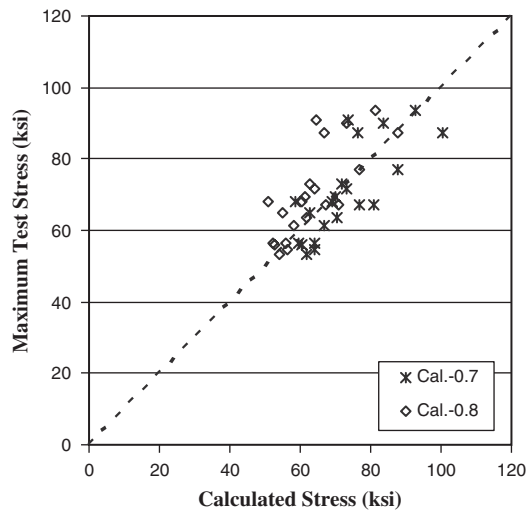


Figure 3.82. Maximum test stress versus calculated stress using factors of 0.7 and 0.8 for Marques and Jirsa (1975), Hamad et al. (1993), and those tested in NCHRP Project 12-60 (1 ksi = 6.89 MPa).

- The epoxy-coated hooked bars developed lower anchorage capacities than uncoated hooked bars. In the #11 hooked bar specimens, the ratios of measured stress to calculated stress were 0.85 to 0.88.
- Transverse reinforcement in the anchorage length of a bar terminated with a standard hook improves the maximum pull-out strength and load versus slip behavior. In the #11 epoxy-coated hooked bar specimens, the ratios of measured stress to calculated stress increased up to 0.98.
- While the minimum concrete cover of 2.5 in. at the end of the hook appeared to be adequate to prevent kicking out of the tail end of the hooked bar, it is proposed that a modification factor of 0.8 be used instead of 0.7. The use of a 0.8 modification factor eliminated almost the entire test to calculated stress ratios less than 1.0. This value of minimum concrete cover can be reduced to d_b if transverse reinforcement is used in the anchorage length of a bar terminated with a standard hook.

CHAPTER 4

Design Recommendations

4.1 Introduction

Article 5.4.2.1 of the *AASHTO LRFD Bridge Design Specifications* (2004) limits the applicability of the specifications for concrete compressive strengths of 10 ksi or less unless physical tests are made to establish the relationships between concrete strength and other properties. A comprehensive article-by-article review of Section 5 of the *AASHTO LRFD Bridge Design Specifications* (2004), pertaining to transfer and development of prestressing strand and splice length and anchorage of free ends by means of standard hooks for mild reinforcement was performed under NCHRP Project 12-60 to identify all provisions that would have to be revised directly or indirectly to extend their use to high-strength, normal-weight concrete up to 15 ksi. These articles are the following:

- Article 5.4.4 Prestressing Steel
- Article 5.5.4.2. Resistance Factors
- Article 5.11 Development and Splices of Reinforcement
- Article 5.11.2 Development of Reinforcement
- Article 5.11.2.1 Deformed Bars and Deformed Wire
- Article 5.11.2.1.1 Tension Development Length
- Article 5.11.2.1.2 Modification Factors that Increase l_d
- Article 5.11.2.1.3 Modification Factors which Decrease l_d
- Article 5.11.2.2 Deformed Bars in Compression
- Article 5.11.2.2.1 Compressive Development Length
- Article 5.11.2.2.2 Modification Factors
- Article 5.11.2.3 Bundled Bars
- Article 5.11.2.4 Standard Hooks in Tension
- Article 5.11.2.4.1 Basic Hook Development Length
- Article 5.11.2.4.2 Modification Factors
- Article 5.11.2.5 Welded Wire Fabric
- Article 5.11.2.5.1 Deformed Wire Fabric
- Article 5.11.2.5.2 Plain Wire Fabric
- Article 5.11.2.6 Shear Reinforcement
- Article 5.11.4 Development of Prestressing Strand
- Article 5.11.4.1 General
- Article 5.11.4.2 Bonded Strand

- Article 5.11.4.3 Partially Debonded Strands
- Article 5.11.5 Splices of Bar Reinforcement
- Article 5.11.5.3.1 Lap Splices in Tension

4.2 Design Recommendations

For prestressing strands, there are five essential recommendations stemming from the research:

1. Adoption of the Standard Test Method for the Bond of Prestressing Strands. Heretofore, this test has been known as the NASP Bond Test.
2. Adoption of a transfer length expression incorporating a factor to account for improved bond with increasing concrete strength. The recommended expression reflects the decrease in transfer lengths as concrete release strengths increase. For release strengths of 4 ksi, the recommended expression would provide a transfer length of 60 strand diameters, which is the same value found in prior editions of the *AASHTO LRFD Bridge Design Specifications*. For release strengths of 6 ksi, the design transfer length would be approximately 50 db. Transfer lengths would be limited to a minimum of 40 strand diameters.
3. Adoption of a development length expression that incorporates factors to account for improved strand bond as concrete strengths increase. The recommended code expression is founded on the same principles as prior editions of the *AASHTO LRFD Bridge Design Specifications*, i.e., the development length is the sum of a transfer length expression plus a flexural bond expression. At “normal” concrete strengths, the development length expression requires 60 strand diameters for transfer length and approximately 90 strand diameters for the flexural bond length, for a total of 150 strand diameters. For a concrete release strength of 6 ksi and design concrete strength of 10 ksi, the development length expression provides a development length of 120 strand diameters. For higher

concrete strengths, the development length is limited to a minimum of 100 strand diameters.

4. Adoption of a modified bilinear build-up of strand stress consistent with the recommended transfer and development length expressions.
5. Adoption of additional restrictions regarding the use of debonded, or shielded, strands.

The following recommendations, discussed in detail in Section 4.3.3, stemming from the work conducted under NCHRP Project 12-60 address the anchorage of Grade 60 mild steel in tension:

1. Development length of black and epoxy-coated reinforcing bars anchored by means of straight embedment length and splices.
2. Anchorage of black and epoxy-coated bars terminated with standard hook.

4.3 Details of the Design Recommendations

4.3.1 Prestressing Strand—Adoption of the Standard Test Method for Bond of Prestressing Strands

Table 5.4.4.1-1 reiterates the requirements for mechanical properties for the prestressing steels that are found in the two AASHTO material specifications. Mechanical properties include the grade or type, the size, the tensile strength (ksi) and the yield strength (ksi). Research findings from NCHRP Project 12-60 support the conclusion that the bond of prestressing strand should be recognized as a material property of the strand and included in Section 5.4.4, “Prestressing Steel,” of the *AASHTO LRFD Bridge Design Specifications*. The research described in Chapter 3 of this report provides supporting evidence that the Standard Test Method for the Bond of Prestressing Strands, found in Appendix H, should be adopted into the LRFD specifications for the purpose of qualifying strand for use in prestressed concrete structures. (Please note that the Standard Test Method for the Bond of Prestressing Strands is also known as the Standard Test for Strand Bond.) There are two issues that require resolution in order to adopt the Standard Test Method for the Bond of Prestressing Strands. First, the repeatability of the test procedure must be clearly shown. Second, minimum threshold values for bond performance need to be established. Both items are addressed below.

4.3.1.1 Standard Test Method for the Bond of Prestressing Strands

Section 3.2 in this report addresses the repeatability and reproducibility of the Standard Test Method for the Bond of

Prestressing Strands. The reproducibility of the test is summarized in Figure 3.7 where the Standard Test Method for the Bond of Prestressing Strands was performed on identical strand samples at Purdue University and at OSU. Altogether, the data illustrated in Figure 3.7 come from tests performed on five different 0.5-in.-diameter strand samples and two different 0.6-in.-diameter strand samples. Figure 3.7 shows that there is a high degree of statistical correlation between the results from the two sites. The coefficient of determination, R^2 , is 0.92. Perhaps even more importantly, Figure 3.7 helps to show that the test results fall very near to the “perfect” line, where nearly identical results are obtained at the two sites independently. The tests at Purdue University were completely blind, as strand designations for the strands tested at Purdue University did not match the strand designations on the same samples at OSU.

The protocols for the NASP Bond Testing used in NCHRP Project 12-60 were based on the NASP Bond Test from May 2004 and are found in Appendix I. However, some refinements were made during the early part of the NCHRP testing at OSU, and the round-robin testing between Purdue University and OSU more closely matched the protocols that were further refined during the NCHRP testing program. These protocols are now titled, “Standard Test Method for the Bond of Prestressing Strands,” and are recommended as the basis for the material requirements to ensure “bond-ability” of prestressing strands with concrete. The final recommended standard is included in Appendix H. Some of the modifications included in the April 2006 edition of the Standard Test Method for the Bond of Prestressing Strands include provisions for minimum acceptance and frequency of testing.

Therefore, it is recommended that the Standard Test Method for the Bond of Prestressing Strands be adopted and made part of the LRFD specifications. Notably, the North American Strand Producers Committee of the American Wire Producers Association has formally, by unanimous vote, adopted the test procedure as their standard for bond. The recommendation from this report is that the Standard Test Method for the Bond of Prestressing Strands be incorporated into the *AASHTO LRFD Bridge Design Specifications* in Section 5.4.4. The LRFD specifications text should state that the material supplier is required to provide certification that the bonding ability of the prestressing strand is acceptable for use in pretensioned and prestressed concrete applications and that the Standard Test Method for the Bond of Prestressing Strands “shall be permitted” to provide acceptability of the prestressing strand product.

4.3.1.2 Minimum Acceptance Value for Strand Bond

Minimum acceptance values for strand bond are incorporated into the Standard Test Method for the Bond of

Prestressing Strands in its current form. The minimum values were determined by analysis of data measured from both transfer length and development length beams. Development length beams were tested with three different 0.5-in. strands for their ability to develop the tension force necessary to support flexural failures in the prescribed development length. Strand A had a NASP Bond Test value of 20,950 lb. Strand B had a NASP Bond Test value of 20,210 lb. The bond values of Strands A and B are contrasted with Strand D, which had a NASP Bond Test value of 6,890 lb. From the testing that was done and discussed in Chapter 3 of this report, it can be determined that beams made with Strands A and B were able to develop their nominal flexural capacity in embedment lengths much shorter than the current requirements for strand development length. Conversely, tests on beams made with Strand D indicate that the bond-ability of this strand is marginal for the rectangular beams and insufficient for the I-shaped beams with respect to the strand's ability to satisfy the current and recommended design provisions for development length. NCHRP Project 12-60 testing indicates that the minimum threshold number resides somewhere between 6,890 lb and 20,210 lb, and that the strand with a bond value of 6,890 lb was acceptable in some of the beams but not in others.

Table 3.28 reports the results of development length tests on rectangular beams made with Strand D. From the table, the following can be seen:

1. For concrete strengths with release strengths as low as 4 ksi, Strand D was developed in the AASHTO-prescribed development length of 73 in.;
2. For the same beams, bond failures regularly occurred at 58 in.; and
3. Bond performance as measured by strand development improved dramatically with increases in concrete strength.

Similarly Table 3.29 reports the results from development length tests on rectangular beams made with Strands A and B. From the table, the following can be seen:

1. Flexural failures were reported on all concrete strengths and at all development lengths, and
2. Strand A was able to develop adequate tensile strength in only 46 in. of embedment for concrete strengths as low as 6,180 lb at release and 8,500 lb at design.

When considering whether the performance of Strand D is adequate for development length, it is important to also consider the development length test results from the I-shaped beams. The results from the I-shaped beams are reported in Table 3.26. In this table, Beams ID-6-5-1-N, ID-6-5-1-S, and ID-10-5-1-S all failed in bond. All three of these tests had

Strand D at embedment lengths of either 72 in. or 88 in. Bond failures occurred when web shear cracking in I-shaped beams propagated through the transfer zones of Strand D. These results from the tests on I-shaped beams indicate that bond performance of Strand D is inadequate.

Comparison of data in the two tables also shows that Strands A and B had superior bond performance when compared with Strand D. The data in the tables show that the correct threshold value for the NASP Bond Test lies somewhere between the NASP Bond Test value for Strand D and the value for Strands A and B.

The data from NASP Round III research, also discussed in Chapter 3, provide additional data points for strands with varying bonding properties (Russell and Brown 2004). In these tests, four different 0.5-in.-diameter strands were used in a testing program that used the NASP Bond Test (August 2001) to assess the bonding properties of the strands. The strands were also cast into beams where transfer lengths and development lengths were measured. Tables 3.31 through 3.33 summarize the results from the Round III testing. Strand FF from the NASP Round III report is the same as Strand D in NCHRP Project 12-60. The data from NASP Round III testing match the data from NCHRP Project 12-60, where beams made with Strand D failed in flexure at 73 in. of embedment but sometimes failed in bond at 58 in. The data from NASP Round III also include testing performed on Strand HH, which had a NASP Bond Test value of 10,700 lb. Beams made with Strand HH failed in flexure at both 73 in. and 58 in., except for one bond failure at an embedment length of 58 in. In this bond failure, the beam achieved nearly 90 percent of its fully developed nominal flexural capacity, exhibited significant ductility, and achieved a flexural strength in excess of that calculated for the beam considering the bilinear stress curves now found in the *AASHTO LRFD Bridge Design Specifications* and the 318 Code. The performance of beams made with Strand FF (NCHRP Project 12-60 Strand D) and Strand HH provides important data points in determining the minimum acceptance values for the Standard Test Method for the Bond of Prestressing Strands.

Therefore, from these test results that incorporate the findings of the NASP Round III tests with those of NCHRP Project 12-60 testing, it is recommended that the minimum threshold shall be 10,500 lb for 0.5-in. strands. In other words, the performance of Strand HH would be minimally acceptable, **and** the value of the NASP Bond Test of 10,700 lb can be rounded to 10,500 lb for simplification. Further, the data support the overall conclusion that the development length performance improves for strand with improving NASP Bond Test values and therefore support the recommendation that the Standard Test Method for the Bond of Prestressing Strands be adopted into the *AASHTO LRFD Bridge Design Specifications*.

Please note the protocols described in the Standard Test Method for the Bond of Prestressing Strands require that a single bond test consist of six individual tests and that the reported “Bond Test Value” is the average value from those six tests. Therefore, the 10,500-lb recommended minimum threshold is an average value in conformance with the protocols found in the Standard Test Method for the Bond of Prestressing Strands. In addition to the requirement for a minimum average Bond Test Value, the test includes a requirement for the minimum value for the lowest value of the set of six individual tests. This second criteria is established to avoid excessive variations in strand bond quality within the same sample of strand. The requirement for the minimum single test value is 9,000 lb for 0.5-in. strands. This second requirement effectively limits the standard deviation, or the statistical variance, for strand produced that may have moderate bonding properties.

In the NCHRP Project 12-60 research, transfer and development length testing was also performed on 0.6-in. strands. The NASP Bond Test was also conducted on 0.6-in.-diameter strands. The results indicated that the NASP Bond Test or the Standard Test Method for the Bond of Prestressing Strands was suitable in predicting the bond behavior of 0.6-in strands. Therefore, the NASP Bond Test is recommended for use for 0.6-in. strands. For 0.6-in. strands, the minimum threshold values are an average value of 12,600 lb and a single test minimum of 10,800 lb.

4.3.2 Transfer and Development Length Expressions for Prestressing Strand

The current ACI and AASHTO design equations for pre-tensioned transfer length and development length do not include concrete strength as a parameter in the design equation. However, test results obtained during NCHRP Project 12-60 strongly suggest that the anchorage ability of the strands is improved as concrete strength increases. The results from both transfer and development length testing support the conclusion that concrete strength is an important factor. These results are supported independently by the results from NASP Bond Tests in varying concrete strengths.

The Standard Test Method for the Bond of Prestressing Strands was used to assess the impact of varying concrete strengths on the bond between strand and concrete. In these tests, the NASP Bond Test was modified simply by casting the strand in concrete (with varying concrete strengths) instead of the sand-cement mortar required in the Standard Test Method for the Bond of Prestressing Strands protocols. Figure 3.9 illustrates the data collected from the NASP Bond Test performed on Strand D, in concrete, and the effects of varying concrete strengths. The figure shows that at a concrete strength of about 4.5 ksi, the prediction curve for Strand D

found in Figure 3.9 corresponds with a NASP Bond Test value (in concrete) of about 6,600 lb. Strand D, tested in mortar using the Standard Test Method for the Bond of Prestressing Strands, had an NASP value of 6,890 lb. In concrete with a strength of 10 ksi, Strand D had a NASP Bond Test value of nearly 12,000 lb. The data from the specimens in concrete support the conclusion that increasing concrete strength improves the bond between strand and concrete.

Figures 3.12 and 3.13 illustrate the results from *all* of the NASP Bond Tests in concrete versus concrete strength on four different strand samples. One of the remarkable features of this dataset is that it includes data from both 0.5-in. and 0.6-in. strands. There are more than 20 data points represented in the figures, all cast within a wide sample of concrete strengths. The unifying factor is that the Standard Test Method for the Bond of Prestressing Strands (in concrete) was performed on each of the samples, and each data point represents the average from at least six individual tests. Furthermore, the coefficient of determination, R^2 , was a remarkable 0.80 for this dataset, which includes two different strand sizes, four different strand samples, and a variety of concrete mixtures. The figures show clearly how the bond of concrete and sand is directly improved by increases in concrete strength. This result is important in determining recommendations for transfer length and development length equations.

Figures 3.12 and 3.13 show two very important things: (1) that the Standard Test Method for the Bond of Prestressing Strands is very robust and (2) that it can be modified with concrete to assess bond performance of strand of all sizes and in various concrete mixtures. As illustrated in Figure 3.12, the power regression between bond strength and concrete strength suggests the relationship:

$$\frac{(NASP_{\text{concrete}})}{NASP} = 0.49139 \bar{f}_{ci}^{0.51702} \quad (4.1)$$

The results from these tests further attest to the suitability of the Standard Test Method for the Bond of Prestressing Strands as a vehicle to measure the bond between prestressing strand and concrete. Further, these results support the argument that the variation in transfer and development lengths should vary with the square root of concrete strength. The results also support the recommendation for the adoption of the Standard Test Method for the Bond of Prestressing Strands by demonstrating that the Standard Test Method for the Bond of Prestressing Strands is useful for various sizes of strands and can predict differences in bond based on variations in concrete strength.

Testing showed that it is possible to describe the relationship between concrete strength and bond strength using the correlations found directly from the NASP Bond Tests in concrete. In those tests, it was found that bond strength varied nearly in proportion with the square root of concrete

strength. It can be observed from the data shown in Figures 3.12 and 3.13 that the bond strength of concrete is almost directly proportional to the square root of concrete strength. The linear regression shown in Figure 3.13 gives the following relationship:

$$\frac{(NASP_{\text{concrete}})}{NASP} = 0.51\sqrt{f'_c} \quad (4.2)$$

Testing also demonstrated that both transfer length measurements and development length requirements were shortened as concrete strength increased. Figures 3.24 through 3.32 show that for all sizes of strand and for all the varying qualities of strand bond, the transfer lengths shorten as concrete release strengths increase. Therefore, the recommended code equation includes the square root of concrete strength at release in order to be consistent with testing results that show shorter transfer lengths with higher concrete strengths. The transfer length recommendation provides a transfer length equal to the current design expression of 60 strand diameters when the concrete release strength is 4 ksi. Using the recommended expression, the transfer length shortens as the concrete release strength increases. Additionally, the expression provides a minimum limit of 40 strand diameters. Thus, the recommended expression for transfer length expression is the following:

$$l_t = \frac{120}{\sqrt{f'_c}} d_b \geq 40d_b \quad (4.3)$$

where

l_t = transfer length (in.),

f'_c = release concrete strength (ksi), and;

d_b = diameter or prestressing strand (in.).

If the concrete release strength is 4 ksi, then the equation results in a transfer length of 60 d_b . As release strength increases, the transfer length decreases. The limit of 40 d_b ensures that all designs consider transfer lengths of some reasonable value. The recommendation effectively limits an additional decrease in transfer length from concrete release strengths greater than 9 ksi. This minimum limit on transfer length is consistent with the testing conducted as part of this research in which the highest release strength achieved on rectangular beams was 9.7 ksi.

The current ACI and AASHTO design equations for development length do not include concrete strength as a parameter. As with the results on transfer length, results from development length testing strongly suggest that the bondability of the strands is improved as concrete strength increases. The experimental results clearly demonstrate that the required development length is shortened as concrete strength increases; higher concrete strength results in shorter development length requirements. Therefore, it is important

to include the effects of concrete strength in the design expression for development length.

Current expressions for development length (both ACI and AASHTO) were developed from the addition of the transfer length and a “flexural bond length.” This approach is supported by past and current research. Therefore, it is recommended to continue with the approach of splitting the development length into a transfer length component and a flexural bond length component. Both components, however, are affected by the concrete strength. Following is an outline of the rationale for developing the recommendation for development length:

1. The current AASHTO development length equation can be used to adequately predict required development lengths for “normal strength concrete” with release strengths in the range of 4 ksi to 6 ksi, provided that the strand itself is qualified by the Standard Test Method for the Bond of Prestressing Strands. The results presented in Chapter 3 of this report demonstrate flexural failures at embedment lengths of 73 in. for all 0.5-in. strands tested in this research program. The embedment length of 73 in. corresponds to 100 percent of the current code provision for development length for these specimens. The results included tests on beams made with concrete strength at release of approximately 4 ksi and approximately 6 ksi at the time of the beam test.
2. The data demonstrate that development length requirements are shortened as concrete strength increases.
3. The required development length calculated from the current code provisions is approximately 150 d_b , although under the 2004, 3rd edition of the AASHTO LRFD Bridge Design Specifications, some variations will exist due to variations in strand stressing, beam geometry, and subsequent variations in computed prestress losses. Only a few specimens contained prestressed strands at the tops of the cross sections. For these, beam tests were conducted for development length. Therefore, no comment can be made regarding the “top bar effect” for prestressing strands. Discussions regarding the κ factor are not included, although the testing demonstrates that the κ factor should be discarded for all sizes of strand. Instead all strands can be qualified for bond through the Standard Test Method for the Bond of Prestressing Strands.
4. Using a transfer length of approximately 60 d_b , and a development length of approximately 150 d_b , the flexural bond length must be approximately 90 d_b .

Thus, the development length expression can then be written as

$$l_d = l_t + \frac{225d_b}{\sqrt{f'_c}} \quad (4.4)$$

where

l_d = development length, (in.),

l_t = transfer length, (in.),

d_b = nominal diameter of the prestressing strand, (in.), and

f'_c = design concrete strength, (ksi).

If a concrete design strength, f'_c , of 6 ksi is seen as a reasonable approximation for “normal concrete strength,” then a coefficient can be computed to correspond with a flexural bond length of 90 strand diameters. That coefficient is $225/\sqrt{6} \approx 90$.

A minimum value is also recommended for the development length expression. The recommended expression for development length, therefore, is based on a limiting concrete strength of approximately 14 ksi, which is slightly less than the maximum concrete strength attained in beams tested in the research program (14.9 ksi). Thus, the recommended development length equation is as follows:

$$l_d = \left[\frac{120}{\sqrt{f'_a}} + \frac{225}{\sqrt{f'_c}} \right] d_b \geq 100d_b \quad (4.5)$$

The proposed development length equation is plotted against the development length test results in Figures 3.49 to 3.51. The result of each beam test, whether flexural failure or bond failure is plotted on a chart showing concrete strength versus embedment length. The curves representing the recommended design equations for development length are also shown on each of the charts. Note that the development length expression is now dependent on the concrete strength. For the purpose of computing the values within the equation and charting the results, the release strength is taken as 66.7 percent of the design strength.

Figure 3.49 shows the results of development length tests on Strand D. Strand D demonstrated below average bond performance with a relatively low NASP Bond Test value of 6,890 lb. Strand D also had measurably longer transfer lengths than Strands A/B. Figure 3.49 indicates that beams made with Strand D experienced bond failures in rectangular beams with embedment lengths of 58 in. for concrete strengths of about 8 ksi and lower. Note that in Figure 3.49, the flexural failures are represented by open symbols (triangles for R-beams and diamonds for I-Beams) and the bond failures are represented by solid symbols. Figure 3.49 clearly shows that as concrete strength increased, Strand D was able to move from bond failures to flexural failures a 58-in. embedment length. Furthermore, Figure 3.49 indicates that I-beams made with Strand D failed in bond at embedment lengths where the proposed design equation would predict adequate development. Therefore, Figure 3.49 shows that Strand D, with an NASP Bond Test value of only 6,890 lb, does not provide adequate bond-ability with concrete.

In contrast to the results from Strand D, Figure 3.50 plots results from development length tests on Strands A/B versus the proposed development length equation. The chart clearly shows that all of the beams tested resulted in flexural failures except for one single shear failure that occurred in an I-shaped beam. Thus, Strands A/B, high performers with an NASP Bond Test value in excess of 20,000 lb, can develop adequate tension force even in relatively short distances.

In Figure 3.52, the results obtained during NASP Round III with Strand HH are shown. Strand HH had a NASP Bond Test value of 10,700 lb. The chart shows that in the beams with two strands, flexural failures occurred at 73 in. (the AASHTO development length expression) and 58 in. The chart indicates that one bond failure occurred at an embedment length of 58 in. on a single strand beam. An embedment length of 58 in. corresponds to about 80 percent of the AASHTO requirement for development length. So in fact, a bond failure is the expected result. These beam test results from Round III provide important support to the recommendation that 10,500 lb should be the minimum average bond value for acceptance of prestressing strand. Clearly, Strand HH performed adequately when the ACI and AASHTO development lengths are provided.

Finally, shown in Figure 3.51 are the results of development length tests on the 0.6-in. strand, Strand A6. Strand A6 demonstrated good bond performance with a NASP Bond Test value of 18,290 lb. That NASP Bond Test value is comparable with the recommended minimum average value for 0.6-in. strands of 12,600 lb. Figure 3.51 indicates that rectangular beams made with Strand A6 experienced bond failures at an embedment length of 58 in., for concrete strengths of about 8 ksi and lower. Note that in the case of 0.6-in. strand these bond failures occurred when the embedment length provided was only 66 percent of the development length required. At an embedment length of 73 in. or so, Strand A6 was able to achieve adequate tension for all concrete strengths tested.

In summary, the results on beam tests clearly demonstrate support for the proposed development length expression for 0.5-in. and 0.6-in. strand. The inclusion of concrete strength is an important parameter that should be included in the design expressions for transfer and development lengths.

4.3.2.1 Additional Requirements for the Use of Debonded Strands

Past research includes some behavioral models that more accurately describe the behavior of beams containing debonded strands. Russell and Burns (1994) and Russell et al. (1994) described the behavior of beams containing debonded strands. Their research indicates that some additional provisions limiting the overall length of the debonded strands should be incorporated into the LRFD Specifications. Early testing performed

by Rabbat et al. (1979) and Kaar and Magura (1965) also support a behavioral approach toward limitations on debonded strands. The experimental programs were reviewed, and recommendations are made to amend the current code provisions. The experimental program did not incorporate testing on beams containing debonded strands. Recommended changes are based on experimental work already performed and identified within the existing body of knowledge.

The current *AASHTO LRFD Bridge Design Specifications* provide limitations on debonding strands. There are limitations on the total percentage of strands that can be debonded and the total number of debonded strands per row, as well as limitations on which strands within the cross section can be debonded. In addition to these existing limitations, the authors recommend three more:

1. Where pretensioned beams are not simply supported, debonding shall not be permitted except where it can be shown that cracking will not occur through the regions where debonding is placed nor through the transfer zones of debonded strands.
2. Debonding shall be limited in length from the end of a member to a distance equal to 0.15 times the span measured from center of bearing to center of bearing.
3. Debonding shall be limited in number and in length to sections where debonding is required to meet the requirements of Article 5.9.4.1. At sections where debonding is not required to meet the requirements of Article 5.9.4.1, debonding shall not be permitted.

4.3.3 Mild Reinforcement Development and Splice Lengths and Anchorage with Standard Hooks in Tension

In Section 12.1.2 of the 318 Code (ACI 2005) an upper limit of 100 psi on the $\sqrt{f'_c}$ term in the anchorage and development length provisions is imposed; in Section 5.4.2.1 of the Interim 2008 *AASHTO LRFD Bridge Design Specifications*, it is stated that design concrete strengths above 10 ksi shall be used only when allowed by specific articles or when physical tests are made to establish the relationships between concrete strength and other properties. The experimental program on mild reinforcement described in NCHRP Project 12-60 was designed to determine, in conjunction with the data already available in the literature, whether these limitations can be removed for concrete compressive strengths up to 15 ksi.

The 1971 provisions in the 318 Code (with slight modifications because f_y and f'_c are stated in terms of ksi and the introduction of epoxy-coated bar factors) are the current provisions for development and splice length of mild reinforcing bars in tension in the *AASHTO LRFD Bridge Design Specifications*. Thus, there are differences between the current 318 Code

provisions and the *AASHTO LRFD Bridge Design Specifications* (2004). In the 1995 edition of the 318 Code, the procedures for calculating development lengths for deformed bars and deformed wire in tension were extensively modified (ACI 1995). The changes resulted in an increase in the development lengths for closely spaced bars and bars with small covers. The basic development length was modified to reflect the influence of cover, spacing, transverse reinforcement, casting position, type of aggregate, and epoxy coating. The basic development lengths remained essentially the same as they were in the 1971 edition of the ACI Code and the *AASHTO LRFD Bridge Design Specifications*, with a few exceptions. One exception is the equation for the basic development length in tension for No. 18 bars. This equation was revised on the basis of a review of available test results on large bars. This change resulted in an increase of 12 percent over the values given by the current *AASHTO LRFD Bridge Design Specifications* for bars of the same size. Also, the top bar factor, which is 1.3 in the 318 Code, is 1.4 in the LRFD specifications. Another important change to the 318 Code, introduced in 1989, was to limit the $\sqrt{f'_c}$ value to a maximum of 100 psi, regardless of the compressive design strength of the concrete (ACI 1989). This limitation meant that development lengths would no longer decrease with concrete strengths greater than 10 ksi. It was noted that research on development of bars in high-strength concretes was not sufficient to substantiate a reduction beyond the limit imposed. This is also the reason given for the limitation imposed in Section 5.4.2.1 of the current LRFD specifications.

In 1977, the 318 Code provisions for tension lap splices of deformed bars and deformed wire encouraged the location of splices away from regions of high tensile stresses and to places where the area of steel provided at the splice location is at least twice that required by analysis. A lap splice of any portion of the total area of steel in regions where (A_s provided/ A_s required) is less than 2.0 had to be at least 1.3 times the development length of the individual bar in tension (Class B splice) in length. If more than one-half of the reinforcement was to be spliced in such regions, lap splices had to be at least 1.7 times the development length of the individual bar (Class C splice) in length. Class A splices in which the length of bar is equal to the development length of the individual bar were only permitted in regions where (A_s provided/ A_s required) is less than 2.0, and no more than 25 percent of the total area is spliced within one lap length. These same provisions are currently in the *AASHTO LRFD Bridge Design Specifications*. The Class C splice has been removed from the 318 Code. It must be noted that the splice factor is associated with the potential mode of failure when multiple bars are spliced at the same location and does not relate to the actual strength of the spliced bar.

The work by Treece and Jirsa (1989) is the basis of the development length modification factors for epoxy-coated bars

in the 318 Code and the *AASHTO LRFD Bridge Design Specifications*. In both, development length is multiplied by a factor of 1.5 for the epoxy-coated bars with a cover of less than $3d_b$ or clear spacing between the bars that is less than $6d_b$. Development length is multiplied by 1.2 for other cases. In either case, the product of the top-bar factor and epoxy-coating factor should not exceed 1.7. The 1.2 factor was selected based on the work of Johnston and Zia (1982). DeVries, Moehle, and Hester (1991), Hadje-Ghaffari, Darwin, and McCabe (1991), and Hadje-Ghaffari et al. (1994) found the current maximum of 1.7 for the product of the top-bar factor and epoxy-coating factor to be too conservative and recommended a value of 1.5. Cleary and Ramirez (1993), based on experimental observations on slab-type specimens, noted that since the experimental data on splitting type failures included only up to maximum cover to bar diameter ratio of 2.67 due to the increase of rib-bearing forces with epoxy-coated reinforcement, the limit of 3 used in the 318 Code for transition between splitting and pull-out failures should be examined experimentally.

The 1983 provisions in the 318 Code for development of bars in tension terminated with standard hooks were a major departure from the 1977 version of the 318 Code as hooked-bar anchorage provisions were uncoupled from provisions for straight-bar development. In the 1983 version of the 318 Code, the hooked-bar embedment length was measured from the critical section to the outside end or edge of the hook. The development length of the hooked bar was calculated as the product of a basic development length and appropriate modification factors. In the 1995 edition of the 318 Code, a factor of 1.2 was introduced in the hooked anchorage requirements (ACI 1995). The requirements in the 3rd edition of the *AASHTO LRFD Bridge Design Specifications* (2004) for anchorage of hooked bars in tension are the same as those in the 2005 318 Code (2005).

Equation 12-1 of the 318 Code (ACI 2005), used for calculating tension splice and the development length requirement, is the following:

$$l_d = \left[\frac{3f_y \psi_t \psi_e \psi_s \lambda}{40\sqrt{f'_c} \left(\frac{c_b + K_{tr}}{d_b} \right)} \right] d_b \quad (4.6)$$

In Equation 12-1, ψ_t is a reinforcement location factor of 1.3 to reflect the adverse effects of the top reinforcement casting position; ψ_e is a coating factor—1.5 with cover less than $3d_b$ or clear spacing less than $6d_b$ and 1.2 for all other cases. The product of ψ_t and ψ_e need not be taken greater than 1.7. The parameter ψ_s is a reinforcement size factor—0.8 for No. 6 bars and smaller and 1.0 for all other cases (the square root of the concrete compressive strength shall not exceed 100 psi as per Section 12.1.2). Other parameters are defined as follows: λ is a factor reflecting the lower tensile strength of

lightweight concrete, d_b is the bar diameter, K_{tr} is $40 A_{tr}/sn$ and represents the contribution of confining reinforcement across potential splitting planes, where A_{tr} is the area of transverse reinforcement within the spacing s that crosses the potential splitting plane, s is the spacing of stirrups and n is the number of bars being spliced or developed along the plane of splitting; c_b is the spacing or cover dimension using the smaller of either the distance from the center of the bar or wire to the nearest concrete surface or one-half the center-to-center spacing of the bars being developed. The ratio of $(c_b + K_{tr})/d_b$ is not to be taken greater than 2.5. However, l_d shall not be less than 12 in. In addition, when calculating anchorage length requirements for tension lap splices, these should be as required for Class A or B splices but not less than 12 in., where a Class A splice is $1.0 l_d$ and a Class B splice is $1.3 l_d$.

Development length for deformed bars in tension terminating in a standard hook (as per Section 7.1 of the 318 Code), l_{dh} , is determined using the equation below, found also in Section 12.5.2 of the 318 Code and applicable modification factors of Section 12.5.3, but l_{dh} shall not be less than the smaller $8d_b$ and 6 in. as indicated in Section 12.5.1 of the 318 Code (ACI 2005).

$$l_{dh} = \left(\frac{0.02 \psi_e \lambda f_y}{\sqrt{f'_c}} \right) d_b \quad (4.7)$$

ψ_e is a coating factor taken as 1.2 for epoxy-coated reinforcement; λ is a factor reflecting the lower tensile strength of lightweight concrete taken as 0.75 (for other cases, these two factors are taken equal to 1.0). Other parameters include the bar diameter of the hooked bar, d_b , concrete compressive strength, f'_c , in psi (the square root of the concrete compressive strength shall not exceed 100 psi as per Section 12.1.2 of the 318 Code). The modification factors of Section 12.5.3 are all less than 1.0 and thus reduce the calculated length on the basis of cover, presence of ties where the first tie encloses the bent portion of the hook within $2d_b$ of the outside of the bend, and when anchorage or development for specified minimum yield strength, f_y , is not specifically required:

1. For #11 bar and smaller hooks with side cover (normal to the plane of the hook) not less than 2.5 in. and for 90-deg hook with cover on bar extension beyond hook not less than 2 in, the factor is 0.7;
2. For 90-deg hooks of #11 and smaller bars that are either enclosed within ties or stirrups perpendicular to the bar being developed, spaced not greater than $3d_b$ along l_{dh} or enclosed within ties or stirrups parallel to the bar being developed, spaced not greater than $3d_b$ along the length of the tail extension of the hook plus bend, the factor is 0.8;
3. For 180-deg hooks of #11 and smaller bars that are enclosed within ties or stirrups perpendicular to the bar being developed, spaced not greater than $3d_b$ along l_{dh} , the factor is 0.8; and

4. Where anchorage or development for f_y is not specifically required, reinforcement in excess of that required by analysis, the factor is (A_s required/ A_s provided).

4.3.3.1 Development and Splice Length of Uncoated and Coated Bars

Article 5.11 of the 3rd edition of the *AASHTO LRFD Bridge Design Specifications* (2004), "Development and Splices of Reinforcement," contained provisions for development length of reinforcement that were essentially the same as those included in editions of the 318 Code up to the 1989 edition. The provisions of the 318 Code were extensively modified for the 1995 edition with a view to formulating a more "user friendly" format while maintaining the same general agreement with professional judgment and research results. Tests on splices of uncoated bars (Azizinamini et al. 1993, 1999a) have indicated that in the case of high-strength concrete some minimum amount of transverse reinforcement is needed to ensure adequate ductility out of the splice at failure. Based on these tests, a proposed modification (Azizinamini et al. 1999b) to the 1999 318 Code calls for the determination of a basic, straight development length for bars in tension, without including the presence of transverse reinforcement, together with a minimum area of transverse steel in the form of stirrups, A_{sp} , crossing potential splitting planes. In these studies, over 70 specimens were tested with concrete compressive strengths ranging between 5 ksi and 16 ksi. The experimental work conducted in NCHRP Project 12-60 aimed to fill the gaps in the existing data to extend the applicability of the LRFD provisions for development and splice length of uncoated and epoxy-coated bars (ASTM A 775) in tension to normal-weight concrete with compressive strengths up to 15 ksi.

Based on the observations from tests conducted during NCHRP Project 12-60 on 18 top-cast beam splice specimens and the examination of an extensive database of previous tests compiled by ACI Committee 408 (presented in previous chapters of this report), it is proposed to extend the *AASHTO LRFD Bridge Design Specifications* to concrete strengths up to 15 ksi using the approach in the 318 Code (ACI 2005), with the following exceptions:

- Remove the bar size factor for No. 6 and smaller bars; thus, $\psi_s = 1.0$ in all cases.
- Use a single factor for epoxy-coated bars of 1.5 regardless of the cover-to-bar diameter ratio.

Beam splice specimens with bottom cast bars were not evaluated in this study. The ACI Committee 408 (2003) indicated that the current approach in the 318 Code overestimated the bar force at failure in many specimens with bottom bars that are available in the ACI Committee 408 database, especially for specimens with concrete compressive strengths greater than 10 ksi. The ACI Committee 408 proposed a modified expression for development and splice length in addition to the removal of the bar size factor to address this issue. In the evaluation of test data conducted under NCHRP Project 12-60, the researchers found that the use of a bottom cast modification factor of 1.2 for uncoated bars anchored in concrete with compressive strengths greater than 10 ksi appeared to address the safety concerns raised by ACI Committee 408. This factor would not be needed for bottom cast epoxy-coated bars (because of the single modification factor of 1.5) or for uncoated top bars. This approach could be used as an alternative to the approach suggested by ACI Committee 408. The researchers note that additional testing of bottom cast uncoated splices is justified with higher strength concretes.

4.3.3.2 Anchorage in Tension of Uncoated and Coated Mild Reinforcement Using Standard Hooks

Article 5.11.2.4 of the *AASHTO LRFD Bridge Design Specifications* was verified for high-strength concrete in the proposed experimental Work Plan for NCHRP Project 12-60 with the exception of the lightweight aggregate factor. Based on the analysis of tests conducted during NCHRP Project 12-60 (21 full-scale tests of hooked-bar anchorages) and of tests of additional specimens in the literature, it is possible to support the extension of the approach in the 318 Code (ACI 2005) provision for anchorage of bars terminated with standard hooks, black and epoxy-coated, to normal-weight concrete with concrete compressive strengths of up to 15 ksi, with the following modifications:

- A minimum amount of transverse reinforcement (at least #3 U bars at $3d_b$ spacing) should be provided in the anchorage length to improve the bond strength of both uncoated and epoxy-coated No. 11 and larger bars terminated in a standard hook.
- A modification factor of 0.8 instead of the current factor of 0.7 for No. 11 and smaller hooks with side cover (normal to the plane of the hook) not less than 2.5 in. and for 90-degree hooks with cover on bar extensions beyond the hook of not less than 2 in.

References

- AASHTO (1998). *AASHTO LRFD Bridge Design Specifications*, 2nd ed., including 1999, 2000, and 2001 interim revisions. AASHTO, Washington, DC.
- AASHTO (2004). *AASHTO LRFD Bridge Design Specifications*, 3rd ed., with 2005 and 2006 interim revisions. AASHTO, Washington, DC.
- AASHTO (2007). *AASHTO LRFD Bridge Design Specifications*, 4th ed., Customary U.S. Units. AASHTO, Washington, DC.
- Abrishami, H. H. and Mitchell, D. (1993). "Bond Characteristics of Pretensioned Strand." *ACI Materials Journal*, Vol. 90, No. 3, May-June, 228–235.
- ACI (1963). *Building Code Requirements for Reinforced Concrete (ACI 318-63)*. American Concrete Institute, Redford Station, Detroit, MI.
- ACI (1989). *Building Code Requirements for Reinforced Concrete (ACI 318-89) and Commentary (ACI 318R-89)*. American Concrete Institute, Farmington Hills, MI.
- ACI (1995). *Building Code Requirements for Structural Concrete (ACI 318-95) and Commentary (ACI 318R-95)*. American Concrete Institute, Farmington Hills, MI.
- ACI (1999). *Building Code Requirements for Structural Concrete (ACI 318-99) and Commentary (ACI 318R-99)*. American Concrete Institute, Farmington Hills, MI.
- ACI (2002). *Building Code Requirements for Structural Concrete (ACI 318-02) and Commentary (318R-02)*. American Concrete Institute, Farmington Hills, MI.
- ACI (2005). *ACI 318-05: Building Code Requirements for Structural Concrete and Commentary*, American Concrete Institute, Farmington Hills, MI.
- ACI Committee 408 (1964). "A Guide for the Determination of Bond Strength in Beam Specimens." *Journal of the American Concrete Institute*, Vol. 61, No. 2, February, 129–135.
- ACI Committee 408 (1966). "Bond Stress—The State of the Art." *ACI Journal Proceedings*, Vol. 63, No. 11, November, 1161–1188.
- ACI Committee 408 (1970). "Opportunities in Bond Research." *ACI Journal Proceedings*, Vol. 67, No. 11, November, 857–867.
- ACI Committee 408 (2003). "Bond and Development of Straight Reinforcing Bars in Tension (408R-03). *Technical Documents*, American Concrete Institute, Farmington Hills, MI.
- Azizinamini, A., Darwin, D., Eligehausen, R., Pavel, R., and Gosh, S.K. (1999b). "Proposed Modifications to ACI 318-95 Tension Development and Lap Splice for High-Strength Concrete." *Structural Journal of the American Concrete Institute*, Vol. 96, No. 6, November-December, 922–926.
- Azizinamini, A., Pavel, R., Hatfield, E., and Gosh, S.K. (1999a). "Behavior of Spliced Reinforcing Bars Embedded in High-Strength Concrete." *Structural Journal of the American Concrete Institute*, Vol. 96, No. 5, September-October, 826–835.
- Azizinamini, A., Stark, M., Roller, J.J., and Gosh, S.K. (1993). "Bond Performance of Reinforcing Bars Embedded in High-Strength Concrete." *Structural Journal of the American Concrete Institute*, Vol. 90, No. 5, September-October, 554–561.
- Barnes, R.W. and Burns, N.H. (2000). "Anchorage Behavior of 15.2 mm (0.6 in) Prestressing Strand in High Strength Concrete." Presentation at PCI/FHWA/FIB International Symposium on High Performance Concrete, September 25–27, Orlando, FL, 484–493.
- Buckner, C.D. (1994). An Analysis of Transfer and Development Lengths for Pretensioned Concrete Structures, FHWA-RD-94-049. FHWA, U.S. DOT, Washington DC.
- Choi, O.C., Hadje-Ghaffari, H., Darwin, D., and McCabe S.L. (1990). "Bond of Epoxy-Coated Reinforcement to Concrete: Bar Parameters." SM Report No. 25, University of Kansas Center for Research, Lawrence, KS.
- Choi, O.C., Hadje-Ghaffari, H., Darwin, D., and McCabe, S.L. (1991). "Bond of Epoxy-Coated Reinforcement: Bar Parameters." *ACI Materials Journal*, Vol. 88, No. 2, 207–217.
- Clark, A.P. (1946). "Comparative Bond Efficiency of Deformed Concrete Reinforcing Bars." *ACI Journal Proceedings*, Vol. 43, No. 4, December, 381–400.
- Cleary, D.B. and Ramirez, J.A. (1993). "Epoxy-Coated Reinforcement Under Repeated Loading." *ACI Structural Journal*, Vol. 90, No.4, July-August, 451–458.
- Cooke, D.E., Shing, P.B., Frangopol, D.M. (1998), "Colorado Study on Transfer and Development of Prestressing Strand in High Performance Concrete Box Girders," University of Colorado Research Series No. CU/SR-97/4, April, 168 pp.
- Cousins, T.E., Johnston, D.W., and Zia, P. (1990). "Transfer and Development Length of Epoxy-Coated and Uncoated Prestressing Strands." *PCI Journal*, Vol. 35, No. 3, July-August, 92–106.
- Cousins, T.E., Stallings, J.M., and Simmons, M.B (1993). "Effect of Strand Spacing on Development of Prestressing Strands," Research Report, Alaska Department of Transportation and Public Facilities, August 1993.
- Darwin, D. and Graham, E.K. (1993a). "Effect of Deformation Height and Spacing on Bond Strength of Reinforcing Bars." SL Report 93-1, University of Kansas Center for Research, Lawrence, KS.

- Darwin, D. and Graham, E. K. (1993b). "Effect of Deformation Height and Spacing on Bond Strength of Reinforcing Bars." *ACI Structural Journal*, November-December, Vol. 90, No. 6, 646–657.
- Darwin, D., Tholen, M.L., Idun, E.K., and Zuo, J. (1996). "Splice Strength of High Relative Rib Area Reinforcing Bars." *ACI Structural Journal*, Vol. 93, No. 1, January-February, 95–107.
- Deatherage, J.H., Burdette, E.G., and Chew, C.K. (1994). "Development Length and Lateral Spacing Requirements of Prestressing Strand for Prestressed Concrete Bridge Girders." *PCI Journal*, Vol. 39, No. 1, January-February, 70–83.
- DeVries, R.A., Moehle, J.P., and Hester, W., 1991. "Lap Splice of Plain and Epoxy-Coated Reinforcements: An Experimental Study Considering Concrete Strength, Casting Position, and Anti-Bleeding Additives," *UCB/SEMM-91/02 Structural Engineering Mechanics and Materials*, University of California, Berkeley, CA, January.
- Ferguson, P.M. and Thompson, J.N. (1965). "Development Length of High Strength Reinforcing Bars." *ACI Journal Proceedings* Vol. 62, No. 1, January, 71–94.
- Furlong, R.W., Fenves, G.L., and Kasl, E.P. (1991). "Welded Structural Wire Reinforcement for Columns." *ACI Structural Journal*, Vol. 88, No. 5, September-October, 585–591.
- Griezic, A., Cook, W.D., and Mitchell, D. (1994). "Tests to Determine Performance of Deformed Welded-Wire Fabric Stirrups." *ACI Structural Journal*, Vol. 91, No. 2, March-April, 211–220.
- Gross, S.P. and Burns, N.H. (1995). *Research Report 580-2: Transfer and Development Length of 15.2 mm (0.6 in) Diameter Prestressing Strand in High Performance Concrete—Results of the Hoblitzell-Buckner Beam Tests*. The University of Texas at Austin, Austin, TX.
- Grundhoffer, T., Menis, P.A., French, C.W., and Leon, R. (1998). "Bond of Epoxy-Coated Reinforcement in Normal and High-Strength Concrete." *ACI Special Publication 180-2*, 261–298.
- Guimaraes, G.N., Kreger, M.E., and Jirsa, J.O. (1992). "Evaluation of Joint-Shear Provisions for Interior Beam-Column-Slab Connections Using High Strength Materials." *ACI Structural Journal*, Vol. 89, No. 1, January-February, 89–98.
- Hadj-Ghaffari, H., Darwin, D., and McCabe, S.L. (1991). "Effects of Epoxy-Coating on the Bond of Reinforcing Steel to Concrete." SM Report No. 28, University of Kansas Center for Research, Inc., Lawrence, KA.
- Hadj-Ghaffari, H., Choi, O.C., Darwin, D., and McCabe, S.L. (1994). "Bond of Epoxy-Coated Reinforcement to Concrete: Cover, Casting Position, Slump, and Consolidation." *ACI Structural Journal*, Vol. 90, No. 1, January-February, 59–68.
- Hamad, B.S., and Itani, M.S. (1998). "Bond Strength of Reinforcement in High-Performance Concrete: The Role of Silica Fume, Casting Position, and Superplasticizer Dosage." *ACI Materials Journal*, Vol. 95, No. 5, September-October, 499–511.
- Hamad, B.S., Jirsa, J.O., and D'Abreu de Paulo, N. (1993). "Anchorage Strength of Epoxy-Coated Hooked Bars." *ACI Structural Journal*, Vol. 90, No. 2, March-April, 210–217.
- Hamad, B.S., and Jirsa, J.O. (1993). "Strength of Epoxy-Coated Reinforcing Bar Splices Confined with Transverse Reinforcement." *ACI Structural Journal*, Vol. 90, No.1, 77–88.
- Hanson, N.W., and Kaar, P.H. (1959). "Flexural Bond Tests of Pretensioned Prestressed Beams." *ACI Journal*, Vol.55, No.7, January, 783–802.
- Hawkins, N.M. and Kuchma, D.A. (2002). "Application of the LRFD Bridge Design Specifications to High-Strength Structural Concrete: Shear Provisions, Phase 1," NCHRP Project 12-56 Interim Report, Transportation Research Board of the National Academies, Washington, DC, February.
- Hester, C. J., Salamizavaregh, S., Darwin, D., and McCabe, S.L. (1993). "Bond of Epoxy-Coated Reinforcement: Splices." *ACI Structural Journal*, Vol. 90, No. 1, 89–102.
- Hyett, A.J., Dube, S., and Bawden, W.F. (1994). "Laboratory Bond Strength Testing of 0.6" 7-Wire Strand from 7 Different Manufacturers," Final Report. Department of Mining Engineering, Queen's University, Kingston, Ontario, November.
- Jacob J. (1998). "Improved Shear Reinforcement Details for the End Regions of Prestressed Concrete Bridge Girders," Masters Thesis. University of Oklahoma, Norman, OK.
- Jirsa, J.O. and Breen, J.E. (1981). *Influence of Casting Position and Shear on Development and Splice Length—Design Recommendation, Research Report No. 242-3F*. Center for Transportation Research, The University of Texas at Austin, Austin, TX.
- Johnston, D.W. and Zia, P. (1982). *Bond Characteristics of Epoxy-Coated Reinforcing Bars*, FHWA-NC-82-002. FHWA, U.S. DOT, Washington, DC.
- Kaar, P.H., LaFraugh, R.W., and Mass, M.A. (1963). "Influence of Concrete Strength on Strand Transfer Length." *PCI Journal*, Vol. 8, No. 5, October, 47–67.
- Kaar, P.H. and Magura, D.D. (1965). "Effect of Strand Blanketing on Performance of Pretensioned Girders." *Portland Cement Association Research and Development Laboratory Bulletin*, December, 24–35.
- Kahn, L.F., Dill, J.C., and Reutlinger, C.G. (2002). "Transfer and Development Length of 15-mm Strand in High Performance Concrete Girders." *Journal of Structural Engineering*, Vol.128, No.7, July, 913–921.
- Kaufman, M.K. and Ramirez, J.A. (1988). "Reevaluation of the Ultimate Shear Behavior of High Strength Concrete Prestressed I-Beams." *ACI Structural Journal*, Vol. 85, No. 3, May-June, 295–303.
- Leonhardt, F. and Teichen, K. (1972). "Druck-Stosse von Bewehrungsstäben." *Deutscher Ausschuss für Stahlbeton Bulletin No. 222*, W. Ernst and Sohn, Berlin, FRG, 1–53.
- Logan, D.R. (1997). "Acceptance Criteria for the Bond Quality of Strand for Pretensioned Prestressed Concrete Applications." *PCI Journal*, Vol.42, No.2, March-April, 52–90.
- Maeda, M., Otani, S., and Aoyama, H. (1991). "Bond Splitting Strength in Reinforced Concrete Members." *Transactions of the Japan Concrete Institute*, Vol. 13, 581–588.
- Mansur, M.A., Lee, C.K., and Lee, S.L. (1987). "Deformed Wire Fabric as Shear Reinforcement in Concrete Beams." *ACI Structural Journal*, Vol. 84, No. 5, September-October, 392–399.
- Marques, J.L. and Jirsa, J.O. (1975). "A Study of Hooked Bar Anchorages in Beam-Column Joints." *Journal of the American Concrete Institute*, Vol. 72, No. 5, May, 198–209.
- Mathey, R.G. and Clifton, J.R. (1976). "Bond of Coated Reinforcing Bars in Concrete." *ASCE Journal of the Structural Division*, Vol. 102, No. ST1, 215–229.
- Meyer, K.F. (2002). "Transfer and Development Length of 0.6-inch Diameter Strand in High Strength Light Weight Concrete." Ph.D. dissertation, Georgia Institute of Technology, Georgia.
- Mitchell, D., Cook, W.D., Khan, A.A., and Tham, T. (1993). "Influence of High Strength Concrete on Transfer and Development Length of Pretensioning Strand." *PCI Journal*, Vol. 38, No. 3, May-June, 52–66.
- Nilson, A.H. (1997). *Design of Concrete Structures, 12th ed.*, McGraw-Hill, New York, NY.
- Orangun, C.O.; Jirsa, J.O.; and Breen, J.E. (1977). "A Reevaluation of Test Data on Development Length and Splices," *ACI Journal Proceedings*, Vol. 74, No. 3, 114–122.
- Ozyildirim, C. and Gomez, J.P. (1999). *High-Performance Concrete in a Bridge in Richlands, Virginia*. Virginia Transportation Research Council, Charlottesville, VA.

- Pfister, J.P. and Mattock, A.H. (1963). "High Strength Bars as Concrete Reinforcement, Part 5. Lapped Splices in Concentrically Loaded Columns." *Journal of the PCA Research and Development Laboratories*, Vol. 5, No. 2, May, 27–40.
- Pincheira, J. A., Rizkalla, S.H., Attiogbe, E.K. (1989). "Performance of Welded Wire Fabric as Shear Reinforcement under Cyclic Loading." *ACI Structural Journal*, Vol. 86, No. 6, November-December, 728–735.
- Rabbat, B.G., Kaar, P.H., Russell, H.G., and Bruce, R.N. (1979). "Fatigue Tests of Pretensioned Girders with Blanketed and Draped Strands." *PCI Journal*, Vol. 24, No. 4, July-August, 88–114.
- Roberts-Wollmann, C., Cousins, T., Gomez, J., and Ozyildirim, C. (2000). "Use of High Performance Concrete in a Bridge Structure in Virginia." Presented at the PCI/FHWA/FIB International Symposium on High Performance Concrete, September 25–27, Orlando, FL.
- Rose, D.R. and Russell, B.W. (1997). "Investigation of Standardized Tests to Measure the Bond Performance of Prestressing Strand." *PCI Journal*, Vol. 42, No. 4, July-August, 56–80.
- Russell B.W. (1992). "Design Guidelines for Transfer, Development, and Debonding of Large Diameter Seven Wire Strands in Pretensioned Concrete," Ph.D. dissertation, University of Texas at Austin, Austin, TX.
- Russell, B.W. (1994). "Impact of High Strength Concrete on the Design and Construction of Pretensioned Girder Bridges." *PCI Journal*, Vol. 39, No. 4, 1994, 76–89.
- Russell, B.W., and Brown, M.D. (2004). "Evaluation of Test Methods in Assessing Bond Quality of Prestressing Strands," Final Report, NASP Round III Strand Bond Testing. Oklahoma State University, Stillwater, OK, August.
- Russell, B.W., and Burns, N.H. (1993). *Design Guidelines for Transfer, Development and Debonding of Large Diameter Seven Wire Strands in Pretensioned Concrete Girders*. Report No. 1210-5F. Center for Transportation Research, The University of Texas at Austin.
- Russell, B.W., and Burns, N.H. (1994). "Fatigue Tests on Prestressed Concrete Beams Made with Debonded Strands." *PCI Journal*, Vol. 39, No. 6, 99–106.
- Russell, B.W., and Burns, N.H. (1996). "Measured Transfer Lengths of 0.5 in. and 0.6 in. Strands in Pretensioned Concrete." *PCI Journal*, Vol.41, No.5, September-October, 44–63.
- Russell, B.W., and Burns, N.H. (1997). "Measurement of Transfer Lengths in Pretensioned Concrete Elements." *Journal of Structural Engineering*, Vol.123, No.5, May, 541–549.
- Russell, B.W., Burns, N.H., ZumBrunnen, L.G. (1994). "Predicting the Bond Behavior of Prestressed Concrete Beams Containing Debonded Strands." *PCI Journal*, Vol. 39, No. 5, 60–77.
- Russell, B.W., and Paulsgrove, G.A. (1999a). "NASP Strand Bond Testing Round One Pull-Out Tests and Friction Bond Tests of Untensioned Strand," Final Report 99-03. The University of Oklahoma, Fears Structural Engineering Laboratory, Norman, OK.
- Russell, B.W., and Paulsgrove, G.A. (1999b). "Assessing Repeatability and Reproducibility of the Moustafa Test, the PTI Bond Test and the NASP Bond Test," Final Report 99-04. The University of Oklahoma, Fears Structural Engineering Laboratory, Norman, OK.
- Russell, H.G., Miller, R.A., Ozyildirim, H.C., and Tadros, M. K. (2006). *Compilation and Evaluation of Results from High-Performance Concrete Bridge Projects, Volume I: Final Report*, FHWA-HRT-05-056. FHWA, U.S. DOT.
- Sakurada, T., Morohashi, N., and Tanaka, R. (1993). "Effect of Transverse Reinforcement on Bond Splitting Strength of Lap Splices." *Transactions of the Japan Concrete Institute*, Vol. 15, 573–580.
- Shahawy, M.A., Issa, M., and Batchelor, B. (1992). "Strand Transfer Lengths in Full Scale AASHTO Prestressed Concrete Girders." *PCI Journal*, Vol. 37, No. 3, May-June, 84–96.
- Shing, P.B., Frangopol, D.M., McMullen, M.L., Hutter, W., Cooke, D.E., and Leonard, M.A. (2000). "Strand Development and Transfer Length Tests on High Performance Concrete Box Girders." *PCI Journal*, Vol. 45, No. 5, September-October, 96–109.
- Tabatabai, H. and Dickson, T.J. (1993). "The History of the Pretensioned Strand Development Length Equation." *PCI Journal*, Vol.38, No. 6, November-December, 64–75.
- Tessema Eden. (2006). "The Effect of High Strength Concrete on Bondability of Prestressing Strands." Masters Thesis, Oklahoma State University, Stillwater, OK.
- Treece, R.A. and Jirsa, J.O. (1989). "Bond Strength of Epoxy-Coated Reinforcing Bars." *ACI Materials Journal*, Vol. 86, No. 2, March-April, 167–174.
- Xuan, X., Rizkalla, S., Maruyama, K. (1988). "Effectiveness of Welded Wire Fabric as Shear Reinforcement in Pretensioned Prestressed Concrete T-Beams." *ACI Structural Journal*, Vol. 85, No. 4, July-August, 429–436.
- Zhongguo, (J.) M., Tadros, M.K., Baishya, M. (2000). "Shear Behavior of Pretensioned High-Strength Concrete Bridge I-Girders." *ACI Structural Journal*, Vol. 97, No. 1, January-February, 185–192.
- Zia, P. and Moustafa, T. (1977). "Development Length of Prestressing Strands." *PCI Journal*, Vol. 22, No. 5, 54–65.
- Zuo, J. and Darwin, D. (1998). "Bond Strength of High Relative Rib Area Reinforcing Bars." SM Report, No. 46, University of Kansas Center for Research, Lawrence, KA.
- Zuo, J. and Darwin, D. (2000). "Splice Strength of Conventional and High Relative Rib Area Bars in Normal and High Strength Concrete." *ACI Structural Journal*, Vol. 97, No.4, July-Aug., 630–641.

APPENDICES

Appendix A of the contractor's final report for NCHRP Project 17-25 contained the figures and tables for the report, and Appendix B contained the report reference list. In this publication, these materials have been incorporated into the text of the report.

Appendices C through I of the contractor's final report are available on the TRB website at http://trb.org/news/blurb_detail.asp?id=9210. Titles of Appendices C through I are the following:

- Appendix C: Rectangular Beam Summaries—Strand D
 - Appendix D: Rectangular Beam Summaries—Strands A&B
 - Appendix E: Rectangular Beam Summaries—Strand A (0.6 in.)
 - Appendix F: I-Beam Summaries—0.5-in. Strand
 - Appendix G: I-Beam Summaries—0.6-in. Strand
 - Appendix H: AASHTO Mxxx—Standard Test Method for the Bond of Prestressing Strands
 - Appendix I: NASP Test Protocols
-

Abbreviations and acronyms used without definitions in TRB publications:

AAAE	American Association of Airport Executives
AASHO	American Association of State Highway Officials
AASHTO	American Association of State Highway and Transportation Officials
ACI-NA	Airports Council International-North America
ACRP	Airport Cooperative Research Program
ADA	Americans with Disabilities Act
APTA	American Public Transportation Association
ASCE	American Society of Civil Engineers
ASME	American Society of Mechanical Engineers
ASTM	American Society for Testing and Materials
ATA	Air Transport Association
ATA	American Trucking Associations
CTAA	Community Transportation Association of America
CTBSSP	Commercial Truck and Bus Safety Synthesis Program
DHS	Department of Homeland Security
DOE	Department of Energy
EPA	Environmental Protection Agency
FAA	Federal Aviation Administration
FHWA	Federal Highway Administration
FMCSA	Federal Motor Carrier Safety Administration
FRA	Federal Railroad Administration
FTA	Federal Transit Administration
IEEE	Institute of Electrical and Electronics Engineers
ISTEA	Intermodal Surface Transportation Efficiency Act of 1991
ITE	Institute of Transportation Engineers
NASA	National Aeronautics and Space Administration
NASAO	National Association of State Aviation Officials
NCFRP	National Cooperative Freight Research Program
NCHRP	National Cooperative Highway Research Program
NHTSA	National Highway Traffic Safety Administration
NTSB	National Transportation Safety Board
SAE	Society of Automotive Engineers
SAFETEA-LU	Safe, Accountable, Flexible, Efficient Transportation Equity Act: A Legacy for Users (2005)
TCRP	Transit Cooperative Research Program
TEA-21	Transportation Equity Act for the 21st Century (1998)
TRB	Transportation Research Board
TSA	Transportation Security Administration
U.S.DOT	United States Department of Transportation